Quantitative Analyse des anorganischen Lösungsinhalts wässriger Proben mittels portabler laserinduzierter Plasmaspektroskopie (pLIBS):

Entwicklung der Methodik, Anwendung und Evaluation

Quantitative Analysis of the Inorganic Solution Content of Aqueous Samples Using Portable Laser-Induced Plasma Spectroscopy (pLIBS):

Methodological Development, Application and Evaluation

Von der Fakultät für Georessourcen und Materialtechnik der
Rheinisch-Westfälischen Technischen Hochschule Aachen

zur Erlangung des akademischen Grades eines
Doktors der Naturwissenschaften
genehmigte Dissertation

vorgelegt von
Nils Schlatter, M. Sc.
aus Freinsheim

Berichtende: Herr Univ.-Prof. Dr. Bernd Georg Lottermoser
Herr Univ.-Prof. Dr. habil. Andre Wilhelm Banning

Tag der mündlichen Prüfung: 17.06.2024

This page intentionally left blank.

Contents

Abstract

The inorganic solution content of aqueous samples is currently still analysed almost exclusively in the laboratory using conventional laboratory methods such as ion chromatography (IC) or atomic absorption spectroscopy (AAS). These methods are costly, time-consuming and not always practical. Many of the field methods developed to date lack the ability to quantify a large number of elements simultaneously in real time. The research objective of this thesis is therefore to evaluate whether and how aqueous solutions can be quantitatively analysed on site for inorganic solution content using portable laser-induced plasma spectroscopy (pLIBS).
Laser-induced plasma spectroscopy (LIBS) is an atomic spectroscopic method in which a pulsed laser is focused on a small area of the surface of a sample. This creates a plasma, the vaporised sample material is atomised and ionised and the electromagnetic radiation released is then analysed.
The first application of LIBS to aqueous solutions took place as early as 1984, albeit with stationary laboratory equipment. Difficulties in directly analysing the liquid surface with LIBS subsequently led to different types of sample preparation. Until now, the analysis of aqueous solutions has been limited to stationary or large, transportable LIBS devices. However, with advancing miniaturisation, analysis is also possible with portable devices.
This thesis documents the method development, application and evaluation of a portable method. Using the pLIBS Z-300 (SciAps), liquid-to-solid conversion is used as sample preparation in order to avoid the physical issues associated with analysing liquid surfaces and to reduce the detection limits by concentrating the sample during evaporation. Aluminium foil is used as a substrate because it is inexpensive, readily available and has few spectral interferences. To optimise the distribution of the evaporation residue and prevent the so-called *coffee ring effect*, a thin pencil layer is applied to the metal surface. The calibrations are created with dilution series from AAS standards. A 3D-printed sample holder guarantees the focusing and analysis of the evaporation residue and makes the method reproducible. Consisting of a base into which the aluminium foil is inserted and a stencil that is placed on top, the device can be mounted during the measurement process on the one hand and automatically focused on the other.
For calibration, dilution series with concentrations between 0.1 and 1000 mg/L are prepared from single-element AAS standard solutions. A drop of 0.75 μL is added with a pipette through the stencil onto the surface-enhanced Al-foil and then evapo-

rated on a hot plate. A square grid of 10 * 10 analysis points per vaporised drop with four individual analyses per point guarantees the complete detection of the evaporation residue. In the device-specific software, several lines of the element of interest with as little interference and as high intensity as possible are selected and an intensity ratio is formed with the strongest Al lines for each concentration. These can be used to create calibration lines for the elements of interest in a spreadsheet.
When analysing the spectra, which were also used for calibration, it is shown using the calibration curves that the three elements Li, Na and K can be quantified in standard solutions from 0.1 to around 100 mg/L (Li, Na) and 160 mg/L (K). At higher concentrations, the signal is no longer directly proportional to the concentration. In addition, the surface enhancement leads to a significantly improved shape and distribution of the evaporation residue and consequently to more reproducible results. At 0.006 to 0.011 mg/L, the detection limits for the three alkali metals are well below the concentration of 0.1 mg/L of the lowest standard solution used. When applied to mineral waters, with further calibrations for Ca, Mg, Sr, Cl, NO_3 and SO_4, similar results are obtained. In low mineralised waters up to about 1000 μS/cm, the dissolved ions can be quantified with the exception of NO_3. In addition, self-absorption of the emitted light occurs in the plasma, which cancels out the proportionality of concentration and signal intensity. The effect can be investigated in more detail using mixed standard solutions. Divalent ions are more susceptible to self-absorption than monovalent ions. Potentially toxic elements such as Cr, Ni, Cu, Zn, As, Se, Cd and Pb can also be quantified in standard solutions using the method. Although the calculated detection limits for these elements are below 0.03 mg/L, it is not possible to create calibration curves below the concentration of 0.1 mg/L for Zn and As. In addition, when comparing produced and predicted concentrations, only Cr shows plausible results for the concentration range below 0.1 mg/L. Only Cu can currently be reliably quantified in the range of the limit values for drinking water set by the World Health Organisation (WHO) and the German Drinking Water Ordinance.
The results show that the method developed cannot compete with laboratory methods such as AAS or ICP-MS in the field of trace analysis. However, it has a major advantage when rapid results or cost-effective preliminary screening are required. The distribution and shape of the evaporation residue can be optimised in the future by further developing the application process or the applied material. Self-absorption prevents the analysis of higher concentrations and must be mathematically minimised, which not only enables the analysis of higher concentrations but also increases reproducibility. The hot plate in combination with the sample holder can also be further developed with a metal version to further facilitate the methodology in the field. The calibration of further elements opens up a broader field of application in different sectors and thus leads to a significant market potential.

Zusammenfassung

Die Analyse des anorganischen Lösungsinhalts wässriger Proben findet derzeit noch fast ausschließlich mittels konventionellen Labormethoden wie Ionenchromatographie (IC) oder Atomabsorptionsspektroskopie (AAS) im Labor statt. Dabei sind diese Methoden kosten- und zeitintensiv und nicht immer praktikabel. Vielen entwickelten Feldmethoden fehlt es bisher an der Möglichkeit in Echtzeit eine Vielzahl von Elementen gleichzeitig quantifizieren zu können. Das Forschungsziel dieser Arbeit ist es deshalb zu evaluieren, ob und wie wässrige Lösungen mit der portablen laserinduzierten Plasmaspektroskopie (pLIBS) quantitativ vor Ort auf den anorganischen Lösungsinhalt analysiert werden können.
Laser-induzierte Plasmaspektroskopie (LIBS) ist eine atomspektroskopische Methode, bei der ein gepulster Laser auf einen kleinen Bereich der Oberfläche einer Probe fokussiert wird. Hierdurch entsteht ein Plasma, das verdampfte Probenmaterial wird atomisiert und ionisiert. Die hierdurch freiwerdende elektromagnetische Strahlung wird anschließend analysiert.
Die erste Anwendung von LIBS auf wässrige Lösungen fand bereits 1984 statt, allerdings mit einem stationären Laborgerät. Schwierigkeiten bei der direkten Analyse der Flüssigkeitsoberfläche mit LIBS führten in der Folge zu unterschiedlichsten Arten der Probenvorbereitung. Bisher beschränkt sich die Analyse wässriger Lösungen auf stationäre oder große, transportable LIBS-Geräte. Mit der voranschreitenden Miniaturisierung ist die Analyse aber auch mit portablen Geräten möglich.
In der vorliegenden Dissertation erfolgt eine Dokumentation hinsichtlich der Methodenentwicklung, -anwendung und -evaluierung hierzu. Unter Verwendung des pLIBS Z-300 (SciAps) wird die Flüssig-zu-Feststoffumwandlung als Probenvorbereitung verwendet, um einerseits die physikalischen Probleme bei der Analyse der Flüssigkeitsoberfläche zu umgehen und andererseits die Nachweisgrenzen durch Aufkonzentration beim Verdampfen der Probe zu verringern. Aluminiumfolie dient als Substrat, da diese kostengünstig und leicht verfügbar ist sowie wenige spektrale Interferenzen aufweist. Um die Verteilung des Abdampfrückstandes zu optimieren und den sogenannten *Kaffeering-Effekt* zu verhindern, wird eine dünne Bleistiftschicht auf die Metalloberfläche aufgetragen. Die Kalibrierungen werden mit Verdünnungsreihen aus AAS-Standards erstellt. Ein 3D-gedruckter Probenhalter garantiert das Fokussieren und Analysieren des Abdampfrückstandes und macht die Methode reproduzierbar. Bestehend aus einer Basis, in die die Aluminiumfolie eingelegt wird und einer Schablone, die aufgelegt wird, kann das Gerät einerseits beim Messvorgang fixiert und andererseits automatisch fokussiert werden.
Für die Kalibrierung werden Verdünnungsreihen mit Konzentrationen zwischen 0,1 und 1000 mg/L aus Einzelelement-AAS-Standardlösungen hergestellt. Ein Tropfen

mit 0,75 μL wird mit einer Pipette durch die Schablone auf die oberflächenoptimierte Al-Folie gegeben und anschließend auf einem Heiztisch verdampft. Ein quadratisches Raster von 10 * 10 Analysepunkten pro verdampftem Tropfen mit jeweils vier Einzelanalysen pro Punkt garantiert die gesamte Erfassung des Abdampfrückstandes. In der geräteeigenen Software werden mehrere möglichst interferenzfreie und intensitätsstarke Linien des Elements von Interesse ausgewählt und mit den stärksten Al-Linien für jede Konzentration jeweils ein Intensitätsverhältnis gebildet. Aus diesen Verhältnissen können in einer Tabellenkalkulation Kalibriergeraden für die Elemente von Interesse erstellt werden.
Bei der Analyse der Spektren, die auch für die Kalibrierung eingesetzt wurden, zeigt sich unter Verwendung der erstellten Kalibriergeraden, dass die drei Elemente Li, Na und K in Standardlösungen von 0,1 bis etwa 100 mg/L (Li, Na) und 160 mg/L (K) quantifizierbar sind. Bei höheren Konzentrationen ist das Signal nicht mehr direkt proportional zur Konzentration. Außerdem führt die Oberflächenoptimierung zu einer deutlich verbesserten Form und Verteilung des Abdampfrückstands und in Folge zu reproduzierbareren Ergebnissen. Die Nachweisgrenzen für die drei Alkalimetalle liegen mit 0,006 bis 0,011 mg/L deutlich unter der Konzentration der niedrigsten verwendeten Standardlösung von 0,1 mg/L. Bei der Anwendung auf Mineralwässer, mit weiteren Kalibrierungen für Ca, Mg, Sr, Cl, NO_3 und SO_4, zeigen sich ähnliche Ergebnisse. In gering mineralisierten Wässern bis etwa 1000 μS/cm können die gelösten Ionen mit Ausnahme von NO_3 quantifiziert werden. Darüber hinaus tritt Selbstabsorption des emittierten Lichts im Plasma auf, welche die Proportionalität von Konzentration und Signalintensität aufhebt. Mit Mischstandardlösungen kann der Effekt genauer untersucht werden. Dabei zeigen sich zweiwertige Ionen anfälliger für Selbstabsorption als einwertige.
Potentiell toxische Elemente wie Cr, Ni, Cu, Zn, As, Se, Cd und Pb können mit der Methode ebenfalls in Standardlösungen quantifiziert werden. Die errechneten Nachweisgrenzen liegen für diese Elemente zwar unter 0,03 mg/L, jedoch ist es für Zn und As nicht möglich Kalibriergeraden unter der Konzentration von 0,1 mg/L zu erstellen. Außerdem zeigt beim Abgleich von hergestellten und prognostizierten Konzentrationen nur Cr plausible Ergebnisse für den Konzentrationsbereich unter 0,1 mg/L. Im Bereich der von der WHO und der deutschen Trinkwasserverordnung festgelegten Grenzwerte für Trinkwasser kann derzeit nur Cu verlässlich quantifiziert werden.
Die Ergebnisse zeigen, dass die entwickelte Methode nicht im Bereich der Spurenanalytik mit Labormethoden wie AAS oder ICP-MS mithalten kann. Sie ist aber deutlich im Vorteil, wenn schnelle Ergebnisse oder ein kostengünstiges Vorabscreening gefragt sind. Die Verteilung und Form des Abdampfrückstands kann in Zukunft mit einer Weiterentwicklung des Auftragungsprozesses oder des aufgetragenen Materials noch optimiert werden. Die Selbstabsorption verhindert die Analyse höherer Konzentrationen und muss mathematisch minimiert werden, wodurch nicht nur die Analyse höherer Konzentration möglich wird, sondern sich auch die Reproduzierbarkeit erhöht. Auch der Heiztisch in Kombination mit dem Probenhalter kann durch eine Metallversion weiterentwickelt werden, um die Methodik im Feld weiter zu erleichtern. Die Kalibrierung weiterer Elemente eröffnet ein noch breiteres Anwendungsfeld in unterschiedlichsten Branchen und führt damit zu einem signifikanten Marktpotential.

Acknowledgements

First of all, I would like to thank Prof Dr. Bernd G. Lottermoser for offering the possibility of writing my Ph.D. and for supervising the thesis. I also want to thank my second supervisor Prof. Dr. habil. Andre W. Banning. Furthermore, I wish to express my gratitude to Dr. Rafael Schäffer, who has already supervised my Master's thesis and co-published its results with me. On one hand, I gained significant insights on how to prepare academic papers, while on the other hand, his stimulating scientific conversations motivated me. Another acknowledgement is owed to my colleagues, with whom I had the opportunity to discuss several matters contributing to this work. Special thanks are extended to Johannes Emontsbotz for providing invaluable support in the construction of the sample holder described in this study. His assistance was instrumental in gaining access to a 3D printer and creating a computer aided design (CAD) model. Based on my initial sketch, we collaboratively developed a model and iteratively refined it through multiple prototypes. I also wish to express my gratitude to Jan-Niklas Sander for proposing the idea to mount the sample to the LIBS and subsequently the idea of creating the sample holder. Johannes Sieger has also inspired me with his comments, for which I would like to thank him very much. Kim Nikolas Fiedler motivated me with his analytical approach and gave me valuable feedback on generated data. Leonard Krebbers was the person I greatly exchanged the progress of my work with, as well as the interpretation of the data. Our conversations consistently provided me with motivation and many new ideas. I express sincere gratitude to him for his contribution. Furthermore, I would like to thank Stefanie Schmidt for always supporting my work, performing, and evaluating my reference measurements in the laboratory and collaborating with me on two academic papers. I would like to also thank Guillaume Freutel and Simon Illgner for contributing to the success of this thesis with their two Master's theses.

I thank my family for their support on the long road to this thesis, especially my parents for believing in me and letting me go my way. In return, they had to endure countless incomprehensible descriptions of my studies and work over the years. I appreciate that they have positively triggered my thirst for knowledge through their passion for travelling and I am very grateful that I was allowed to live out of my urge to explore the unknown. I would like to separately thank my grandfather for always fuelling my thirst for knowledge, believing in me, and helping me get this far. Finally, I would like to express my great gratitude to my fiancée, whose support and encouragement have been invaluable during challenging times.

Contributions to the Thesis

The basic idea for the research question and the vast majority of the research work were developed and carried out independently by the author. However, ideas and contributions from other people are always incorporated into a doctoral thesis, and may even lead to the success of the work in the first place. In the following, these contributions of others are elaborated and documented. All sources used for this thesis are cited and listed in the bibliography. Some sections have already been published as journal articles or posters and are identified as such.

Guillaume Freutel conducted a master's thesis under the guidance of the author of this work, which elucidates the utilisation of LIBS in the minerals sector and he contributed to the publication described in section 1.4. In detail he wrote the drafts of the sections 1.4.2, 1.4.3, and 1.4.5. Furthermore, he devised figure 1.3.

The proposal by Jan-Niklas Sander to mount the sample to the LIBS ultimately gave rise to the concept of developing a dedicated sample holder.

Johannes Emontsbotz provided invaluable assistance with the computer-aided design (CAD) modelling of the sample holder and shared his 3D printer for recursive modelling and subsequent printing.

Stefanie Schmidt has done the IC and ICP-MS analysis for the second paper described in section 3.2 as well as writing of the relating part of the subsection 3.2.2.

Simon Illgner has also conducted a master's thesis under the guidance of the author of this work, in which the feasibility of analysing Ca, Mg, Sr and Zn using the method developed by the author was evaluated. The requisite measurements were subsequently augmented and processed by a multitude of additional measurements conducted by the author of this work, and were then published in a publication. His contribution to the article described in section 3.2 was the laboratory work already carried out in his Master's thesis as well as proofreading.

The spreadsheet-based approach to hydrochemical data evaluation used within this thesis, is the idea of Rafael Schäffer and is documented in his doctoral thesis as well as in two publications (Schäffer, 2018; Schäffer and Dietz, 2023). He instructed the author of this work in the creation and utilisation of a spreadsheet calculation tool for the evaluation of hydrochemical data at TU Darmstadt. This tool was subsequently developed and tailored to the author's specifications for use within this thesis.

The comments provided by the reviewers of the three principal articles included in this thesis have resulted in notable enhancements to the articles in question.

The contributions of the author's former colleagues, both in the form of numerous

comments made during research seminars and in other informal settings, also played a significant role in the success of the work. Leonard Krebbers, Johannes Sieger and Kim Nikolas Fiedler deserve special mention here.
Bernd G. Lottermoser assumed responsibility for the supervision, funding acquisition, proofreading of the majority of the texts, and provided annotations, suggestions, and additional insights.
The free translator DeepL (https://www.deepl.com/de/translator) and the AI writing assistant DeepL Write (https://www.deepl.com/de/write) were used to improve the English language within this thesis and proofreading of the final document was carried out by Cäcilia Boller.

List of Figures

List of Tables

List of Abbreviations

AAOPM 3D anodic aluminum oxide porous membrane
AAS atomic absorption spectroscopy
AMD acid mine drainage
ARD acid rock drainage
AES atomic emission spectroscopy
BASE Bielefeld Academic Search Engine
CAD computer aided design
CCD charge-coupled device
CRE coffee ring effect
CRM certified reference material
DOI digital object identifier
DP double pulse
EC electric conductivity
ED electrical deposition
EDX energy-dispersive X-ray spectroscopy
E$_h$ redox potential
EoI element of interest
ESD electrospray deposition
EvR evaporation residue
FFM fused filament fabrication
FWHM full width half maximum
GC geometric constraint
HF hydrofluoric acid
HG hydride generation
IID internal integration delay
IB ion balance

IC ion-exchange chromatography
ISEs ion-selective electrodes
ICP-MS inductively coupled plasma mass spectrometry
ICP-AES inductively coupled plasma atomic emission spectroscopy
ICP-OES inductively coupled plasma optical emission spectroscopy
IDG isolated droplet generator
IID internal integration delay
IQR inter-quartile range
IR intensity ratio
IUPAC International Union of Pure and Applied Chemistry
LAC liquid-to-aerosol conversion
LB liquid bulk
LCD liquid-crystal display
LED light-emitting diode
LIBS laser-induced breakdown spectroscopy
LIF laser-induced fluorescence
LJ liquid jet
LoD limit of detection
LPO laser protection officer
LPSW laser-patterned silicon wafer
LSC liquid-to-solid conversion
MeGe membrane generation
MLR multiple linear regression
MRE Institute of Mineral Resources Engineering
MW microwave enhancement
Nd:YAG neodymium-doped yttrium aluminum garnet
NIST National Institute of Standards and Technology
NIR near-infrared
NP nanoparticle-enhanced
n-SE non-surface-enhanced
PLA polylactic acid
pLIBS portable laser-induced breakdown spectroscopy
PMMA polymethyl methacrylate
ppb parts per billion
ppm parts per million
PTEs potentially toxic elements

PTFE polytetrafluoroethylene
pXRF portable X-ray fluorescence
R^2 coefficient of determination
R resonant
RE resonance-enhanced
REE rare earth elements
RMSE root mean square error
RSD relative standard deviation
RSO radiation safety officer
S standard deviation based on the regression
SD standard deviation
SDGs sustainable development goals
SE surface-enhanced
SEM scanning electron microscope
SNR signal-to-noise ratio
SP single pulse
SPEs screen-printed electrodes
SW silicon wafer
T temperature
t_b gate width
TBL triple bottom line
TDS total dissolved solids
t_d gate delay
THV threshold value
TRL technology readiness level
WDX wavelength dispersive X-ray analysis
WHO World Health Organisation
Z atomic number

Glossary

Atomic absorption spectroscopy (AAS) A frequently utilised analytical technique for the quantitative determination of chemical elements. It employs the absorption of characteristic light from a light source specific to a particular element by free atoms (Gey, 2021).

Acid mine drainage (AMD) Mine water produced by the artificially induced oxidation of sulfides by exposure to unstable (oxidising) environmental conditions. Has a significantly adverse impact on the environment due to its low pH levels (pH < 5.6) (Lottermoser, 2010, 2017).

Acid rock drainage (ARD) The low pH in water is formed in the same way as AMD, but occurs naturally when sulfides are exposed to oxidising conditions through natural processes such as weathering (Lottermoser, 2010, 2017).

Aerosol Tiny solid or liquid particles dispersed in air or gas (Harris, 2010).

Aqueous solution A solution in which water is used as the solvent.

Blank The term *blank sample* is used to describe a sample that consists of a solution lacking the analyte. The purpose of using a blank sample is to determine the sources of contaminants that were artificially introduced (Harris and Harris, 2014).

Bremsstrahlung X-ray radiation, generated by the deceleration of electrons, is observable as a continuous spectrum (Beckhoff, 2006).

Brine Type of water with a very high solution content. There are different definitions of the threshold, e.g. $\geq$ 40 g/L NaCl in mining (Hölting and Coldewey, 2019) or 14 g/kg in balneologically utilised waters (Wisotzky et al., 2021).

Calibration curve Plot showing the detector signal in relation to the concentration of the analyte, obtained through analysis of standard solutions (Harris and Harris, 2014).

Coffee ring effect (CRE) Ring shaped evaporation residue when droplets are dried on non-hydrophobic surfaces (Bae et al., 2015; Liu et al., 2020; Li et al., 2022). This effect is due to a capillary flow which, depending on the contact angle of the drop, conducts the vaporising liquid more or less strongly from the inside to the outside (Deegan et al., 1997).

Continuum radiation Radiation in a LIBS analysis resulting from Bremsstrahlung and recombination events that propagates across a wide wavelength spectrum (Cremers and Radziemski, 2013).

Detection limit (LoD) The analytical method's limit of detection (LoD) refers to the minimal value of an analyte that can be detected with certainty (Harris and Harris, 2014).

Deionised water To obtain pure water, ions are removed from the solution by distillation and deionisation, using a cation and anion exchanger (Harris, 2010).

Dilution series Series of standards with different concentrations prepared from a stock solution (Harris and Harris, 2014).

Dissolved Substances that pass through a filter with a pore size of 0.45 μm are deemed dissolved (Wisotzky et al., 2021). This evaluation is based solely on the size of the filter and not on other factors such as the chemical composition of the substance.

Electrical conductivity (EC) Typically measured as an on-site parameter, the electrical conductivity (κ) of a solution is analysed as the resistance between two electrodes and is expressed in S/cm or μS/cm (Hölting and Coldewey, 2019) . This is possible because ions dissolved in water form an electrically conductive solution (Hölting and Coldewey, 2019).

Evaporation residue (EvR) The residual content left on a surface following the evaporation of the liquid.

Full width half maximum (FWHM) Is the frequency interval between those frequencies at which the intensity has dropped by half compared to the centre frequency (Demtröder, 2011).

Gate delay (t_d) The time elapsed between the pulse arrival at the sample surface and recording of the signal (Cremers and Radziemski, 2013). A longer gate delay minimises background noise caused by continuum radiation, which overlays the characteristic lines during the early stages of plasma formation (Singh and Thakur, 2020). Figure 1 shows the temporal evolution of the LIBS plasma with spectra obtained with very short as well as longer gate delays. It is evident that the continuum radiation decreases with increasing time elapsed since the laser impact, and the spectrum demonstrates reduced noise levels.

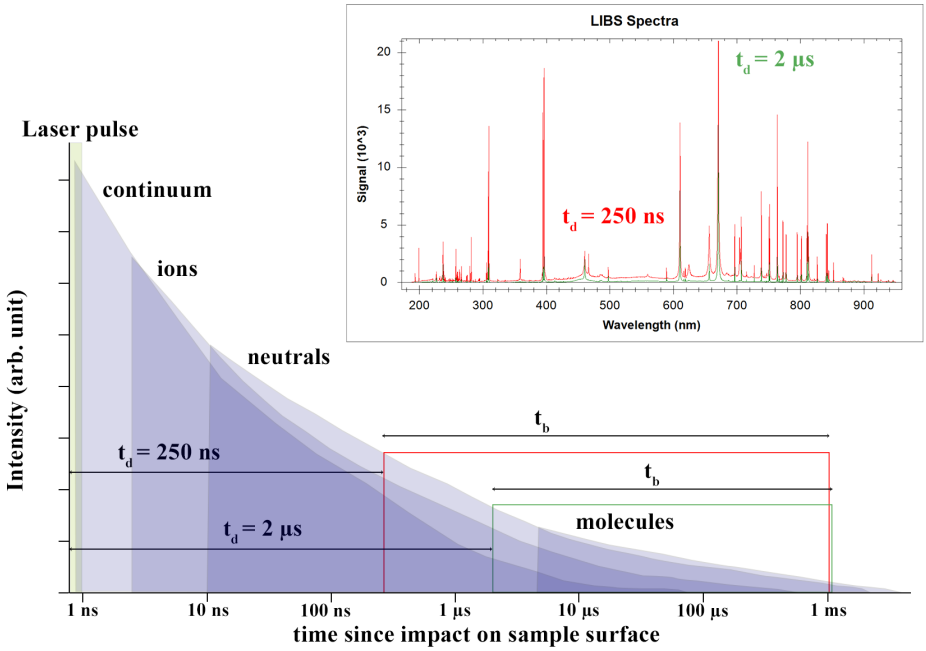

Figure 1: Temporal evolution of a LIBS plasma with an explanation of the gate delay (t_d) and gate width t_b. The spectra for Li analysis using two different gate delays are included. The shortest gate delay possible with the Z-300 is 250 ns and was used for comparison purposes, while the gate delay of 2 μs was employed for all the analyses in this thesis. It is evident that the continuum radiation decreases with increasing time elapsed, since the laser impact, and the spectrum demonstrates reduced noise levels. Modified after Cremers and Radziemski (2013) and Fabre (2020) and supplemented with own data.

Gate width (t_b) Time period during which plasma light is acquired (Cremers and Radziemski, 2013). Refer to Figure 1 for a visual representation. The shortest achievable gate width (t_b) with the Z-300 is 1 ms (Judge et al., 2021), which was used for all analyses in this thesis.

Greenness / green chemistry Approach to making chemical analyses more sustainable by reducing energy and resource consumption and avoiding waste (Harris, 2010; Gałuszka et al., 2015).

Handheld (h-) According to Senesi et al. (2020), *field-portable* refers to compact, lightweight, self-contained units that can be comfortably used whilst being held in the hand of an operator. In this dissertation, the terminology *portable* is used for all kind of field instruments and it is used interchangeably with *handheld* for the purpose of simplification.

Hydrochemistry Hydrochemistry is a sub-discipline of hydrogeology and deals with the chemistry of water. Its aim is to study the temporal and spatial influences and interrelationships with the physical, chemical, and physico-chemical (and in some cases biological) processes taking place in the groundwater-bearing medium (Hölting and Coldewey, 2019). Thus, the most important task of hydrochemistry is to quantify the chemical composition of (ground) water (Hölting and Coldewey, 2019).

Hydrophilic surface Water is a polar solvent due to the formation of dipoles in its molecules (Boyd, 2020). Consequently, it adheres to charged surfaces, which are described as hydrophilic (water loving) (Boyd, 2020).

Hydrophobic surface Less charged or uncharged surfaces are more difficult to wet because the cohesion between water molecules is greater than with the surface (Boyd, 2020). These surfaces are referred to as hydrophobic (water hating) (Boyd, 2020).

Inductively coupled plasma mass spectroscopy (ICP-MS) An atomic emission technique in which the sample is atomised in a high-temperature plasma. The energy for the plasma comes from a high-frequency electric field (Harris, 2010). After ionisation in the plasma the ions are separated by mass (Harris, 2010).

Inductively coupled plasma atomic emission spectroscopy (ICP-AES) An atomic emission technique in which the sample is atomised in a high-temperature plasma.

The energy for the plasma comes from a high-frequency electric field. The light emitted by the excited atoms is used for elemental analysis (Harris, 2010).

Ion balance Is a plausibility check of a water analysis (Hölting and Coldewey, 2019). For this purpose, the equivalent concentrations of the cations and anions of a solution are balanced (Wisotzky et al., 2021).

Ion chromatography (IC) Probably, the most commonly used method for determining the most prevalent cations and anions. It involves separating the ions using cation exchange processes and analysing the ion-specific electrical conductivity (Gey, 2021).

Inorganic Substances of non-animal or plant origin (Wisotzky et al., 2021). Used in this thesis to differentiate from dissolved organic compounds.

In-situ It refers to an analysis conducted on-site with no sample transportation and negligible or no sample treatment (Gałuszka et al., 2015).

Intensity ratio (IR) Is employed for the purpose of normalisation through division of the intensity of chosen emission line(s) of the element of interest (numerator) with the emission line(s) of an internal standard (denominator) (Guezenoc et al., 2019).

Internal integration delay (IID) Auxiliary variable without units utilised by the Z-300 to adjust the gate delay. The value can be recomputed to a gate delay through multiplication by a factor.

Inter-quartile range (IQR) It represents the height of the rectangular box in a box plot, which contains half of the data (Walser, 2011).

Laser Anacronym for *"light amplification by stimulated emission of radiation"*. Consisting of three components: Amplifying medium, energy pump, and a resonator (Demtröder, 2011). The most commonly used laser medium in LIBS is Nd:YAG, which typically has pulse durations in the nanosecond range (Palleschi, 2022b).

Laser-induced breakdown spectroscopy (LIBS) Elemental analysis employing a low-energy pulsed laser and a focused lens for producing a plasma that evaporates a minute portion of the sample's surface. The resulting plasma light is gathered and analysed for atoms, ions, and simple molecules (Cremers and Radziemski, 2013).

Linearity A measure of the extent to which data points follow a straight line, indicating proportional response to analyte amount (Harris, 2010).

Linear range Section of the calibration curve (range of concentration) where the intensity is directly proportional to the concentration of the analyte (Harris, 2010).

Liquid-to-solid conversion Sampling technique taking advantage of a solid target in LIBS analysis with phase conversion (Harun and Zainal, 2018b).

Matrix The matrix encompasses all substances present in an aqueous solution, aside from the analyte (Harris and Harris, 2014).

Matrix effect Small differences in the matrix (e.g. different concentrations of the analyte) can change the physical and chemical properties to such an extent that the intensity of the emitted signal is no longer proportional to the concentration (Palleschi, 2022b).

Mineral water Groundwater that originates from underground sources that are naturally or artificially tapped and has certain nutritional and physiological effects due to its constituents. The composition and temperature remain steady within the range of natural fluctuations and are not influenced by the flow of the spring (BGBI, 1984).

Mine water It refers to all water present at mining sites, both on the surface and underground. This water may originate from ground, surface or meteoric sources and undergoes reactions with rocks and minerals (Lottermoser, 2010).

Multiple linear regression (MLR) Since there are many different spectral lines per element, more than one line can be used for calibration. The statistical technique MLR utilises two or more lines in the determination of concentration (Fu et al., 2018a).

On-site parameters Even though inorganic water chemistry is nowadays almost exclusively investigated in the laboratory, some parameters still have to be analysed in the field as they can vary due to a changing environment. These are called on-site parameters and typically include organoleptic testing, temperature (T), electric conductivity (EC), pH-value, oxygen concentration, and redox potential (E_h) (Hölting and Coldewey, 2019).

pH The pH is the negative decadal logarithm of the hydronium ion activity. For diluted solutions: of the concentration of hydronium ions (Wisotzky et al., 2021).

Piper diagram The piper diagram is used to visualise and compare water samples to determine water types (Wisotzky et al., 2021). Comprised of combined triangular diamond diagram and developed by Piper (1944).

Plasma "A gas that is hot enough to contain free ions and electrons, as well as neutral molecules." (Harris, 2010)
"Local assembly of atoms, ions, molecules, and free electrons, overall electrically neutral, in which the charged species often act collectively. Plasmas are characterised by a variety of parameters, such as the degree of ionisation, the plasma temperature, and the electron density. A weakly ionised plasma is one in which the ratio of electrons to other species is less than 10%. LIBS plasmas typically fall in the category of weakly ionised plasmas." (Cremers and Radziemski, 2013)

Portable (p-) According to Senesi et al. (2020), *field-portable* refers to laboratory-level systems that can be transported to the field using a vehicle, operated by multiple individuals, and may require installation work. In this thesis, the terminology *portable* is used for all kind of field instruments and it is used interchangeably with *handheld* for the purpose of simplification.

Potentially toxic elements (PTEs) The term *"heavy metal"* is commonly used in literature as a collective term for elements linked to pollution or potential toxicity to living organisms (Duffus, 2002; Pourret and Hursthouse, 2019). However, this is misguided as different elements are included in various sources, some of which are not metals but metalloids, and some not heavy by definition (Duffus, 2002; Pourret and Hursthouse, 2019). Therefore, Pourret and Hursthouse (2019) suggests using the term PTEs to group elements that may harm living organisms.

Pre-concentration Step to increase the concentration of the analyte prior to the analysis (Harris, 2010).

Qualitative A qualitative test assesses the presence or absence of the analyte of interest. A positive result indicates the analyte is present while a negative result indicates its absence (Song et al., 2001).

Semi-quantitative A semi-quantitative analysis estimates the analyte concentration in the sample (Bertin, 1978). The confidence interval around the measured value is wider than that of a corresponding quantitative analysis (Song et al., 2001). An example of a semi-quantitative analysis is a test strip with multiple increments.

Quantitative Quantitative analysis determines the concentration of an analyte in a sample (Harris and Harris, 2014).

Redox potential (E_h) Redox potential is a measure of the oxidation-reduction state of water through the measurement of its electrical potential (Wisotzky et al., 2021).

Schoeller diagram Facilitates the visualisation and comparison of water samples in a vertical diagram. It utilises a logarithmic scale to represent the concentration on the ordinate and analytes on the abscissa. The diagram was originally developed by Schoeller (1965). Similarities and distinctions can be determined among various water samples by joining the points with straight lines (Schäffer, 2018). The result is a distinctive signature unique to each water sample (Schäffer, 2018). Congruent signatures are observed in water samples from the same source or identical aquifers. Parallel or subparallel signatures indicate a hydrochemical relationship, such as dilution (Schäffer, 2018).

Screen-printed electrodes (SPEs) Affordable and portable electrochemical instruments for analysing ions in water (Lu et al., 2018). Manufactured by printing different types of inks onto screen plates (Lu et al., 2018). Allow rapid in-situ analysis with high reproducibility, sensitivity and accuracy (Lu et al., 2018).

Sensitivity The concept of sensitivity entails how well a measuring device responds to variations in analyte concentration. It also determines a method's capacity to differentiate minute concentration variations in different samples (Harris and Harris, 2014).

Self-absorption A nonlinear saturation effect observed in calibration curves, leading to the cancellation of the proportionality between the concentration of the analyte and the measured intensity of the emission lines (Palleschi, 2022a).

Self-reversal A phenomenon in LIBS spectra, in which a narrow dip appears on top of the emission line, may potentially be misinterpreted as two distinct lines. It is linked to self-absorption, but manifests solely in the existence of spatial disparities in plasma temperature and electron number density (Palleschi, 2022a).

Signal-to-noise ratio (SNR) The signal-to-noise ratio defines the strength of a signal relative to the strength of the accompanying background noise (Harris and Harris, 2014).

Spectral line of neutral atom Analysis using LIBS involves the emission of characteristic lines of the elements present in the sample in their atomic, ionic, or molecular state, in addition to continuum radiation Fabre (2020). Atomic lines are labelled with the Roman numeral I, which should not be confused with redox states.

Spectral line of singly-ionised atom Analysis using LIBS involves the emission of characteristic lines of the elements present in the sample in their atomic, ionic, or molecular state, in addition to continuum radiation Fabre (2020). Ionic lines are labelled with the Roman numeral II. According to Fabre (2020), singly ionised ions are commonly detected, while double ionised ions decay fast (within nanoseconds). Trivalent ions, on the other hand, are not detected.

Standard solution A standard solution comprises an aqueous solution with a well-defined concentration of one or more substances (Harris and Harris, 2014).

Stiff diagram The Stiff diagram is used to visualise and compare water samples by building polygons with equivalent concentrations of an equal number of selected cations on the left and anions on the right side. Initially developed by Stiff (1951) as single diagram it can also be used to compare different waters in multi-stiff diagrams (Schäffer et al., 2021).

Surface enhancement (SE) This process refers to enhancing a non-hydrophobic surface to counteract the coffee ring effect. This is usually accomplished by increasing the surface's hydrophobicity (e.g. Jijón and Costa (2011)) or utilising geometrical constraints (e.g. Wu et al. (2021)).

Transportable (t-) In this thesis, the term *transportable* refers to all instruments constructed for in-situ application that are not lightweight ($>$ 10 kg), lack a portable energy source, and are not compact in size.

Triple bottom line (TBL) Sustainable development is based on three *bottom lines* or dimensions: economic/profit, social/people, and environmental/planet (Almici, 2022).

Technology readiness level (TRL) Scale with nine levels developed by NASA as a standardised instrument for assessing the degree of technological maturity for the use in further development of complex systems (Olechowski et al., 2020).

Total dissolved solids (TDS) The total dissolved solids of a water sample is determined by summing up the dissolved components (Wisotzky et al., 2021).

Trace element Substance usually occurring only in very small quantities in nature (Wisotzky et al., 2021).

X-ray fluorescence spectrometry (XRF) Method for the detection of elements by means of their X-ray emission (Cremers and Radziemski, 2013).

Chapter 1

Introduction

1.1 Motivation

Clean and accessible water is indispensable for both humans and animals (United Nations, 2023). Subsequently, it is also included in the 17 sustainable development goals (SDGs) (United Nations, 2023), which are political objectives aiming at guaranteeing global sustainable development, including the triple bottom line (TBL). Goal 6 claims to ensure access to water and sanitation for all humans by defining six targets (United Nations, 2015). One of these is to provide equal access to safe and affordable drinking water. Another is to improve the water quality by reducing pollution, emitting less, and at the same time recycling and treating more water. Moreover, in order to counteract water scarcity, the efficiency of water utilisation is to be significantly increased by 2030 and the sustainable extraction and supply of fresh water is to be ensured. This should significantly reduce the number of people suffering from water scarcity. Furthermore, it is aimed to implement integrated water resource management at all levels by 2030, including transboundary cooperation. The sixth objective of Goal 6 comprises three initiatives: safeguarding and rehabilitating water-linked ecosystems, facilitating global collaboration in water-related affairs, and backing and empowering local communities to enhance management of water and sanitation (United Nations, 2023).

The growing world population with an increasing demand for fresh water and, at the same time, an increasing amount of produced service and waste water, with increased land requirements exacerbating the situation (van Vliet et al., 2021). This makes it more difficult to achieve the targets set. Further complexities arise due to the effects of climate change including extreme weather events, droughts, and discrepancies in water distribution (IPCC, 2023).

Knowledge of the inorganic chemistry of water resources is therefore an important pillar in achieving the targets that have been set. There are manifold pollution sources, be it natural or anthropogenic ones. One common discussed pollution source is the mineral resource extraction (van Vliet et al., 2021). Mining not only unearths

the minerals and elements that are exploited, but also causes environmental issues through the alteration of minerals that are no longer stable under the environmental conditions at the Earth's surface or simply because mines need to be dewatered. Oxidising of reduced species can lead to acid mine drainage, which accelerates alteration and solution of potentially toxic elements (PTEs) (Lottermoser, 2010, 2017). However, this process can also take place naturally, without any human support. This can happen when rocks containing reduced minerals, such as sulfides, are unearthed by natural processes like rockfalls or erosion in general. This emphasises that natural processes can also be sources of water pollution.

Another issue in groundwater contamination is arsenic (As), which is a serious problem in Bangladesh for example (Ahmad and Khan, 2023). Prior to the 1970s, the population in Bangladesh experienced diarrhoeal diseases and cholera due to the use of biologically polluted surface water (Ahmad and Khan, 2023). Consequently, tube wells were installed throughout the country and campaigns were launched to shift from the traditional use of surface water to groundwater, resulting in a widespread use of shallow groundwater sources (Ahmad and Khan, 2023). However, high geogenic concentrations of arsenic are widespread throughout the country in shallow aquifers, affecting 62 out of 64 districts (Ahmad and Khan, 2023). This has resulted in many people suffering from arsenicosis. The highest concentration measured was 1670 mg/L, while the median and mean concentrations were 0.004 and 0.055 mg/L, respectively (Ahmad and Khan, 2023). The drinking water threshold in Bangladesh is 0.05 mg/L. Compared to the threshold of 0.01 mg/L defined by the WHO (WHO, 2022), this threshold is very high. But as the world's population continues to grow, so does the population pressure and thus the need for drinking water (van Vliet et al., 2021).

However, there is also geogenic inorganic groundwater contamination in specific regions of Germany, such as arsenic (As) and uranium (U) (Banning, 2021). Both elements can be mobilised due to changing Eh-pH conditions and ion exchange reactions, and accumulate in aquifers (Banning, 2021). The adverse effects of U on human health mainly arise from its toxicity rather than its radioactivity (Banning, 2021).

Catastrophes such as the pollution of the Oder river in the summer of 2022, which led to a mass extinction of fish (Free et al., 2023), show how helpless industrialised nations can be. It took weeks and weeks until the source of the pollution was found: A high solution content paired with hot weather supported the growth of a poisonous algal bloom. The incident could have been avoided if the polluter, a mining company, had limited the discharge of mine water into the receiving watercourse depending on the water levels of the river. In New South Wales (Australia), where dryness is a more common issue, they implemented a trading scheme for the release of mine water to the receiving waters in the Hunter Valley coal area (Krogh et al., 2013). It regulates the allowed water discharge according to the water levels and the EC in a certain part of the river by trading discharge licences (Krogh et al., 2013; Timms and Holley, 2016). This could have been a potential solution for the Oder event. But the consequences could also have been minimised if the cause had been found more quickly. Here and in other cases, analysing water samples for the inorganic solution content is time-critical. For many applications, it would be desirable if samples did

not have to be sent to the laboratory first and if statements about the chemistry could already be made in the field. Thus, a preselection of samples to reduce costs or direct actions should be made possible. However, to this day, there is no reliable direct field method present to analyse water samples simultaneously for several main ions and PTEs like lead or arsenic with a low limit of detection (LoD). Finding such a reliable fast method would help revealing many environmental problems, not only in mining, but also in other industries, and could thus generally lead to cleaner water around the world.

1.2 Research Gap, Aim, and Questions

To find such a method, there is no need to invent a completely new analysis technique. Instead, well-established laboratory methods can be utilised. For example, miniaturised laboratory devices, such as a transportable ion chromatography systems for field application (Elkin, 2014), can be used. However, many of these miniaturisation attempts lack true portability as they are usually not handheld, lightweight, or self-powered (Gałuszka et al., 2015).
Following the acquisition of the SciAps Z-300 portable laser-induced breakdown spectroscopy (pLIBS) analyser at the Institute of Mineral Resources Engineering (MRE), RWTH Aachen University, potential research areas with this new technology were investigated. The pLIBS meets the criteria for true portability and allows a multiple element analysis. As it will be outlined in Section 1.4, despite being a relatively new technique, pLIBS has already found numerous applications in solids analysis and is proving to be a competitor to the portable X-ray fluorescence (pXRF). In particular, it has found a wide application in positive material identification, for example, in scrap sorting (Piorek, 2019; Poggialini et al., 2020). Nevertheless, this measurement technology is also spreading rapidly in the field of geosciences (Harmon et al., 2009; Harmon and Senesi, 2021; Lawley et al., 2021).
However, to this date there appears to be no research in water analysis using pLIBS, although there has been a lot of research using laboratory laser-induced breakdown spectroscopy (LIBS) equipment (e.g. Cremers et al. (1984); Yueh et al. (2002); Zhao et al. (2010); Lee et al. (2011, 2012); Aguirre et al. (2013); Cahoon and Almirall (2012); Bae et al. (2015); Yang et al. (2018); Ma et al. (2020a); Nakanishi et al. (2021); Skrzeczanowski and Długaszek (2022); Tian et al. (2022)). Possible reasons for this will be discussed in the following sections (e.g. Section 1.4). As outlined in Section 1.1, the identification of a portable technique capable of a multi-elemental analysis of elements in aqueous solutions would have significant implications and offer a variety of potential applications. With the promising research found for stationary and online LIBS devices, one question arises:

(How) can aqueous solutions be quantitatively analysed for their inorganic solution content using a pLIBS, in particular by the SciAps Z-300?

Henceforth, the central research objective of the thesis is to develop a method that allows the use of the SciAps Z-300 for a quantitative analysis of aqueous solutions for inorganic solution content. The main research question is to be answered in Chapters 1 - 4, with the following subordinate questions structured by chapter. A short answer to each of the questions listed can be found in the conclusions (Sect. 5.1).

Chapter 1: Introduction To give an introduction to the quantitative analysis of the inorganic solution content of aqueous samples with LIBS in general, the following research questions will be answered:

- When was LIBS developed and how has the technology evolved since its introduction?
- How long have pLIBS devices been on the market?
- What are the physical principles behind LIBS and how are the devices constructed?
- What are the differences to the comparable pXRF technique?
- What needs to be considered when working with pLIBS?
- Are there safety regulations and legal requirements for transport and use?
- What functions are available on current devices?
- What applications in the raw materials sector are known to date?
- When was elemental analysis of aqueous solutions by LIBS introduced and where is research being carried out on this subject?
- What are common challenges encountered during elemental analysis of aqueous solutions using LIBS?
- What methods for sample preparation exist to date and what is their share of use?
- Which types of aqueous solutions are analysed?
- Which types of devices are used?
- What are the most important acquisition settings?
- Which elements are usually investigated?
- What LIBS setups exist to enhance analyses?
- What sensitivity do different methods show for various elements?
- What could the future development in this field look like?

Chapter 2: Method Development The development of the method for quantitative analysis of dissolved elements in aqueous solutions with pLIBS is characterised by many subordinate research questions, which are answered in Chapter 2:

- Is a liquid-to-solid conversion (LSC) method appropriate for use with the SciAps Z-300?
- Which substrate should be selected?
- What is required to improve the LSC method?
- What type of standard can be chosen and which elements should be considered?
- What are the calibration steps and is the manufacturer's calibration software sufficient?
- How can a pLIBS be held in place during analysis and what can be done to improve the speed and repeatability of the focusing process?
- How can the process of evaporation also be carried out in the field?
- How can calibration be managed using a spreadsheet?
- How can the developed calibrations be used to analyse unknown samples?

Chapter 3: Application and Evaluation The application and evaluation of the method on different water samples raises further sub-questions, which are answered in Chapter 3:

- Is it possible to quantitatively determine Li, Na, and K in aqueous standard solutions using pLIBS?
- Is the developed surface-enhanced liquid-to-solid conversion technique suitable?
- Is it possible to create linear calibration curves?
- What are the detection limits achieved for the three elements?
- Which concentration ranges can be analysed?
- What is the effect of surface enhancement on the spread and shape of the evaporation residue?
- Does the surface enhancement improve sensitivity or reproducibility?
- How do the findings compare with other methodologies detailed in literature?
- Is it possible to quantitatively determine typical cations and anions in bottled mineral water using pLIBS?

- Is it possible to create linear calibration curves for all desired concentration ranges of all selected elements?
- What are the detection limits achieved for the selected elements?
- Which concentration ranges can be analysed?
- What are the results when the calibrations are applied to mixed standard solutions with a known concentration of the elements?
- Are there any matrix effects and what is the influence of self-absorption?
- Is it possible to quantitatively determine PTEs in aqueous solutions using pLIBS?
- Is it possible to use mixed standard solutions for calibration?
- Is it possible to create linear calibration curves for all desired concentration ranges of all selected elements?
- What are the detection limits achieved for the selected elements?

Chapter 4: Discussion Limitations, possible improvements, comparison with other techniques, and the market potential are discussed in the fourth chapter with the following research questions:

- How can the spread and shape of the evaporation residue be further optimised?
- How can self-absorption be reduced or eliminated?
- How does the developed method compare to other instruments?
- What is the current stage of development of the method?
- What is the market potential of the method?

1.3 Structure of the Thesis

The research for this cumulative dissertation started in June 2020 and comprises three papers that have been published in peer-reviewed journals. These publications represent the methodical development steps and are supplemented by additional information in further chapters within this thesis to aid in a better understanding and comprehensive discourse of the topic. The thesis is meticulously organised and structured into five chapters and an appendix:

1. In the opening chapter, the motivation for this PhD thesis is discussed (Sect. 1.1) and the research gap, aim, and questions are defined (Sect. 1.2). Moving forward, the use of pLIBS systems in the raw materials sector will first be evaluated and the comparatively new type of analysis compared with the more established method of pXRF (Sect. 1.4). Subsequently, the elements that can be analysed relatively well in aqueous samples using LIBS will be identified (Sect. 1.5). Different types of sample preparation and various measurement methods as well as their strengths and weaknesses will be analysed.

2. Chapter 2 outlines the steps taken to develop the final field method using the SciAps Z-300. This includes preliminary tests with various measurement settings (Sect. 2.1), the creation of a custom sample holder for on-site water analysis (Sect. 2.2), and a portable hot plate (Sect. 2.3). The chapter closes with a description of the calibration steps using spreadsheets (Sect. 2.4).

3. Chapter 3 covers the application and evaluation of the developed method. It is first validated on standard solutions (Sect. 3.1) and then on more complex mineralised bottled mineral waters (Sect. 3.2). An overview of the method's capability for analysis of potentially toxic elements (PTEs) is also provided (Sect. 3.3).

4. In a comprehensive discussion, the fourth chapter summarises the problems encountered when applying the method (Sect. 4.1, 4.2) and proposes potential solutions. The method is compared to other field analyses (Sect. 4.3) and laboratory-based measurement techniques. Furthermore, the stage of development and market potential are critically assessed (Sect. 4.4).

5. The fifth chapter concludes by answering the research questions (Sect. 5.1) and identifying future research areas (Sect. 5.2).

6. The appendix includes a list of related publications (Sect. A.1), some background data (Sect. B.1), working materials (Sect. B.2), and the list of the digital attachments (Sect. B.3).

1.4 Evaluation of the Use of Field-Portable LIBS Analysers in the Mineral Resources Sector

All content in this section was originally published in the Georesources article entitled *"Evaluation of the Use of field-portable LIBS Analysers for on-site chemical Analysis in the Mineral Resources Sector"*. Key questions have been added and some minor typesetting and layout work have been done.

Authors: Nils Schlatter, Guillaume Freutel, and Bernd G. Lottermoser

Received: 3 February 2022; **Revised:** 16 May 2022; **Published:** 18 July 2022

Keywords: Mining; Raw Materials; Measuring technology; Analysis; Innovation; Efficiency

Key questions:

- When was LIBS developed and how has the technology evolved since its introduction?
- How long have pLIBS devices been on the market?
- What are the physical principles behind LIBS and how are the devices constructed?
- What are the differences to the comparable pXRF technique?
- What needs to be considered when working with pLIBS?
- Are there safety regulations and legal requirements for transport and use?
- What functions are available on current devices?
- What applications in the raw materials sector are known to date?

1.4.1 Introduction

Over the past few decades the advent of portable hightech field tools such as portable X-ray fluorescence (pXRF) instruments have revolutionised chemical data acquisition in the mining value chain. Times have dramatically changed. Previously, the ability to make an objective assessment and decision on the significance of a sample's chemistry took weeks or even months of waiting for a commercial laboratory to prepare and analyse a sample and then report the results. These pXRF instruments are now increasingly used within the mineral resources sector as they have many clear advantages. The technology allows for real-time 'fit for purpose' data to be collected

in the field. No advanced training, as in the case of a laboratory environment, is needed to use the equipment, although appropriate work safety and radiation protection training for operators is required. Portable field instruments are now available to the user to fast track the decision making process in the field. Results are obtained almost immediately and allow rapid real-time assessments and decision-making on-site, assuming the instruments are used correctly and their limitations understood by the user. The potential of saving costs in screening samples for laboratory analyses are particularly attractive. Making these decisions in a timely manner leads to more efficient and cost-effective exploration, mining and environmental practices. However, as pXRF devices use X-rays, operators need to have completed radiation safety training and certification, and safety regulations have to be adhered to. Moreover, elements with a low atomic number (Z), such as Li (lithium), cannot be analysed due to the technical limitations of the system (Lemière, 2018). Given the operational simplicity of portable instruments and their affordability in relation to bench-top laboratory analysers as well as their operational simplicity, portable instruments could become "the equipment of choice" for resource characterisation and environmental monitoring (Fig. 1.1). In this respect these portable units are able to meet the system-independence criterion, i. e. they can stand alone and do their job with few or no other supporting facilities or devices.

Figure 1.1: pLIBS analysis to determine the lithium content of a pegmatite. Unlike pXRF analysis, the sample can be held in the hand as no ionising radiation is used.

Another relatively new but very promising qualitative and quantitative field method is the portable laser induced breakdown spectroscopy (pLIBS). Meanwhile, pLIBS has proved to be capable of identifying solid materials, especially alloys. It has also been used for the geochemical analysis of geological materials with the detection of light elements such as Si (silicon), Li, K (potassium) and Be (beryllium), providing information for geochemical mapping and provenance analysis. The latest pLIBS analysers are not only capable of generating qualitative results within seconds but can also deliver quantitative results if a matrix fitting calibration is performed. Moreover, heat maps displaying changes in elemental concentrations can be created for small sample areas and, unlike pXRF systems, pLIBS can even analyse low-order elements. All in all, it appears that pLIBS analysers may offer real advantages over pXRF devices (Senesi et al., 2021). This review will outline equipment development, operating principles, safety aspects, legal requirements as well as transport regulations and will also discuss how pLIBS can be applied in the mineral resources sector.

1.4.2 Development of pLIBS Analysers

Laser-induced breakdown spectroscopy is a type of atomic emission spectroscopy that uses a highly energetic laser pulse as an excitation source. A plasma is formed by focussing the laser beam, which atomises and excites sample surfaces. The first scientific publication on LIBS appeared in the early 1960s, after the development of the laser (Baudelet and Smith, 2013). In 1981, laser pulses were amplified for the first time with the help of a focusing unit, so that a thermal plasma was formed by the excitation of the atoms. The acronym LIBS was introduced, which is still used today (Loree and Radziemski, 1981).
In 1996 a prototype of a pLIBS system was developed to detect metal contamination in soils and paints. Several components of the pLIBS system were integrated in a single case weighing 14.6 kg (Yamamoto et al., 1996):

Figure 1.2: Transport case and pLIBS system shown next to a geologist's hammer.

- Accumulator
- Detector
- Spectrograph
- Notebook for processing the data

The first pLIBS system (Porta-LIBS-2000) came on the market in the early 2000s. This unit contained a Nd:YAG laser that emitted laser pulses with a wavelength of 1,064 nm and could detect electromagnetic radiation in the wavelength range from 200 to 1,100 nm on a charge-coupled device (CCD) sensor. The 14.6 kg pLIBS system measured 18 * 33 * 46 cm and was no bigger than a briefcase (Pierce and Christian, 2006). Progressive technical advances and component miniaturisation of components led to the development of today's pLIBS analysers. In 2013 SciAps Inc. introduced the pLIBS model Z-500, which was followed by other systems from a range of manufacturers (Rai and Thakur, 2020) (Fig. 1.2).

1.4.3 Operating Principles of pLIBS Analysers

The schematic representation of the process flow of a LIBS system is shown in Fig. 1.3. A high-powered laser pulse is directed onto the sample's surface by a focusing unit. At the point of impact the sample heats up to several 10,000 °C until a thermal plasma is formed and a small volume of the sample begins to vaporise. The molecular bonds break, and the thermal plasma expands, resulting in atomisation and excitation

of the atoms. Thus, the electrons are at an elevated energy level and with the return to their initial state, background continuum radiation is emitted, which initially consists mainly of bremsstrahlung. In addition, light with characteristic wavelengths is also emitted. Both electromagnetic radiations are concentrated by means of converging lenses, detected by a fibre-optic sensor, and transmitted via an optical fibre to the spectrometer. The latter contains both a dispersive element and a detector. With the dispersive element, the wavelengths are broken down into their components and the radiation is then projected onto a detector, which outputs the spectral information as an electrical signal. The wavelength (abscissa) and spectral line intensity (ordinate) are plotted on a histogram. Finally, the chemical elements can be identified by the characteristic spectral lines in the spectrum, and mass concentrations can then be determined via the spectral line intensity (Rai and Thakur, 2020).

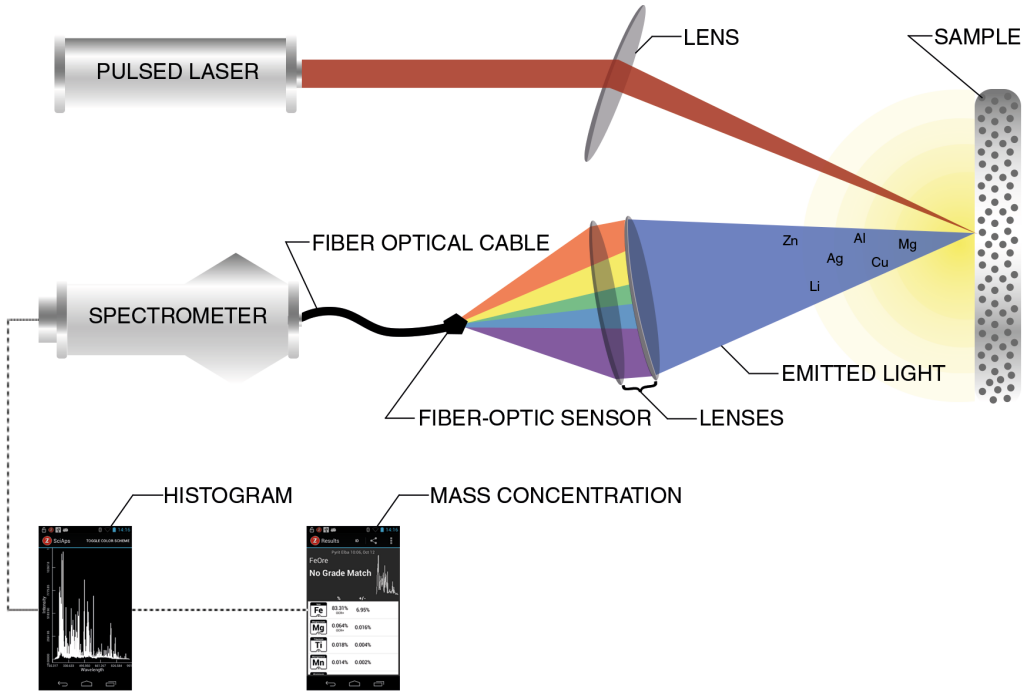

Figure 1.3: Schematic representation of the process flow of a LIBS system (Jarvikivi (2018), modified)

1.4.4 Comparison of pLIBS and pXRF Analysers

Fig. 1.4 shows two examples of pLIBS and pXRF devices. Both types of analysers are almost the same size with only minor differences in dimensions. Table 1.1 shows the most important advantages and drawbacks of pLIBS and pXRF in direct comparison to one another. The pLIBS has a base, into which the battery is inserted, making it easier to put the device down after use. For the pXRF analyser, the battery is inserted in the handle, which is used for the application of argon cartridges in the LIBS.Both devices are supplied with a wrist strap for safe use and also come equipped with touch screens. Measurements can be initiated either by pressing the trigger on the top of the handle or via the software using the touch screen or an external computer. Both instruments are ruggedised for use in the field and in tough operating environments. Analyses using the pXRF device are based on ionising radiation, whereas the LIBS analyser uses a pulsed laser beam. pXRF and pLIBS analyses are therefore non-destructive, with pLIBS measurements causing minute ablations of surface materials and leading to dark stains on sample surfaces after measurement.
These spots are barely visible to the naked eye. Several laser spots within a defined raster can be analysed when dealing with larger sample areas. Such a grid pattern can also be used to create a heat map of element distributions. Maintenance is only needed when it comes to cleaning the quartz window. An internal wavelength calibration is automatically performed by the device before the first measurement and when temperature changes occur.

Figure 1.4: Two commercially available portable analysers: On the left the pLIBS SciAps Z-300 (21.0 * 29.2 * 11.4 cm, 1.8 kg with battery) and on the right the pXRF Olympus Vanta C (24.2 * 28.9 * 8.3 cm, 1.7 kg with battery).

Table 1.1: Advantages and disadvantages of pLIBS and pXRF devices (Lemière, 2018; Senesi et al., 2021; Fu et al., 2018b).

pLIBS	**pXRF**
elements Z 1 - 92	elements $Z > 12$
almost non-destructive	(ablation of pg or ng) non-destructive
low acquisition costs compared to laboratory methods, but slightly higher acquisition costs than pXRF	comparatively low acquisition costs compared to laboratory methods
low maintenance and operating costs (Ar-cartridges, cleaning, quartz window)	low maintenance and operating costs (window, radiation safety training)
laser protection officer (LPO) not necessary; documented instruction reasonable	radiation safety officer (RSO) required (repetition of training every 5 years); yearly documented instruction of users by the RSO required
spot size < 3 mm possible	spot size < 3 mm not possible
sensitivity to surface contamination, but cleaning with laser shots possible	sensitivity to surface contamination, cleaning not possible with the device
bulk analysis, single grain analysis and 2D heat maps with elemental distribution and sub millimetre spatial resolution	only bulk analysis
analysis speed (< 1 s)	comparatively slow analysis, especially if different voltages are used
simultaneous capture of the full elemental composition	tube voltage and anode (Rh, Ag, W) determine elemental range and limit of detection
Ar-atmosphere for signal enhancement	no protective atmosphere
less material needed for analysis (pg to ng)	more material needed for analysis (typically sample cups, few g)

1.4.5 Safety Aspects, Legal Requirements and Transport Regulations for pLIBS Devices

The use of pLIBS instead of pXRF devices has the advantage that no ionising radiation is applied, which enormously simplifies transport and use. Yet, even when using optical radiation, especially in the near-infrared (NIR) range (1,064 nm), certain safety regulations must be observed.
NIR light is particularly dangerous because the body's own glare protection (corneal reflex) is only triggered by visible light. A person would therefore not notice exposure to NIR light. In addition, the pulsed laser is extremely focused and emits a high amount of energy to a very small spot. As NIR light is able to penetrate into the eye and through all skin layers, exposure to laser and NIR light can be very harmful. The SciAps Z-300 uses a Class 3B laser, which normally requires the designation of a responsible person. However, when used properly, the laser falls into Class 1, which can be used without restrictions. Nevertheless, users should be instructed and made aware of the dangers of laser exposure and must wear laser safety goggles. Special attention should also be paid to the possible reflection of laser light by polished and shiny surfaces.

pLIBS analysers are relatively light in weight and can be transported in small suitcases. In fact, there are hardly any restrictions regarding their transportation. When transporting by air it is only necessary to observe the relevant regulations applying to lithium-ion batteries and argon cartridges. For example, the batteries must be transported as hand luggage. While argon gas is neither flammable nor reactive, the argon cartridges may explode during a fire due to increased internal pressures. Therefore, these cartridges should not be exposed to high temperatures. When transporting pXRF instruments, it is necessary to register with the relevant authorities and, furthermore, a RSO has to travel with the device.

1.4.6 Convenience of pLIBS Devices

Even though pLIBS analysers are highly complex measuring devices, they are relatively user-friendly. Qualitative elemental analysis can be carried out within seconds and without any knowledge of the operating principles. In addition, rather large databases can be purchased for positive material identification, which makes the user's own calibration for these materials superfluous. Unlike the pXRF devices, sample preparation is usually not necessary. Errors due to inhomogeneities can be avoided by scanning the sample, and surface contaminants can be eliminated by cleaning with laser shots before taking measurements. In fact, scanning a sample with the device can be used not only to analyse the average chemical composition but also to display chemical information in 2D, through the generation of heat maps that display elemental distributions (Fig. 1.5).

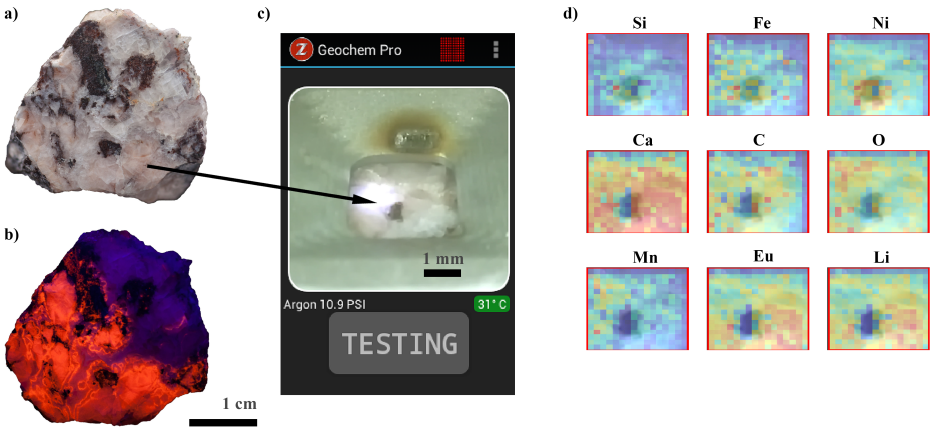

Figure 1.5: Element distribution maps: **a)** Section of a sample consisting mainly of calcite from Příbram, Czech Republic. **b)** The calcite shows strong fluorescence under short-wave UV light caused by Eu^{3+} and Mn^{2+}. **c)** In a 16 * 16 laser raster, the elemental distributions of a tiny section from the cut including an inclusion are analysed. **d)** The difference in the elemental composition of the inclusion and the calcite is clearly visible.

If sample cups are needed for the bulk chemical analysis of samples using pLIBS, then they should be prepared in a slightly different way than for pXRF analysis. The laser beam of the pLIBS would destroy the protective foil that is normally attached to the powdered sample material. Moreover, the pressure applied, when compressing the powder, should be much higher (more than 3 t/cm^2), so that dust generation is reduced and intensities are increased (Fabre et al., 2021). To compensate for wavelength shifts due to thermal expansion of the spectrometer, the stainless steel inside the unit is analysed as a reference material by default before first use. The positions of the emission lines are automatically corrected with the factory-stored calibration, and the user is prompted again, if a new calibration is required (Crocombe et al., 2021). Maintenance is generally only required in the form of regular cleaning of the front quartz window, as a small volume of the sample material can fuse with the focusing unit. The quartz window can be replaced if it is no longer suitable for cleaning.
Some background information is needed, however, when it comes to quantitative analysis. The background continuum reduces the accuracy of the measurements and the signal is initially superimposed by bremsstrahlung. Since the latter decays very quickly and the characteristic light lasts longer, it is recommended that the start of the detection phase is controlled (Cremers and Radziemski, 2013). The time span between the laser pulse and the switching-on of the detector is referred to as the gate delay (t_d). The SciAps Z-300 model allows this parameter to be controlled for each analysis. However, care should be taken to ensure that all measurements are done with the same acquisition settings. Fig. 1.6 shows how important this setting is: The overall intensities are higher without gating, but the background disturbs the evaluation so that the signal-to-noise ratio (SNR) is significantly higher with longer gate delay.

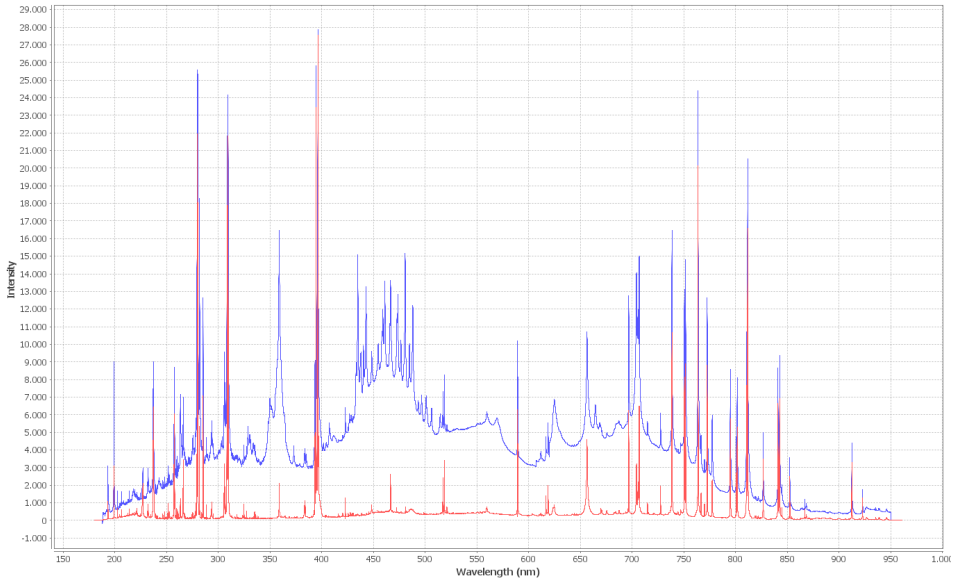

Figure 1.6: Importance of the acquisition setting *gate delay*. The spectrum of an aluminium foil was recorded once with gating (2000 ns, red spectrum) and once without gating (250 ns, blue spectrum, lowest possible gating).

The SciAps Z-300 uses small Ar-cartridges to create an atmosphere of inert gas, which prevents ignition and improves signal intensity. Quantitative analysis calls for calibration with standards of known concentration, and pLIBS analyses usually require matrix matching calibrations. This is based on the fact that the intensity of a spectral line is proportional to the concentration in the sample, provided no self-absorption takes place (Cremers and Radziemski, 2013). Many different calibration techniques have now been developed, but a detailed description of the calibration methods is beyond the scope of this article. Detailed information on the subject can be found in Fu et al. (2018b). Calibrations for the SciAps Z-300 are performed using the complementary Profile Builder software. Here the most suitable peaks for the elements of interest are identified and used to create an intensity ratio with internal standards. The intensity ratios are then used to create linear regressions for element quantification.

1.4.7 Applications of pLIBS in the Resources Sector

Field-portable LIBS devices are now being increasingly used in the mineral resources sector. Their fields of application can be assigned to four groups:

1. pLIBS devices are now most widely used for material identification, and especially for sorting scrap. Examples include the rapid sorting of Al alloys (Piorek, 2019) and the analysis of steel samples (Poggialini et al., 2020).

2. pLIBS analysers are increasingly used in geochemical characterisation studies, as there have been recent advances in equipment design and capabilities. Quantitative measurements have been performed to determine, for example:

    - F (fluorine) in tungsten ore (Foucaud et al., 2019)
    - The geochemistry of volcanic rocks (Yant et al., 2020)
    - The presence of Ti (titanium) inclusions in ferrous rocks (Connors et al., 2016)
    - Trace element abundances of Be, Cs (caesium), F, Rb (rubidium) in Li ore minerals (Fabre et al., 2021)
    - Classification of Cu (copper) ore minerals (Wójcik et al., 2020)
    - 25 minor and trace elements in 835 diverse geological samples (Ytsma et al., 2020)
    - rare earth elements (REE) in a uranium oxide matrix (Manard et al., 2018)

3. The development of additional functions such as sample scanning to generate 2D elemental distribution maps has produced a new range of applications for pLIBS. Such a new function has allowed chemical imaging of rock and mineral surfaces (Lawley et al., 2021).

4. Another novel field of application is the source tracing of gold samples and has provided a lowcost field-based tool for responsible mineral supply chain management. In this case, the Ag content in commercial Au alloys and native Au was used to determine the geographical origin of gold samples (Pochon et al., 2020).

Since pLIBS devices are designed for field applications, their greatest advantage is transportability to remote places and the generation of instant analytical data on site. Moreover, there is a clear advantage over pXRF systems, because transporting pXRF analysers is problematic due to radiation protection issues and the need for a RSO. Another benefit is that no comprehensive sample preparation is needed for pLIBS analysis. When very rapid results, high data density and/or high sample throughput are required, pLIBS analysers are even better suited than pXRF devices as each analysis is done within seconds. Furthermore, as the method is almost non-destructive, valuable samples or small amounts of sample materials can be analysed. However, if the sample is to be retained in an absolutely pristine condition, then the pXRF system should be used. On the other hand, if lighter elements ($Z < 13$) have to be analysed, especially Li, then pLIBS has to be applied. The capability of pLIBS to analyse lighter elements is one of the most important advantages of pLIBS over pXRF. This is particularly important for geological samples, as some of the most abundant elements on the Earth's crust are H (hydrogen) (Z = 1), Na (sodium) (Z = 11), and Mg (magnesium) (Z = 12). The same applies to the elements Al and Si, which are usually poorly quantified by pXRF. Moreover, analytical measurements for C (carbon) are possible with pLIBS, opening up many areas of application. In addition, the small spot size of the laser allows element distribution maps to be created by sample scanning, which is not possible with pXRF. In conclusion, pLIBS devices can be used as a fast, qualitative, on-site screening method when limited financial resources are available or instant results are needed. Quantitative pLIBS analyses require matrix fitting calibrations, which are slightly more time-consuming.

1.4.8 Conclusion and Outlook

Handheld LIBS devices are already used in numerous fields of the mineral resources sector. This trend will increase over the next few years as the method becomes better known and our understanding of its analytical capabilities and applications improves. The advantages of pLIBS over pXRF are already obvious and could result in pLIBS becoming at least as widespread as the already established pXRF technique. In future, further equipment developments and improvements need to address better detection limits, calibration techniques and data processing algorithms. Finally, there is an urgent need for pLIBS protocols that outline the best practices for the collection of chemical data on geological materials, similar to the best practice guidelines that already exist for pXRF analyses.

1.5 Laser-Induced Breakdown Spectroscopy Applied to Elemental Analysis of Aqueous Solutions – A Comprehensive Review

The content in this section was originally published in the *spectroscopy journal* with the title *"Laser-Induced Breakdown Spectroscopy Applied to Elemental Analysis of Aqueous Solutions – A Comprehensive Review"*. Key questions have been added and some minor typesetting and layout work have been done.
DOI: https://doi.org/10.3390/spectroscj2010001 (Schlatter and Lottermoser, 2024).

Authors: Nils Schlatter and Bernd G. Lottermoser

Received: 25 November 2023; **Revised:** 23 December 2023; **Accepted:** 15 January 2023; **Published:** 17 January 2024

Keywords: Laser-induced breakdown spectroscopy (LIBS); elemental analysis; aqueous solutions; trace elements; environmental analysis; detection limits; liquid sample preparation techniques, signal enhancement

Key questions:

- When was elemental analysis of aqueous solutions by LIBS introduced?
- Where is research being carried out on the subject of elemental analysis of aqueous solutions using LIBS?
- What are common challenges encountered during elemental analysis of aqueous solutions using LIBS?
- What methods for sample preparation exist to date and what is their share of use?
- Which types of aqueous solutions are analysed?
- Which types of devices are used?
- What are the most important acquisition settings?
- Which elements are usually investigated?
- What LIBS setups exist to enhance analyses?
- What sensitivity do different methods show for different elements?
- What could the future development in this field look like?

1.5.1 Introduction

The analysis of aqueous solutions for different elements is important for numerous reasons, such as environmental analysis (Hartzler et al., 2023), resource estimation (Zuber et al., 2020), hydrogeochemical research questions (Koch et al. 2005), process control in nuclear fuel reprocessing plants (Wachter and Cremers, 1987), industrial control (Kuwako et al., 2003; He et al., 2019; Nakanishi et al., 2021), food analysis (Bocková et al., 2018), and medical applications (St-Onge et al., 2004). Today, elemental analysis of aqueous solutions is typically performed in the laboratory using well-established methods such as ion-exchange chromatography (IC), atomic absorption spectroscopy (AAS), inductively coupled plasma atomic emission spectroscopy (ICP-AES), and inductively coupled plasma mass spectrometry (ICP-MS) (Bhatt et al., 2020a; Schlatter et al., 2023).
Another possible analytical technique that is capable of analysing aqueous solutions is LIBS. The atomic emission spectroscopy technique was developed shortly after the introduction of the first lasers in the 1960s (Baudelet and Smith, 2013). It involves a low-energy, pulsed laser focused on a sample by a lens. A small volume of the sample is vaporised in a plasma which is created by the high energy density at the surface and the emitted light is collected and sent to a spectrometer where it is dispersed. With the use of a detector the signals are recorded and digitised. The spectrum can be evaluated with a suitable software and the atoms, ions and simple molecules contained in the plasma can be determined qualitatively via the characteristic lines (Cremers and Radziemski, 2013). By using certified reference materials (CRMs), it is possible to establish a calibration that also quantifies the elements and molecules present.
The advantages of LIBS are typically minimal sample preparation, low instrumentation cost, rapid analysis, simultaneous detection of multiple elements, and the possibility of in situ analysis, real-time analysis, and remote analysis (Tang et al., 2021; Harun and Zainal, 2018b). In particular, the analysis of solids, including soils, geological samples, archaeological samples, metals, and alloys using pLIBS devices has developed enormously in the last few years (Senesi et al., 2021) and the applications are hardly limited. As a result, pLIBS has established itself as a powerful competitor and companion to pXRF in field analysis of solids, as it is theoretically capable of analysing the entire periodic table of elements (cf. Fig. 1.7) (Senesi et al., 2021; Harmon and Senesi, 2021). However, the analysis of aqueous solutions with LIBS, whether in the laboratory or in the field, has since played a rather niche role among potent and widely used analytical methods such as ICP-MS, ICP-AES, AAS, and IC (Schlatter et al., 2023). This may be due to the complicated interactions involved in the formation of plasma at the surface of the liquid (Bhatt et al., 2020a), or simply because the other methods have become so well-established that it has been difficult for LIBS to establish itself.
In the meantime, numerous sample preparation techniques and experimental setups that circumvent the problems mentioned, have been developed and presented in the literature (Harun and Zainal, 2018b; Keerthi et al., 2022). These enable detection limits for several elements that compete with the ICP-MS.

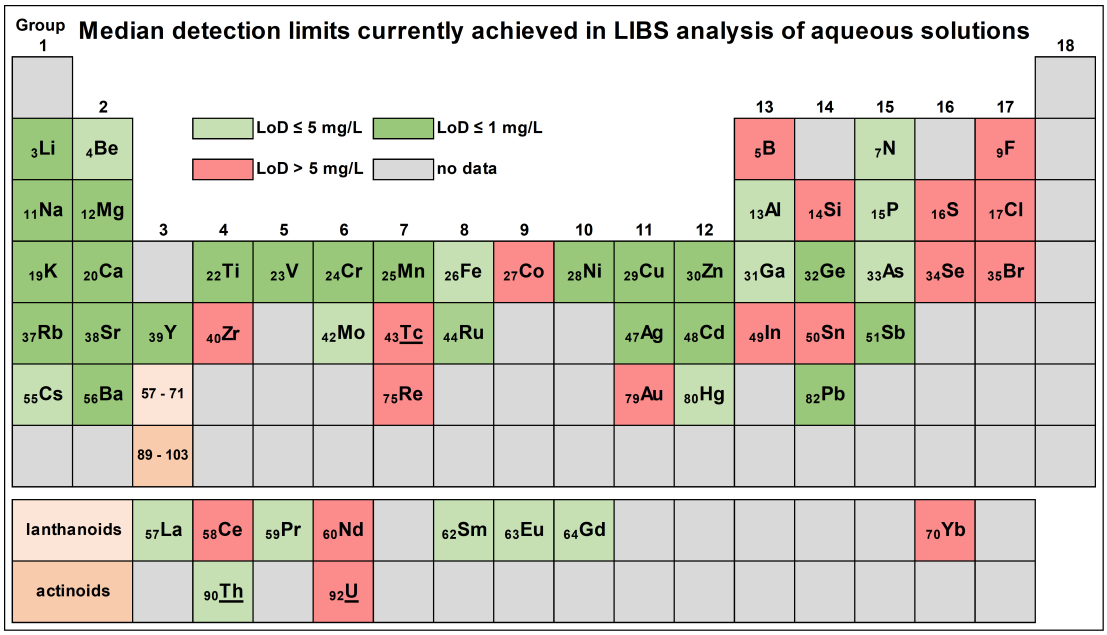

Figure 1.7: Graphical Abstract: Median detection limits currently achieved in LIBS analysis of aqueous solutions.

Figure 1.8 illustrates the constant increase in publications on the topic of aqueous solution analysis by LIBS since the first application in 1984 by Cremers et al. (1984). Harun and Zainal (2018b) already gave a comprehensive overview of different sample preparation techniques in liquid analysis. However, the diversity and variety of different instrument types, sample preparation techniques, LIBS experimental setups, and acquisition settings can be confusing to new users. This may hinder the more widespread use of LIBS in laboratories for aqueous analysis. Therefore, the main aim of this review is to provide a comprehensive overview of our existing knowledge on the analysis of elements dissolved in aqueous solutions using LIBS and to provide an initial guide for new LIBS users.
Firstly, historical and spatial aspects of research into elemental analysis in aqueous solutions using LIBS are discussed. Sample types and sample preparation techniques to overcome the physical issues are then elaborated on. It is highlighted which sample preparations have given surpassing results and which are not recommended. The focus is less on a comprehensive discussion of the various methods of sample preparation, but rather on which methods are more commonly used and give better results for a specific application. The different types of instruments and their main advantages and disadvantages are also presented. For signal enhancement, different experimental setups are used and their main advantages and disadvantages are discussed. In addition, the most important acquisition settings are presented, as they strongly influence the analysis results. The analysis of the frequency of the different acquisition settings and the different sample preparation techniques used may help scientists who want to use LIBS for their research to make an informed choice for a particular application.
Another aim of this work is to demonstrate the opportunities and limitations of LIBS analysis of elements dissolved in aqueous solutions and associated research gaps. Al-

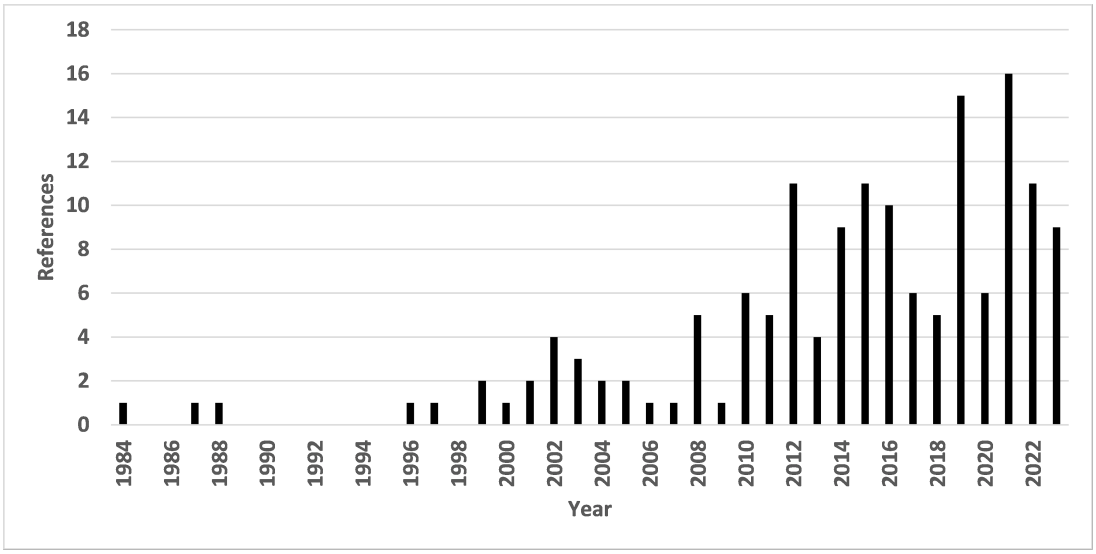

Figure 1.8: Number of references reporting one or more detection limits for the analysis of aqueous solutions by LIBS from 1984 to this date. Data based on the literature reviewed.

though in theory any element can be analysed by LIBS (Senesi et al., 2021), it turns out that some elements are less quantifiable than others. There is a large number of publications that provide detection limits for a wide variety of elements dissolved in aqueous solutions using LIBS. For example, the very early publication by Cremers et al. (1984) showed the possibility to analyse Li, Na, K, Rb, Cs, Be, Mg, Ca, B, and Al in aqueous solutions. Since then, numerous other elements have been successfully tested, their and detection limits documented, such as for PTEs like Cr and Pb (Ma et al., 2019) or lanthanides (Maity et al., 2022). The present work presents these detection limits explicitly for the analysis of aqueous solutions for as many elements as possible. The aim is to give a simple, accessible sense of which elements are commonly investigated, which are rarely studied and, more importantly, a sense of the sensitivity per element. The results of the literature review are among other things presented in this work in the form of an annotated periodic table (cf. Fig. 1.7), thus providing a quick overview of the analysis of aqueous solutions for a wide range of elements using LIBS. Moreover, the reviewed publications are briefly presented with the sample preparation techniques, sample types, LIBS experimental setups and acquisition settings used, as well as recommendations are given. Therefore, this review contributes to a better understanding of LIBS as a technique for the analysis of dissolved elements in aqueous solutions.

1.5.2 Methods

A comprehensive literature review was conducted using databases and search engines such as Scopus, PubMed, Google Scholar, GeoRef, Web of Science, ResearchGate, and

Bielefeld Academic Search Engine (BASE) with no annual limit on the search query. However, this review only documents research published until August 2023. Typical search items were:
element name, LIBS/LIPS, water analysis, quantitative analysis, environmental analysis, aqueous, aqueous solution, solution, surface-enhanced, hydride, hydride generation, water, aquatic, liquid, aerosol, metal ion, cation, and anion.
All references, and the references therein, covering the analysis of aqueous solutions using any form of LIBS were collected. Sample types within the references included the dilution series of stock solutions; aqueous artificial solutions such as industrial or waste waters; biological solutions such as blood, urine, or wine; natural solutions such as river water, rainwater, or groundwater; and natural saline solutions such as seawater or brine. The focus of the literature review was clearly based on the analysis of aqueous solutions with any form of LIBS, excluding other liquids like oils, liquid metals, melts, resins, emulsions, and colours. Also, colloidal or particulate analysis in liquids was excluded in the review. These exclusions were made to keep the matrix reasonably similar for comparison in terms of viscosity, density, and general composition, as there is a strong matrix dependence of LIBS analysis (Legnaioli et al., 2022).
The focus of this review was not to describe in meticulous detail every possible method of sample preparation technique used with LIBS, or every LIBS configuration, as such comprehensive reviews of sample preparation techniques can be found elsewhere (Harun and Zainal, 2018b; Keerthi et al., 2022).
Instead, it is intended to provide a guidance to scientists wishing to use LIBS for the first time in their research on aqueous solutions. It is therefore aimed to be a comprehensive collection of published literature on the subject of aqueous solution analysis. The purpose is to give an idea which elements typically work well with LIBS applied to aqueous solutions and which methods have achieved low limits of detection (LoDs).
All selected publications (from 1984 to 2023) were systematically investigated for the following settings and parameters:

- Element(s) investigated,
- LoD(s) achieved,
- Sampling method/ sample pre-treatment,
- Peculiarities in LIBS setup and beam geometry,
- Laser wavelength used,
- Pulse energy used,
- Year of publication,
- First author country of affiliation,
- Sample type.

This long period, in fact the entire timeframe since the beginning of water analysis using LIBS, was chosen to obtain a comprehensive database. To compare the performance of analytical methods quickly and easily, the LoD is commonly used (Poggialini et al., 2023b). This indicates the lowest concentration of a particular element that can be reliably determined. Typically, the LoD is determined by a calibration line that plots the measured signal as a function of analyte concentration for standards of known concentration (Poggialini et al., 2023b). The current attitude towards LIBS is often that the analyses are characterised by high detection limits (parts per million (ppm) to %) (Fabre, 2020; Poggialini et al., 2023b). This may often be sufficient for geochemical applications or material characterisation, but for the analysis of elements dissolved in water, the typical unit of analysis is mg/L or μg/L, equivalent to ppm or parts per billion (ppb), using the simplification where the density of water is 1 g/cm^3. However, the use of a special sample treatment can lead to a significant improvement in sensitivity and therefore in LoD.

By far the most commonly used calculation to determine the LoD in LIBS analysis is the 3σ-IUPAC criterion: the LoD is equal to three times the standard deviation of the background signal at the lowest solution concentration divided by the slope of the calibration line (Poggialini et al., 2023b). This formula is used although it is outdated and LIBS calibrations are associated with non-linearity due to self-absorption, leading to miscalculation of the LoD (Poggialini et al., 2023b). When the detection limits are compared independently of the method used, but for one type of instrument (LIBS), they should also give an indication of whether the elements are generally poorly or well analysed by the instrument compared to other elements. This should be true if enough detection limits are available. If certain elements have not been analysed or have only been analysed infrequently, this may, except in the case of a lack of interest, also indicate that there are difficulties in quantifying these elements with the measuring instrument. For ease of comparison, all LoDs reported in the literature reviewed were converted to mg/L. For further simplification, values documented in auxiliary measuring units such as ppm were recalculated to mg/L on a 1:1 basis.

To allow a quick assessment of whether an element is more or less quantifiable by LIBS in aqueous solutions, a periodic table of the elements based on the one by the National Center for Biotechnology Information was used to illustrate the detection limits achieved in literature (NCBI, 2024). The median of all LoDs found per element was used for comparison instead of the mean to compensate for outliers. To give an impression of the data quality, the number of LoDs used for calculation is printed below the median LoD. Several LoD values can come from one reference if different sample preparation techniques, different LIBS configurations, or different spectral lines were used. For an even faster impression, the background of the elements is coloured according to threshold values. These were defined as high analytical performance with a LoD of less than 1 mg/L, greater than 1 but less than 5 mg/L for medium analytical performance, and higher than 5 mg/L for low analytical performance.

A colour code has also been introduced for quicker assessment of data quality in the other figures evaluating the detection limits. Here, red bars indicate a value calculated from less than five LoDs. A dark green colour code indicates a more reliable database with more than five LoDs used for calculation.

All data collection and analyses were done in a spreadsheet, which is available as a

digital supplement. It also contains additional figures, such as a second periodic table using means rather than medians. The file is intended as a guide for researchers aiming to work with LIBS on aqueous solutions. A separate worksheet called "Inf" is provided for guidance through the document. All references reviewed and evaluated are documented in a worksheet called *"references"*, including their titles and digital object identifier (DOI), if available. Illustrations of different sample preparation techniques were created with artistic liberty using Photoshop CS6, based on the descriptions and figures in the literature reviewed.

1.5.3 Results

Historical Aspects

Over 153 publications on the subject of the analysis of aqueous solutions using LIBS were identified as having been published between 1984 and August 2023 and reporting at least one LoD for at least one element. Figure 1.8 shows the number of references for the analysis of aqueous solutions by LIBS from 1984 to date reporting at least one LoD for at least one element. It also shows a clear and constant increase in the number of publications, suggesting that research is continuing in this area.
The first usage of LIBS for the analysis of aqueous solutions probably dates back to 1984, when Cremers et al. (1984) analysed Li, Na, K, Rb, Cs, Be, Mg, Ca, B, and Al in aqueous solutions. They directed the pulsed laser directly into the liquid and monitored the spark light to receive a spectra. This early publication already showed a very low detection limit for the alkali elements (0.006 – 1.2 mg/L), but significantly higher ones for elements of the thirteenth group (20 – 80 mg/L) (Cremers et al., 1984). This trend seems to continue to this day. Also, Cremers et al. (1984) encountered the problem of direct liquid analysis with LIBS. When they focused the laser from the top, bubbles disturbed the analysis. Therefore, they modified to focus from the side or the bottom. However, the sample cell made of quartz did not resist for a long time due to the high pressure produced (Cremers et al., 1984). Since then, it has been shown in many publications that the direct bulk analysis of liquids is prone to several physical issues, such as splashing, liquid evaporation, and plasma cooling (Bhatt et al., 2020a), leading to low sensitivity and low precision (Zhang et al., 2021a). Therefore, many different sample preparation techniques have been adapted and developed to bypass these issues. For example, LSC (Schlatter et al., 2023), liquid-to-aerosol conversion (LAC) (Aras et al., 2012), and liquid jet (LJ) (Abu Kasim et al., 2022) can solve the problems by using a different sampling technique.
Looking at countries where research is being carried out on this topic, several research-intensive localities stand out. Figure 1.9 illustrates the number of references by country from 1985 to 2023 that report one or more LoD for the analysis of aqueous solutions by LIBS. For simplification, the country of the work affiliation of the first author in the literature reviewed was used for classification. Most of the research on the analysis of aqueous solutions has been done in China, followed by the United States of America, India, Spain, Germany, Canada, and Brazil. LIBS was first used as a liquid analysis

method in the USA in 1984 (Cremers et al., 1984). Based on the literature reviewed, outside the USA, the method was first applied and published in Germany in 1996 (Knopp et al., 1996). This was followed by publications in Italy in 1997 (Arca et al., 1997), France in 1999 (Fichet et al., 1999), and the Czech Republic in 2000 (Samek et al., 2000). In China, where most publications on the topic currently come from, LIBS was first used to analyse aqueous solutions in 2010 (Lu et al., 2010), based on the literature reviewed.

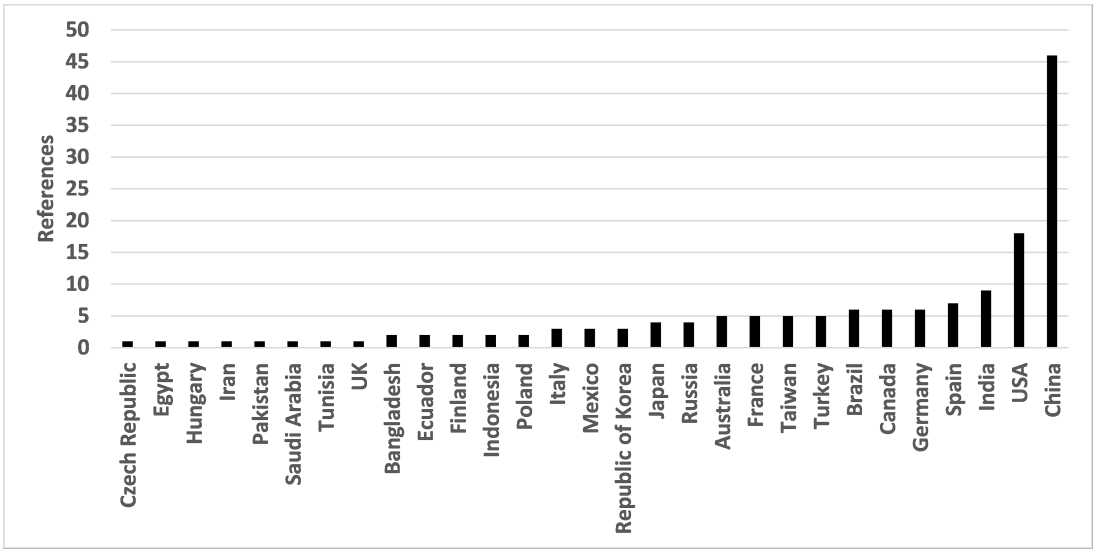

Figure 1.9: Number of references per country reporting one or more detection limits for the analysis of aqueous solutions by LIBS from 1984 to date. The affiliation of the first author is used for classification. Data based on the literature reviewed.

Types of Aqueous Solutions

As stated in the section describing the methods, some liquids have been excluded due to the strong matrix dependency of LIBS analysis (Legnaioli et al., 2022). The focus is therefore solely on elemental analysis in aqueous solutions. However, the sample types are still quite diverse due to the different applications in literature. Table 1.2 shows five classes of sample types, which were used for a proof of concept in the literature reviewed. For each class, examples are given and the elements analysed per class are indicated. In most cases, only dilution series of stock solutions were used, both for calibration and for proof of the developed method, even though the final application would be classed differently. Quite a few references applied their developed calibration to artificial, biological, natural, or natural saline water. Therefore, the list of elements for the stock solution is the most comprehensive one.

Table 1.2: Sample types used in the literature reviewed for calibration and verification, and elements analysed therein. Data based on the literature reviewed.

Sample type	Example	Elements analysed
Stock solution (ss)	Prepared solutions	Li, Be, B, N, F, Na, Mg, Al, Si, P, S, Cl, K, Ca, Ti, V, Cr, Mn, Fe, Co, Ni, Cu, Zn, Ga, Ge, As, Se, Br, Rb, Sr, Y, Zr, Mo, Tc, Ru, Ag, Cd, In, Sn, Sb, Cs, Ba, La, Ce, Pr, Nd, Sm, Eu, Gd, Yb, Re, Au, Hg, Pb, Th, U
Artificial (art)	Industrial or waste waters	P, Cr, Ni, Cu, Zn, Ge, Cd, Au, Pb
Biological (biol)	Blood, urine, wine	Ti, Fe, Cu, Sr, Ag, Cs, Pb
Natural (nat)	River water, ground water, rainwater	Li, B, N, Na, Mg, Al, P, S, Cl, K, Ca, Cr, Mn, Ni, Cu, Zn, As, Sr, Ag, Cd, Sn, Sb, Ba, Hg, Pb
Natural saline (nat sal)	Seawater, brine	Li, Na, Mg, K, Ca, Mn, Cu, Sr

Sample Preparation Techniques

As indicated in the introduction, direct analysis of the liquid surface is prone to low sensitivity and repeatability (Zhang et al., 2021a). This is due to effects such as evaporation, splashing and cooling of the plasma leading to energy losses and signal intensity (Bhatt et al., 2020a). Therefore, many different sample preparation techniques have been developed or adapted for LIBS liquid analysis. Some use conversion processes to preconcentrate the analytes for higher sensitivity, others only to circumvent the physical issues. An overview of the most typical preparation techniques reported in the literature reviewed is given in Table 1.3. For illustration purposes and easier understanding, these are also shown schematically in Figure 1.10. Column 3 is the link between the table and the figure, as it contains the connecting letters. Four main categories can be identified according to the aggregate state of the sample material: 1) liquid bulk (LB), 2) liquid-to-solid conversion (LSC), 3) liquid-to-aerosol conversion (LAC), and 4) hydride generation (HG) (cf. Table 1.3). The two main categories, LB and LSC, can be divided into several sub-categories (second column).

Table 1.3: Categories of the most typical sample preparation techniques used in LIBS analysis of aqueous solutions.

Category	Sub-category	cf.	Exemplary reference
Liquid bulk (LB)	Surface	a	Golik et al. (2015); Tolstonogova et al. (2021)
	Inside	b	Goueguel et al. (2015)
	Soaked on FP	c	Xiu et al. (2014)
	ID	d	Meneses-Nava et al. (2021); Cahoon and Almirall (2012)
	LJ capillary	e	Zhang et al. (2018)
	LJ	f	Nakanishi et al. (2021); Abu Kasim et al. (2022)
Liquid-to-solid conversion (LSC)	n-SE	g	Vander Wal et al. (1999); Sarkar et al. (2008)
	SE	h	Matsumoto et al. (2021); Schlatter and Lottermoser (2023)
	FP	i	Yang et al. (2018); Skrzeczanowski and Długaszek (2022)
	IE	j	Kim et al. (2010); Schmidt and Goode (2002)
	Ad/Ab	k	Chen et al. (2010); Ruiz et al. (2019)
	Che/Com	l	Tian et al. (2019); Zheng et al. (2021)
	MeGe	m	Lin et al. (2016)
	NP	n	De Giacomo et al. (2016); Wu et al. (2021)
	ESD	o	Huang et al. (2007); Ripoll and Hidalgo (2019)
	ED	p	Chen et al. (2008); Kurniawan et al. (2015)
	Ice	q	Harun and Zainal (2018a); Sobral et al. (2012)
Liquid-to-aerosol conversion (LAC)		r	Aras et al. (2012); Williams and Phongikaroon (2016)
Hydride generation (HG)		s	Ünal and Yalçın (2010); Ezer et al. (2019)

Abbreviations: FP = filter paper; ID = isolated droplet; LJ = liquid jet; n-SE = non-surface-enhanced; SE = surface-enhanced; IE = ion exchange; Ad/Ab = adsorption/ absorption; Che/Com = chelating/ complexation; MeGe = membrane generation; NP = nanoparticle enhanced; ESD = electrospray deposition; ED = electrical deposition. Letters a - s in the third column are also shown in Figure 1.10 for ease of comparison.

Extensive reviews with detailed descriptions of different LIBS setups and sample preparation techniques can be found in the literature (Harun and Zainal, 2018b; Keerthi et al., 2022), and exemplary references are given for every category and subcategory (cf. Table 1.3). Therefore, this section provides only concise descriptions, divided into four categories:

1) LB

Surface analysis (a) can be performed by focusing the laser directly on the liquid surface (Golik et al., 2015; Tolstonogova et al., 2021). To avoid splashing, the laser can also be focused inside the liquid (b) (Hartzler et al., 2023; Goueguel et al., 2014), or on soaked filter paper (c) (Xiu et al., 2014). Also, the analysis of low-volume isolated droplets can reduce splashing (d) (Meneses-Nava et al., 2021; Cahoon and Almirall, 2012). Furthermore, a liquid jet (LJ) can also be used to reduce splashing, either in a steel capillary (e) (Zhang et al., 2018) or directly on the jet (f) (Nakanishi et al., 2021; Abu Kasim et al., 2022). Here, the laser is focused on the LJ produced by a peristaltic pump (Zhang et al., 2018).

2) LSC
An alternative method is to analyse the evaporation residue (EvR) of a droplet on a substrate (g) (Vander Wal et al., 1999; Sarkar et al., 2010), which should be hydrophobic to compensate for an inhomogeneous distribution. Metallic substrates are commonly used for surface-enhanced (SE) analysis (h) and are prepared for homogeneous droplet distribution by geometric constraints (Matsumoto et al., 2021) or made hydrophobic (Schlatter and Lottermoser, 2023). Filter-paper-supported analysis utilises the technique of evenly distributing the liquid using the filter paper (i) (Yang et al., 2018; Skrzeczanowski and Długaszek, 2022). Either the dried filter paper or the evaporation residue (EvR) beneath it is subsequently analysed. Also, an ion-exchange (IE) membrane can be utilised to preconcentrate the analyte (j) by either placing the membrane in the solution or filtering the solution through it (Kim et al., 2010; Schmidt and Goode, 2002). The membrane is then dried and analysed. Moreover, the analyte can be evenly distributed on a surface through absorption by a substrate, such as wood (Chen et al., 2010), or adsorption by an adsorbent, such as activated carbon (Ruiz et al., 2019), which is then analysed (k). By using a chelating resin (Tian et al., 2019; Zheng et al., 2021) or complexation agent, the analyte can be preconcentrated in a solid form (l). Another option is to produce a membrane by mixing the sample solution with polyvinyl alcohol (m) (Lin et al., 2016). In nanoparticle-enhanced (NP) LSC (De Giacomo et al., 2016; Wu et al., 2021), typically, microdroplets are dried and the particles act as an adsorbent for the analyte, cause field enhancement in the plasma, and increase the number of particles in the plasma (n) (De Giacomo et al., 2016). The electrospray deposition (ESD) (Huang et al., 2007; Ripoll and Hidalgo, 2019) involves spraying a small amount of sample solution onto a heated metallic substrate using a metallic needle with a high voltage between them (o). The resulting dried residue is then analysed (Ripoll and Hidalgo, 2019). For electrical deposition (ED), metallic plates are placed in the sample solution, and a voltage is applied between the cathode and anode. After a few minutes of deposition, the cathode is removed and analysed (p) (Chen et al., 2008; Kurniawan et al., 2015). A straightforward method of LSC is freezing the liquid and analysing the surface of the resulting ice (q) (Harun and Zainal, 2018a; Sobral et al., 2012).
3) LAC
For a LAC generation, a nebuliser is used and the aerosol is focused and analysed (r) (Aras et al., 2012; Williams and Phongikaroon, 2016).
4) HG
To generate hydrides of certain elements, a complex system is required. This system includes a peristaltic pump, a gas-liquid separator, a flow meter, a membrane drying unit, a plasma cell, and chemicals such as acids, reductants, and a carrier gas (Ünal and Yalçın, 2010; Ezer et al., 2019). The resulting hydrides can be analysed in a plasma cell (Ünal and Yalçın, 2010; Ezer et al., 2019).
In order to obtain an overview of the relative frequencies of different sample preparation methods, all LoDs documented in the literature reviewed were classified according to the method used to achieve them. The results are shown in Figure 1.11. Most commonly (50%), the sample was first transferred from the liquid to the solid phase to avoid the physical issues of direct LIBS analysis of aqueous samples (cf. Figure 1.11a).

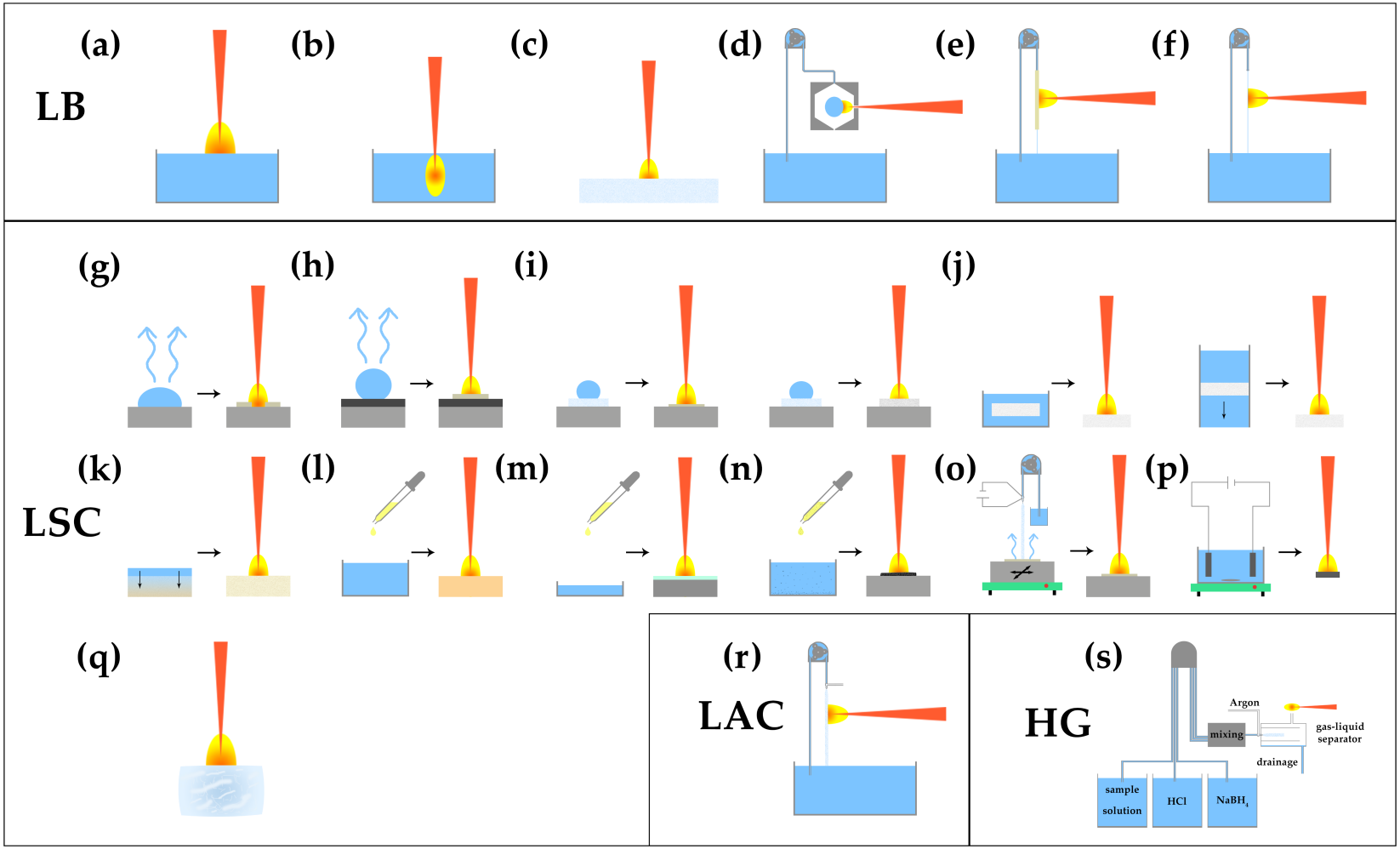

Figure 1.10: Illustration of the most typical sample preparation techniques used in LIBS analysis of aqueous solutions. First row: **Liquid bulk (LB):** a) surface; b) inside; c) soaked on filter paper; d) isolated droplet (ID); e) liquid jet (LJ) capillary; f) LJ. Second to fourth rows: **Liquid-to-solid conversion (LSC):** g) non-surface-enhanced (n-SE) evaporation residue (EvR); h) surface-enhanced (SE) EvR; i) filter paper supported EvR – left: analysing the EvR, right: analysing the dried filter paper; j) ion exchange (IE)- left: immersion in solution, right: flowing through a medium, k) adsorption/ absorption (Ad/Ab); l) chelating/complexation (Che/Com); m) membrane generation (MeGe); n) nanoparticle enhanced (NP); o) electrospray deposition (ESD); p) electrical deposition (ED); q) ice;. Fourth row: r) **Liquid-to-aerosol conversion (LAC)**; s) **Hydride generation (HG)**.

This was followed by an analysis in the liquid phase, with a share of 37%. Conversion to an aerosol with a nebuliser is less common, at 12%. Hydride generation is the least used, but it should be noted that this method is only applicable for certain elements (e.g. As, Sn, Sb, Se, Ge, Pb, Bi, Te) (Ünal and Yalçın, 2010; Bölek et al., 2018). Further classification into subcategories demonstrates that the scientific approaches used by individuals are highly variable (see Figure 1.11b & 1.11c).
Liquid bulk (LB) is dominated by the liquid jet (LJ) method (37%), which does not pre-concentrate the sample solution but avoids splashing (cf. Figure 1.11b). The second most common subcategory (30%) is an analysis directly on the surface of the liquid, which causes the greatest quantification problems. When analysing inside the liquid (15%), there are slightly fewer physical phenomena that negatively affect the analysis compared to a surface analysis (Cremers et al., 1984). Soaking up in filter paper can already lead to a slight pre-concentration (Xiu et al., 2014), but this is less common, at 10%. Analysis of an isolated droplet is probably the most complicated experimental setup within the liquid bulk category and, at 7%, is represented rather rarely.
A special form of the liquid jet is the liquid jet capillary, which was used only very rarely at 1%. LSC is dominated by SE (22%) and non-surface-enhanced (n-SE) (20%) preparation techniques (cf. Figure 1.11c). Both do not only convert the aggregate state, but also pre-concentrate the sample by evaporation (Aguirre et al., 2013). Therefore, higher sensitivity and lower LoDs are possible with these methods (Aguirre et al., 2013). Ad/ab is slightly less common (18%), which also pre-concentrates the sample, followed by filter paper support (FP) (9%). Chelating/ complexation (Che/Com), electrospray deposition (ESD), and ion exchange (IE) all have a share of 6%. Electrical deposition (ED) accounts for 5%, and the remaining methods, such as transfer to ice, account for 8%.

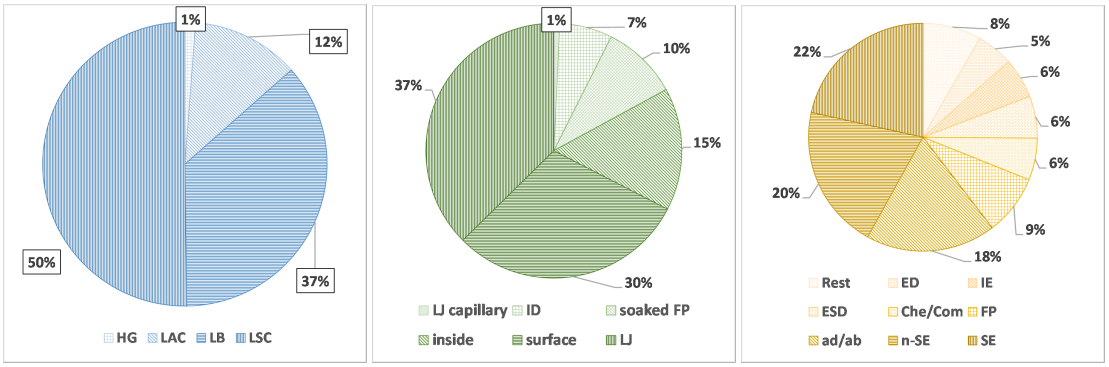

(a) **(b)** **(c)**

Figure 1.11: Percentages of methods used: **a)** Percentages for the main categories. HG = hydride generation, LAC = liquid-to-aerosol conversion, LB = liquid bulk, LSC = liquid-to-solid conversion. **b)** & **c)** Percentages for subcategories for the two most common methods used: **b)** LB, **c)** LSC. LJ = liquid jet, ID = isolated droplet, FP = filter paper, LJ = liquid jet, ED = electrical deposition, IE = ion exchange, ESD = electrospray deposition, Che/Com = chelating/ complexation, ad/ab = adsorption/ absorption, n-SE = non-surface-enhanced, SE = surface-enhanced. Data based on the literature reviewed.

Instrument Types, Experimental Setups and Acquisition Settings

The variety of different lasers, laser manufacturers, and LIBS manufacturers as well as their diverse applications have led to the fact that there is no uniformity in any of the possible settings, nor in the experimental setup. As a result, there may be confusion about which types of LIBS devices, experimental setups, and acquisition settings exist. The following three tables provide a brief overview of some of the different instrument types, experimental setups and acquisition settings (cf. Table 1.4 - 1.6). Both, Table 1.4 and 1.5, provide a short description as well as information on the main advantages and disadvantages of the instrument type or the LIBS setup. For further details, please refer to the listed literature. Table 1.6 provides an overview of the acquisition settings that influence LIBS analysis the most. The brief descriptions are intended to give a sense of the parameters that influence the analyses. More comprehensive information is found in the listed literature.

Table 1.4: Overview of different LIBS instruments used for the elemental analysis of aqueous solutions.

Instrument type	Description	Advantages	Disadvantages	References
Laboratory-based	Laboratory analysis	Sensitive, multi-element detection	Usually inflexible, trained staff needed, expensive	Shao et al. (2023)
Online	Continuous online analysis	On-site, continuous, real-time, multi-element detection	Needs own power supply, large	Sui et al. (2021)
Telescopic	Remote analysis by a telescopic system	Safe, remote, on-site, multi-element detection	Not useful/ necessary for every application	Samek et al. (2000)
Portable/ handheld	In situ analysis possible	Low-cost, on-site, real-time, multi-element detection	Only low energies, less sensitive	Schlatter and Lottermoser (2023)

Table 1.5: Overview of different experimental setups for signal enhancement in elemental analysis of aqueous solutions.

LIBS setup	Description	Advantages	Disadvantages	References
Double-pulse (DP) instead of single-pulse (SP)	First pulse ablates and generates plasma; second pulse reheats or selectively excites the plume	Higher sensitivity, fast and easy sample preparation, remote and in situ utilisation possible, no tuning of the laser wavelength, simultaneous multi-element detection	Not as sensitive as LIBS-LIF or RE-LIBS	Rifai et al. (2012, 2013)
Laser-induced fluorescence (LIF)	First pulse ablates and generates plasma, Second pulse is tuned to specific analytes	Higher sensitivity due to resonant excitation and background-free signal detection, no spectral interference	No simultaneous multi-element detection, tuneable laser and experienced staff needed	Kang et al. (2017); Wang et al. (2019)
Resonance-enhanced (RE)	First pulse ablates and generates plasma; Second pulse is resonant with the major species line	Higher sensitivity, simultaneous multi-element detection, low sample consumption	Tuneable laser and experienced staff needed	Rifai et al. (2013)
Resonant (R)	One laser source is tuned to specific resonant transition	Simpler experimental setup compared to LIF and RE, higher sensitivity compared to SP, simultaneously multi-element detection	Tuneable laser and experienced staff needed	Liu et al. (2021); Rifai et al. (2013)
Microwave enhancement (MW)	Enhancement by extended plasma lifetime through mobilised free electrons and ions	Higher sensitivity for a specific element	Complicated setup, requires a microwave system, no simultaneously multi-element detection	Abu Kasim et al. (2022)

Table 1.6: Overview of the acquisition settings that most influence the LIBS analysis.

Acquisition settings	Unit	Short description	Reference
Repetition rate	Hz	An increased repetition rate allows faster analysis and greater averaging for a better SNR and influences the energy delivered	Cremers and Radziemski (2013)
Pulse energy	mJ	Higher energy results in more and faster ablation	Singh and Thakur (2020)
Pulse duration	ns	ns/ ps/ fs pulses possible; influences the results due to effects such as plasma shielding	Musazzi and Perini (2014)
Gate delay	ns	Gating can improve the results due to less continuum radiation and therefore better SNR with longer delays	Cremers and Radziemski (2013)
Atmosphere	-	Influences the results: Ar $>$ air $>$ He in terms of intensity, plasma temperature, and electron density; He leads to better SNR	Scott et al. (2014)
Wavelength	nm	More energy is delivered at shorter wavelengths to break bonds and ionise	Singh and Thakur (2020)

The most important acquisition settings of the laser are probably the wavelength, the pulse energy, the irradiation intensity (focused pulse power density), and the spatial beam quality (Cremers and Radziemski, 2013). The latter can hardly be compared, based on the presented data in publications. The irradiation intensity is determined by the pulse duration in combination with the pulse energy and the repetition rate. As it is only rarely stated, no comparison was made for the reviewed literature. The wavelengths and pulse energies used are compared below.

In Figure 1.12, the frequencies of different wavelengths used in the literature on aqueous analysis by LIBS is shown. It is clear that the most commonly used laser wavelength is the fundamental 1064 nm one for a Nd:YAG laser, followed by the second harmonic 532 nm. Other wavelengths like 266, 352, 500, and 800 nm are less typical and no reference has used the fifth harmonic. Few references were found using lasers other than Nd:YAG. For example, a Ti:Saphphire laser used an 800 nm wavelength for femtosecond analysis (Golik et al., 2012; Tolstonogova et al., 2021), whereas a pumped dye laser used 500 nm (Knopp et al., 1996).

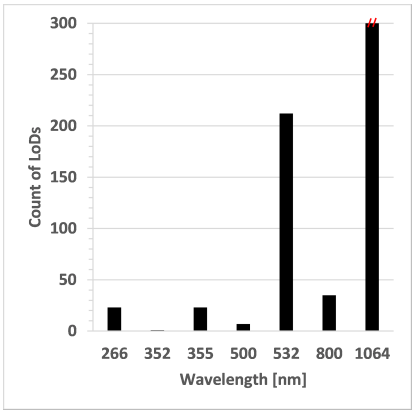

Figure 1.12: Frequencies of different wavelengths used in the literature on aqueous analysis by LIBS. The wavelength is counted more than once per citation if different settings were used, resulting in different LoDs. The data for 1064 nm have been partially hidden for the sake of clarity (N = 435).

The use of pulse energy depends on the instrument type, as different lasers are used within portable, telescopic, standoff, and online instruments. The pulse energy cannot always be changed directly by the user. However, it can be changed indirectly via the frequency or the wavelength. Due to the different LIBS instruments used, as well as the different applications and the possibility of adjusting the pulse energy, a wide range of different pulse energies has been applied as documented by the literature. These range from a fraction of a mJ to several hundred mJ. The highest pulse energy found in the literature reviewed was 800 mJ. However, such high pulse energies are less frequently used, and certain clusters are noticeable with significantly lower energies. Figure 1.13 shows the pulse energies classified in steps of 10 mJ up to 250 mJ. Energies above 250 mJ are rather unusual, and only 12 LoDs were reported for these energies. By comparison, 635 examples could be identified for energies lower than 250 mJ. The pulse energy of 100 mJ was found particularly frequently (74 times), and within the range below 70 mJ many different pulse energies were used. However, the range 0.1 - 9.9 mJ was used more (99 times) than the range 100 - 109.9 mJ (74 times).

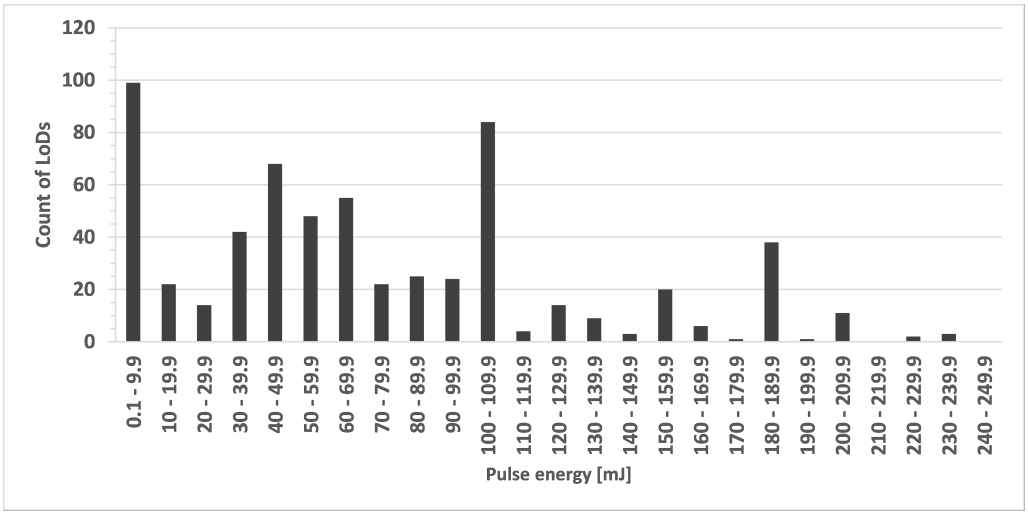

Figure 1.13: Classified frequencies of different pulse energies within the range 0.1 – 250 mJ (intervals of ten 0.1 mJ steps) used in the literature on aqueous analysis by LIBS. The pulse energy is counted more than once per citation if different settings were used, resulting in different LoDs. Pulse energies above 250 mJ and up to 800 mJ are omitted for clarity.

Calibration Techniques and Spectral Treatment (Chemometrics)

Different calibration techniques are not discussed in detail in this review but can be found in literature (Andrade et al., 2008; Mermet, 2010; Cong et al., 2013; Fu et al., 2018b; Babos et al., 2018; Donati and Amais, 2019; Costa et al., 2021; Poggialini et al., 2023a). Spectral processing and data handling are similarly covered in detail elsewhere (Aberkane et al., 2022; Palleschi, 2022b; Wang et al., 2021). Both calibration techniques and spectral treatment have an influence on the LoD achieved, but it is impossible to evaluate the influence as the calibration and spectral treatment methods used cannot be compared between different references on the basis of the information given in the publications.

Self-Absorption and Self-Reversal Correction

Self-absorption takes place when some of the emitted radiation is re-absorbed before it exits the source. As a result, this re-absorbed radiation eventually reaches the detector (Palleschi, 2022b). In quantitative LIBS analysis, self-absorption is usually manifested by broadened spectral lines within the spectra and by non-linear calibration lines in calibration. Higher concentrations of the analyte no longer result in a proportionally higher intensity (Palleschi, 2022b). This makes calibration difficult, especially for large concentration ranges. Various methods have been developed to reduce the effect of self-absorption. However, the effects of different methods cannot be compared based

on the reviewed data. Here, reference should be made to the extensive literature concerning self-absorption (Yi et al., 2016; de Oliveira Borges et al., 2018; Tang et al., 2019; Hou et al., 2019; Rezaei et al., 2020; Palleschi, 2022b).
Self-reversal can arise independently of self-absorption when there are spatial gradients in plasma temperature and electron density, which typically occur at the edge of the plasma. This effect appears as a confined dip at the top of the emission line (Palleschi, 2022b), which looks like two very close and not individually resolved peaks.

Elements Analysed by LIBS in Aqueous Solutions

Based on the literature reviewed, 56 different elements have been analysed in aqueous solutions using LIBS. Of these, three elements are radioactive (Tc, Th, U) and thus at least 53 out of 80 stable elements (66.3%) have been analysed with LIBS in water to this date. Most LoDs were reported for Cr (N = 87) and Pb (N = 76), followed by Cu (N = 49) and Cd (N = 43) (cf. Figure 1.14). For 30 elements five or more LoDs were identified (cf. Figure 1.14, marked in dark green). None of the noble gases, nor H, C, O, or Sc have been analysed to date. Furthermore, some elements of the fifth period (Nb, Rh, Pd, Te, I) and several of the sixth period (Tb, Dy, Ho, Er, Tm, Lu, Hf, Ta, W, Os, Ir, Pt, Tl, (Bi)) have not yet been analysed.

Detection Limits Achieved

In Figure 1.14, the elements are highlighted, depending on whether more or less than five LoDs were found and therefore included in the evaluation. The same colour code has been used in Figure 1.15, which shows the median LoD values for all elements. Dark red bars thus indicate that the median is less reliable than with green bars, as only very few studies down to one detection limit were included in the calculation. It can be seen that by far the lowest LoD median was obtained for Ag. This is followed by V, for which only two detection limits could be used for calculation. Ni, Cu, Li, and Cr also show very low median LoDs with good sample sizes. The worst median LoDs were obtained for F, Tc, U, In, Cl, Yb, and Br, in ascending median order.

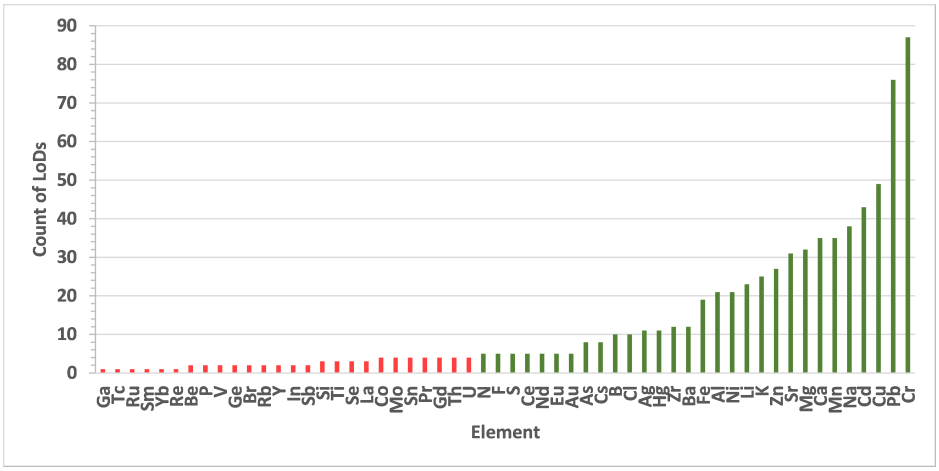

Figure 1.14: Number of detection limits (LoDs) per element in LIBS analysis of aqueous solutions per year. Red: less than five LoDs found; dark green: five or more LoDs found. Data based on the literature reviewed.

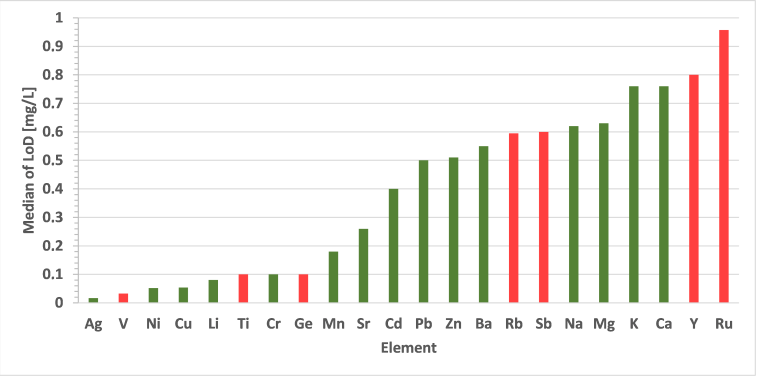

(a)

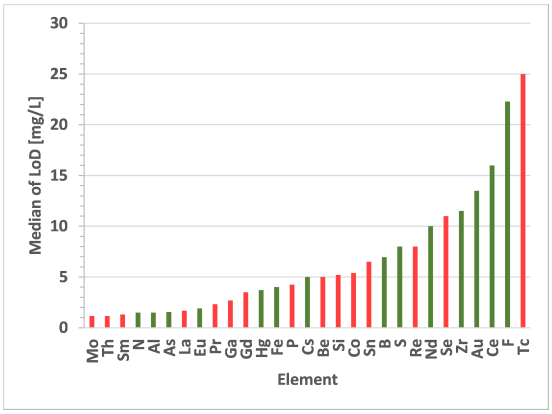

(b)

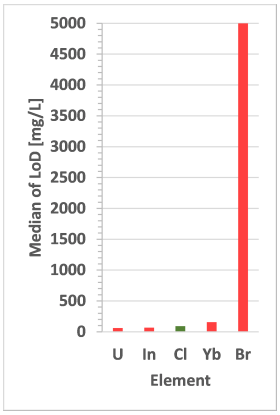

(c)

Figure 1.15: Median of LoD per element in LIBS analysis of aqueous solutions. **a)** Median < 1 mg/L; **b)** Median < 30 mg/L; **c)** Median > 30 mg/L. Red: less than five LoDs included for calculation; dark green: more than five LoDs included for calculation. Data based on the literature reviewed.

Figure 1.16 compares the LoDs obtained using different categories of sample preparation for the two elements with the most comprehensive datasets: Cr and Pb. Here, both elements show significantly lower LoDs for LSC than for LAC or LB for most of the reported LoDs. As HG was only used for Pb and only once, it is difficult to classify it among the other methods. For Pb, there may be a clear order with LAC giving the highest LoD, LB an intermediate LoD, and LSC the lowest LoD. However, there are only five LoDs for LAC, and for Cr LB is worse than LAC.

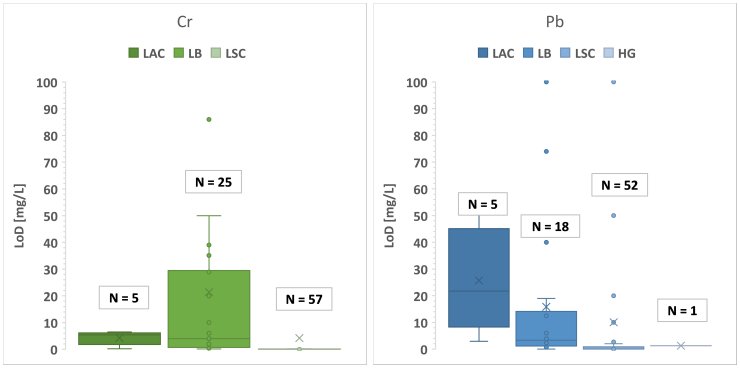

(a) **(b)**

Figure 1.16: Comparison of detection limits (LoDs) achieved in the reviewed literature between different categories of sample preparation: **a)** Cr, **b)** Pb. Two values have been faded out for Cr (LB 200 mg/L and LSC 230 mg/L) and one for Pb (LSC 200 mg/L) for the sake of clarity. Data based on the literature reviewed.

Figures 1.17-1.20 show the range of LoDs using boxplots for the 56 different elements for which detection limits have been found (excluding the transition metals). In general, both the first- and the second-group elements show a medium to high analytical performance according to the classification scheme. In Figure 1.17, some trends are visible: by far, Li shows the lowest LoDs within the alkali and alkaline earth elements, with outliers below 2 mg/L, and therefore is the most sensitive element within the two groups. For Na, the analysis is less sensitive, and K seems to be problematic to analyse. Cs and Be have the highest LoDs within the first and second main groups, but also, together with Rb, the lowest data quality (N = 2 – 8). With the exception of Be, the detection limits for the alkaline earth elements are relatively similar to each other, while the analysis for Sr is somewhat more sensitive.
For group 13 and 14 elements, LIBS analysis in aqueous solutions generally appears to be less sensitive (cf. Figure 1.18). Low to high analytical performance can be observed for elements from Group 13 and Group 14. Ga, In, Si, Ge, and Sn are rarely analysed and less than five LoDs have been found. It is therefore not possible to make any reliable statements other than a trend. B and Al are more frequently analysed. For Al an indifferent analytical performance is observed, with outliers up to 43 mg/L. B shows an outlier of 1200 mg/L, but the same reference also achieved an LoDs of 80 mg/L by using two laser pulses instead of a single one (Cremers et al., 1984). Pb may be an exception in both groups, but was also analysed particularly frequently (N = 76)

and the LoDs resulted to be very scattered. The highest LoD was 200 mg/L, however, most LoDs were below 15 mg/L and the median LoD was 0.5 mg/L. Therefore, high analytical performance can be reported for the analysis of Pb.
In general, elements of Group 15 (Pnictogens) seem to be have been analysed at greater sensitivity than those from Group 13 (Triels) or Group 14 (Tetrels) (cf. Figure 1.19a). However, they are rarely analysed, and no reliable statement can therefore be made for P or Sb. N was analysed only five times, with two very high LoDs (107 and 542 mg/L) but also with three LoDs below 2 mg/L. For As, the highest LoD was 8 mg/L and the median was 1.55 mg/L. In lanthanide analysis, a very different analytical performance can be observed (cf. Figure 1.19b). La, Pr, Nd, and Sm were generally analysed with low LoDs and Ce, Eu, Gd, and Yb with high LoDs. However, only a few references are available for all lanthanides. For La, Pr, Sm, Gd, and Yb, less than five LoDs were found. Unsurprisingly, within the actinides, only Th and U were analysed (cf. Figure 1.19c). Unfortunately, less than five LoDs were found for both, and all LoDs for Th were found in one reference only. However, this reference also analysed U, resulting in significantly higher LoDs (18.5 and 24.6 mg/L) than for Th (0.0007 – 2.25 mg/L). This suggests that Th is probably easier to detect than U.
Both the chalcogens and the halogens, in general, show a poor analytical performance (cf. Figure 1.20). Some of the detection limits were achieved indirectly via other elements or compounds. Although relatively few detection limits were found for the elements within the two groups, it can be assumed that these reflect a trend that only a poor analytical performance can be achieved for these elements. The transition metals, as a group of elements, show no clear trends and are therefore not shown here. However, elements of the fourth period, such as Cr, Ni, Cu, and Zn, show comparatively low LoDs.
Figure 1.21 summarises the collected data in the form of a periodic table of elements. The median of the detection limit is given for each element, if one was found. The coloured highlighting, with green for median detection limits up to and including 1 mg/L, light green up to and including 5 mg/L, and red above 5 mg/L, quickly shows which areas of the periodic table can be analysed well with LIBS and which are rather poor.

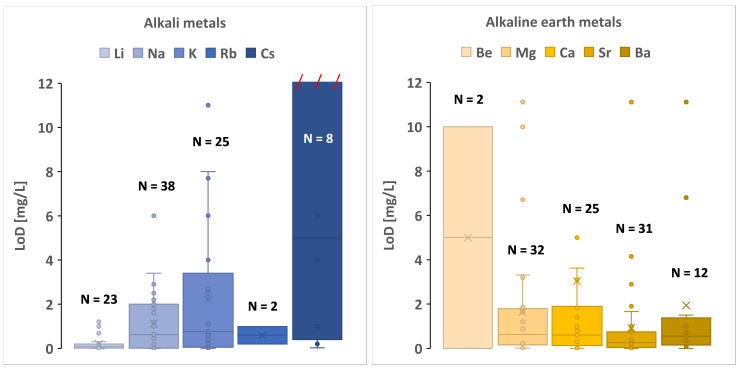

(a) **(b)**

Figure 1.17: Ranges of LoDs for **a)** the alkali metals and **b)** alkaline earth metals. Cs has been partially dismissed for the sake of clarity. Data based on the literature reviewed.

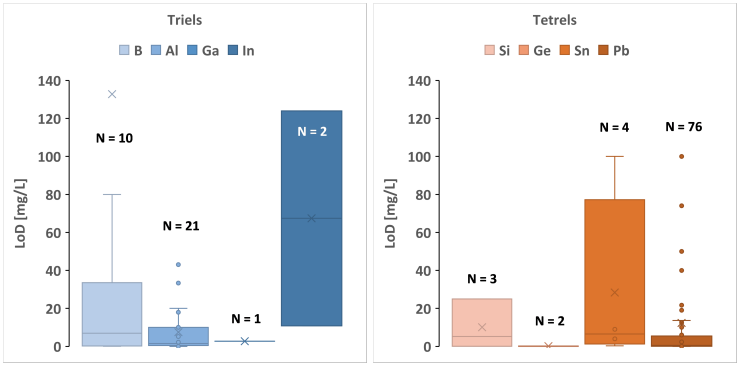

(a) (b)

Figure 1.18: Ranges of LoDs for **a)** triels, and **b)** tetrels. In has been partially hidden for the sake of clarity. Also, one LoD of B and one of Pb have been omitted (1200 and 200 mg/L). Data based on the literature reviewed.

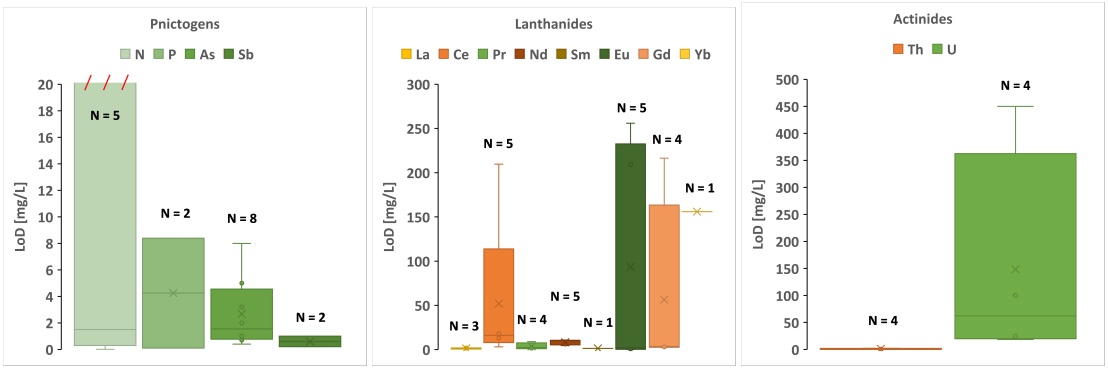

(a) (b) (c)

Figure 1.19: Ranges of LoDs for **a)** pnictogens, **b)** lanthanides, and **c)** actinides. N has been partially hidden for the sake of clarity (107 and 542 mg/L). Data based on the literature reviewed.

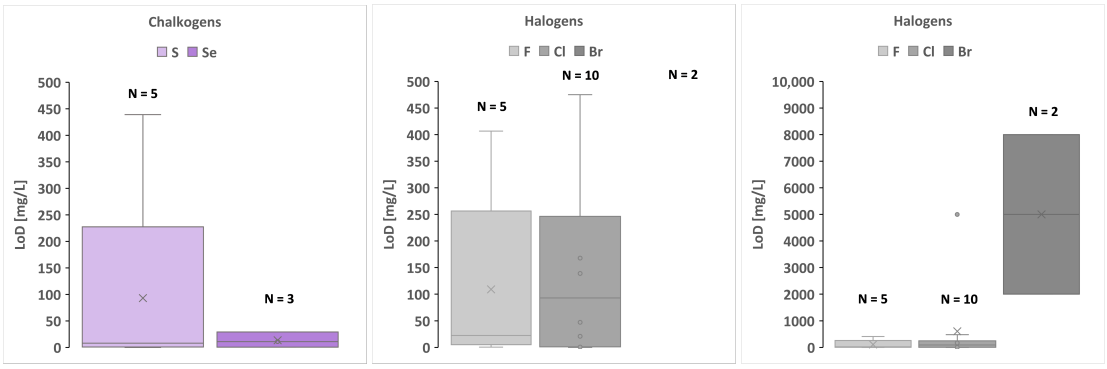

(a) (b) (c)

Figure 1.20: Ranges of LoDs for **a)** chalcogens, and **b+c)** halogens. Data based on the literature reviewed.

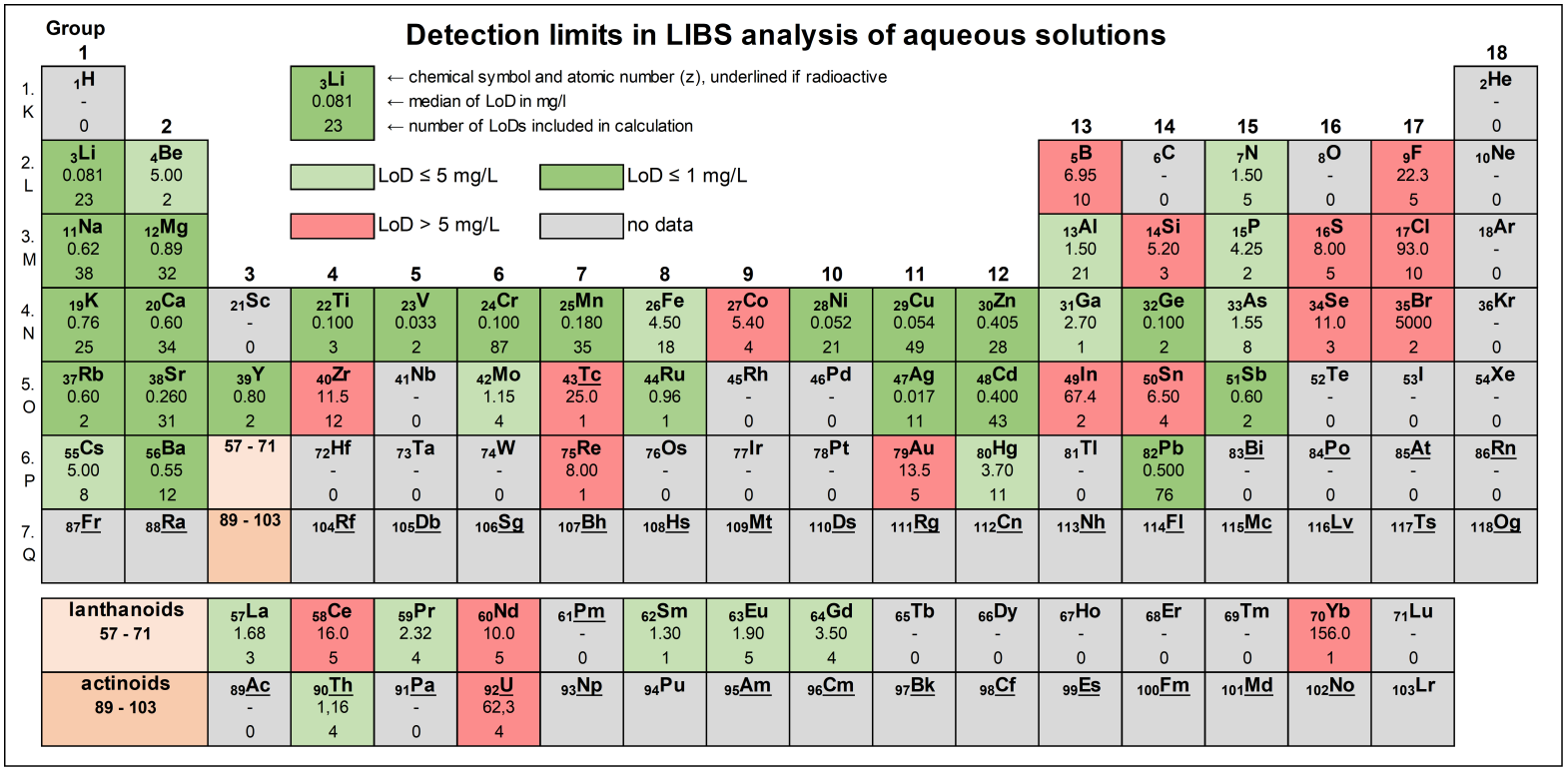

Figure 1.21: Median detection limits reported in a periodic table of elements. The median value of the reported LoDs is plotted beneath the element. As the same numbers of detection limits were not found for each element, the number of detection limits included in the calculation is also given to indicate the data quality. Threshold values have been set for faster assessment. Median detection limits below 1 mg/L are marked green, up to 5 mg/L light green and above 5 mg/L red. The underlying periodic table was created freely according to NCBI (2024). Comparable graphics have already been created by Busser et al. (2018) and Casanova et al. (2023).

1.5.4 Discussion

Sample Preparation Techniques

It has been shown that there is no standard approach to aqueous LIBS analysis in terms of sample preparation, LIBS experimental setup, or acquisition settings (cf. Table 1.3, Figure 1.10 - 1.13). Several very different techniques were used, each with its own advantages and disadvantages (cf. Table 1.3 – 1.6). This is due to the variety of possible applications, ranging from basic research in laboratory analysis, typically using standoff or self-arranged LIBS (Shao et al., 2023), to remote analysis for hazardous substances, using telescopic systems (Samek et al., 2000), and to in situ analysis for environmental concerns using online (Sui et al., 2021) or portable instruments (Schlatter et al., 2023). Therefore, both the LIBS setup and the sample preparation technique should be selected according to the desired application.
However, one of the sample preparation methods listed in Table 1.3 can be excluded in the choice of sample preparation. This method, being the surface analysis of bulk liquids, has many limitations, such as high laser energy requirements and low sensitivity, which have been extensively described in literature (e.g. Contreras et al. (2018)), and is therefore not recommended. Instead, splashing and liquid evaporation compensation methods should be applied. An analysis inside the liquid is a bit more promising but is subject to shot-to-shot variability (Goueguel et al., 2015).
Furthermore, in situ applications require sample preparation techniques that are easy to use in the field. Therefore, methods such as LB soaked on FP, SE-LSC, and LSC FP are recommended. However, when selecting a sample preparation technique, it should be noted that several sample preparations also pre-concentrate the sample solution and thus can lower the LoDs significantly (e.g. most LSC techniques). This can help to achieve LoDs significantly below 1 mg/L. As portable instruments are typically less sensitive than laboratory devices using higher energies, sample preparation should include pre-concentration steps. For on-line or laboratory analysis, more complex LIBS setups with more complicated sample preparation techniques can be chosen (e.g. LJ, LAC). Here, pre-concentration may be helpful but are not imperative. Some LJ analysis already reached sensitivities comparable to commercial ICP-AES devices without any pre-concentration (Nakanishi et al., 2021) and could also be used for online and real-time analysis. For Na, cylindrical jets showed a lower sensitivity compared to sheet jets (Nakanishi et al., 2021). The special form of a LJ capillary effectively reduces splashing (Zhang et al., 2018) but brings along a more complicated experimental setup and costly consumables.
When only hydride-generating elements (e.g. As or Se) are to be analysed, HG is a good choice as it significantly improves sensitivity by eliminating spectral and chemical interference (Ünal and Yalçın, 2010). However, this method is limited to a small group of elements, which can form hydrides (e.g. As, Sn, Sb, Se, Ge, Pb, Bi, Te), and it requires a complicated measurement setup. Coupling LIBS with ion-exchange techniques can also be a good option to improve sensitivity and reduce matrix effects in LIBS liquid analyses (Kim et al., 2010). However, this also requires a complicated setup, which reduces the advantage of a simple and fast sample preparation over other

methods such as IC. The same is true for the isolated droplet technique. An easy way to avoid splashing is the LSC technique of freezing the sample (Harun and Zainal, 2018a; Sobral et al., 2012). This sample preparation does not require much expertise or a complicated setup and could also be performed in situ using liquid nitrogen (Sobral et al., 2012). However, no pre-concentration is achieved this way.
ESD achieves pre-concentration, but many chemicals are required, as well as additional parts and experimental knowledge. ED also pre-concentrates the samples and therefore has an improved sensitivity (Chen et al., 2008; Kurniawan et al., 2015). The main drawback is a comparatively long time required for analysis due to the deposition process ($\ll$ 10 min). Ad/ab on wood chips (Chen et al., 2010) or graphene oxide (Ruiz et al., 2019) is also quite time consuming but can be conducted cost-effectively and additionally improves sensitivity. Chelating (e.g. Tian et al. (2019)) is even more time-consuming, requires more chemicals, and is usually not possible for a multi-element analysis. However, it can be more efficient in analyte enrichment than FP (Tian et al., 2019). As described by Lin et al. (2016), membrane generation (MeGe) is very similar to chelating, but requires even more time in sample preparation due to the long drying process. This makes the method less favourable in comparison to other presented methods.
Analysis in an isolated droplet, either with an isolated droplet generator (IDG) or by acoustic levitation (Meneses-Nava et al., 2021), adds complexity in the experimental setup, which minimises its advantages over conventional analytical techniques. NPs have the potential also to improve the sensitivity (De Giacomo et al., 2016; Wu et al., 2021) and are easier to introduce in sample preparation. When using LSC of a droplet on a surface with no adsorption/absorption step, some form of SE is recommended to improve the homogeneous distribution and shape of the EvR. Without any SE, an effect typically referred to as the coffee ring effect (CRE) occurs, leading to a lowered repeatability due to an inhomogeneous distribution of the EvR (Liu et al., 2020; Schlatter and Lottermoser, 2023). The SE can be implemented by making the surface more hydrophobic to improve the distribution of the EvR (Schlatter and Lottermoser, 2023) to introduce a geometric constraint (geometric constraint (GC)) technique (Ma et al., 2020a; Ahlawat et al., 2023) or to combine both (Wu et al., 2021).

Instrument Types, Experimental Setups, and Acquisition Settings

Furthermore, it is also possible to improve the various sample preparations with a special LIBS setup. These include, e.g., double pulse (DP), laser-induced fluorescence (LIF), resonance-enhanced (RE), resonant (R), or microwave enhancement (MW) LIBS. The main advantages and disadvantages of the special setups are presented in Table 1.5. Depending on the design of the LIBS, such setups may not be possible, or lead to complexity that diminishes the main advantage of LIBS over other laboratory methods in being simple in sample preparation (Cremers and Chinni, 2009). The simplest method to use is DP, which typically enhances the signal ten times and for some elements up to 50 times (Cremers and Chinni, 2009). The other experimental setups are more complicated, require more experienced staff, and do not all allow

multi-elemental detection, but can improve sensitivity (cf. Table 1.5).
The acquisition settings (cf. Table 1.6) also affect the sensitivity and should likewise be adapted to the method. For example, the gate delay should be long enough to minimise the influence of continuum radiation, which typically occurs at the very beginning of the breakdown and provides no useful information, in addition to degrading the signal-to-noise ratio (Zhang et al., 2021a). However, with overly long gate delays, the signal becomes weaker. Although it is possible to set an optimum delay time for each element individually, using different delay times for different elements prevents simultaneous detection. For this reason, when analysing multiple elements, a gate delay should be selected which is suitable for all the elements to be detected.
Another enhancement possibility, which is often easy to implement, is to use a purge gas such as Ar, which also amplifies the signal intensity significantly (Scott et al., 2014). Even some portable LIBS units are already equipped with Ar cartridges for signal amplification (Schlatter and Lottermoser, 2023).
A change in pulse duration, pulse energy, wavelength, or repetition rate essentially influences the energy that is supplied to the sample and is thus available for the formation of the plasma (cf. Table 1.6). Moreover, increasing the repetition rate reduces the analysis time and improves averaging (Cremers and Radziemski, 2013). Typical lasers used in LIBS liquid analysis are Nd:YAG lasers with a fundamental wavelength of 1064 nm (cf. Figure 1.12). Using different wavelengths can improve detection. For example, the CO_2 wavelength of 10.600 nm is particularly suitable for the analysis of water, as it absorbs in the infrared range (Cremers and Radziemski, 2013). However, the wavelengths used were between 266 and 1064 nm (cf. Figure 1.12). The wavelengths of 532, 355, (352), and 266 nm are the second to fourth harmonics of the Nd:YAG laser, with a fundamental wavelength at 1064 nm.
According to Cremers and Radziemski (2013), typical pulse energies for LIBS are between 10 and 500 mJ. In the literature reviewed, pulse energies between 0.2 and 800 mJ were found (cf. Figure 1.13), with most in the range 0.2 to 100 mJ. Energies below 10 and around 100 mJ are the most common (cf. Figure 1.13). To ablate enough material to produce a strong signal, the pulse energy must be high enough . However, a low energy pulse combined with a shorter pulse width and higher repetition rate will also result in a higher power density (Cremers and Radziemski, 2013). Handheld devices generally operate with lower pulse energies. For example, the SciAps Z-300 uses a pulse energy of 5 - 6 mJ, a frequency of 50 Hz (10 Hz), and a pulse width of 1 ns (Wise et al., 2022).

Elements and their Reported Detection Limits

Looking at the elements analysed, several areas of interest stand out (cf. Figure 1.14). Frequent testing of PTEs such as Cr (N = 87) or Pb (N = 76) is particularly striking. There is a very strong interest in the detection of these elements because they are problematic elements in drinking water (Rai et al., 2008). Also, Cu and Cd are analysed

very frequently which are also problematic elements (Rai et al., 2008). Furthermore, there is a second group of elements, that are often analysed: Na, (Mn), Ca, Mg, Sr, K, and Li. These are typical cations in natural waters and therefore of interest in natural water analysis.
An interesting observation is that arsenic (As) is less often analysed than Cr, Pb, Cu, Cd, and Zn, although it is a very problematic element in drinking water (Haider et al., 2014). This may be because As is not as well analysed by LIBS as other elements such as Li and Cr. According to Cremers and Radziemski (2013), the most common and useful spectral range for LIBS analysis is 200 - 900 nm. Unfortunately, there are few strong lines for As in this range that can be used for quantification. Therefore, for As quantification, it is recommended to use pre-concentration methods or to choose HG.
S, N, F, Br, and P (and to a lesser extent Cl) are also relatively rarely analysed, although they are typically present as anions in natural water. This is also due to the fact that these elements are not analysed by LIBS as well as other elements such as Li and Cr. These six elements have among the highest ionisation energies of the 56 elements for which detection limits have been found. The ionisation energy plays a major role for these elements, as the lines typically chosen for quantification lie in or near to the infrared range (except for P) and are difficult to excite due to the high ionisation energy (Ma et al., 2020b). The intensities are therefore usually so weak that low concentrations cannot be detected (Ma et al., 2020b, 2022b). For example, the strongest lines for F and Cl are below 200 nm, below the range of typical CCD detectors and within a range where a vacuum is required in the light path (Asimellis et al., 2005). Therefore, a detour via indirect analysis is usually used (for example, molecular emission, as compounds such as CaF and CaCl show higher intensities) (Tang et al., 2021). Another option is to analyse the excess of a more easily analysable element (e.g. Ag or Ba) that reacts with the anions through precipitation (Ma et al., 2020b).
It is also interesting to note that some atypical elements such as Tc were analysed in water. The reason for this is the possibility of remote LIBS analysis. Samek et al. (2000) analysed Tc with a telescopic LIBS system over a distance of 3 m. Also, the catastrophe of the Fukushima nuclear disaster has led to development of LIBS aqueous analysis for elements like Cs, Sr, and Zr (Ramli et al., 2017; Ruas et al., 2017; Shimazu et al., 2021; Matsumoto et al., 2021).

Limitations of the Data Review

There are a number of limitations that need to be considered when interpreting the data reviewed, in order to avoid drawing premature conclusions and to be able to interpret the graphs and data, especially the periodic table of elements, correctly. First of all, the review was limited to publications available between 1984 (Cremers et al., 1984) and August 2023. Moreover, although most of the reported LoDs have been calculated using the 3σ-IUPAC criterion, some have been calculated using other formulae, and some may be overly optimistic as they are often calculated incorrectly (Poggialini et al., 2023a). In addition, very different instrument types, experimental setups, and sample preparation methods were used among the reviewed literature

to achieve the LoDs, including steps of pre-concentration and indirect analysis (e.g. Wakil and Alwahabi (2020); Tang et al. (2021); Ma et al. (2020b, 2022b)).
Another factor that should not be neglected is the lasers and spectrometers used, which strongly influence the possibilities of analysis, for example, through different possible energies and resolutions (e.g. full width half maximum (FWHM)). A distinction should be made between laboratory-based, online, telescopic, and portable devices (see Table 1.4), if one wants to directly compare the detection limits of two analyses of different LIBS types. Here, the application also plays a major role. For in-situ measurements, higher LoDs are usually accepted if direct decisions can be made on the basis of the measured concentrations and if more detailed laboratory analyses are still possible afterwards (Schlatter et al., 2023). Acquisition settings can either be a preset by the instrument or they can be set by the user. Different gate delays, gate widths, pulse energies, repetition rates, and wavelengths also result in different detection limits. Furthermore, the atmosphere used in LIBS analysis also plays an important role in the detection limit achieved (Scott et al., 2014). For example, Ar and He improve the signal intensity and thus lead to better detection limits. However, various atmospheres were used in the compared literature, leading to problems with comparability.
The use of different calibration techniques affects the calculated LoD, as does the use of different spectral lines (atomic/ionic/molecular) for the same element. This was, for example, clearly shown for Zr in Ruas et al. (2017). In addition, it is also possible to use several lines per element and ratios of different lines for calibration (Palleschi, 2022b) to reduce the negative matrix effects.
When analysing aqueous solutions with several dissolved elements, it is also important to ensure that the lines used for quantification are not excessively close together, as they will be falsely detected as one peak by the sensor (e.g. Cd I 467.81 nm & Zn I 468.01 nm , cf. Figure 1.22).

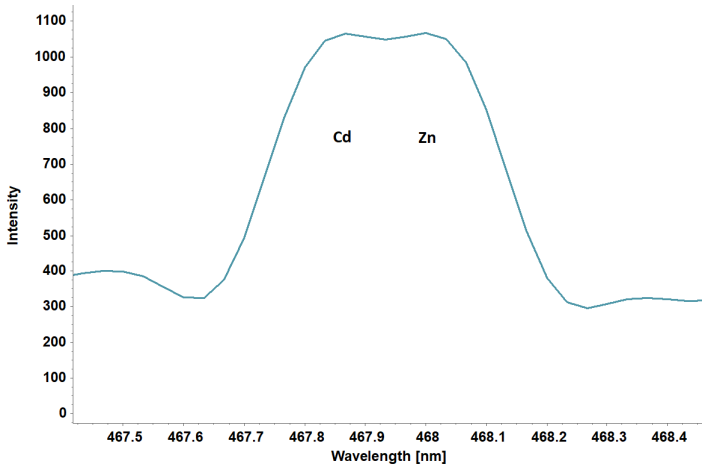

Figure 1.22: The two closely spaced lines of Cd (467.81 nm) and Zn (468.01 nm) appear to merge into a single peak when a solution containing both elements at 125 mg/L is analysed by a portable LIBS using the SE-LSC method described in Bhatt et al. (2020a).

The choice of the best spectral lines or the best ratios can lead to improved LoDs for the intended application. However, the multiplicity of the lines or of the ratios of lines used limits the comparability of the LoDs between the literature to some extent. The difference in the liquids analysed also has an influence on which detection limit is achieved due to their different matrices (cf. Bol'shakov et al. (2021)). LIBS analysis is very susceptible to matrix effects (Palleschi, 2022b). Aqueous solutions with complex matrices therefore generally lead to higher detection limits. To avoid this problem, certain liquids were excluded in advance and only aqueous solutions were considered.
Last but not least, a very important factor is the number of references per element. A threshold of five references has been applied to illustrate sufficient data in several graphs (e.g. Figure 1.14 and 1.15). However, if these five LoDs per element are reported in one reference for different lines used in the calibration, there is no statistical improvement in comparison to one reported LoD.
Overall, however, the limitations listed cannot be avoided, otherwise, the sample size would be further reduced. However, if a sufficient number of LoDs are available for each element, the limitations also become relative. Despite the limitations, this review provides a quick and comprehensive overview and can serve as a guide for further research in this area. Detailed information can be found in the Supplementary Data (https://www.mdpi.com/article/10.3390/spectroscj2010001/s1), which also lists all of the references used.

Future Directions

It is unlikely that LIBS will be widely used in the laboratory for aqueous analysis in the near future, because there are already well-established methods such as IC, AAS, and ICP-MS. However, the possibility of the miniaturisation of LIBS and the handheld or on-line instruments already available offer a great opportunity. In 2009 there was no truly handheld LIBS instrument (Cremers and Chinni, 2009). It was only 10 years ago, in 2013, when the first truly handheld LIBS analyser was introduced by SciAps Inc (Woburn, MA, USA) (Senesi et al., 2021). Since then, there has been a lot of research with such handheld instruments within the area of solids analysis (Pochon et al., 2020; Lawley et al., 2021; Fabre et al., 2022; Wise et al., 2022), but still little in the field of liquids analysis (Schlatter and Lottermoser, 2023; Schlatter et al., 2023). Therefore, there is a distinct potential to investigate LIBS as a novel technique in liquids analysis. LIBS may also offer benefits simply through the fact that LIBS analysis allows immediate decisions to be made and a pre-selection of samples for laboratory analysis. Also, the miniaturisation of instruments (online and portable/handheld) offers a new field in which LIBS could establish itself, as it is able to simultaneously analyse the entire periodic table of elements in water with comparatively low LoDs. This is a cost-effective and efficient approach compared to investigations solely relying on laboratory analyses. Moreover, pre-concentration methods can significantly improve sensitivity and therefore the acceptance of LIBS.

1.5.5 Conclusions

This review has provided a guidance on how to use LIBS for elemental analysis in aqueous solutions, which elements can be analysed, and which methods achieve low LoDs. Over 153 publications (1984 to August 2023) could be identified, which covered the topic of elemental analysis of aqueous solutions. Five classes of sample types could be identified, with most of the research on diluted stock solutions, but also with applications on artificial, biological, natural, and natural saline waters. The majority of the research on this topic is currently conducted in China.
Direct liquid analysis using LIBS is prone to low sensitivity due to splashing and cooling of the plasma. Therefore, many sample preparation techniques have been developed or adapted to improve sensitivity. Sample preparation in LIBS aqueous analysis can be classified into four main categories: liquid bulk (LB), liquid-to-solid conversion (LSC), liquid-to-aerosol conversion (LAC), and hydride generation (HG). The most common category is LSC, followed by LB and LAC. HG is quite seldom used, but also only applicable for a few elements. The most used subcategories within LSC are surface-enhanced (SE), non-SE, and adsorption/absorption (ad/ab). Within LB, the most used subcategories are liquid jet (LJ), surface, and inside.
Four different instrument types are used for analysis: laboratory-based, online, telescopic, and portable/handheld. In addition, there are different experimental setups in use for signal enhancement, e.g., double-pulse (DP) instead of single pulse (SP), laser-induced fluorescence (LIF), resonance-enhanced (RE), resonant (R), and microwave (MW) enhancement.
Furthermore, several acquisition settings strongly influence the elemental analysis in aqueous solutions: repetition rate, pulse energy, pulse duration, gate delay, atmosphere, and wavelength. Typically the fundamental wavelength of the Nd:YAG laser is used (1064 nm), but the second harmonic is also used quite often. All other wavelengths have been used seldom within the reviewed literature. Very different pulse energies have been used among the literature; however, 100 mJ was used the most. The range from 0.1 – 9.9 mJ was used even more frequently than the range 100 – 109.9 mJ. In total, 56 different elements have by now been analysed in aqueous solutions using LIBS, including three radioactive elements.
Most LoDs have been reported for Cr and Pb, and for 30 elements five or more LoDs are reported. In particular, the analyses of Ag, Ni, Cu, Li, and Cr performed well in the literature reviewed, with median LoDs less than or equal to 0.1 mg/L and more than ten LoDs were included in the calculation. The analyses of Mn, Sr, Cd, Pb, Zn, Ba, Na, Mg, K, and Ca also performed quite well in the literature reviewed with a median LoD lower than or equal to 1 mg/L and more than five LoDs included in the calculation. Elements of the 15th - 17th group of the periodic table tend to show higher detection limits in the analysis with LIBS, because they typically have higher ionisation energies and, in some cases, only lines in the infrared range can be selected. As a result, the intensities of the selected lines are often not sufficient at low concentrations. This is especially relevant for S, N, F, Br, P and Cl, which typically occur as anions in water. It is recommended to choose an indirect determination via molecular emissions or excessive elements by precipitation for these elements.
There is no uniformity in the literature when choosing a sample preparation technique

and selecting an experimental setup. This is because there are advantages and disadvantages depending on the choice made, and, therefore, the most appropriate method for the particular application should be chosen. However, the analysis of bulk liquid at the surface gives the least reliable results and should thus be excluded. HG only works for hydride-generating elements and is complicated to set up, but can lead to a significant improvement in sensitivity. If the setup can be implemented, this method can help to quantify hydride-generating elements that are not as well analysed as Cr or Li, such as As. DP often has an advantage over SP, especially for liquid samples, but is not possible with every instrument. However, the conversion from the liquid phase to a gas or solid phase also has certain advantages. For example, the SE LSC leads to a preconcentration of the sample, as only the EvR, i.e. the elements of interest, are analysed. As a result, the sensitivity increases significantly, and elements with generally poorer sensitivity can be analysed better.
Since the relative standard deviation (RSD) for LIBS analysis is usually quite high, multiple measurements should be considered to increase the accuracy. However, since the analysis time for LIBS is very short and the time can be reduced by increasing the repetition rate, this is not a problem for analytical methods with small sample quantities.
Overall, LIBS is a powerful analytical technique capable of a simultaneous multi-element analysis, not only of solids but also of aqueous solutions. As long as the limitations are known and certain sample preparations and experimental setups are used, any element can be detected in water. Advantages such as low acquisition cost, rapid and simultaneous detection of multiple elements and the possibility of in situ or remote analysis are convincing arguments for using LIBS as an alternative to established analytical techniques in the elemental analysis of aqueous solutions.

Supplementary Materials

The following supporting information can be downloaded at:
https://www.mdpi.com/article/10.3390/spectroscj2010001/s1,
Spreadsheet S1: LIBS applied to elemental analysis of aqueous solutions.

The following references are not cited in the text but are part of the reviewed data:

Aguirre et al. (2015); Alamelu et al. (2008); Aras and Yalçın (2016); Archontaki and Crouch (1988); Bae et al. (2015); Bhatt et al. (2017, 2021); Bocková et al. (2017); Bukhari et al. (2012); Cáceres et al. (2001); Carvalho et al. (2019); Charfi and Harith (2002); Chen et al. (2015); Cheri and Tavassoli (2011); Contreras et al. (2018); de Jesus et al. (2014); Fang and Ahmad (2012); Fichet et al. (2001); Gaubeur et al. (2015a,b); Godwal et al. (2008); Goueguel et al. (2014); Groh et al. (2010); Haider et al. (2014); Hartzler et al. (2019); He et al. (2019); Huang et al. (2002, 2004); Huang and Lin (2005); Huang et al. (2013); Janzen et al. (2005); Järvinen et al. (2013, 2014); Jiang et al. (2021); Jijón and

Costa (2011); Jijon and Costa Vera (2012); Kumar et al. (2003); Lee et al. (2011, 2012); Lin et al. (2022); Liu et al. (2020); Loudyi et al. (2009); Ma et al. (2022a); Méndez-López et al. (2023); Metzinger et al. (2014); Niu et al. (2019); Papai et al. (2019); Pearman et al. (2003); Poggialini et al. (2022); Popov et al. (2016); Raimundo et al. (2021); Rezk et al. (2016); Sarkar et al. (2012, 2008); Sawaf and Tawfik (2014); Sheng et al. (2019); Shi et al. (2014); Simeonsson and Williamson (2011); Singh and Sarkar (2019); Skrzeczanowski and Długaszek (2021); Tian et al. (2022); Wakil and Alwahabi (2019); Wall et al. (2016); Wang et al. (2014, 2015, 2023); Wen et al. (2016, 2023); Wu et al. (2018); Xing et al. (2021); Yang et al. (2016, 2017); Yao et al. (2012); Ünal Yeşiller and Yalçın (2013); Yueh et al. (2002); Zhang et al. (2022); Zhao et al. (2010, 2019); Zhong et al. (2015, 2016); Zhu et al. (2011, 2023); Wang et al. (2022); Ripoll et al. (2021)

Chapter 2

Method Development

As shown in Section 1.5, there are many approaches to the elemental analysis of aqueous solutions using LIBS devices. None of these methods have been used with a handheld LIBS to date. Thus, this thesis aims to identify a suitable technique for an in-situ application employing a pLIBS. In the following chapter the process leading to the final method is detailed, outlining the rationale behind selecting a specific approach and the process of adapting it to the SciAps Z-300.
Section 2.1 describes the process of finding an adaptable solution to the pLIBS with lessons learned. In Section 2.2, the construction of a necessary component for the application of the selected method is outlined. To complete the method and to enable its application in the field, a further component is required, which is presented in Section 2.3. Section 2.4 concludes with a brief explanation of the spreadsheet required for calibration and analysis. The most important laboratory equipment used in this thesis is listed in the appendix, along with their respective errors (cf. Appendix B.2).

2.1 First Attempts of Analysing Aqueous Solutions Using pLIBS

After thoroughly screening the literature, some initial evaluations were done to test the general suitability of a LSC method with a handheld device, in particular the SciAps Z-300. This kind of sample preparation involves the evaporation of microdroplets from the sample solution on a substrate, and the subsequent analysis of only the EvR. This results in an increased sensitivity due to the preconcentration step (Aguirre et al., 2013; Ma et al., 2020a).
First, the substrate had to be chosen with respect to the background of creating an easy applicable field method. The considerations are described in Section 2.1.1. It was promptly decided to avoid using a deposition via filter paper, as suggested by Yang et al. (2018), to prevent any loss of total dissolved solids (TDS) in the paper. Addi-

tionally, eliminating this step reduces costs and enhances the greenness of the method (Gałuszka et al., 2015) by decreasing waste production. Therefore, a SE method was chosen to improve the distribution of the EvR and therefore reproducibility. Section 2.1.3 details the selection decisions on the elements to be calibrated. Within section 2.1.2 the initial assessment of the SE-LSC method's suitability using a NaCl solution is provided. After the preliminary test, the first calibration was carried out using K as an example (see Section 2.1.4). The individual steps are dealt with in detail in the following paragraphs. A summary of the findings from the first attempts to analyse aqueous solutions with the pLIBS are discussed in Section 2.1.5.

Key questions:

- Is a LSC method appropriate for use with the SciAps Z-300?
- Which substrate should be selected?
- What is required to improve the LSC method?
- What type of standard can be chosen and which elements should be considered?
- What are the calibration steps and is the manufacturer's calibration software sufficient?

2.1.1 Substrate Selection

Several materials with different properties have been examined in the literature as potential substrates for LSC. For example, graphite planchets (Singh and Sarkar, 2019) or carbon planchets (Vander Wal et al., 1999) were used. The decision was made due to several reasons as followed (Vander Wal et al., 1999):

- no reaction with either the aqueous solution or the EvR
- no spectral interferences by the substrate
- no *"diatomic or cluster emission from the substrate material"*
- inexpensive
- simple to use
- readily available

Also silicon wafer (SW) and laser-patterned silicon wafer (LPSW) substrates have been tested for LSC (Bae et al., 2015). The bare SW satisfies most of the aforementioned reasons for selecting it as the substrate. Nevertheless, upon the drying of droplets on the

SW, the EvR appears to be rather non-uniform with a higher concentration of analytes at the periphery. This phenomenon is commonly known as the CRE (Bae et al., 2015; Keerthi et al., 2022), and it typically manifests on surfaces that lack hydrophobic properties. Therefore Bae et al. (2015) used a LPSW to control the wettability of the surface. It significantly mitigates the CRE and promotes a more uniform distribution of the EvR.
Aras and Yalçın (2016) utilised an oxide-coated SW instead, in order to increase the surface area available for the immobilisation of metal ions. Glass was also tested as a potential substrate, but a particularly hydrophobic coating was added to compensate for the CRE (Wu et al., 2021). Another material used as a substrate is an 3D anodic aluminum oxide porous membrane (AAOPM) (Shi et al., 2014). It enhances the signal by forming a strong metal-oxygen bond between hydroxyl groups and metal ions present on the substrate's surface, increasing the matrix-to analyte contact area. This efficiently couples a laser beam to the material due to the substrate's unique nanochannel distribution (Shi et al., 2014). Furthermore, Keerthi et al. (2022) compared three different substrates namely glass, polymethyl methacrylate (PMMA), and polytetrafluoroethylene (PTFE). CRE was observed on the glass substrate, with fluctuations in intensity depending on the analysed spot on the EvR. The hydrophilic surface of the glass leads to an increase in the deposition of EvR along the edges of the evaporating droplet. More hydrophobic surfaces possess a higher contact angle and hence a smaller contact area, leading to the suppression of the CRE (Keerthi et al., 2022). This is the case for PTFE and PMMA, for example.
However, as shown in literature, metallic surfaces are particularly suitable for several reasons (Aras and Yalçın, 2016): On the one hand, reaching thermal equilibrium between the atoms to be determined and the plasma occurs more quickly (Aguirre et al., 2013; Kocot et al., 2016). On the other hand, high temperatures and electron densities are achieved through interaction with the metallic substrate, which enhances the signal (Aguirre et al., 2013; Kocot et al., 2016).
This is why various metals have been examined as substrates. For example, Yang et al. (2016) tested a magnesium alloy containing Al and Zn. Ma et al. (2019) tested Zn, Mg-alloy, Ni and Si. Wang et al. (2023) applied Cu with a laser patterned surface as a substrate, and Metzinger et al. (2014) utilised Al, Cu, and Zn. Many others also tried Al due to its low price and good availability (de Jesus et al., 2014; Bocková et al., 2017; Wang et al., 2022; Aguirre et al., 2013; Gaubeur et al., 2015a,b).
To ensure the developed method within this thesis remains simple and cost-effective, it is crucial to use materials that are affordable and easy to handle. Therefore, the substrate should be, above all, inexpensive, readily available, and the preparation should be achievable within a relatively short time.
Cleaning the substrate with abrasive paper and ethyl alcohol, as implemented in Yang et al. (2016), would unnecessarily waste time in the field and require additional chemicals and materials. Thus, the price of the metal has to be very low as it can only be used once (Kocot et al., 2016). Aluminium foil fulfils this criterion. Furthermore, most of the strong spectral lines of Al are between 200 and 450 nm, avoiding spectral interference with most metals (Zhao et al., 2010). In addition, Al-foil has a high degree of purity due to its manufacturing process in fused salt electrolysis (Zhao et al., 2010). The price is comparatively very low, as it is a consumer product. Furthermore,

aluminium possesses exceptional thermal conductivity and a passivating oxide layer, which is important when using in the field. The reasons listed above led to the selection of aluminium as the sample carrier.

2.1.2 Evaluation of the General Suitability of the Method

Since it was not certain at the beginning whether LSC would lead to reproducible results with a portable device, it was tested whether acceptable results could be achieved with a simple NaCl solution before purchasing standard solutions. For this purpose, a saline solution was prepared from table salt and double-distilled water with a concentration of roughly 250 mg/L. Using a micropipette (Eppendorf Research® plus 0.1–2.5 μl), 1 μL drops were applied to a SE Al-foil. Surface enhancement was done according to Jijón and Costa (2011): A thin pencil layer was applied to an Al-foil. Three Faber Castell Pitt Graphite crayon pencils with varying levels of hardness (4B, 6B, and 9B) were subjected to testing. Jijon and Costa Vera (2012) already experienced that the grade of hardness has an influence on the sensitivity. They tested HB, 4B, and 9B pencils on silicon and stainless steel, finding out that 4B works best for most cases (Jijon and Costa Vera, 2012). The droplets were evaporated by placing the aluminium foil with the droplets on the hot plate for several minutes, and it was visually checked, whether the solution had evaporated. Afterwards, the EvRs were targeted with the help of the internal camera of the Z-300 and analysed. By doing this, initial observations could be made:

- Since aluminium foil has two different surface textures resulting from the production process, it prompts the question of which is better suited. When applying the pencil layer, it turned out that it is very difficult to coat the glossy side with all the pencils tested. With the matt side, however, this is easier. Therefore, the matt side is preferably to be coated.
- The optimal outcome was achieved by utilising the softest pencil grade (9B) as it was significantly more manageable to apply onto the aluminium foil. The decision in favour of this practical consideration excluded the prospect of potentially enhanced sensitivity, as articulated by Jijon and Costa Vera (2012), on the basis that it is difficult to achieve a uniform SE with the 4B pencil.
- The EvR of 1 μL droplets are easily visible to the eye.
- Droplets of 1 μL result in an EvR of about 1 - 2 mm.
- The droplets can be applied precisely to a particular area and remain in place even when the foil is tilted.
- The droplets evaporate rapidly on the laboratory hot plate ($<$ 1 min) and the EvR is uniformly circular when SE is applied.

- Targeting with the internal camera poses difficulties as measurements occur at the lower edge rather than centrally located in the measuring field.
- The analysed area is smaller than the EvR. Therefore, the droplet should be reduced in size and/or the analysed area enlarged.
- The droplets on the unprepared Al-foil spread unevenly and the EvR is larger in size and more irregular in shape and distribution.
- With increased solution content, the quartz window requires frequent cleaning.
- If a measurement is cancelled due to the absence of a sample, contamination on the quartz window is often the reason.
- Wavelength calibration is prompted after some time, however, it may be useful to complete a smaller series of measurements in order to obtain similar data.

2.1.3 Selection of Elements and Standards

Using LIBS, the entire periodic table of elements could be analysed in theory (Senesi et al., 2021). In Section 1.5 the results of a comprehensive literature review on liquid analysis are presented, and pictured on a periodic table of elements (see Fig. 1.21). It provides information on which elements have been analysed in aqueous solutions using LIBS to this date and the average (median) LoD achieved per element. This table assists in gaining an understanding of the relative importance of different elements in water testing: Those that are rarely or not at all analysed are either of less interest, are rarely found in water, or pose difficulties for analysis using LIBS.
Table 1.2 displays the elements examined, based on the type of sample. Most of the research has only been examined on standard solutions and not on samples as represented in reality. This is due to the many unpredictable influences of different matrices as LIBS analysis is highly matrix dependent. For this reason, and in order to be able to calibrate the device at all, standard solutions were initially used in this work. The elements to be calibrated were initially selected with the intention to differentiate from a comparable instrument such as pXRF. The latter can usually only analyse elements with $Z > 12$ (Lemière, 2018). For this purpose, elements with a low Z were chosen, which are also typically found as cations in natural aqueous solutions (Li, Na, and K). Following positive results, the range of elements was extended to include other cations typical of natural waters (Ca, Mg and Sr). In addition, SO_4, NO_3, and Cl were selected to allow a comparability with IC analyses and to be able to analyse bottled mineral waters. Next, typical elements of polluted industrial or mining water were selected to enable the application of the method for environmental screening (Cr, Ni, Cu, Zn, Cd, As, Se, Pb). Al could not be considered because of the substrate selection. To analyse Al, it would be necessary to choose another metal foil with a low interference. However, this is likely to result in increased costs.
The analysis of Si was discontinued for safety precautions as the solute present in the AAS standard solution has the potential to form hydrofluoric acid (HF), as the solute

is $(NH_4)_2SiF_6$. All standard solutions purchased are listed in Table B.1 in the appendix. Except for the anionic standard (IC standard solution), all are AAS standard solutions (ROTI®Star, Carl Roth, Karlsruhe, Germany). This decision was made because AAS is a spectroscopic method that exhibits similarities in analysis type. Additionally, the literature reviewed also utilised AAS standard solutions for calibration in LIBS aqueous analysis (e.g. Choi et al. (2014); Skrzeczanowski and Długaszek (2021)). Besides being less expensive than IC or ICP-MS standard solutions, they are convenient to manage and produce dilution series with, as the matrix relies on diluted nitric acid.

2.1.4 First Calibration Attempt Using Potassium as an Example

Building on the experiences from the preliminary test (Sect. 2.1.2) a first calibration for potassium was carried out. The following sections outline the main procedures involved.

Mixing of the Standard Solutions

For calibration of the selected elements in Section 2.1.3, dilution series of the purchased AAS standard solutions were produced by diluting with 2% nitric acid using pipettes and volumetric flasks. The 2% HNO_3 was produced by dilution of an aliquot (ROTIPURAN® $\geq$65%, Carl Roth, Karlsruhe, Germany) with distilled deionised water of 18 MΩ. Calculation of the necessary volumes of both the stock solution and the solvent were carried out using Pearson's square. Volumetric flask volumes were minimised during mixing to reduce waste. Whenever feasible, exclusively pipettes were employed for volume measurement. For instance, a particular quantity of stock solution and diluent was directly pipetted into a centrifuge tube when high concentrations were desired. For storage of the dilution series, centrifuge tubes with a border were used (Centrifuge tubes SPL 50 ml, with border (PP), Semadeni AG, Germany). Information on the standard solutions and the working material can be found in the appendix (cf. B.1 and B.2).

Adjusting the Gate Delay (t_d)

Explanation of both- the gate delay (t_d) and t_b- can be found in the glossary (cf.). Please also refer to Figure 1. As discussed in Section 1.5, adjusting the t_d is crucial for improving the SNR in LIBS analysis. Hence, a series of tests were conducted by varying the gate delay while maintaining a constant concentration of the standard solution at 1000 mg/L. The SciAps Z-300 uses a default internal integration delay (IID) of 19, corresponding to 645.2 ns t_d, when gating is enabled. For the calculation of the delay time on the SciAps Z-300, the following formula is used (SciAps, 2021):

$$t_d(ns) = 250 + 20.8 * \text{IID} \tag{2.1}$$

A total of twelve different gate delays were tested to determine the optimal one (see Table 2.1). Generally, it appears that the majority of peaks experience a decline in absolute intensity as the gate delay increases. The highest absolute intensities are found at an IID of 0, whereas the lowest are found at 132. Simultaneously, the background noise also decreases. Furthermore, as the IID increases, the peaks become narrower. An optimum eventually is reached at an IID of 84 (approximately 2 μs), which is a t_d frequently used in literature (e.g. Ma et al. (2019); Yang et al. (2018)). It is also possible to adjust the t_b, however, the shortest possible value is 1 ms (SciAps, 2021), which is sufficient for analysis. Consequently, the default value of t_b was used (1 ms).

Table 2.1: Different gate delays tested

IID [-]	t_d [ns]	Approx. t_d [ns]
0	250.0	250
5	354.0	350
10	458.0	450
19	645.2	650
24	749.2	750
31	894.2	900
36	998.8	1000
48	1248.4	1250
60	1498.0	1500
84	1997.2	2000
108	2496.4	2500
132	2995.6	3000

IID = internal integration delay; t_d = gate delay

Calibration Steps

The best practice guide for developing LIBS calibrations was distributed with the device (SciAps, 2021). However, it focuses on the analysis of solids in particular alloys, and its steps are not fully applicable to the developed method. Nevertheless, some steps are adapted from the best practice guide to the newly developed method.
Profile Builder is a software required for creating custom calibrations with the SciAps Z-300, whereby the software on an external computer can only be used as long as the device is connected. SciAps Utility can be used to analyse data that is already stored on the computer when a connection is not possible. However, for calibration purposes, it is recommended to use Profile Builder. In the following, a step by step procedure is described. Both on the Z-300 and in the computer software, a series of steps is required:

1. Turn the Z-300 on
2. Connect the device and the Computer via USB
3. Select *"Tethering"* on the settings dashboard of the Z-300, then *"USB tethering"*

4. Return to the main menu and make sure the remote service is enabled
5. Open Profile Builder on the computer
6. Select *"USB"* and click *"Connect"*

Establishing a connection with the device may last a few minutes, but will only work if the device has been assigned to an IP address. This information is located at the bottom left field, and the software indicates if it has been properly configured with a green highlight (see Figure 2.1). If the device is connected, there are various *modes* available to select (see Figure 2.1).

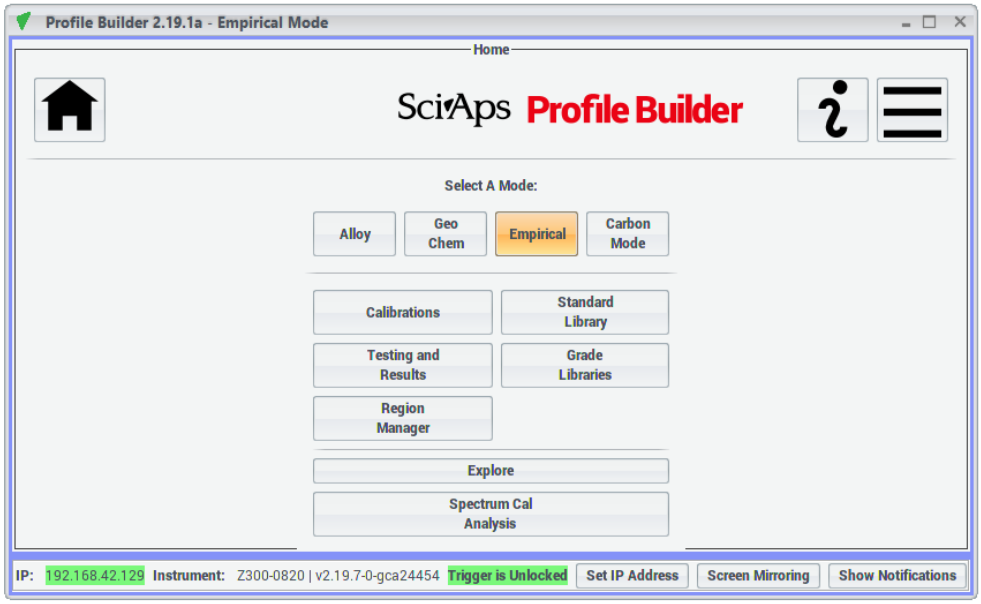

Figure 2.1: Main menu of the SciAps Z-300. Various modes are available for selection.

The *Alloy*, *Geochem*, and *Carbon* modes analyse elemental concentrations using the manufacturer's in-house calibrations. The *Empirical* mode provides the possibility of employing custom calibrations and is therefore selected in the Profile Builder software. A new calibration is set up:

1. Select *"Calibrations"*
2. Select *"Add new"* and enter a name
3. Select the elements of interest
4. Select *"Set unit to ppm"*
5. Add a list of the dilution series concentrations

6. Acquire data for the selected standards, ensuring that wavelength calibration has been performed beforehand
7. Build curves: set intensity ratios for each element of interest

The last step is to be further explained. First, the denominator must be defined, acting as a normalisation factor for the numerator signal. To do this, appropriate lines must be selected. When using aluminium foil as a substrate, Al lines can be chosen as the denominator, as these are constant across all samples. The lines chosen should be strong and prominent in all samples. It is also possible to select more than one denominator as well as to choose more than one line per element. However, the use of C as the second element in the denominator was discontinued due to typically weak C lines. Instead, five Al lines were selected. Figure 2.2 illustrates two of the five selected aluminium lines.

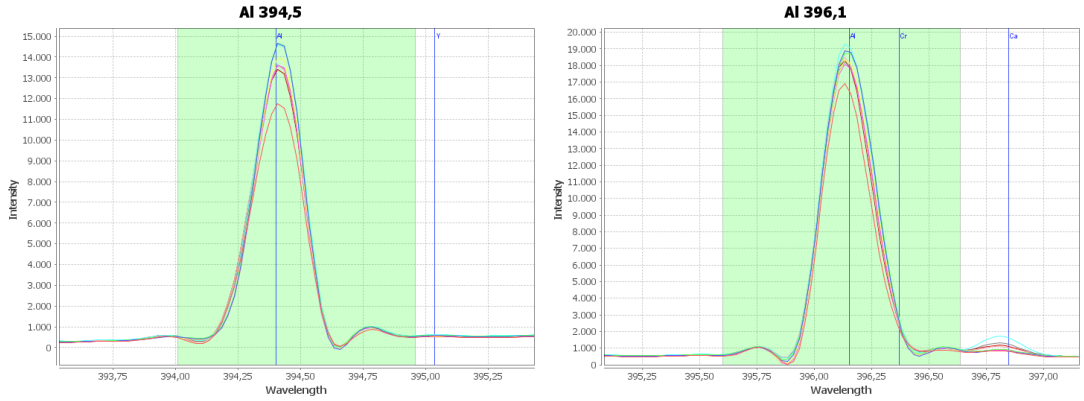

(a) **(b)**

Figure 2.2: Two of the five chosen lines of aluminium as an internal standard. They exhibit high intensity and no interferences with other elements.

Next, the numerator (analyte) is to be selected. It is recommended to choose lines of the element of interest (EoI) that exhibit the following characteristics (SciAps, 2020):

- are within the same spectrometer as, and near the denominator lines,
- are strong, but not saturating across the calibration range,
- have little overlap or interference from other elements,
- produce good calibration curves,
- produce a linear calibration with low root mean square error (RMSE) and small/no offset.

If the signal is weak, multiple lines should be used. The use of multiple lines also helps to keep the matrix effect low (Palleschi, 2022b). Therefore, in this thesis several

lines per element were chosen. An example is shown in Figure 2.3. Background removal can help to define the region limits (green background) of integration. Smoothing can also improve the SNR (Palleschi, 2022b), so Savitzky-Golay smoothing was applied (SciAps, 2020).

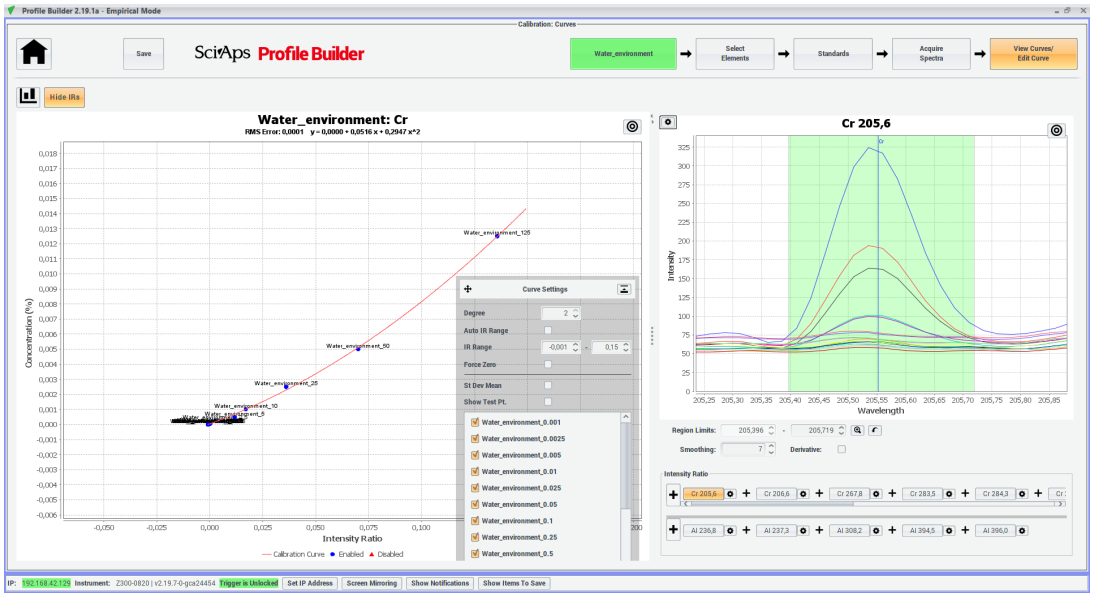

Figure 2.3: Calibration of Cr in aqueous solutions using Profile Builder.

Now an intensity ratio (IR) can be calculated by the software and the calibration can be fit using a polynomial. There are different options:

- Linear or quadratic fit
- Activate/ deactivate data points
- Force zero (forces y-intercept)

In a step-by-step process, different options should be tested. The aim is to reduce the RMSE number. Any data points that are outliers must be removed in order to obtain a proper calibration curve. As there were difficulties in performing further calibrations in the Profile Builder, it was decided to continue calibration using a spreadsheet. The process and rationale are explained in the next section.

Features and Limitations of the Model Builder Onboard Software

Certain limitations were observed when using the software provided by SciAps, the manufacturer of the Z-300. The software is suitable for simple calibrations with a

small number of standards and features a clear menu navigation. Additionally, a wide range of highly specific functions are accessible, simplifying work processes. All functions can be found intuitively thanks to the straightforward but organised interface. However, one drawback is that the software can only be used if the Z-300 is connected at the same time. This means that data that has already been generated and saved on the computer must be viewed with another software if the device cannot be accessed. As the amount of data increases, the connection to the device can also take a long time due to the bottleneck of the USB 2.0 connection. Moreover, the software clearly was designed for the analysis of solids. The linear equation displayed in the software only considers percentages. With a calibration in the range of ppm or mg/L, important decimal places are missing when calculating the concentration. It can be assumed that the software does not include all decimal places in the calculation, as spreadsheet tests have demonstrated.
In addition, the calibration regression can only be established using measured values. When averaging numerous measured values (more than three per concentration), the software often freezes as the data sets are too large. It would therefore be beneficial to first compute an average value of all measured concentrations and then determine a point on the calibration line. In this thesis, sometimes more than 20 points (averaged spectra) per concentration could have been chosen from, but it was not possible to select more than two or three per concentration.
Apart from linear and quadratic regression, exponential or logarithmic functions could have been advantageous too. Also, an *"undo"* function does not exist in the Profile Builder. If the integration range is accidentally moved, all intensity ratios automatically change irreversibly. This cancels out any comparability of the data. Only closing the software immediately without saving and restarting it solves this issue. All in all, it was decided to use a spreadsheet for further processing of the IR instead. Some explanation on the spreadsheet file can be found in Section 2.4.

2.1.5 Lessons Learned

1. Filter paper can be used for improvement of LSC, but it results in a loss of the analyte and reduces sensitivity.
2. A metallic substrate enhances the signal, as thermal equilibrium between atoms and plasma is reached more quickly, leading to high temperatures & high electron density.
3. An organic substrate leads to low precision, poor linearity and reduction of plasma energy during the vaporisation of the sample.
4. Al as a metallic substrate is inexpensive, available, easy to process, and has a fairly high purity.
5. Al can be used as an internal standard in the denominator of the IR.
6. The matt side of the aluminium foil was more suitable for LSC.

7. The EvR was fairly visible with droplets of 250 mg/L NaCl solution.
8. Evaporation on uncoated Al caused the coffee ring effect (CRE).
9. The shape of the EvR was irregular, and the distribution of TDS was inhomogeneous when applied on non-SE Al-foil.
10. Droplets of 1 μL were too large upon evaporation.
11. Droplets of 0.75 μL fitted best in size.
12. The reproducibility of the approach is presently poor.
13. Sampling locations varied between analyses and only a part of the EvR was sampled.
14. The raster size must be increased and the sample must be secured to the SciAps Z-300 during analysis.
15. A hydrophobic coating of the Al-foil is required.
16. Pencil layers (9B hardness) are an inexpensive and fast solution for coating.
17. Profile Builder is a useful software for calibrating solids. Nevertheless, there are constraints with its use in aqueous solution analysis.

2.2 Design and Construction of a Sample Holder for Surface-Enhanced Liquid-to-Solid Conversion Using pLIBS

Key questions:

- How can a pLIBS be held in place during analysis and what can be done to improve the speed and repeatability of the focusing process?

2.2.1 Introduction

Following lessons learned a sample holder was developed (cf. Section 2.1.5). This holder aims to improve the reproducibility and streamline the SE-LSC technique. It was printed on a commercial 3D printer. 3D-printing has multiple scientific applications, such as in medicine (Oleksy et al., 2023), geology (Hasiuk, 2014), ecology and evolution (Walker and Humphries, 2019), as well as cultural heritage and museums (Cooper, 2019). On the one hand, it enables three-dimensional visualisation, but on the other hand also low-cost prototyping (Chiulan et al., 2017), facilitating the development of useful tools in research. The final sample holder presented in this section allows SE-LSC with a pLIBS and thus in-situ analysis of aqueous solutions, which is currently mainly done in the laboratory (Schlatter et al., 2023). The development steps are well-documented, and interested researchers can request the 3D model. This allows others to reproduce or even improve the SE-LSC method. With minor adaptations to the sample holder, it should also be possible to use the technique with other pLIBS or even pXRF instruments.

2.2.2 Design Fundamentals

The sample holder is required in the SE-LSC process for mounting during the rastering of the EvR. It also greatly assists in focusing, as this does not need to be done manually by visual inspection of the EvR. As manual focusing is a very time-consuming step, the efficiency of the method was also improved. Furthermore, it should improve reproducibility as focusing will become more constant. By use of the recesses as a marker, the droplets can also be applied more consistently. In addition, smaller droplets are possible as there is no need to visually check the EvR of the former droplets for focusing. Therefore, faster evaporation is possible. Last but not least, the sample holder facilitates the handling of the thin, easily deformable metallic foil (e.g. Al), especially in the field.
The design of the sample holder is based on the shape of the nose of the pLIBS analyser SciAps Z-300, which is shown in Figure 2.4. The analysis window, where the laser beam exits, is clearly visible. Instead of reproducing the whole shape of the nose in the stencil, the screw holes are used for mounting and securing the sample holder. The

original screws used to fasten the front element are quite high, leaving only a small amount of space for securing a sample holder. Therefore, the screws were changed to flathead ones. The recess next to the analysis window was used as an additional fixing point and as a marker for the droplet application. The use of the screw holes and the recess for fixation saved space on the sample holder by allowing more measurement fields to be placed next to each other on the same area. It also allowed the stencil to be made flatter without the risk of slipping. The sample holder was designed in a CAD software (Fusion 360, Autodesk, San Rafael, USA).

Figure 2.4: The nose of the pLIBS SciAps Z-300. The screw holes and recess next to the analysing window are visible at the front part of the nose.

The prototypes and the final version were printed using thermoplastic polylactic acid (PLA) (Prusament Galaxy Silver, Prusa Research, Czech Republic) on a commercial 3D fused filament fabrication (FFM) printer (Prusa i3 MK3S+ with Bondtech Extruder, Prusa Research, Czech Republic). PLA is the most common and affordable 3D printing material for FFM printing (Chiulan et al., 2017) and therefore well suited for prototyping. The 3D model was sliced using the software Prusa Slicer (Prusa Research, Czech Republic) (cf. Figure 2.5). The printing temperature was adjusted to 215 °C and the bed temperature to 60 °C. A 0.4 mm nozzle was used and the printing time of the final version was 4 h 37 min, consuming about 68 g material. No supports were needed and no post-cleaning was required.

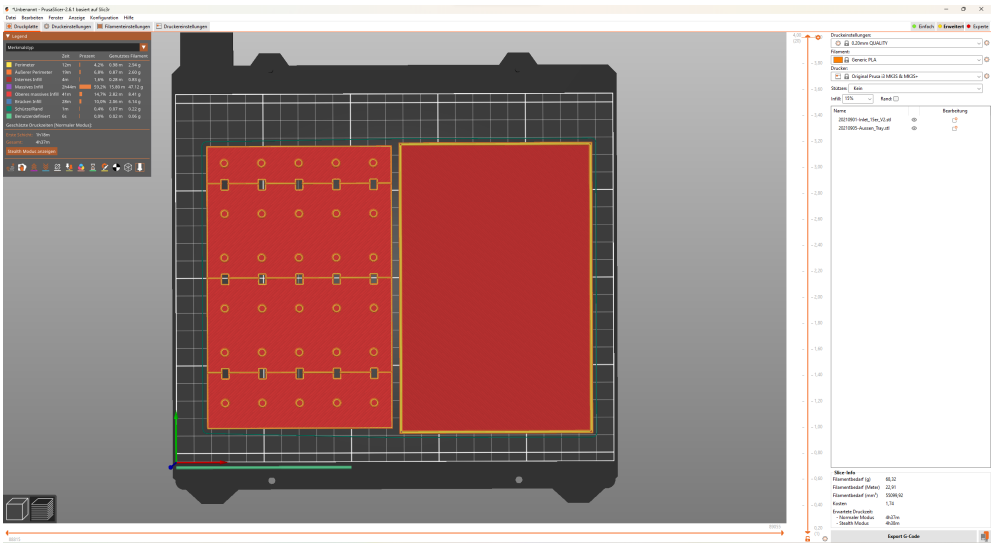

Figure 2.5: The final sample holder in in the software Prusa Slicer (Prusa Research, Czech Republic).

2.2.3 Experimental Results

The final sample holder consists of a base and a stencil (cf. Figure 2.6, number 3 and 4). The base is a thin rectangular plate on which a thin frame on the edges above the plate can hold the stencil accurately, but at the same time, leaving some space in between for inserting the sample carrier made of metal foil. The stencil is also a rectangular plate with a base that is the same height as the frame. The final version of the sample holder has a total of 15 recesses, approximately the size of the Z-300 measurement window. These are arranged in three rows of five recesses each. A ridge marks the centre of the window and runs from left to right in each row. This fits exactly into the recess next to the measurement window on the nose of the Z-300 and provides both a more stable fixation and a more targeted placement of the droplets through the recess onto the Al-foil. Above and below the recess is a cylindrical protrusion that fits into the screw holes of the Z-300, ensuring rapid focusing and securing of the pLIBS. For easy documentation, the individual measuring fields have been numbered with a waterproof pen.

Figure 3.1 shows the final method described in Schlatter and Lottermoser (2023) and Schlatter et al. (2023). First, the sample foil (Al) was surface-enhanced by a hydrophobic pencil layer. Then the foil was attached between the base and stencil of the sample holder. Next, the liquid was applied by a pipette through the recess. 0.75 μL have been used per sample in Schlatter and Lottermoser (2023) and Schlatter et al. (2023). After all samples were applied to the sample foil, the latter was removed from the sample holder and heated to dryness on a hot plate for several minutes. It was visually checked whether the droplets have evaporated. Afterwards, the sample foil was reattached between base and stencil and the analysis could be performed. The sam-

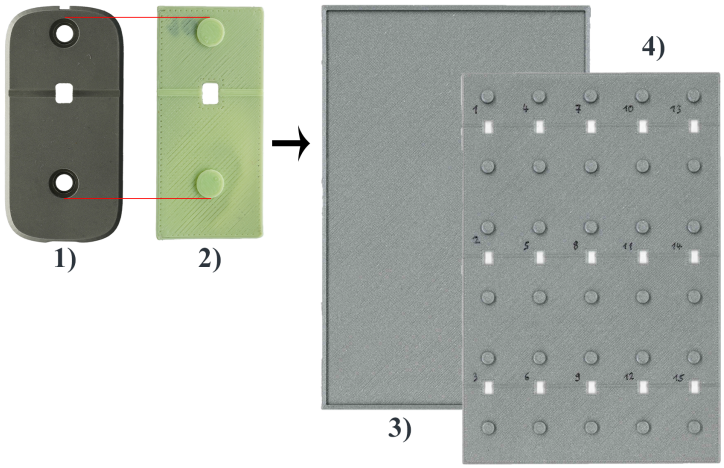

Figure 2.6: Design process of the sample holder. 1) Front element of the SciAps Z-300. 2) Prototype for fixation to the front element. 3) Base. 4) Final sample holder with 15 recesses for analysis.

ple holder ensures direct focusing on the EvR and fixation while the analysis is being carried out. There is no need for visual inspection for the EvR as these are in the same place as where the droplets have been placed.

2.2.4 Discussion

General Results: The results using the sample holder are documented in Schlatter and Lottermoser (2023) and Schlatter et al. (2023). Using it significantly improved the reproducibility while the SE-LSC method enhanced the sensitivity. Moreover, it made the process faster, as there was no need for focusing. In addition, no slipping of the portable device or the sample was possible while the laser rastered over the EvR. As the Al-foil is fixed between the base and the stencil, the method can also be used in the field, where the thin foil alone would be difficult to handle. The choice of Al as a sample support is justified by its relatively high thermal conductivity, easy availability, high purity, and very reasonable price. If the analysis of Al in aqueous solutions is required, or a different metal is desired, another metal foil can be selected.

Metal instead of thermoplastics version: There is also the possibility of producing a metal version of the sample holder to make it even more efficient, as the step of removing the aluminium foil for heating will no longer be necessary. This step is necessary with the current version because PLA is a thermoplastic material that changes its shape when heated. For the production of a metal version, a metal with particularly good thermal conductivity should be chosen and the design of the sample holder should be slightly modified by using a thinner base. However, it should be tested

whether the aluminium foil can be easily removed from the metal version after analysis. This is easily done with the plastic version, as the template can be bent, allowing the base and template to be easily separated. Once removed, the stencil returns to its original shape. If this is not possible with the metal version, the base and stencil would have to be adapted to make the stencil easier to separate, e.g. with some kind of protrusion on the frame.

Adoption to other portable devices: The presented version of the sample holder perfectly fits to the SciAps Z-300. However, the market is constantly changing and new generations of portable devices such as the Z-900 series arrive. This will not be a major problem, as small design changes will allow the use on other portable instruments, as the basic layout of pLIBS and pXRF instruments remains the same (Lemière and Uvarova, 2020).

2.3 Construction of a Hot Plate for Field Use

Key question:

- How can the process of evaporation also be carried out in the field?

In order to be able to use the developed method in the field, as planned, it is necessary to evaporate the droplets in-situ. However, typical laboratory hot plates need to be connected to a power supply and have a high power consumption. Transporting a strong power supply such as a car battery would limit portability which is essential to the method. However, most functions of such hot plates are not required for the purpose of this work. For example, stirring is not required and adjustable temperatures up to 300 °C are not necessary. Therefore, a lightweight prototype of a field hot plate has been designed using commercially available batteries and a simple heating element. It consists of relatively basic components:

- One circular Cu-plate of 10 cm in diamater
- One heating element (Thermo Tech, 12 V/DC, 15 W)
- Heat protection for the housing of the hot plate (one sandstone core)
- 3D printed upper part of the housing
- One two-pole lustre terminal
- One battery housing with a switch and cables
- Eight AA batteries (1.5 V each)
- 3D printed base of the housing

Figure 2.7 displays the prototype of the field hot plate, weighing approximately 520 g and measuring 13 * 13 * 3.8 cm. The 3D printed housing holds the different components. It was designed in a CAD Software (Fusion 360, Autodesk, San Rafael, USA) exported as .stl file, sliced using the software Prusa Slicer (Prusa Research, Czech Republic), and printed on a commercial 3D FFM printer (Prusa i3 MK3S+ with Bondtech Extruder, Prusa Research, Czech Republic) using PLA.
To keep the heat transfer to the housing low, a spacer is embedded in the housing. In the prototype, this consists of a short sandstone core which supports the Cu plate. The heating element is attached to the underside of the Cu plate and connected with batteries in the battery housing. To reach 12 V for the heating element, eight AA batteries with 1.5 V are connected in series. A small switch starts the hot plate and the Cu plate begins to heat up. The battery housing is located inside the casing, with a recess that

the switch can be operated from the outside.
Once switched on, the hot plate takes approximately four to five minutes to heat up, followed by a further two minutes for the droplets to evaporate. The mobile hot plate was originally designed for a smaller sample holder. Therefore, the heating element and the Cu plate are slightly smaller than the latter. In future, both should be selected slightly larger to match the whole 3D printed sample holder. With further optimisations, in combination with a metal version, the base could be integrated directly into the hot plate, replacing the Cu plate to allow evaporation and measurement to take place without moving the base of the sample holder. This would create an all-in-one solution. For a measurement, the Al-foil would then have to be inserted, the stencil placed over it, the drops applied, evaporated and then the TDS measured with the LIBS.

(a) **(b)** **(c)**

Figure 2.7: Prototype of a field hot plate. **a)** The hot plate is shown on the 3D printer used. **b)** The hot plate is shown in more detail. The recess to the right of the centre allows access to the switch and prevents accidental activation **c)** The hot plate's internal structure is shown, with the battery case visible on the left.

2.4 Creating a Spreadsheet for Calibration and Analysis

Key questions:

- How can calibration be managed using a spreadsheet?
- How can the developed calibrations be used to analyse unknown samples?

Due to the limitations of the Profile Builder software described in Section 2.1.4, an spreadsheet was created to process and evaluate the measurement data for calibration and unknown samples. IR were calculated in the Profile Builder software and exported as .csv files. These were imported and further processed in the spreadsheet file, which consists of several spreadsheets (cf. Table 2.2):

Table 2.2: Explanation of the individual spreadsheets.

Name	Explanation
Inf:	Basic information on how to use the spreadsheets is provided. It also displays the meta data of the analysis and lists the abbreviations used.
Cali:	An overview of the statistics of the calibration curves is provided.
Curves:	The different calibration curves are plotted for all elements over the different concentration ranges.
SD:	SD and RMSE values are calculated for different concentration ranges.
IR in:	The IR values for the calibration are inserted.
IR-blank:	The mean of the blank values is subtracted from the IR values to subtract the background.
IR cache:	Values are prepared for "IR-blank" so that they can be plotted.
Medi IR:	Median IR values are calculated from *"IR-blank"*.
Mean IR:	Mean IR values are calculated from *"IR-blank"*.
C:	The predicted concentrations are calculated based on the different calibrations listed in *"cali"*.
Medi c:	The median values of the predicted concentrations are calculated.
Mean c:	The mean values of the predicted concentrations are calculated.
Anal in:	IR values of unknown samples can be inserted in *"anal in"* to analyse a sample.
Anal-bl_1:	Blank IR values are subtracted from inserted IR values.
Out (bl1):	The final results of the analysis can be found here.

These spreadsheets not only allow calibration, but also statistical evaluation of calibrations and analysis of unknown samples. To enable other users to use the file, detailed documentation have been included within the file, which can be found in the digital appendix.
For calibration, first, the IR values are added in *"IR in"*. The first column contains the predicted values. The IR values are then added column-wise, organised by elements and assigned to the corresponding predicted values. Next, outliers are eliminated by the 1.5 inter-quartile range method. At the top section of this spreadsheet, the IR

values of the blank values are added and median, mean, and SD are calculated for all EoIs. In *"IR-blank"*, the mean of the blank values is subtracted from all IR values. The values in *"IR cache"* are copied from *"IR-blank"*, and *"NV"* is added to empty cells in order to enable plotting in diagrams. The next two spreadsheets calculate median and mean values per predicted concentration of every EoI. Median values are utilised to create the calibration curves, with the IR values from the *"IR cache"* spreadsheet also incorporated on the plots. Multiple calibration curves were constructed for one EoI due to the inability to use linear fits across the entire concentration range. However, for certain concentration ranges, particularly with higher concentrations, there was a requirement for exponential, polynomial or potency fits. The obtained formulae have been transferred to the *"cali"* spreadsheet, including the coefficient of determination (R^2) values. A distinction was made between an ultra-low concentration range, a low, a medium and a high concentration range. However, these were determined individually for each element, as different slopes of the calibration lines were determined. The defined ranges can be located within Rows 64 to 68 in the spreadsheet titled *"cali"*. Formulas for the different concentration ranges were applied depending on the predicted value and were highlighted with different colours. With the latter three spreadsheets of the document, it is possible to plot predicted against prepared concentrations to test the calibrations. Furthermore, the spreadsheet *"SD"* analyses the results and standard deviation (SD), from which RMSE values can be calculated for different concentration ranges. The measure of the differences between true and predicted values are also represented in spreadsheet *"cali"*. In the latter, RSD values are also calculated based on the SD values. Moreover, the limit of detection is determined by different formulae. The 3σ-IUPAC criterion, as outlined by IUPAC (1976), is the most widely used and thus adopted in subsequent publications.

The stored calibrations for each EoI can be applied within the same document to analyse IR, using identical measurement settings. The IR values simply need to be added to the *"anal in"* table. Thresholds enable the selection of the appropriate calibration curve, if there are several concentration ranges for a given EoI. The background is automatically subtracted in *"anal-bl"* and the results are subsequently displayed in the *"out (bl1)"* spreadsheet.

The hydrochemical diagrams presented within this work were created using a spreadsheet according to the manual found in Schäffer (2018). The method described within this thesis is a simple way of plotting hydrochemical measurement data, which typically comes in a tabular form. Data is directly plotted onto Stiff or Piper diagrams within a spreadsheet without the need for additional software. This not only eliminates the need to purchase additional software, but also an elaborate preparation of the data for another software (Schäffer, 2018).

The basis for the creation of the Piper diagrams is the use of a pre-built blank diagram which is placed under a hidden Cartesian coordinate system. By automatically converting the measured values into coordinates, the measured data is then plotted onto the diagram. For more detailed information on the individual calculation steps and the more detailed description of the creation, please refer to Schäffer (2018).

In the present work, the calculations for the diagrams were not changed. Additions were only made in the calculation of the ion balance and in the calculation of the species types of carbonic acid. On the one hand, this makes it possible to include

further anions and cations in the ion balance and, on the other hand, the exact species distribution is calculated at the measured pH value and temperature.
The Stiff diagrams also uses the conversion of measured values into coordinates, but they do not require any prefabricated diagrams in the background. For higher resolution export, the freely available add-in Daniels XL Toolbox was used (Kraus, 2014). It allows to change colour models, resolution, and file types when exporting plots.

Chapter 3

Application and Evaluation

The findings of the literature review (Chapter 1) and the method development (Chapter 2), concerning the elemental analysis of aqueous solutions using pLIBS, are put into practice and assessed on samples within this chapter. Section 3.1 presents the evaluation of the final method on standard solutions of three elements. The next section is dedicated to the application on natural waters with an extended set of elements (Sect. 3.2). The last section of this chapter provides a perspective for the analysis of PTEs (Sect. 3.3).

3.1 Quantitative Analysis of Li, Na, and K in Single Element Standard Solutions Using Portable Laser-Induced Breakdown Spectroscopy (pLIBS)

The content of this section was originally published in the Journal Geochemistry: Exploration, Environment, Analysis (GEEA) under the title: *"Quantitative analysis of Li, Na, and K in single element standard solutions using portable laser-induced breakdown spectroscopy (pLIBS)"*. Key questions have been added and some minor typesetting and layout work have been done.
DOI: 10.1144/geochem2023-019 (Schlatter and Lottermoser, 2023).

Received: 4 March 2023; **Revised:** 13 April 2023; **Accepted:** 13 April 2023; **Published:** 26 May 2023

Authors: Nils Schlatter and Bernd G. Lottermoser

Keywords: handheld LIBS; inorganic water analysis; SciAps Z-300; surface-enhanced; liquid-to-solid conversion; light alkali elements; monitoring

Key questions:

- Is it possible to quantitatively determine Li, Na, and K in aqueous standard solutions using pLIBS?
- Is the developed surface-enhanced liquid-to-solid conversion technique suitable?
- Is it possible to create linear calibration curves?
- What are the detection limits achieved for the three elements?
- Which concentration ranges can be analysed?
- What is the effect of surface enhancement on the spread and shape of the evaporation residue?
- Does the surface enhancement improve sensitivity or reproducibility?
- How do the findings compare with other methodologies detailed in the literature?

3.1.1 Introduction

Today, common practice in quantitative water analysis is to measure on-site parameters like water temperature (T), pH, EC, hydrogen carbonate content, and sometimes E_h directly at the place of sampling as these parameters can change upon sample transport and storage (Coldewey and Göbel, 2015). Thereupon, the collected water samples have to be filtrated, sealed, and stored in a cool place to prevent changes in their chemistry due to precipitation (Coldewey and Göbel, 2015). Afterwards, they are transported to a laboratory for further analyses using ion-exchange chromatography (IC), atomic absorption spectroscopy (AAS), and/or inductively coupled plasma mass spectrometry (ICP-MS) techniques. Such laboratory analyses are costly, time-consuming, and not always feasible, especially if samples are taken in remote places and cooling cannot be ensured, preventing the necessary rapid analysis. Consequently, there is a need for a fast, quantitative measuring device for use in the field (Mukherjee et al., 2021).
For a few years now, portable laser-induced breakdown spectroscopy (pLIBS) has been established for different geological applications e.g. in-situ Li quantification in rocks and minerals (Fabre et al., 2022; Wise et al., 2022), in-situ slag analysis (Schilder et al., 2021), geochemical imaging of rocks (Lawley et al., 2021), and geochemical fingerprinting (Pochon et al., 2020). With laser-induced breakdown spectroscopy (LIBS) it is theoretically possible to analyse the whole periodic table with very little sample material and in a very short time (Senesi, 2014; Lemière and Uvarova, 2020; Senesi et al., 2021).
In contrast to solid materials, there are some physical constraints when measuring

liquids with LIBS such as energy losses due to evaporation of the liquid (Lazic and Jovićević, 2014; Bhatt et al., 2020b; Zhang et al., 2021b), cooling of the plasma due to hydrogen (Lazic and Jovićević, 2014) and intense splashing (Bhatt et al., 2020b). All in all, this leads to poorer detection sensitivity and accuracy (Zhang et al., 2021b). This could be one reason why LIBS has never been used for in-field water analysis by now. However, a lot of research has been done to analyse liquid samples with LIBS in the laboratory, with very different approaches and limits of detection (LoD) in the trace element range (Cremers et al., 1984; Yueh et al., 2002; Zhao et al., 2010; Lee et al., 2011, 2012; Aguirre et al., 2013; Cahoon and Almirall, 2012; Bae et al., 2015; Yang et al., 2018; Ma et al., 2020a; Nakanishi et al., 2021; Skrzeczanowski and Długaszek, 2022; Tian et al., 2022). A very comprehensive overview of different methods applied to the analysis of liquids with LIBS can be found in the literature (Harun and Zainal, 2018b). Many of these proposed methods provide reproducible results with low LoD, but most of them use complicated experimental set-ups, for example, measuring in liquid jet (Yueh et al., 2002; Nakanishi et al., 2021) or liquid-to-aerosol (Cahoon and Almirall, 2012) which cannot easily be adapted for field use. Therefore, not only a portable device with a simpler measurement setup is needed, but also the method of sampling and analysis must be adapted.
The aim of this study is to establish whether pLIBS combined with a surface-enhanced (SE) liquid-to-solid conversion (LSC) method can quantify light alkali element concentrations in standard solutions. The three alkali metals Li, Na, and K were selected as an example because the latter two are typical cations in natural waters (Wisotzky et al., 2018) and Li is becoming increasingly important due to its use in Li-ion batteries (Goldberg et al., 2022b). Results of this study show that pLIBS is well suited for the quantitative analysis of light alkali metals in single element standard solutions. Hence, this study contributes to the development of a method that may be used for comprehensive analysis or screening of cation concentrations of water samples in the field.

3.1.2 Materials and Methods

Instrumentation

In this study, the pLIBS analyser SciAps Z-300 was used. It contains a pulsed Nd:YAG Class 3B laser, which produces a laser light with a wavelength of 1064 nm and an energy of 5 – 6 mJ/pulse with a duration of 1 ns (Wise et al., 2022). The firing rate can be adjusted by the user within the range of 1 to 50 Hz. The emitted light is detected in the spectral range from 190 to 950 nm on three spectrometers consisting of time-gated CCD (Wise et al., 2022). By default, the light is collected after a gate delay (t_d) of ca. 650 ns over a 1 ms integration time. This parameter can be changed by the user to improve the results. In this study, a t_d of 2 μs was used (see Section 3.1.2). Two databases for spectra are implemented for the analysis of emission lines: one based on the National Institute of Standards and Technology (NIST) and one by the manufacturer. Within the spectral range between 190 and 950 nm, every element has

at least one emission line and the database of SciAps is adapted on the device (Wise et al., 2022). The Z-300 can also operate with an argon atmosphere, if Ar-cartridges are inserted in the handle. This enhances the signal intensity and increases plasma temperature and electron density (Scott et al., 2014; Wise et al., 2022). Another feature of the Z-300 is the ability to create a grid pattern. This is made possible by an integrated XY table and enables the user to create elementary heat maps or to calculate the average concentration per area (Lawley et al., 2021).
For better reproducibility when shooting different locations in one analysis, a self-designed stencil, fitting the nose of the SciAps Z-300, was made using a 3D printer (see Fig. 3.1). It is supported by a base where the substrate for LSC can be placed in between. Joined together, the result is a lightweight sample holder, which can also be used in the field. The substrate in between can be removed and reinserted after evaporating the sample solution to be analysed, without a change in the locations, because a thin metallic foil adapts itself to both the base and the stencil. The template has several small recesses through which the sample solution can be applied and through which the evaporation residue (EvR) can later be analysed with the laser. To hold the pLIBS firmly in place during a measurement, there are two cylindrical elevations above and below the measurement window that fit into the screw recesses of the nose of the Z-300. Furthermore, slightly above the centre of the measurement window, there is another linear, horizontal elevation that fits into a recess in the nose of the Z-300 and, at the same time provides an indication of where the droplets must be placed.

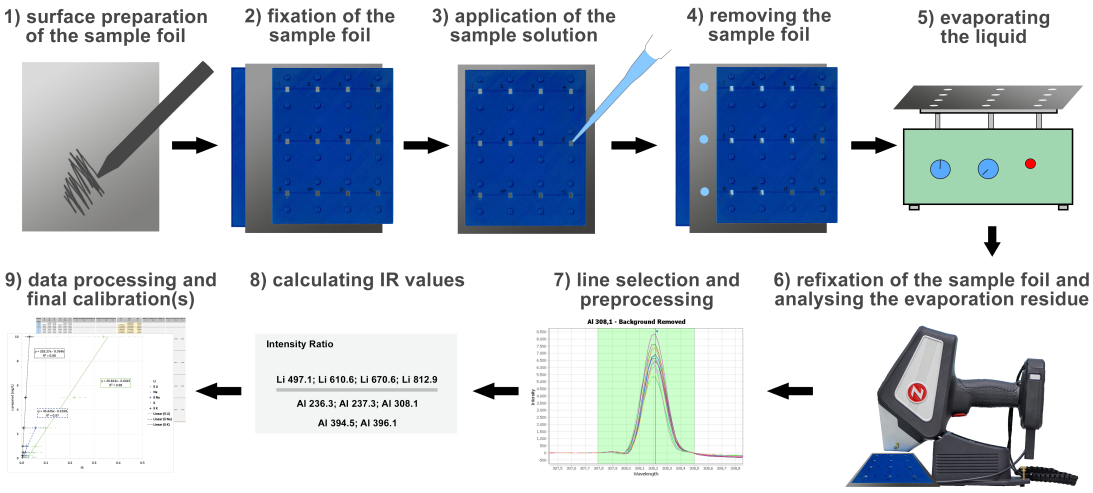

Figure 3.1: Step by step procedure for quantitative analysis of Li, Na, and K in single element standard solutions using handheld laser-induced breakdown spectroscopy.

Development of the Method

The development of the method described below includes the measurement of the EvR, which corresponds to the total dissolved solids (TDS) of a solution as long as all undissolved components, such as colloids, have been filtered out. There are two reasons for this analytic approach. Firstly, solids are easier to analyse with LIBS than liquids. Energy losses caused due to vaporisation of the liquid (Lazic and Jovićević, 2014; Bhatt et al., 2020b; Zhang et al., 2021b), cooling of the plasma by hydrogen (Lazic and Jovićević, 2014), and intense splashing (Bhatt et al., 2020b) lead to poorer detection sensitivity and accuracy (Zhang et al., 2021b). This is why a lot of research has been conducted to solve these problems with different approaches (Cremers et al., 1984; Yueh et al., 2002; Zhao et al., 2010; Lee et al., 2011, 2012; Aguirre et al., 2013; Cahoon and Almirall, 2012; Bae et al., 2015; Yang et al., 2018; Ma et al., 2020a; Nakanishi et al., 2021; Skrzeczanowski and Długaszek, 2022; Tian et al., 2022). A very comprehensive overview of different methods applied to the analysis of liquids is given in the literature (Harun and Zainal, 2018b). Many of these proposed methods provide quantitative results at the μg/L scale, but this work aims to present an easy-to-apply method with a pLIBS, which can later on also be used in the field. Therefore, complicated experimental set-ups for example measuring in liquid jet (Yueh et al., 2002; Nakanishi et al., 2021) or liquid-to-aerosol (Cahoon and Almirall, 2012) cannot be implemented.
The second reason for analysing the TDS instead of the solution, is to enhance the sensitivity of the method. Before very accurate ICP-MS analyses with a LoD well below μg/L were available, pre-concentration was the method of choice to obtain results for very low concentrations of analytes in solutions. Also, a very extensive overview of different pre-concentration methods can be found in the literature (Harun and Zainal, 2018b). One of these is the liquid-to-solid conversion (LSC), which uses the deposition on a non-absorbent metal substrate (Aguirre et al., 2013; Yang et al., 2018; Ma et al., 2020a).
Using a metallic substrate to analyse microdroplets with LIBS has several important advantages: it results in a rapid thermal equilibrium between the atoms to be determined and the plasma (Aguirre et al., 2013; Kocot et al., 2016). Furthermore, the interaction with the metallic surface generates high temperatures and high electron densities, which leads to an improved signal (Aguirre et al., 2013; Kocot et al., 2016). As suggested by other authors, Al in the form of thin foil was used as a substrate because it does have the most spectral lines in the 200 – 450 nm range, which avoids overlapping with most metals (Zhao et al., 2010). Moreover, due to the manufacturing process of Al-foil, it is usually relatively pure, readily available, and affordable (Zhao et al., 2010). The properties of Al being a good thermal conductor and forming a passivating oxide layer are also positive for the desired application.
Nevertheless, there is a problem with the non-homogenous droplet distribution on a metal surface like Al and consequently the shape and homogeneity of the EvR (Jijón and Costa, 2011; Bae et al., 2015; Yang et al., 2018; Ma et al., 2020a; Tian et al., 2022). The reasons for this are relatively hydrophilic surface properties of Al and the low surface tension of liquids, especially at higher impurities and temperatures, which lead to widespread EvR (Ma et al., 2020a). One approach to solve this problem is to apply

the droplets to the metal surface through a filter paper (Yang et al., 2018) and another is to restrict the droplets with a geometric barrier (Ma et al., 2020a; Tian et al., 2022). Furthermore, it is possible to increase the hydrophobicity of the surface. A thin pencil layer helps the distribution of water droplets, because pencil lead consists mainly of non-polar components such as clay and wax, leading to a highly hydrophobic surface (Jijón and Costa, 2011; Black et al., 2006). When drying, the distribution of the EvR is more uniform and narrow with this hydrophobic layer (Black et al., 2006). In this work, both geometric restriction and the use of filter paper were omitted in order to keep preparation time and substrate costs low. Instead, the surface was made more hydrophobic by adding a pencil layer. Hence, a soft graphite pencil (Pitt Graphite crayon, 9B by Faber Castell) was used to prepare the surface of the Al-foil by painting it with light pressure, which is termed surface-enhanced (SE) (see Fig. 3.1, step 1). Sample solutions were applied on the substrate as droplets from an Eppendorf Research® plus 0.1 - 2.5 μL pipette (see Fig. 3.1, step 3). Droplets of 0.75 μL fitted best in size with the used grid size (see Section 3.1.2).

Sample Preparation

Three aqueous single element AAS standard solutions with a concentration of 1000 mg/L in 2 % nitric acid were used for the calibration (ROTI®Star, Carl Roth, Karlsruhe, Germany). Sixteen different concentrations ranging from 0.1 to 1000 mg/L were prepared from each of the standard solutions by diluting it with 2 % nitric acid (diluted from ROTIPURAN® $\geq$65 %, Carl Roth, Karlsruhe, Germany). Distilled deionised water (18 MΩ) was used for dilution of the nitric acid.

Acquisition Settings and Analysis

To obtain reproducible results, the acquisition settings used for the analysis must always be identical. Settings used in this study have been empirically determined in various test series. In contrast to other authors (Aguirre et al., 2013; Ma et al., 2020a), not a specific spot or a small area of the EvR was analysed, but the entire surface of the dried droplet by using the ability of the device to create a grid pattern. A number of 100 locations in combination with the step size of 25 μm was used to scan the whole EvR of the former droplet and a small area around it. An area of ca. 6 mm^2 (2.5 * 2.4 mm) was analysed. The mean diameter of the EvR was about 1.7 mm, giving an area of 2.27 mm^2, assuming that it is perfectly circular. As the number of shots averaged has to be at least four, the same number was chosen for the data shots per location in order to average each of the 100 locations. Cleaning shots are possible with the SciAps Z-300 (Lawley et al., 2021), but are not necessary as standard solutions were analysed. Therefore, the input value used was zero. With changing the IID, gating can be applied. In a quantitative analysis, it is advisable to use gating, since continuum radiation is mainly emitted from the very beginning, which does not provide any viable information about the chemistry. On the contrary, this even worsens the SNR (Zhang

et al., 2022). When gating is applied, an IID of 19 is the default value in the SciAps Z-300, which corresponds to 645.2 ns. The formula for calculating the delay time (t_d) on the SciAps Z-300 is (SciAps, 2021):

$$t_d(ns) = 250 + 20.8 * \text{IID} \tag{3.1}$$

An ungated use (IID = 0) will therefore lead to a delay time of 250 ns. In this study, an IID of 84 was chosen (t_d = 1997.2 ns $\approx$ 2 μs) due to the results of a test series with twelve different delay times ranging from an IID of 0 to 130 (t_d = 250 – 2954 ns).
For all pre-tests, a standard concentration of 1000 mg/L was chosen to get the highest signals possible, and all other acquisition settings than IID were kept the same. An IID of 84 seemed to fit best for all three elements at the chosen concentration, as the relative concentration of the elements increased up to 84 and possibly reached a plateau with longer IIDs. Too long delay times must be avoided in order to prevent losing the signal.
The atmosphere in which the analyses are carried out has a significant influence on the observed spectra. This is because the atmosphere affects the plasma temperature, the electron density, the mass ablation, and the shielding of the plasma (Scott et al., 2014). The latter in turn influences the emission intensity and peak resolution (Scott et al., 2014). Using an argon atmosphere instead of normal air enhances the signal intensity and increases plasma temperature as well as electron density (Scott et al., 2014). Therefore, argon was used in this study, without changing the default argon flush.
Coordinates of the start and end positions may differ slightly from device to device and should be adjusted before use. In this study, the coordinates in combination with the step size of 25 were chosen to produce a grid size slightly larger than the size of the EvR (start location with coordinates: 100, 100, 70, and end location: 350, 350). Finally, the test rate was set to 50 Hz. For the analysis, one droplet of 0.75 μL was applied through each recess of the self-designed stencil (Fig. 3.1.2, step 3). To achieve LSC, the Al-foil was then heated on a hot plate for several minutes, and it was visually checked whether the solution had evaporated (Fig. 3.1.2, step 5). Finally, the EvR was analysed (Fig. 3.1.2, step 6).
To investigate the differences in signal intensity between SE and n-SE, eight additional analyses were performed with a 1000 mg/L Na single element standard solution, keeping all settings the same as for calibration. Four droplets were applied to SE Al-foil and four to n-SE, resulting in one single droplet for each analysis.
In order to obtain information about the spread and shape of the EvR, two series of additional measurements were carried out on Al-foil: One without surface preparation (blank Al-foil) and one SE. Sample solutions were applied as in the calibration analysis. For the two series, the GeoChem Pro App was used with a raster size of 16 * 16 and default acquisition settings to achieve heat maps (10 Hz, 256 locations, no cleaning shots, 300 ms argon flush, shots to average 1, linear averaging, and drift correction). Since the size of the EvR was within the maximum grid size of the GeoChem Pro App, focusing was done visually by means of the EvR.

Calibration Settings

LIBS analysis is particularly susceptible to so-called matrix effects. Small differences in the matrix (e.g. different concentrations of the analyte) can change the physical and chemical properties to such an extent that the intensity of the emitted signal is no longer proportional to the concentration (Legnaioli et al., 2022). To reduce the influence of possible matrix effects, multivariate calibration was performed in form of a multiple linear regression (MLR) (Legnaioli et al., 2022). All different spectral lines of the three EoIs used are listed in Table 3.1. By using the EoI as numerator and Al from the substrate as denominator, the IR were calculated. Since Al-foil was used as substrate, the intensities of Al can be used as an internal standard in the denominator to normalise the numerator (analyte) (Guezenoc et al., 2019; Legnaioli et al., 2022). Integration was done with Profile Builder by SciAps, and derivative of 0^{th} order and Savitzky-Golay smoothing were applied using seven and nine as input values for the analytes and Al, respectively. Smoothing was applied to filter out noise (Aberkane et al., 2022), allowing the values that visibly gave the best curve to be chosen.

Table 3.1: List of emission spectral intensities used for calibration

Calibration	**Li**	**Na**	**K**
Lines used as numerator λ [nm]	497.1; 610.6; 670.6; 812.9	330.1; 569.0; 588.9; 589.5; 818.1; 819.8	422.6; 691.1; 693.6; 766.6; 769.6
Lines used as denominator (Al-lines) λ [nm]	236.3; 237.3; 308.1; 394.5; 396.1		

With these settings, IR were calculated and exported as .csv file for further analyses in a spreadsheet (Fig. 3.1, step 8 & 9). The means of blank IR values of each element were subtracted from all other IR values before the resulting IRs were used to create calibration curves (Fig. 3.1, step 9). After eliminating outliers by the 1.5 inter-quartile range (IQR) method, about 12 to 25 values per concentration were used (Fig. 3.2, 3.3, and 3.4). Three linear fits were made for each element as the slope of the calibration changes with increasing concentration as effects like self-absorption increase with higher concentrations (Legnaioli et al., 2022).
For Li the three ranges were 0.1 – 10, 10 – 100, and 100 – 1000 mg/L, for K 0.1 – 10, 10 – 160, and 160 – 1000 mg/L and for Na 0.1 – 2.5, 2.5 – 100, and 100 – 1000 mg/L. LoDs for the EoI were calculated according to the 3σ-IUPAC criterion (IUPAC, 1976) and are listed in Table 3.2. Further statistical parameters like the coefficient of determination (R^2) of the calibration lines, the RMSE of the regression and the residual standard deviation based on the regression (S) are given within the three concentration ranges.

Table 3.2: Statistical assessment of the method

EoI	LoD mg/L	Range mg/L	Y	R^2	RMSE mg/L	S mg/L
Li	0.006	0.1 - 10	29.81x - 0.64	0.98	0.23	0.23
		10 - 100	38.16x - 2.84	0.99	11.22	11.38
		100 - 1000	162.52x - 398.62	0.84	102.98	104.00
Na	0.011	0.1 - 2.5	45.63x - 0.10	0.97	2.09	2.12
		2.5 - 100	189.11x - 12.35	0.96	1.20	1.36
		100 - 1000	6408.2x - 3677	0.58	229.21	231.34
K	0.007	0.1 - 10	335.27x - 0.76	0.98	1.08	1.09
		10 - 160	290.77x + 1.10	0.97	10.43	10.55
		160 - 1000	747.28x - 354.73	0.86	258.99	262.56

Limit of detection (LoD) calculated according to the 3σ-IUPAC criterion (LoD = 3*σB/k) (IUPAC, 1976), coefficient of determination (R2), root mean square error (RMSE), and residual standard deviation (S) for the three elements of interest (EoI): Li, Na, and K. σB = standard deviation of the background signal at the lowest solution concentration, k = slope of the calibration line

3.1.3 Results and Discussion

Calibration Curves

Figures 3.2, 3.3, and 3.4 show the calibration curves for the EoI with three defined concentration ranges each. Highly positive correlations are given for all EoI and across all concentrations. Table 3.2 shows the statistics of the method. LoDs, R^2, RMSE, and S are given for the EoIs in the different concentration ranges. For the lowest range, the coefficient of determination is quite high (between 0.97 and 0.98) for the three elements, whereas RMSE and S values are quite low. As expected, with increasing concentration, RMSE and S values increase and R^2 decreases. The statistics are reasonable for the medium concentration range. In the third range (100 – 1000 mg/L for Li and Na, 160 – 1000 mg/L for K), a strong dispersion of the single predicted values can be observed leading to low R^2 and high RMSE and S values.

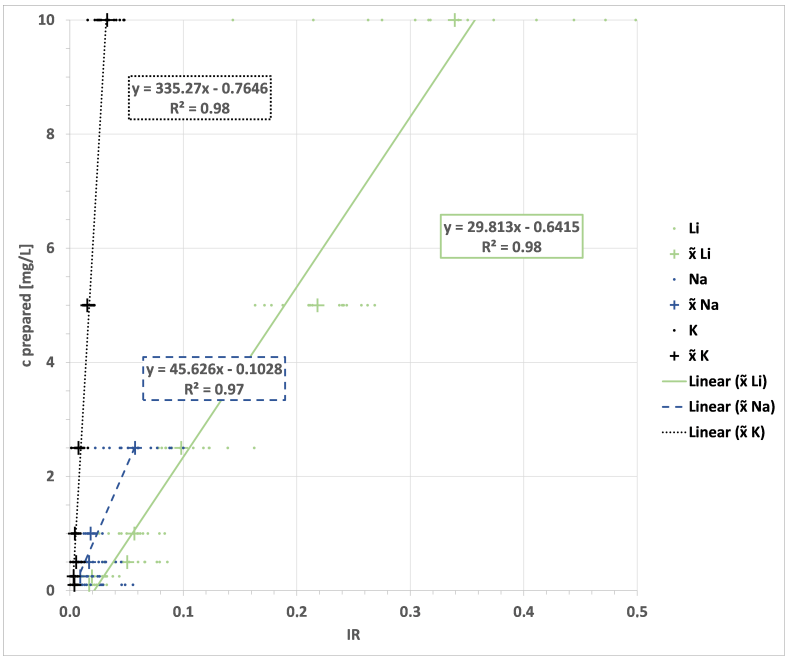

Figure 3.2: Calibration curves for Li, Na, and K between the prepared concentration and the calculated intensity ratio (IR) for the concentration ranges: 0.1 – 10 mg/L (Li, K) and 0.1 – 2.5 mg/L (Na).

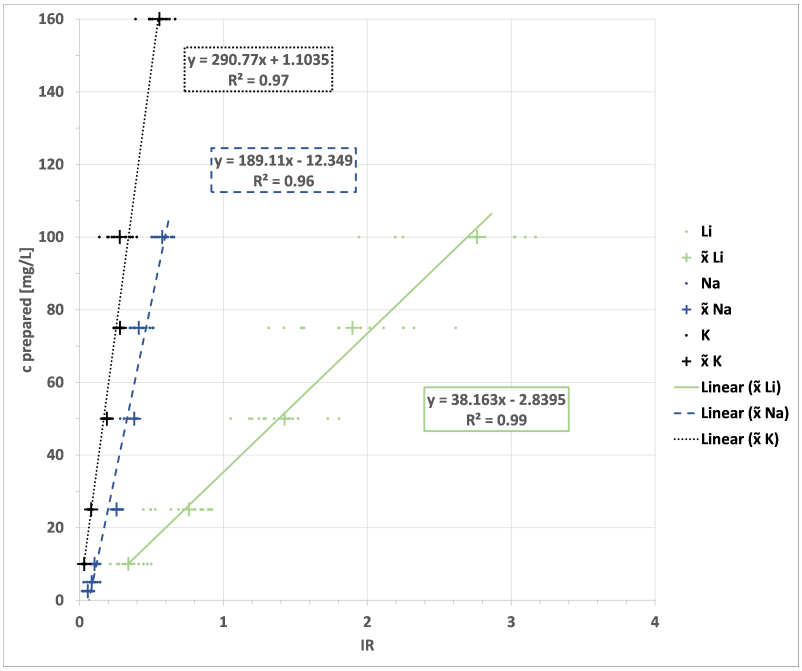

Figure 3.3: Calibration curves for Li, Na, and K between the prepared concentration and the calculated intensity ratio (IR) for the concentration ranges: 10 – 100 mg/L (Li), 2.5 – 100 mg/L (Na), and 10 – 160 mg/L (K).

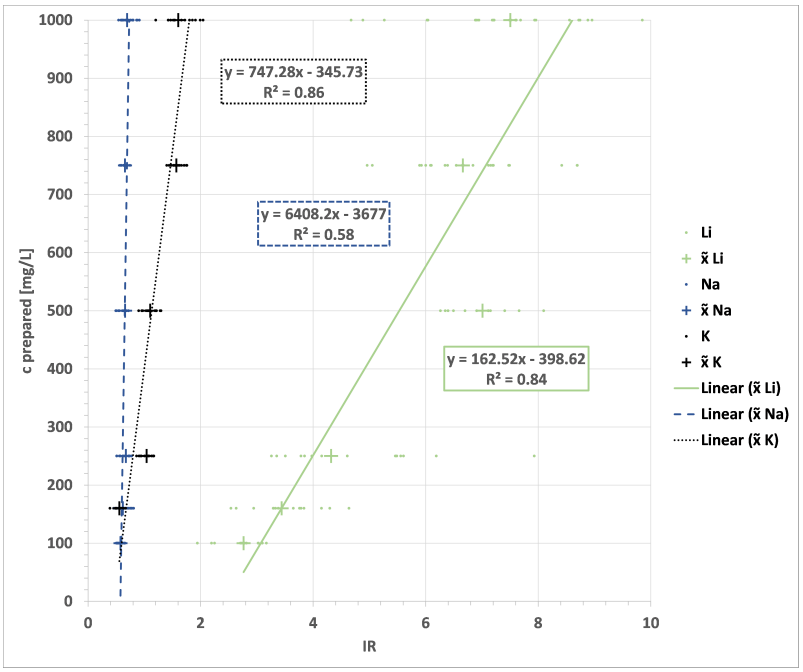

Figure 3.4: Calibration curves for Li, Na, and K between the prepared concentration and the calculated intensity ratio (IR) for the concentration ranges: 100 – 1000 mg/L (Li, Na) and 160 – 1000 mg/L (K).

Figures 3.5 and 3.6 show the calibration curves between the predicted and the prepared concentration for three EoIs based on the formulae of the calibration curves in Figure 3.2 and 3.3. The red solid lines show an ideal correlation, whereby prepared and predicted values match exactly. The other lines show the actual correlations. It can be seen that the correlation is quite high for all lines with slopes close to one. From these results, it can be stated that the calibration curves created are suitable for predicting the concentration of Li and Na in the range of 0.1 – 100 mg/L and K in the range of 0.1 – 160 mg/L.

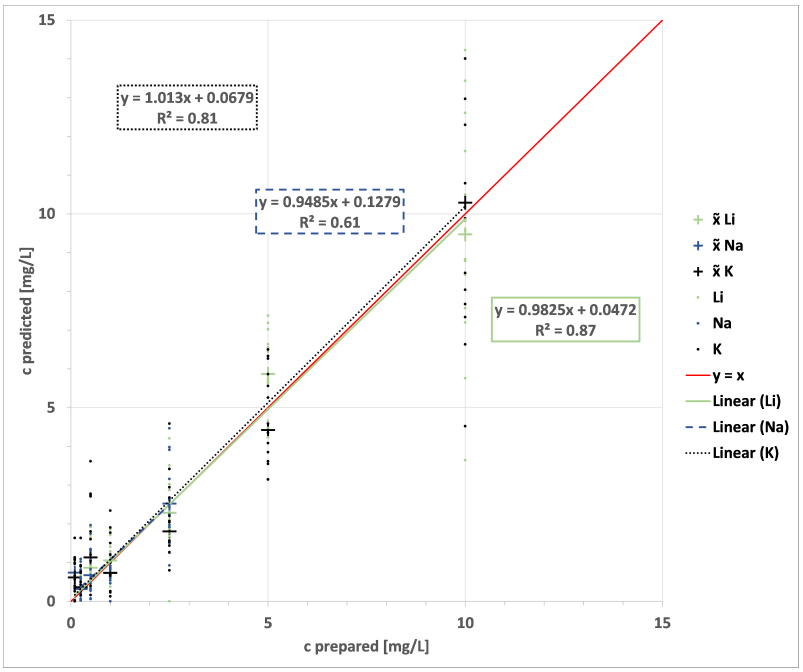

Figure 3.5: Calibration curves for Li, Na, and K between the prepared and the predicted concentration for the two concentration ranges: 0.1 – 10 mg/L (Li, K) and 0.1 – 2.5 mg/L (Na).

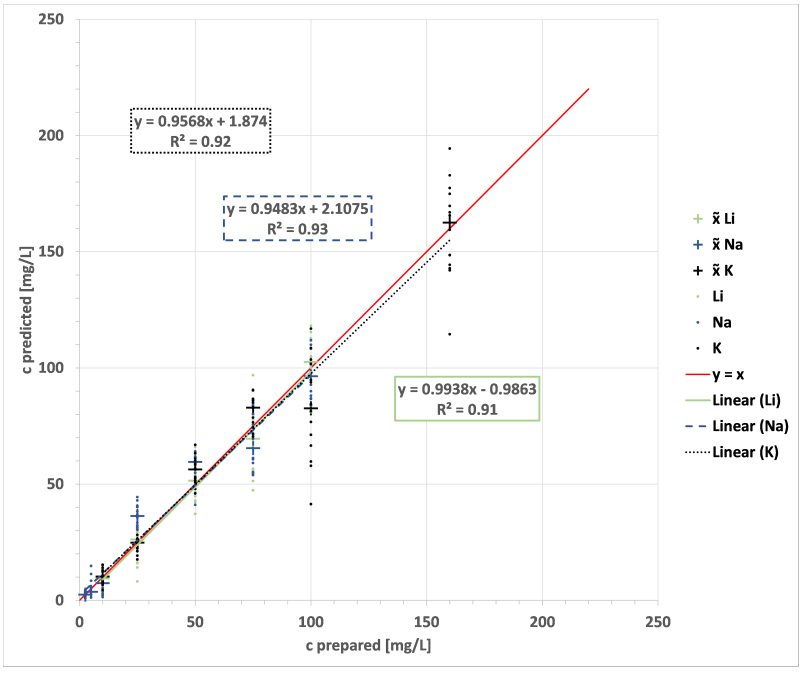

Figure 3.6: Calibration curves for Li, Na, and K between the prepared and the predicted concentration for the three concentration ranges: 10 – 100 mg/L (Li), 2.5 – 100 mg/L (Na) and 10 – 160 mg/L (K).

Spread and Shape of the Evaporation Residue

As other authors have shown, n-SE Al-foil is not well suited as a base for the application of aqueous droplets due to its low hydrophobicity, leading to irregular shapes of the EvR (Bae et al., 2015; Yang et al., 2018; Ma et al., 2020a; Tian et al., 2022; Jijón and Costa, 2011). Figure 3.7 shows two-dimensional maps of the distribution of the EvR derived from a 0.75 μL droplet on an Al-foil for different concentrations and different surfaces. In the first row, the Li distribution is shown for n-SE and for SE trials in the second row. A clear difference can be seen with increasing concentration. The EvR of the n-SE trial is distributed over a larger area, is more irregularly shaped, and the concentration distribution is more inhomogeneous in comparison to the SE method. Moreover, with higher concentrations this effect gets even worse as the surface tension coefficient is lower impacted by more impurities and higher temperature (Ma et al., 2020a). Thus, the use of blank Al-foil leads to lower accuracy and precision. It is also obvious that with the SE-method presented by Jijón and Costa (2011), the EvR produced in this work has a more uniform size and concentration distribution when a pencil layer is applied to the surface compared to n-SE (Fig. 3.7, e – h).

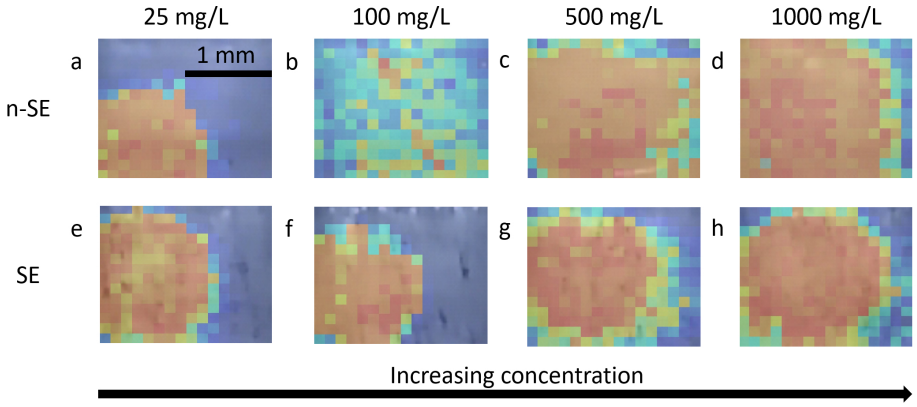

Figure 3.7: 2D maps of the spread and shape of the evaporation residue (EvR) of a 0.75 μl droplet on the substrate for different concentrations of Li in the range 25 - 1000 mg/L. Blue–violet colour indicates no detectable Li concentration and orange–red a high concentration. (a)-(d) Blank Al-foil. (e)-(h) Surface-enhanced (SE) Al-foil.

If the surface enhancement has led to a more homogeneous distribution and shape of the EvR, the signal intensities for Na should differ less with SE than in experiments without SE, as there are fewer differences in concentration per area (Bae et al., 2015; Ma et al., 2020a). In addition, the intensities should be higher with SE, since the droplets spread out further with n-SE and thus the concentration in the EvR per area is smaller (Ma et al., 2020a). At the same time, hardly any differences should be discernible between SE and n-SE in the case of Al lines, since the EvR only makes up a thin layer and no additional Al is added. To investigate this, eight analyses were carried out with the same measurement settings as for calibration with a 1000 mg/L

Na standard solution. For every single analysis a single EvR has been analysed. Four droplets were applied to SE Al-foil and four to n-SE and subsequently evaporated. Figures 3.8, 3.9, and 3.10 show the intensities of some exemplary Na and Al lines for the four independent analyses with and without SE, respectively. The variations in the signal intensity are therefore not only dependent on the fluctuations of the laser, but also on the difference in distribution and shape of the EvR. Slight differences between SE and n-SE are visible in the strong lines of Al at 394.5 and 396.1 nm (Fig. 3.8). In the SE trials, there are hardly any deviations in signal intensity between the four measurements. In comparison, a slight deviation is visible in the n-SE trials. Approximately 900 units are between the red and the green line. For the Na lines, the difference between SE and n-SE is more pronounced (Fig. 3.9). The two lines at 588.9 and 589.5 nm show no distinct variation for the SE trials. In comparison, the intensities for n-SE fluctuate strongly. The utter intensity may be higher for one analysis (the green one), but all other measurements are obviously lower in intensity and differ clearly from each other. At 818.1 and 819.8 nm, variations for the SE trials are conspicuous but the same sequence (red, yellow, green, and blue) is visible for the lines in the SE trial in Figure 3.10. At the same time, the signal intensities of the two lines in the n-SE experiments are clearly less intense and diverge more strongly. This observation is consistent with the results of Ma et al. (2020a) and Tian et al. (2022), who also observed higher intensities for the most geometrically constrained EvR and lower intensities for more widespread ones.

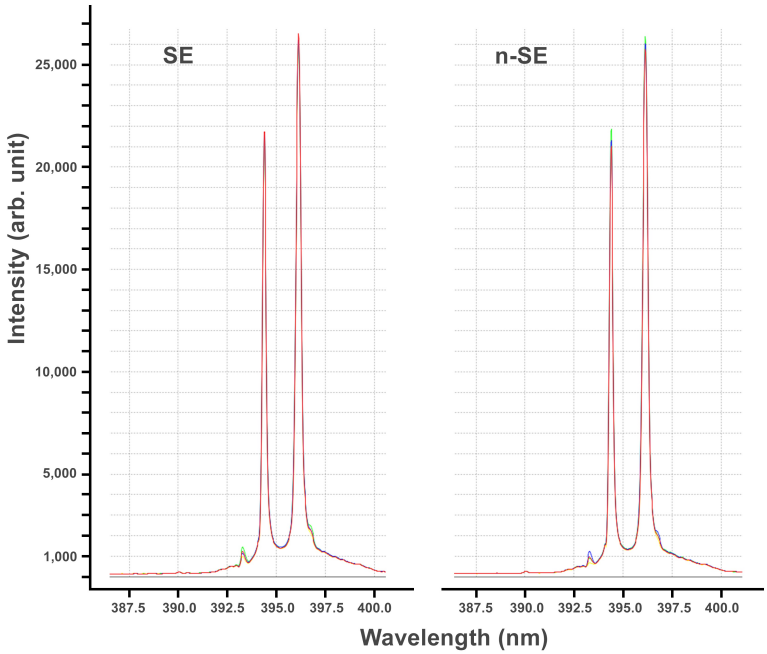

Figure 3.8: Extracts from the spectra of the analysis of four evaporated 1000 mg/L Na single-element standard solution droplets on SE (left) and four on non-SE Al-foil (right). Two strong lines of the substrate Al at 394.5 and 396.1 nm are compared for SE and non-SE trials.

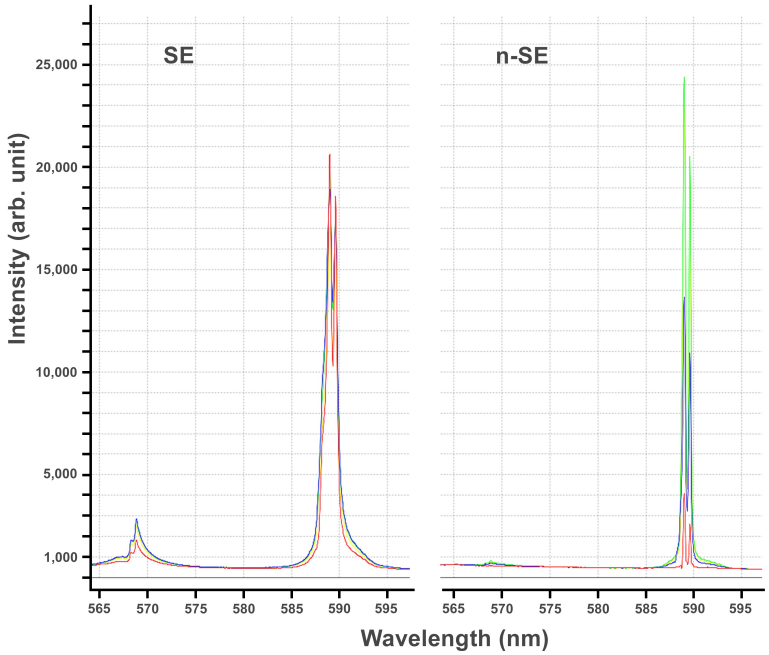

Figure 3.9: Extracts from the spectra of the analysis of four evaporated 1000 mg/L Na single-element standard solution droplets on SE (left) and four on non-SE Al-foil (right). Two strong lines of the evaporation residue at 588.9 and 589.5 nm are compared for SE and non-SE trials.

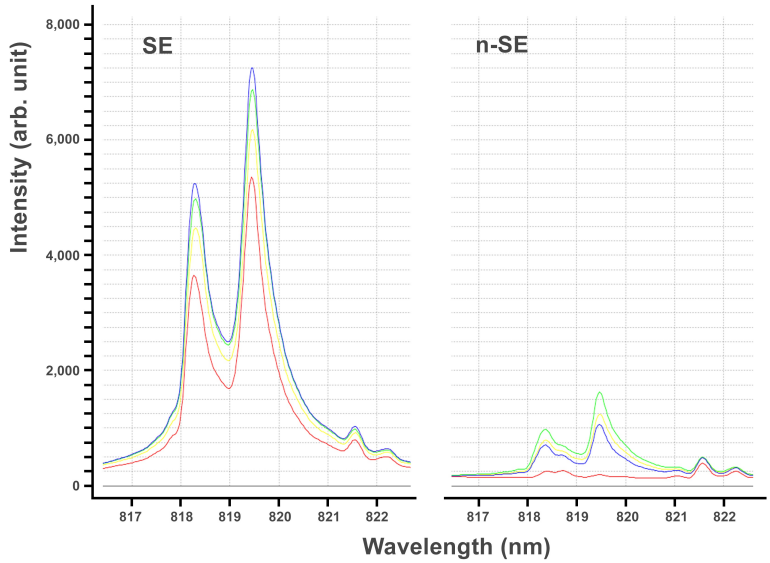

Figure 3.10: Extracts from the spectra of the analysis of four evaporated 1000 mg/L Na single-element standard solution droplets on SE (left) and four on non-SE Al-foil (right). Two strong lines of the evaporation residue at 818.1 and 819.8 nm are compared for SE and non-SE trials.

Since the intensities for Al lines are more or less the same for the SE and n-SE experiments, but not for the Na lines, it can be stated that surface enhancement leads to more reproducible results than without it. Given that the intensities of Al lines are very similar between analyses, Al is well suited as denominator in the IR, since a good internal standard should be constant between different analyses (Guezenoc et al., 2019).
As other authors have shown the use of Al as substrate leads to a signal enhancement (Aguirre et al., 2013). But surface preparation is needed to ensure the repeatability, by having an EvR with a more uniform size and concentration distribution (Jijón and Costa, 2011; Bae et al., 2015; Yang et al., 2018; Ma et al., 2020a; Tian et al., 2022). This is achieved by the thin hydrophobic layer of non-polar components such as clay and wax applied by the pencil scratches, resulting in more regular and tinier droplets, as well as in a more uniform and narrower EvR, when dried. Such an improvement has been shown before by Jijón and Costa (2011) and Black et al. (2006), but has never been used for analysis with a pLIBS. From these findings it can be deduced that the SE LSC method combined with the self-designed stencil is suitable for analysis of single element standard solutions with pLIBS for concentrations between 0.1 and 160 mg/L.
Nevertheless, with higher concentrations, R^2, RMSE as well as S deteriorate strongly (Table 3.2) which can be explained as follows: As the EvR is only a small part of the analysed area (see Acquisition settings and analysis), there is a larger expanse analysed without giving information on the concentration of the liquid. This leads to at least two Gaussian distributions for the intensities within the 100 averaged spectra in one analysis. One at a very low to zero concentration for locations, whereby only the SE-foil was analysed and one at the desired concentration, where the EvR was analysed. Therefore, the slope of the calibration curve decreases with higher concentrations. This effect has not been observed by other studies, because either only a small part of a large EvR (Jijón and Costa, 2011; Aguirre et al., 2013; Yang et al., 2018; Ma et al., 2020a) or almost the entire EvR has been analysed (Tian et al., 2022).
For low concentrations, the effect of two distributions is not noticeable. However, the higher the concentration, the more the two differ. This leads to lower accuracy and precision with higher concentrations because errors due to shot by shot variation of the signal (Guezenoc et al., 2019), homogeneity of the concentration distribution (Bae et al., 2015), and shape of the EvR (Bae et al., 2015) are amplified. The analysis of alkali metal concentrations above 160 mg/L is therefore not reliable with the current method and must be improved in further studies. Hence, variations in the area of the EvR or in the concentration distribution have to be further minimised. This could be achieved by applying the carbon, clay, and wax film by an automated process, since the surface may not be perfectly homogeneous when applied by hand. Droplet and EvR distribution may be improved this way and at the same time the more homogenous pencil layer would also affect the uniformity of the Al signal intensity upon analysis. Moreover, statistical procedures could be a solution to eliminate zero values produced by analysing the area around the EvR. However, the distribution of the droplets also depends on surface tension, which in turn depends on the temperature and the solution's content (Ma et al., 2020a). This could be another reason why the analytical data of this study vary significantly more at higher alkali metal concentrations. Influences on the droplet and EvR distribution, such as ionic strength, therefore need to be further investigated in the future when analysing natural waters.

Comparison to Other Methods

This study documents the first step in the development of an in-situ analytical technique. Further investigations, such as the application to mixed standard solutions and natural waters to analyse possible matrix effects and differences in EvR distribution, are required in the future. Nevertheless, it is necessary to compare the strengths and weaknesses with similar methods, some of which are already established.
There have been attempts to analyse the inorganic water chemistry by pXRF. This method has proven to detect and analyse different solved elements with a wide range of quantification and low LoDs (Pearson et al., 2018; Tighe et al., 2020; Tiihonen et al., 2022). For example, K, Mn, Ca, Fe, Cu, and Zn were analysed with pXRF using standard plastic sample cups filled with the water to be analysed and covered by Prolene© thin-film (Pearson et al., 2018). High coefficients of determination were achieved by using partial least squares regression (Pearson et al., 2018).
Tighe et al. (2020) developed a portable screening method for lead (Pb) in drinking water using pXRF and a simple water bottle. They pre-concentrated Pb by using an activated carbon felt in front of a filter cap and could even analyse samples below the EPA limit of 15 ppb for Pb in drinking water (Tighe et al., 2020). A specially developed filter was used in another study achieving a LoD of 0.035 mg/L for Zn by pre-concentration (Tiihonen et al., 2022).
However, the biggest problem with X-ray fluorescence is that elements with low atomic numbers (Z) like Li, Na, Mg, and usually K cannot be analysed or can only be analysed poorly (Lemière, 2018). Therefore, it is not possible to compare pXRF data with the results of this study. However, it can be assumed that other elements such as the alkaline earth elements or PTEs such as Cu, Pb, Cd, and Cr can also be analysed with the presented method. For example, Jijón and Costa (2011) have already quantified Li, Sr, Ba, and Rb using a similar surface-optimised method with a laboratory-based LIBS. Furthermore, PTEs such as Cu, Pb, Cd, and Cr (Yang et al., 2018) or the rare-earth elements (Yang et al., 2017) have already been quantified using laboratory-based LIBS and SE. In theory, it is possible to analyse any element with LIBS (Senesi, 2014; Lemière and Uvarova, 2020; Senesi et al., 2021). However, more research is needed, especially with portable devices.
Furthermore, pLIBS has not been used to date for liquid analysis, thus, laboratory and online methods are used for comparison (Table 3.3). Laboratory-based LIBS setups partly have lower detection limits for the three EoIs than the developed portable method (Lee et al., 2011). However, compared to an online setup, the LoDs achieved in this study are significantly lower (Sui et al., 2021). In addition, the measurement setups of the compared methods are partly very difficult to transfer to a portable device. Sui et al. (2021) used an ultrasonic nebuliser LIBS setup. This can hardly be adapted to a portable device like the SciAps Z-300. The same applies to the work of Lee et al. (2011), who used a nebuliser and a dual-pulse LIBS instead of a single pulse. Zhang et al. (2018) compared two different setups to directly analyse the liquid, namely liquid capillary and liquid jet mode. Both modes require a complex set-up and are not easily implemented for field use and especially not on a portable device.

Table 3.3: Comparison of LoDs of different methods analysing liquids with LIBS

Element	Device	LoD mg/L	Method	References
Li	Portable	0.006	SE, LSC, metallic substrate	This work
	Online	0.29	nebuliser	(Sui et al., 2021)
	Lab-based	0.0805	SE, LSC, glass substrate, colloidal	(Zhang et al., 2021b)
		0.0008	nebuliser, dual pulse LIBS	(Lee et al., 2011)
Na	Portable	0.011	SE, LSC, metallic substrate	This work
	Online	0.58	Nebuliser	(Sui et al., 2021)
	Lab-based	1	Capillary	(Zhang et al., 2018)
		2.1	Liquid jet	(Zhang et al., 2018)
		3.4	SE, LSC, filter paper	(Skrzeczanowski and Długaszek, 2022)
K	Portable	0.007	SE, LSC, metallic substrate	This work
	Online	0.95	Nebuliser	(Sui et al., 2021)
	Lab-based	2.8	SE, LSC, filter paper	(Skrzeczanowski and Długaszek, 2022)
		0.6	SE, LSC, silicon Wafer substrate	(Bae et al., 2015)

LoD = limit of detection; SE = surface-enhanced; LSC = liquid-to-solid conversion; for simplification, ppm values were recalculated to mg/L on a 1:1 basis

In contrast to the online setup presented in Sui et al. (2021), where sampling, nebulisation, measurement, data processing, evaluation, storage, and display of results are automated, a portable device such as pLIBS requires trained users. Therefore, operator skills are an important consideration in the application of the method presented. When developing the method, care was taken to make it as easy to use as possible. For example, the used spreadsheet can handle exported IR values and automatically calculate concentrations by selecting the correct calibration range, according to the given IR value, using predefined thresholds. Nevertheless, steps such as SE, sampling, pipetting, and evaluation with the developed spreadsheet can influence the results. Therefore, users of the method should be trained accordingly.
Using the self-designed sample holder, 15 measurements take a little less than half an hour. This means that only about 2 min are needed for an analysis with 400 laser shots. If preparation time in the form of droplet application and evaporation of the liquid is added, the time needed is still less than the 15 to 20 min described in similar research (Tiihonen et al., 2022; Zhang et al., 2022). The sample holder enables a clearly shorter measurement time due to fixed start positions of the laser that make focusing unnecessary, but it also prevents shifting during the measurement. At the same time, it also makes it possible to analyse samples with very low solution content, whose EvR would not be visible to the eye, or only with difficulty, and thus focusing would not be possible at all.
As one analysis is done with a 0.75 μL droplet, the sample quantities necessary are negligible. Even if several measurements with the same sample are desired, the sam-

ple quantity is in the µL range and thus far below the quantity required for typical laboratory methods such as AAS, IC or ICP-MS, which are typically within the mL range. Furthermore, in comparison to the methods with pXRF, there is a clear advantage of the presented method when the sample quantity is limited. For instance, 10 mL are needed for the analysis described in Tiihonen et al. (2022) and 2 L for the one in Tighe et al. (2020). The sample cups described in (Pearson et al., 2018) hold between 9 and 25 mL. This means that the required sample volume is also significantly larger here.
The costs of the developed method strongly depend on the argon consumption, which leads to costs of about 0.05 € per measurement, if Ar-cartridges are used. In addition, there are the costs for the Al-foil, the pencil and the pipette tips. The cost of the Al-foil is negligible as a few 1000 measurements are possible on a single roll and it is available for less than 2 €. The same applies to the pencil. With the pipette tips costing about 0.07 € each, the total cost of consumables is about 0.13 € per analysis. However, if a sample is measured several times, the costs are reduced by the share of the pipette tip. Compared to the method described by Tighe et al. (2020), where the consumables cost about $0.05, there is a slightly higher cost per analysis. However, compared to the method of Tiihonen et al. (2022), whose filter is 8 €, the method developed in this work is significantly cheaper. Using syringe filters to filter out undissolved substances in natural waters would add approximately 1 € per sample.
In addition, the method presented within this study requires no chemicals except for calibration, and only few consumables such as commercially available graphite pencils and Al-foil, pipette tips, and Ar-cartridges. However, if natural waters are to be analysed in the future, additional filters would be necessary to exclude all non-dissolved components such as colloids before evaporation.
Clearly, the documented analytical approach and applied materials for the quantitative analysis of single element standard solutions using pLIBS demonstrate that there is a significant potential for the further development of field-based pLIBS analysis of natural waters.

3.1.4 Conclusions

To date, pLIBS has not been evaluated whether the technique is capable of quantitative analysis of dissolved metals in waters, although laboratory LIBS instruments have already proven to be viable for trace element analysis. The aim of this study was to establish whether pLIBS combined with a surface-enhanced (SE) liquid-to-solid conversion (LSC) method can quantify light alkali element concentrations in single element standard solutions. A SE LSC method was developed and adapted to the pLIBS SciAps Z-300 resulting in detection limits significantly lower than 1 mg/L. LSC, adapted to a portable device, is a powerful method to circumvent the physical constraints, when analysing liquid samples with pLIBS, because it lowers the LoD by pre-concentration. At the same time, the surface enhancement with a pencil layer on Al-foil improves the spread and shape of the evaporation residue and leads to better droplet homogeneity.

By using a self-designed sample holder that includes a base and a stencil, between which the substrate for LSC can be placed, sample measurement time is reduced and sample shift during analysis is prevented. Moreover, it makes manual focusing superfluous, as the fixation leads to exactly the EvR being analysed. The sample holder is designed specifically for the SciAps Z-300 pLIBS, but should also work with any other pLIBS with few adjustments.
Using the method described within this paper, a very high precision for low concentrations (0.1 – 10 mg/L, or 2.5 mg/L for K) of 0.23, 2.12, and 1.09 mg/L for Li, Na, and K, respectively, was achieved. At intermediate concentrations (10 – 100 mg/L for Li, 2.5 – 100 mg/L for Na, and 10 – 160 mg/L for K), high precision was obtained for Na (1.36 mg/L) and an acceptable precision for Li and K (11.38 mg/L, 10.55 mg/L). At concentrations higher than 100 (Li, Na) or 160 mg/L (K), the method needs to be improved, because variations in EvR area and concentration distribution become increasingly pronounced at higher concentrations. Statistical analyses of the effect of the analysed area without EvR on the distribution of the averaged spectra intensities could help to improve the method in future.
Results of this study demonstrate that it is possible to use pLIBS instruments to quantify aqueous concentrations of alkali elements in single element standard solutions, provided a suitable sample pre-treatment is achieved. Thus, the results also show that pLIBS instrumentation has the potential to be further developed into a rapid, cost-effective, and simple field-based method for the quantitative analysis of metals in water samples.

3.2 Utilising Portable Laser-Induced Breakdown Spectroscopy for Quantitative Inorganic Water Testing

The contents of this section were originally published in the MDPI journal Chemosensors as an article entitled *"Utilising Portable Laser-Induced Breakdown Spectroscopy for Quantitative Inorganic Water Testing"*. Key questions have been added and some minor typesetting and layout work have been done.
DOI: 10.3390/chemosensors11090479 (Schlatter et al., 2023)

Authors: Nils Schlatter, Bernd G. Lottermoser, Simon Illgner, and Stefanie Schmidt

Received: 19 July 2023; **Revised:** 18 August 2023; **Accepted:** 26 August 2023; **Published:** 1 September 2023

Keywords: portable laser-induced breakdown spectroscopy; pre-screening; handheld; inorganic water analysis; hydrochemistry; in-field water analysis; SciAps Z-300; water-quality testing

Key questions:

- Is it possible to quantitatively determine typical cations and anions in bottled mineral water using pLIBS?
- Is it possible to create linear calibration curves for all desired concentration ranges of all selected elements?
- What are the detection limits achieved for the selected elements?
- Which concentration ranges can be analysed?
- What are the results when the calibrations are applied to mixed standard solutions with a known concentration of the elements?
- Are there any matrix effects and what is the influence of self-absorption?
- How do the results compare with other findings detailed in literature?

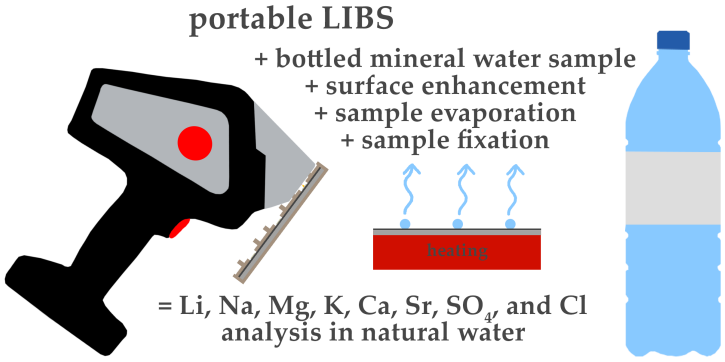

Figure 3.11: Graphical Abstract: Utilising Portable Laser-Induced Breakdown Spectroscopy for Quantitative Inorganic Water Testing.

3.2.1 Introduction

An understanding of water quality is traditionally obtained using laboratory-based analyses and continuous monitoring techniques (Zulkifli et al., 2018; Yaroshenko et al., 2020; Jan et al., 2021). This is despite the need for fast, reliable, and, if possible, inexpensive in-field measurement methods, particularly in remote regions. Although hand-held instruments like pXRF and pLIBS have been established in geochemical analyses of solid samples for many years (Lemière and Uvarova, 2020; Lemière and Harmon, 2021; Harmon and Senesi, 2021; Schlatter et al., 2022), inorganic water analyses are still performed almost exclusively in the laboratory (Yaroshenko et al., 2020). Typical equipment used includes ion chromatography (IC), atomic absorption spectroscopy (AAS), and inductively coupled plasma-mass spectroscopy (ICP-MS). These techniques require trained staff and proper sample transport, storage, and handling prior to analysis. Furthermore they are expensive to maintain and are time consuming (Tiihonen et al., 2022). This often prevents quick action, as it can take more than a week from the time the sample is taken to the actual analysis of samples and data generation. In addition, in less developed countries, analyses are less likely to be carried out due to the cost and expertise required. Therefore, reliable field instruments are needed to quantify as many elements and compounds as possible. In on-site analysis, lower sensitivity and higher detection limits are usually accepted, if immediate results and higher data density are feasible, especially if pre-screening is performed (Gałuszka et al., 2015; Lemière and Uvarova, 2020).
Typical field-ready measuring equipment for inorganic water analysis available on the market includes photometers, test kits, and ion selective electrodes. The main reason why field methods have not yet been widely adopted for measuring the inorganic chemistry of waters is presumably due to the fact that reliable methods for simultaneous determination of a range of elements have not been developed to date. Laser-induced breakdown spectroscopy (LIBS) is an atomic emission spectroscopy technique capable of simultaneously determining the complete elemental chemistry of a sample. A focused, pulsed laser beam is directed at a sample to form a plasma

containing the elements of the small sample volume that is being ablated. By spectral analysis of the emitted light, it is possible to obtain qualitative and quantitative data on the elements present, provided a suitable calibration is used (Lemière and Uvarova, 2020; Harmon et al., 2021). Although LIBS currently plays a rather niche role in water analysis, several studies have shown that laboratory-based LIBS systems can be used to simultaneously quantify almost any element in water with very low detection limits (Cremers et al., 1984; Yueh et al., 2002; Zhao et al., 2010; Lee et al., 2011, 2012; Cahoon and Almirall, 2012; Aguirre et al., 2013; Bae et al., 2015; Yang et al., 2018; Ma et al., 2020a; Nakanishi et al., 2021; Skrzeczanowski and Długaszek, 2022; Tian et al., 2022; Zhang et al., 2022). For example, Na has been quantitatively analysed in aqueous solutions with a detection limit of 0.57 μg/L (Nakanishi et al., 2021). Mg, Ca, Sr, and Ba have been detected down to 0.3, 0.6, 1.0, and 0.7 ppm, respectively (Cahoon and Almirall, 2012), and Mg, Cr, Mn, and Re have been detected down to 0.1, 0.4, 0.7, and 8 mg/L, respectively (Yueh et al., 2002).
However, many of these laboratory applications described use complicated experimental setups, such as measurement in a liquid jet (Yueh et al., 2002; Nakanishi et al., 2021) or liquid-to-aerosol conversion (LAC) (Cahoon and Almirall, 2012). This is because direct bulk liquid analysis by LIBS is prone to low sensitivity and accuracy due to energy losses as a result of liquid evaporation, plasma cooling, and intense splashing (Bhatt et al., 2020a). A simpler sample preparation method, which is also feasible in the field and adaptable to a pLIBS instrument, is the liquid-to-solid conversion (LSC). At the same time, this method offers the advantage that the detection limits are lowered by pre-concentration. Therefore, in a previous work, a surface-enhanced (SE) LSC method was adapted to a pLIBS for quantitative analysis of Li, Na, and K in standard solutions containing nearly no other cations (Schlatter and Lottermoser, 2023). Instead of directly shooting the liquid with the laser, the evaporation residue (EvR) was analysed on a commercially available aluminium foil, which was SE with a thin pencil layer. Low detection limits could be achieved by LSC while avoiding negative physical effects such as splashing and cooling of the plasma that occur when analysing liquid samples. Moreover, by preparing the aluminium foil with a pencil layer, the surface became more hydrophobic, and therefore, the EvR were distributed more homogenously, leading to better reproducibility. A self-designed template that fits on the nose of the SciAps Z-300 guaranteed fixation during the analysis of 100 positions in a fixed grid on and around the EvR. Results of the study showed that a portable LIBS analyser is well suited for the quantitative analysis of light alkali elements in standard solutions up to 160 mg/L (Schlatter and Lottermoser, 2023). To our knowledge, that was the first time that a handheld LIBS instrument had been used to quantify dissolved elements in aqueous solutions using an LSC technique. The portability of the method opens up new possibilities for on-site screening and quantitative analysis of inorganic water chemistry.
However, to date, the method has only been applied to single-element standard solutions. In order to identify possible matrix effects and to further adapt the method for field use, bottled mineral waters from different manufacturers and as diverse in chemistry as possible were chosen as examples in this study (see Figure 3.11, Table 3.4, and Figure 3.12). When using bottled mineral waters from grocery stores, it is possible to choose from a wide range of different mineralised waters, as the manufacturers in the

European Union are obliged to print analysis results on their bottles. These may often not be particularly up to date, but they provide a rough guide on the likely chemical composition of bottled waters. There has also been a lot of research into testing bottled mineral water for mineralisation (Birke et al., 2010b,a; Reimann and Birke, 2010; Demetriades et al., 2012). As can be seen in Figure 3.12, the choice of bottled mineral water allowed very different types of water to be selected. This is important in order to have a diverse test series to study possible matrix effects on.
In this study, the analytical approach of the former study by Schlatter and Lottermoser (2023) was extended to include elements and compounds (Ca^{2+}, Mg^{2+}, Sr^{2+}, Cl^-, $SO_4{}^{2-}$, and $NO_3{}^-$) to cover the main cations and anions in natural waters and documented on bottled mineral water. The results of this study therefore contribute to the ongoing development of hydrochemical field testing tools.

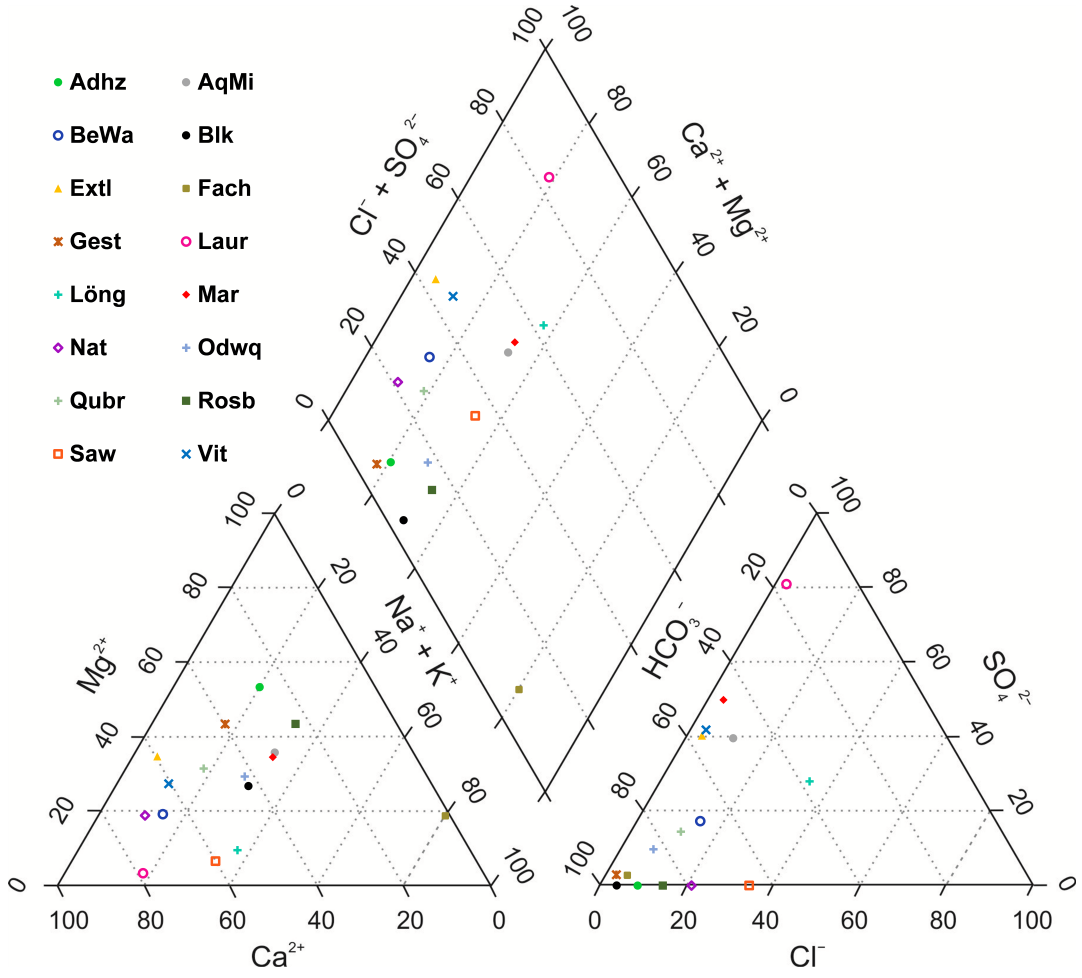

Figure 3.12: Piper plot of the bottled mineral waters. The chemical data were obtained by IC and field photometer (hydrogen carbonate) analyses.

Table 3.4: List of bottled mineral waters analysed by this study.

Abbr.	Name/Brand	Spring	Location	State	Country	Bottle	TDS mg/L	EC μS/cm
Adhz	Adelholzener	Adelholzener Alpen Quell	Bergen	BY	De	PET	511	598
AqMi	Aqua Mia	Geotaler	Löhne	NW	De	PET	1284	1575
BeWa	Bergische Waldquelle	Bergische Waldquelle	Haan	NW	De	PET	159	257
Blk	Blank sample	-	laboratory	-	-	HDPE		1.3
Extl	Extaler-Mineralquell	Extaler-Mineralquell	Rinteln-Exten	NI	De	TP	1603	1708
Fach	Staatl. Fachingen	Staatl. Fachingen	Fachingen	RP	De	glass	4306	2726
Gest	Gerolsteiner Naturell	Naturell	Gerolstein	RP	De	PET	807	878
Laur	Lauretana	Lauretana	Graglia	21	It	PET	17	20.5
Löng	K-Classic	Quelle Löningen	Löningen	NI	De	PET	162	275
Mar	Marius-Quelle	Marius-Quelle	Sachsenheim	BW	De	PET	2435	2650
Nat	Naturalis still	Urstromquelle	Wolfhagen	HE	De	PET	126	212
Odwq	Odenwald-Quelle	Odenwald Quelle	Heppenheim	HE	De	PET	760	727
Qubr	Quellbrunn Werretaler	Werretaler	Löhne	NW	De	PET	729	971
Rosb	Rosbacher Naturell	Rosbacher Naturell	Rosbach v.d. Höhe	HE	De	PET	1235	1363
Saw	Sawell	Genussquelle 3	Emsdetten	NW	De	PET	377	589
Vit	Vittel	Vittel Bonne Source	Vittel	88	Fr	PET	490	444

BY = Bavaria, NW = North Rhine-Westphalia, NI = Lower Saxony, RP = Rhineland-Palatinate, BW = Baden Württemberg, HE = Hesse, 21 = Piemont, 88 = Département des Vosges, De = Germany, It = Italy, Fr = France, PET = polyethylene terephthalate, HDPE = high-density polyethylene, TP = Tetra Pak, TDS = total dissolved solids (as indicated), EC = electrical conductivity (as measured).

3.2.2 Materials and Methods

Sample Preparation

Water samples were taken from commercially available bottled mineral waters purchased from supermarkets. Fifteen different brands were chosen, and waters with the most diverse chemistry according to their information labels were selected to obtain a diverse test series (Table 3.4 and Figure 3.12). Only non-carbonated bottled water was selected to compensate for precipitation by degassing. With two exceptions (Fach., glass, and Extl., Tetra Pak), all mineral waters were bottled in PET. Two 50 mL samples of each mineral water were prepared by filling centrifuge tubes. One was acidified with HNO_3 to prevent precipitation (cation sample). The anion sample was not prepared further. An additional blank sample was prepared from distilled deionised water (18 MΩ) in the same way as the mineral waters. A portion of each anion sample was used for the analysis of physico-chemical parameters (T, EC, pH, and HCO_3^-) and pLIBS analysis before all samples were sealed with Parafilm® and

sent directly to the laboratory for subsequent IC and ICP-MS analysis (Technical University of Darmstadt, Darmstadt, Germany). For subsequent measurements, aqueous single-element AAS standard solutions on a 2% nitric acid basis with a concentration of 1000 mg/L were used for the calibration of the cations ROTI Star©, Carl Roth, Karlsruhe, Germany). From each of the standard solutions, 16 different concentrations ranging from 0.1 to 1000 mg/L were prepared by diluting with 2% nitric acid. The latter was made by diluting 65% nitric acid (ROTIPURAN® $\geq$ 65%, Carl Roth, Karlsruhe, Germany) with distilled deionised water (18 MΩ). Li^+, Na^+, and K^+ were prepared as single-element standard dilution series. Mg^{2+} and Ca^{2+} were mixed with each other as paired standard dilution series. Concentrations above 500 mg/L were prepared as single-element standards. The same procedure was used for Zn^{2+} and Sr^{2+}. In addition, a water-based multi-element anion IC standard solution containing Cl^-, $SO_4{}^{2-}$, and $NO_3{}^-$ was used to calibrate the main anions by dilution with distilled deionised water at concentrations ranging from 0.5 to 1000 mg/L. Furthermore, mixed solutions were prepared by using the single-element standard solutions in equal amounts and diluting with 2% nitric acid. Six mixed solutions containing Li, Na, and K (ranging from 2 to 250 mg/L) and six containing Li^+, Na^+, K^+, Mg^{2+}, Sr^{2+}, and Ca^{2+} (ranging from 1 to 125 mg/L) were prepared. Cl^-, $SO_4{}^{2-}$, and $NO_3{}^-$ were not included in the mixed standards, as the cationic single element standards already contained nitrate in different quantities.

Instrumentation

As in the previous study Schlatter and Lottermoser (2023), the commercially available pLIBS analyser SciAps Z-300 (SciAps, Woburn, MA, USA) was used. It contains a class 3B Nd:YAG laser that produces laser light with a wavelength of 1064 nm and an energy of 5 – 6 mJ/pulse with a duration of 1 ns and an adjustable firing rate of between 1 and 50 Hz (Wise et al., 2022). Three spectrometers consisting of time-gated CCDs detect the emitted light in the spectral range of 190 – 950 nm by three spectrometers (Wise et al., 2022). The acquisition settings of the pLIBS analyses have been detailed in a previous study (Schlatter and Lottermoser, 2023). Due to the small size of the EvR after LSC and the possibility of laying a raster over an area with the SciAps Z-300, it was possible to analyse the whole EvR and a small area around it. One hundred locations were fired at four times each in order to obtain data. For each location, the four individual analyses were averaged into a spectrum, resulting in 100 spectra per sample. Since fresh samples were applied to the SE aluminium foil, no cleaning shots were needed, and this setting was set to zero. The use of gating can improve the SNR because the continuum radiation, which contains no useful information and occurs mainly at the beginning of a measurement, has a lower proportion with a slightly delayed measurement (Zhang et al., 2022). In the previous study, the gate delay for Li, Na, and K was optimised (Schlatter and Lottermoser, 2023). In order to obtain comparable data, the gate delay was not further adjusted in this work. An IID of 84 was used, corresponding to a delay time (t_d) of approximately 2 μs. In order to achieve signal enhancement (Wise et al., 2022; Scott et al., 2014), an Ar atmosphere was used

for the measurements. The coordinates were set to start at 100, 100, 70, and end at 350, 350. Finally, the test rate was set to 50 Hz. A custom sample holder designed for the SciAps Z-300, as described in Schlatter and Lottermoser (2023), was used to facilitate and speed up handling by securing the substrate and the device itself.

Liquid Analysis

First, the pH and EC of each bottled mineral water were determined. For this purpose, the bottled waters were poured into centrifuge tubes large enough to fit the probes of the pH and conductivity electrode. This method has already been described by Schäffer et al. (2022) and helps to reduce the required sample volume. In this study, a slightly larger sample volume of about 20 – 25 mL was used. Conductivity and temperature were measured first (CA 10141 with conductivity probe XCP4ST1, Chauvin Arnoux, Asnières-Sur-Seine, France), making sure that the probe was thoroughly cleaned with distilled water and then dried before measurement. Afterwards, the pH value was analysed with a likewise cleaned probe (HI 991002 with pH/ORP probe HI1297, Hanna Instruments, Vöhringen, Germany). Hydrogen carbonate was measured with a field-ready photometer (HI775 Checker HC, Hanna Instruments, Vöhringen, Germany) using a sample of maximum 15 mL. For the comparative measurements in the laboratory, one cation and one anion sample were prepared each, the former being acidified with 10 droplets of 10% nitric acid (diluted ROTIPURAN® $\geq$ 65%, Carl Roth, Karlsruhe, Germany) to prevent precipitation. The samples were analysed for the main cations and anions with IC at the Institute of Applied Geosciences of Technical University of Darmstadt (Metrohm 882 Compact IC plus, Metrohm, Herisau, Switzerland).
Sr and Zn were analysed using ICP-MS (Analytik Jena Plasma Quant MS Elite®, Jena, Germany). Instrumental conditions were optimised using a 1 μg/L tuning solution (diluted 10 mg/L Analytik Jena Tuning solution, Jena, Germany), leading to high sensitivities of the containing elements Be, In, Pb, and Th in the tuning solution with simultaneous low oxide and a doubly charged ion ratio. Helium was used as a collision gas in the integrated collision–reaction cell (iCRC) for the minimisation of potential interferences. A 10 μg/L Y solution (diluted ROTI® Star 1000 mg/l Y, Carl Roth, Karlsruhe, Germany) was added online via a peristaltic pump to all samples and standards in order to compensate for drifts of the ICP-MS system. Standard deviations of laboratory analyses are provided in Table 3.8.
The ion balances were calculated from the equivalent concentrations of the cations and anions according to DIN-38402-62:2014-12 (2014). High ion balance deviations are an indication that certain ions have not been recorded or have been recorded incorrectly. The algebraic sign is an indicator of whether the error could be on the anion or cation side. Another plausibility check is the calculation of the EC of a water sample from the main cations and anions (Rossum, 1949). This method was used to evaluate whether there were any inconsistencies between the measured and calculated conductivity, indicating that certain cations or anions had not been detected or had been incorrectly detected.

The underlying method for the analysis of cations and anions in water with pLIBS has been presented in detail by Schlatter and Lottermoser (2023) for the three alkali elements Li, Na, and K. Here, the SE Al-foil, prepared with a thin layer of pencil, was placed between the base and the stencil and the sample solutions were applied through the recesses using a micropipette (cf. Figure 3.13). A total of 0.75 μL of the sample solutions was applied to the Al-oil in the same way, each time with the help of an auxiliary line. This way, 15 droplets can be placed on one sample foil. After application, the Al-foil was removed and heated on the hot plate to achieve LSC until only the EvR remained. The aluminium foil was then placed back between the base and the stencil and the EvR was analysed with the pLIBS. Standard deviations and relative standard deviations of replicate pLIBS analyses are provided in Table 3.9. By securing the nose of the device, it is possible to quickly switch between the individual samples without additional focusing. In addition, the measuring device does not slip during the measurement of the 100 spots per EvR.

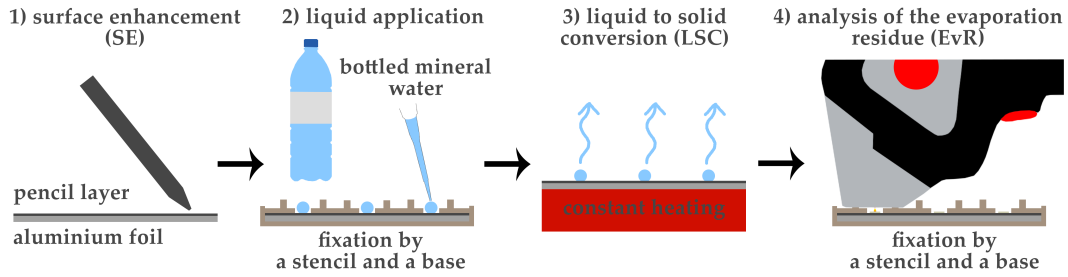

Figure 3.13: Summary of the method involving surface enhancement, fixed liquid application, liquid-to-solid conversion (LSC), and fixed analysis by portable LIBS

Calibration Settings

With the calibrations in this work, it should later be possible to examine as wide a range of differently mineralised waters as possible. It can thus be assumed that the matrices in the EvR will also vary strongly. However, even small changes in the matrix, e.g., due to different concentrations of the analytes, alter the physical and chemical properties in the plasma to such an extent that the emitted signal is no longer proportional to the concentration. This leads to so-called matrix effects (Legnaioli et al., 2022). To compensate for matrix effects, multivariate calibration was performed for all elements of interest (EoI) using multiple linear regression (MLR). Using the intensities of Al in the denominator, to normalise the numerator (analyte), adds an internal standard (Legnaioli et al., 2022; Guezenoc et al., 2019), as Al foil was used as a substrate. Intensity ratios (IRs) were calculated by using the intensities of the EoI in the numerator (analyte) and Al intensities in the denominator. The intensities chosen for both the EoIs and Al were selected to avoid a possible overlap of nearby peaks of other EoIs due to peak broadening and to maintain an equal sequence of intensities as the concentration of the analytes increases and constant intensity at

the intensities of the standard. For this reason, small changes were also made to the lines used for Li, Na, and K compared to Schlatter and Lottermoser (2023). The spectral lines used for calibration in this study are listed in Table 3.5. However, the integration was performed in the same way in SciAps' Profile Builder, applying the zeroth order derivative and Savitzky–Golay smoothing with 7 and 9 as input values for the analytes and Al, respectively, to filter out noise (Schlatter and Lottermoser, 2023).
For more extensive possibilities in calibration, the IRs were calculated with these settings, exported as a .csv file, and used in a spreadsheet for calibration. Subsequently, outliers were eliminated by the 1.5 IQR method. For most concentrations, 15 IR values were used for calibration, of which at least 12 remained after outlier elimination. Some higher concentrations were tested with up to 27 IR values. The mean of the respective IR values per element for blanks was then subtracted from all IR values. Due to effects such as self-absorption at higher analyte concentrations (Legnaioli et al., 2022), the slope of a single calibration curve over the entire concentration range (0.1 – 1000 mg/L) changes strongly. Skrzeczanowski and Długaszek (2022) encountered the same problem when analysing K, Na, Ca, and Mg in liquid solutions dried on filter paper. They had to use two calibration lines over the concentration range of 10 – 1000 mg/L (Skrzeczanowski and Długaszek, 2022). Therefore, in this work, three concentration ranges were defined for all cationic species, which were chosen differently due to the different slopes for the individual elements. Only two concentration ranges were defined for the anionic species. Wherever possible, linear calibration lines were used. For higher concentration ranges, exponential or quadratic calibrations were often required. The different concentration ranges are listed in Table 3.5. According to the 3σ-IUPAC criterion (IUPAC, 1976), LoDs for the EoI were calculated and are also listed in Table 3.5. Within the concentration ranges, other statistical parameters are given, such as the R^2 of the calibration lines, the RMSE of the regression, and the residual standard deviation based on the regression (S).

Table 3.5: Statistical assessment of the calibrations for single-element standards (Li, Na, K) and paired-element standards (Mg/Ca, Zn/Sr, NO_3/SO_4/Cl).

z	EoI	State	λ nm	LoD mg/L	Range mg/L	y	R^2	RMSE mg/L	S mg/L
3	Li	I	497.1	0.006	0.1-2.5	28.133x-0.3725	0.918	0.17	0.18
		I	610.4		2.5-100	37.973x-2.3069	0.995	6.65	6.71
		I	670.8		100-1000	$11.632x^{2.1134}$	0.954	202.18	204.19
		I	812.9						
11	Na	II	330.2	0.014	0.1-2.5	45.219x+0.0149	0.971	2.00	2.03
		I	589.0		2.5-100	184.47x-11.45	0.960	3.54	4.01
		I	589.6		100-1000	$8152.3x^{8.359}$	0.538	1131.01	1141.34
		I	818.3						
		I	819.5						
12	Mg	II	279.6	0.008	0.1-10	78.378x-0.0589	0.979	0.00	0.00
		II	279.8		10-100	173.46x-14.439	0.973	6.83	6.93
		II	280.3		100-1000	-	-	-	-
		I	285.2						

Table 3.5: Cont.

z	EoI	State	λ nm	LoD mg/L	Range mg/L	y	R^2	RMSE mg/L	S mg/L
		I	293.6						
		I	382.9						
		I	383.2						
		I	383.8						
		I	516.7						
		I	517.3						
		I	518.4						
19	K	I	691.2	0.006	0.1-10	343.08+9.4034	0.987	0.49	0.49
		I	693.9		10-160	292.55x+9.7589	0.973	10.70	10.82
		I	766.5		160-1000	$62.902e^{1.6945x}$	0.913	266.10	269.77
		I	769.8						
20	Ca	II	315.9	0.021	0.1-2.5	23.014x-0.0512	0.990	0.03	0.03
		II	317.9		2.5-100	103.34x-12.964	0.893	3.79	3.82
		II	318.1		100-1000	$-527.31x^2$+2456.7x-1766.7	0.889	155.42	157.59
		II	370.6						
		II	393.3						
		II	396.8						
		I	422.6						
		I	430.2						
		I	430.8						
		I	443.5						
		I	445.5						
		I	526.5						
		I	527.0						
		I	558.9						
30	Zn	II	202.6	0.0005	0.1-2.5	621.9x-0.1649	0.988	0.07	0.07
		I	213.9		2.5-50	544.01-0.4883	0.998	1.38	1.40
		I	334.5		50-1000	$2449.2x^2$+1115.7x-94.322	0.989	102.14	103.02
		I	468.0						
		I	481.1						
		I	636.2						
38	Sr	II	215.3	0.0008	0.1-5	38.764x+0.0607	0.999	0.14	0.14
		II	216.6		5-75	$136.68x^2$-0.3885x+3.2393	0.998	7.64	7.74
		II	338.1		75-1000	$6.1616e^{3.7x}$	0.851	4708.79	4754.73
		II	407.7						
		II	416.2						
		II	421.6						
		II	430.6						
		I	460.7						
		I	496.2						
		I	525.7						
		I	548.1						
7	N	II	567.6	0.002	0.5-160	2014.3x	0.853	105.13	105.97
		II	568.6		160-1000	$100.07e^{7.0029x}$	0.872	195.30	197.96
16	S	I	921.2	0.0002	0.5-160	175098x+106.97	0.647	93.42	94.12
		I	922.8		160-1000	$109.42e^{2043.1x}$	0.829	621.23	629.69
		I	923.7						
17	Cl	I	833.3	0.0004	0.5-160	33588x	0.976	97.18	98.04
		I	837.6		160-1000	$18.869e^{561.95x}$	0.912	1113.22	1126.09
		I	857.5						
		I	858.6						
		I	894.8						

Table 3.5: Cont.

z	EoI	State	λ nm	LoD mg/L	Range mg/L	y	R^2	RMSE mg/L	S mg/L
13	Al*	I	236.7						
		I	237.3						
		I	308.2						
		I	394.4						
		I	396.1						

z = atomic number, EoI = element of interest (EoI), λ = wavelength of the lines used for calibration (* Al used as internal standard), LoD = limit of detection: calculated according to the 3σ-IUPAC criterion (LoD = 3*σB/k) (IUPAC, 1976), y = formula used for calibration, R^2 = coefficient of determination, RMSE = root mean square error, S = residual standard deviation, σ = standard deviation of the background signal at the lowest solution concentration, k = slope of the calibration line

3.2.3 Results

In Table 3.5, the statistical evaluation of the calibrations for single-element standards (Li, Na, K) and paired-element standards (Mg/Ca, Zn/Sr, NO_3/SO_4/Cl) is shown. The calculated LoDs were quite low (<0.03 mg/L) and therefore notably lower than the lowest concentration used for calibration (0.1 mg/L). In general, high coefficients of determination (R^2) were obtained for the low and medium concentration ranges. The third concentration range generally suffered from lower R^2 and higher RMSE and S (e.g., Na, Sr). The analysis of anionic species was generally less sensitive than that of cationic species, as indicated by the high to very high RMSE and S. It was not possible to establish a calibration line for Mg above 100 mg/L, as the IR did not increase with further increases in concentration. The calibration curves for Sr are shown in Figure 3.14. In order not to go beyond the scope of this paper, the other calibration curves are not shown here.

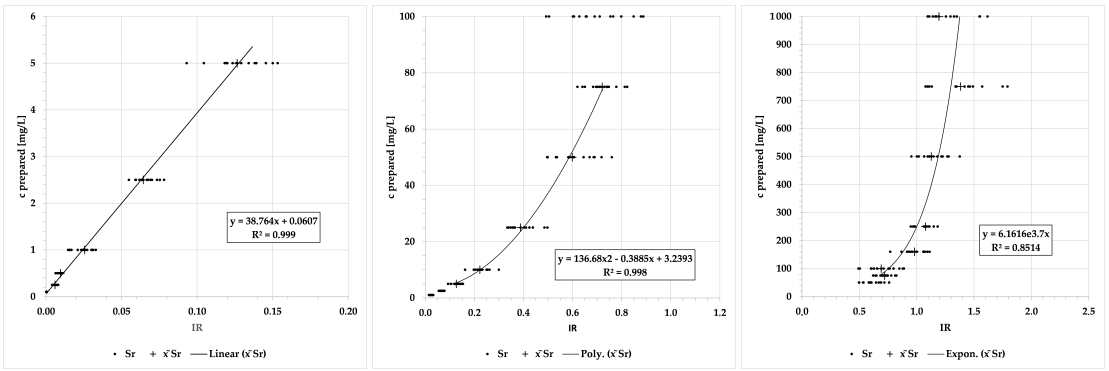

(a) **(b)** **(c)**

Figure 3.14: Calibration curves for Sr between the prepared concentration and the calculated intensity ratio (IR) for the concentration ranges **(a)** 0.1 – 5 mg/L, **(b)** 5 – 75 mg/L, and **(c)** 75 – 1000 mg/L.

By applying the calibration curves provided in Table 3.5, subtracting the respective IR blank values (see Table 3.7) and using the respective threshold values (THVs) from Table 3.7 to select the correct concentration range, the results of the analysis of the bottled mineral waters were obtained and are given in Table 3.6. The values were compared with the laboratory analyses (IC and ICP-MS). The absolute and relative deviations are provided. In addition, ion balances (IBs) of all waters are presented and were compared between the laboratory and the pLIBS analysis. The ECs calculated from the laboratory and pLIBS analyses are shown and the latter were compared with values measured before the analysis. As highly mineralised bottled mineral waters, typically above 1000 μS/cm, showed very low accuracy, these were excluded from evaluation in order to increase clarity. In addition, Zn and NO_3 were excluded, as they showed low analytical performance (low accuracy - in particular, inconsistent overestimation).

Table 3.6: Results of the analysis with the pLIBS compared to laboratory analysis (lab), excluding SO_4 and Zn. pLIBS values are presented as the mean of five measurements (Adhz: 15). All bottled mineral waters with a conductivity > 1000 μS/cm were omitted. SDs are given in Table 3.8 and 3.9. Laboratory analyses were performed using IC, except for Sr (ICP-MS). The absolute deviation (dev) and the relative deviation (r-dev) of the pLIBS from the laboratory value are given for each value. The IB was calculated using additional hydrogen carbonate values measured with a field photometer. EC was calculated according to Rossum (1949) for both laboratory and LIBS analysis.

Abbr.		Li	Na	Mg	K	Ca	Sr	SO_4	Cl	Unit	IB	EC	
											eq-%	μS/cm	
Adhz	lab	<LoD	11.95	30.63	1.26	18.40	1.891	28.46	18.95	mg/L	-41.3	496	lab
	pLIBS	<LoD	16.11	22.69	0.32	18.74	1.460	<LoD	16.71	mg/L	-44.9	434	pLIBS
	dev	0.022	4.16	7.94	0.95	0.34	0.431	28.46	2.24	mg/L		598	meas
	r-dev	78.6	34.8	25.9	74.8	1.9	22.8	100	11.8	%	-3.7	-164	dev
BeWa	lab	<LoD	6.19	6.96	0.97	30.16	0.103	21.81	15.46	mg/L	-0.7	252	lab
	pLIBS	<LoD	9.41	7.06	1.86	40.15	<LoD	17.98	11.08	mg/L	30.2	277	pLIBS
	dev	0.022	3.21	0.10	0.88	9.99	0.1022	3.83	4.37	mg/L		257	meas
	r-dev	78.6	51.9	1.4	91.1	33.1	99.2	17.5	28.3	%	30.9	20	dev
Blk	lab	<LoD	<LoD	<LoD	<LoD	0.24	0.004	1.68	2.01	mg/L	-171.2	17	lab
	pLIBS	<LoD	<LoD	<LoD	0.01	<LoD	<LoD	<LoD	0.28	mg/L	-193.6	9	pLIBS
	dev	0.022	0.005	0.051	0.047	0.077	0.003	1.68	1.73	mg/L		1	meas
	r-dev	78.6	26.3	86.4	88.7	78.6	79.4	100	86.2	%	-22.4	8	dev
Gest	lab	<LoD	11.86	39.42	4.45	31.57	0.529	24.23	20.61	mg/L	-45.8	684	lab
	pLIBS	<LoD	13.71	22.08	4.96	33.25	0.363	10.98	6.36	mg/L	-61.8	573	pLIBS
	dev	0.022	1.85	17.34	0.52	1.69	0.166	13.25	14.25	mg/L		878	meas
	r-dev	78.6	15.6	44.0	11.6	5.3	31.4	54.7	69.2	%	-15.9	-305	dev
Laur	lab	<LoD	0.97	0.34	0.36	1.38	0.010	3.21	2.13	mg/L	-73.2	26	lab
	pLIBS	<LoD	0.46	0.04	0.01	1.74	<LoD	42.50	0.95	mg/L	-163.0	81	pLIBS
	dev	0.022	0.51	0.29	0.35	0.36	0.009	39.29	1.18	mg/L		21	meas
	r-dev	78.6	52.1	86.9	98.3	26.2	91.8	1225	55.3	%	-89.9	60	dev
Löng	lab	<LoD	15.05	3.23	1.70	30.33	0.066	40.08	28.79	mg/L	4.8	281	lab
	pLIBS	<LoD	21.31	3.23	4.17	30.05	0.001	24.99	22.56	mg/L	29.1	278	pLIBS
	dev	0.022	6.25	0.00	2.47	0.28	0.065	15.09	6.22	mg/L		275	meas
	r-dev	78.6	41.5	0.0	145	0.9	98.8	37.6	21.6	%	24.3	3	dev
Nat	lab	<LoD	6.28	7.01	3.09	22.48	0.057	12.02	9.29	mg/L	46.8	177	lab
	pLIBS	<LoD	5.21	6.05	2.60	37.28	0.001	0.00	6.36	mg/L	98.8	182	pLIBS
	dev	0.022	1.07	0.96	0.49	14.80	0.056	12.02	2.94	mg/L		212	meas

Table 3.6: Cont.

Abbr.		Li	Na	Mg	K	Ca	Sr	SO_4	Cl	Unit	IB eq-%	EC μS/cm	
	r-dev	78.6	17.0	13.7	15.8	65.9	98.6	100	31.6	%	52.1	-30	dev
Odwq	lab	0.036	13.04	23.87	5.83	41.52	0.834	17.56	24.54	mg/L	-42.7	592	lab
	pLIBS	<LoD	22.15	15.25	10.54	36.16	0.694	35.49	19.86	mg/L	-57.1	602	pLIBS
	dev	0.030	9.11	8.62	4.71	5.37	0.140	17.94	4.68	mg/L		727	meas
	r-dev	83.3	69.9	36.1	80.7	12.9	16.8	102	19.1	%	-14.4	-125	dev
Rosb	lab	<LoD	59.91	65.13	3.09	30.59	0.284	18.15	91.57	mg/L	-9.2	1016	lab
	pLIBS	0.057	57.49	42.53	7.67	37.75	0.001	0.0002	44.85	mg/L	-16.4	876	pLIBS
	dev	0.029	2.42	22.60	4.58	7.17	0.284	18.15	46.72	mg/L		1363	meas
	r-dev	103	4.0	34.7	148	23.4	100	100	51.0	%	-7.3	-487	dev
Saw	lab	<LoD	18.73	3.52	1.17	71.03	0.722	58.00	52.78	mg/L	3.7	524	lab
	pLIBS	<LoD	41.18	4.29	0.62	65.17	0.296	0.0002	32.02	mg/L	60.5	439	pLIBS
	dev	0.022	22.45	0.78	0.55	5.86	0.427	58.00	20.76	mg/L		589	meas
	r-dev	78.6	120	22.1	47.1	8.2	59.0	100	39.3	%	56.8	-150	dev
Vit	lab	0.055	6.02	19.45	5.07	54.26	0.877	113.17	6.87	mg/L	5.0	511	lab
	pLIBS	<LoD	5.93	11.94	7.16	43.63	0.764	70.51	4.33	mg/L	1.5	390	pLIBS
	dev	0.049	0.09	7.51	2.09	10.63	0.113	42.65	2.54	mg/L		444	meas
	r-dev	89.1	1.5	38.6	41.4	19.6	12.9	37.7	37.0	%	-3.6	-54	dev
Median	r-dev	78.6	34.8	34.7	80.7	19.6	79.4	100.0	37.0	%			

Adhz = Adelholzner, BeWa = Bergische Waldquelle, Blk = blank sample, Gest = Gerolsteiner, Laur = Lauretana, Löng = Löningen, Nat = Naturalis, Odwq = Odenwaldquelle, Rosb = Rosbacher, Saw = Sawell, Vit = Vittel.

Figures 3.15 - 3.17 show correlations between pLIBS predicted concentrations and laboratory concentrations for all EoIs, excluding bottled mineral waters with a conductivity greater than 1000 μS/cm. Out of these, Figure 3.15 shows only the singly charged cations (alkali metals) and Figure 3.16 the doubly charged cations (alkaline earth elements). The correlations for the anionic species, excluding NO_3, are illustrated in Figure 3.17.

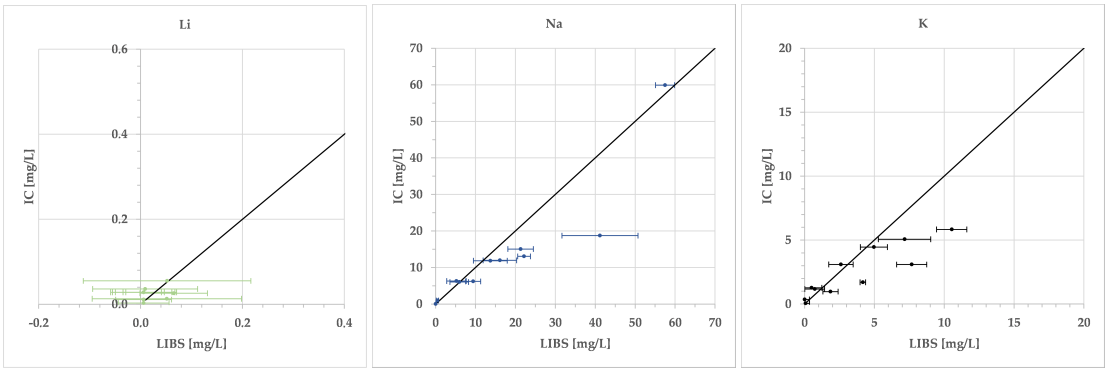

(a) **(b)** **(c)**

Figure 3.15: Correlations of LIBS predicted concentrations versus IC for the light alkali metals. Li and K values were adjusted by subtracting a slightly higher value than the blank IR value, otherwise the results would be overestimated. An optimal correlation is indicated by the black line (results for AqMi, Extl, Fach, Mar, and Qubr are not included).

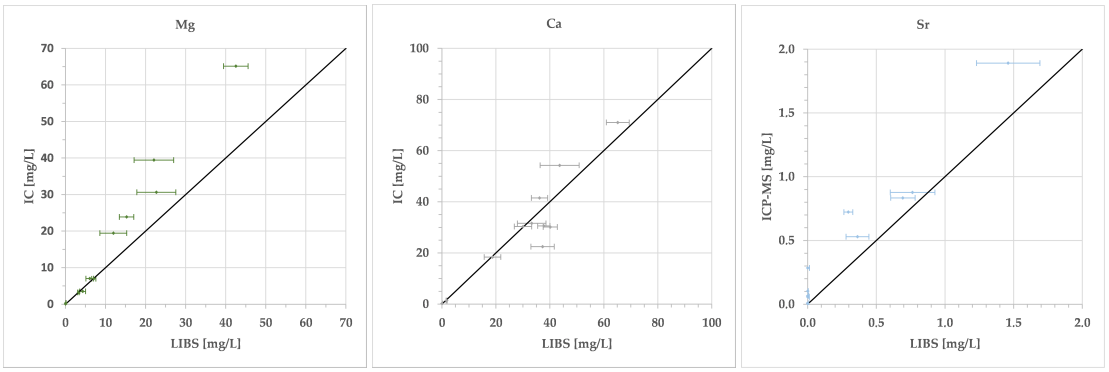

(a) **(b)** **(c)**

Figure 3.16: Correlations of LIBS predicted concentrations versus IC or ICP-MS analyses (Sr) for the alkaline earth metals. An optimal correlation is indicated by the black line (results for AqMi, Extl, Fach, Mar, and Qubr are not included).

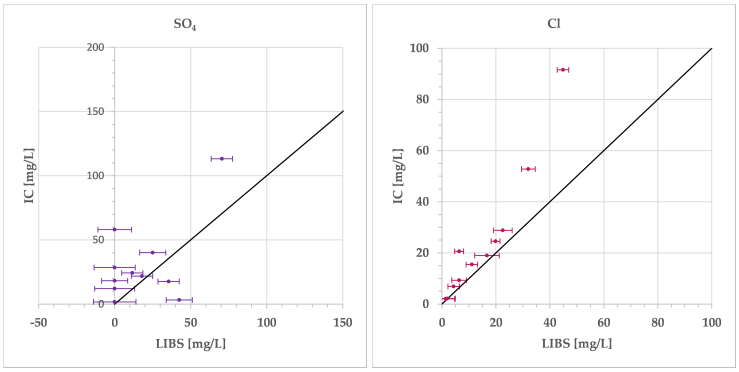

(a) **(b)**

Figure 3.17: Correlations of LIBS predicted concentrations versus IC for the anionic species, excluding SO_4. An optimal correlation is indicated by the black line (results for AqMi, Extl, Fach, Mar, and Qubr are not included).

Figure 3.18 shows combined Stiff diagrams for all selected bottled mineral waters. Stiff plots simplify the comparison of waters (Schäffer and Dietz, 2023) and are usually applied to compare different waters - for example, to illustrate spatial or temporal differences in water chemistry. Here, combined Stiff diagrams were used to compare the same water in different analyses (pLIBS and laboratory). For each water sample, a Stiff diagram is shown for the laboratory and for the pLIBS analysis results. Perfectly matching analyses should produce exactly the same polygon for both analyses. Since an additional photometer was used for the HCO_3 concentrations, the results for laboratory and LIBS analyses are identical for HCO_3.

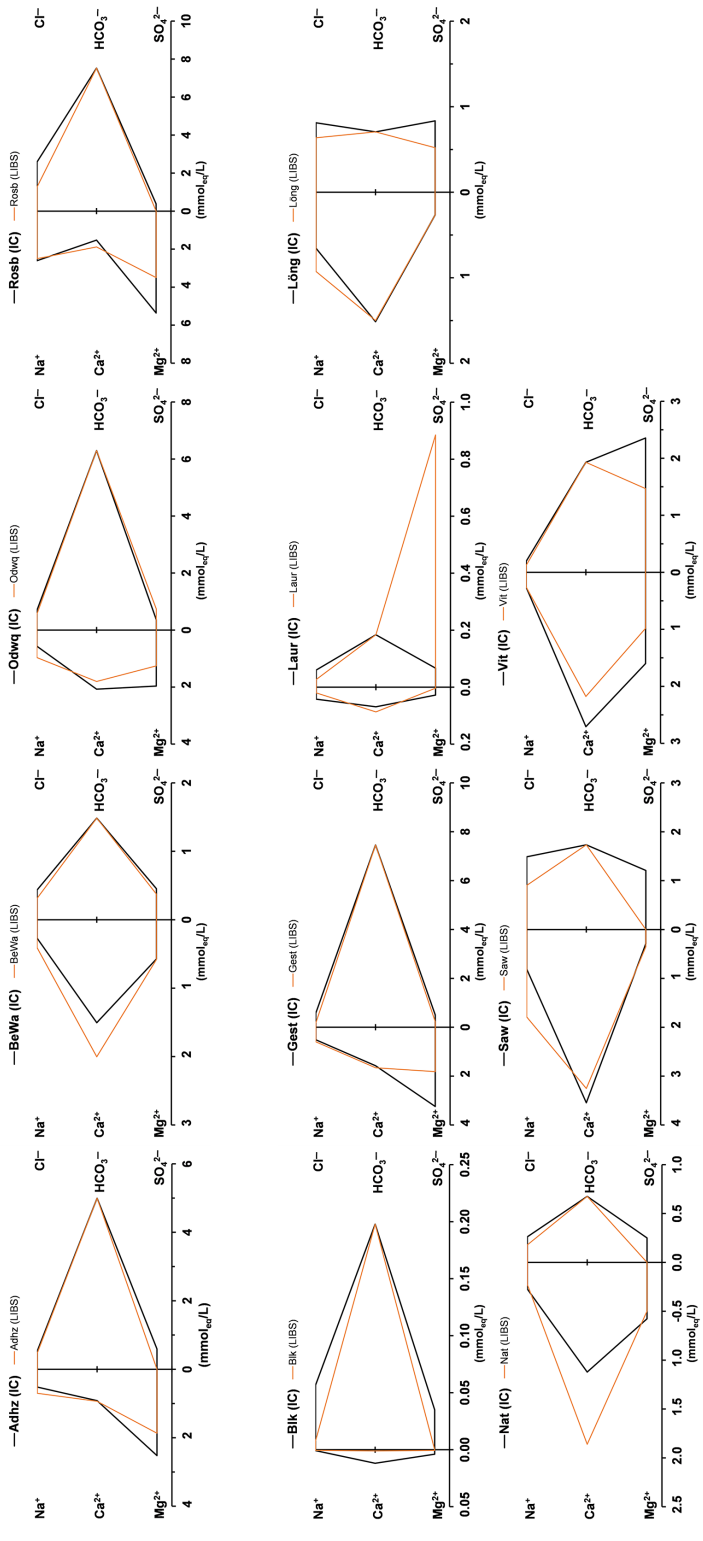

Figure 3.18: Combined Stiff diagrams of the analysis results of the selected bottled mineral waters. One shows the diagram for the IC and one for the pLIBS results. HCO_3 concentrations were measured with a field-ready photometer and were therefore identical for both analyses.

Figures 3.19 and 3.20 show the results of applying the calibrations used for single-element or paired-element standard solutions (Table 3.5) to mixed standard solutions. The first of the two figures shows the results of the mixed test series containing all three singly charged cations simultaneously (cf. Figure 3.19). K concentrations appear to have been slightly underestimated for prepared concentrations below 10 mg/L and overestimated for prepared concentrations between 40 mg/L and 75 mg/L. For higher concentrations, the prepared concentrations were clearly underestimated. Li concentrations were slightly overestimated for concentrations up to 30 mg/L, fit relatively well for concentrations up to 80 mg/L, and were underestimated for even higher concentrations. Na concentrations up to 20 mg/L seem to have fit well, but at higher prepared concentrations the predicted concentrations also seem to have been underestimated.

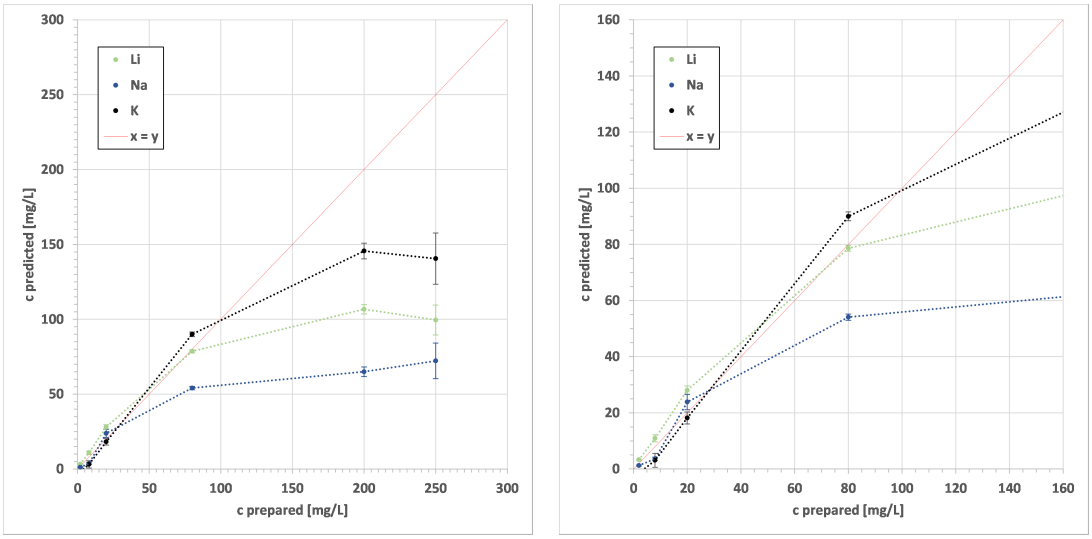

(a) **(b)**

Figure 3.19: Results of applying the calibrations to a series of tests using mixed solutions of known concentration containing equal concentrations of Li, Na, and K. The right graph **(b)** shows a section of the left graph **(a)** for better comparison with Figure 3.20.

Figure 3.20 shows the results of the test series with mixed standards containing all six cations simultaneously. Compared to the mixed standards with less different cations, all three alkali elements seem to have behaved differently. The overestimation at low concentrations and underestimation at high concentrations was even more pronounced for Li, Na, and K in the second series of tests. Li, in particular, changed and ended up behaving very similarly to Na. It is noticeable that the alkaline earth metals (doubly charged cations) Mg, Ca, and Sr behaved similarly to each other but quite differently to the alkali elements (singly charged cations). They were more clearly underestimated at higher concentrations but not overestimated at low concentrations. For all elements in both test series, there appeared to be a plateau

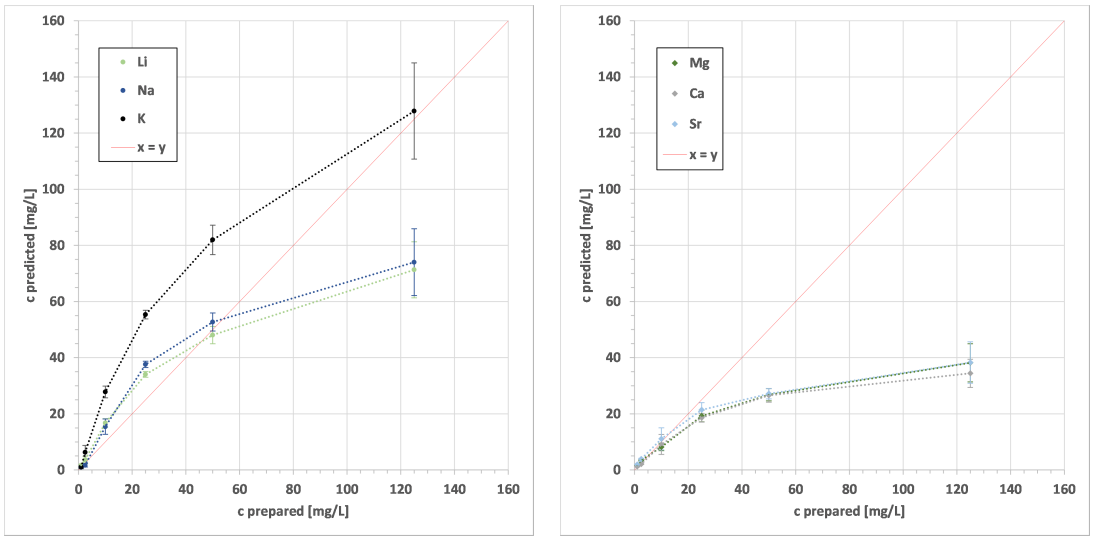

(a) **(b)**

Figure 3.20: Results of applying the calibrations to a series of tests using mixed solutions of known concentration containing equal concentrations of Li, Na, K, Mg, Ca, and Sr. The light alkali elements are shown on the left **(a)** and the alkaline earth metals on the right **(b)**.

at higher concentrations, where even higher concentrations did not produce more signal and therefore a predicted concentration. Attenuation at higher concentrations appeared to have been greater for alkaline earth elements (divalent cations) than for alkali elements (monovalent cations). A series of attenuations can be formed from low to high: $K < Li < Na < Mg < Sr < Ca$.

3.2.4 Discussion

All calculated LoDs were quite low (in the ppb range). However, these low detection limits are deceptive. The lowest concentrated standard used was 0.1 mg/L for the cations and 0.5 mg/L for the anions. Nevertheless, the highest LoD calculated was 0.021 mg/L (Ca). It is particularly striking that the detection limits for the anions were particularly low. Earlier research has shown that the quantitative analysis of sulphur and chlorine with LIBS is subject to some difficulties and that indirect determination is often necessary to achieve low detection limits (Ma et al., 2020b; Tang et al., 2021). This is due to the low excitation in the plasma caused by the high ionisation energy of Cl and S (Ma et al., 2020b). However, Poggialini et al. (2023b) pointed out that the determination of LoDs with the outdated IUPAC formula used in this work is not particularly appropriate for multivariate LIBS analysis (Poggialini et al., 2023b). Yet, since this formula is currently the most widely used calculation of the LoD and compara-

bility with Schlatter and Lottermoser (2023) should be ensured, a different calculation was not used. Although the absolute detection limits may be somewhat higher in reality, it has been shown that very low concentrations (<0.1 mg/L) can be detected in standard solutions with pLIBS.
It may seem cumbersome to have several calibration curves within one EoI for different concentration ranges, but by using THVs (cf. Table 3.7), the selection of the correct range, and therefore the formula can be completed automatically in a spreadsheet. The advantage of having multiple calibration curves for an EoI at different concentration ranges is that the changing slope of a single curve can be better represented. If self-absorption correction is applied in the future, it may not be necessary to have several concentration ranges but rather only one calibration curve, as the slope will no longer change as much.
The high determination coefficients for Li, Na, and K in Schlatter and Lottermoser (2023) could also be achieved for other elements and compounds, especially at low to medium concentrations (cf. Table 3.5). At higher concentrations (generally > 100 mg/L), the determination coefficients were higher than expected. For Mg, no calibration line could be established, as the IR did not increase with increasing concentration. This is an indication of strong self-absorption (Legnaioli et al., 2022).
Zn, and NO_3 were excluded from the evaluation, as they showed low analytical performance. For Zn, on the one hand, the test series was not diverse enough to make statements about the applicability to natural waters and, on the other hand, the measured values were clearly overestimated. NO_3 concentrations showed no clear correlation between pLIBS and IC analysis, with a strong tendency of overestimation. For the pLIBS analysis of NO_3, it cannot be excluded that the results were partly falsified. It is possible that some cation samples were used for the pLIBS measurements instead of the unaltered anion samples. In contrast to the anion samples, these were acidified with HNO_3 (see liquid analyses) to prevent the cations from precipitating during transport to the laboratory for IC and ICP-MS analyses. Since only very small amounts of diluted high-purity nitric acid were used, this should only have had an influence on the nitrate concentrations. This would explain why there was no correlation between pLIBS and IC analyses for nitrate.
The median of the relative deviation for all Ca analyses with pLIBS compared to laboratory analyses was fairly good, at 19.6% (cf. Table 3.6). Figure 3.16 shows a fairly good correlation between pLIBS and IC data for Ca up to 75 mg/L.
The median of the relative deviation for all Na and Mg analyses with pLIBS compared to laboratory analyses was reasonable, at 34.8% and 34.7%, respectively (cf. Table 3.6). Figure 3.15 shows a fairly good correlation between pLIBS and IC data for Na with only one conspicuous outlier with a very high standard deviation (9.52 mg/L). Figure 3.16 shows a correlation between pLIBS and IC data for Mg, with a tendency for higher concentrations to be underestimated. This trend could be interpreted as a progressive exponential function, which could indicate an increase in self-absorption with increasing concentration. The median of the relative deviation for all Cl analyses with pLIBS compared to laboratory analyses was still reasonable, at 37.0% (cf. Table 3.6). Figure 3.17 shows a fairly good correlation between pLIBS and IC up to 30 mg/L, with a tendency to underestimate higher concentrations, similar to Mg (cf. Figure 3.16), from which the same conclusions can be drawn. The median of the rel-

ative deviation with pLIBS compared to laboratory analyses was quite high for Li, Sr, and K, at 78.6, 79.4, and 80.7%, respectively (cf. Table 3.6). However, the test series was not very diverse for Li, with most values close to or below the LoD of the IC analyses (0.027 mg/L). It is therefore hardly surprising that most of the values for the pLIBS Li analysis were also close to or below the LoD of the pLIBS analysis. A large part of the relative deviation for Li thus resulted from the different LoDs between pLIBS and IC analysis. As the test series was not diverse enough for Li concentrations (cf. Figure 3.15), it is also difficult to say whether there was a good correlation between pLIBS and IC analysis. For Sr, the deviation also mainly came from very low concentrations. Many pLIBS results were below the LoD of 0.0008 mg/L. However, there was a correlation between pLIBS and IC data for concentrations up to 2 mg/L (cf. Figure 3.16). For K, Figure 3.15 shows a fairly good correlation between pLIBS and IC data, with a tendency for all concentrations to be slightly overestimated.
The median of the relative deviation for all SO_4 analyses with pLIBS compared to laboratory analyses was quite high, at 100.0% (cf. Table 3.6). In addition, the correlation between pLIBS and IC data was quite poor (cf. Figure 3.17).
The IB can help to identify possible analytical discrepancies between cationic and anionic species concentrations. Therefore, a negative IB indicates excessive findings of anionic species concentration or underestimation of cationic species concentration. A positive IB indicates an analysed anionic species concentration which is too low or a cationic species concentration which is too high. Seven out of eleven results of IB calculated with pLIBS had a negative IB, which indicates that anions were mostly overestimated and/- or cations were underestimated. Ideally, the calculated ECs for both analyses (pLIBS and laboratory) should match the measured EC value. A deviation from the measured value is a clear indication of non-analysed or incorrectly analysed ions. If the calculated EC value of the laboratory measurement differs from the measured value, it can be assumed that ions were either precipitated, samples were contaminated, or they were measured incorrectly. Looking at the values in Table 3.6, one water stands out as having had a deviation of more than 30% for the laboratory EC measurements: the blank one. This was mainly due to the low mineralisation of the deionised water, where minimal absolute differences in the analysis resulted in large percentage deviations. For the pLIBS analysis, five of the eleven waters showed a deviation of more than 30% (Blk, Gest, Laur, Löng, Saw). This is an indication that the total of all determined ions for these waters differ from the real solution content.
Furthermore, precipitation of $CaCO_3$, prior to both pLIBS and IC analysis, can be observed by comparing the analysis results with the values indicated on the bottles (Adhz, Gest, Odwq, Rosb, Vit). However, other cations or anions do not appear to have been affected and precipitation occurred prior to analysis, as shown by comparative measurements with newly purchased bottles and re-measurements of the original samples.
The Stiff diagrams perfectly illustrate the differences between pLIBS and laboratory analyses (cf. Figure 3.18). Based on the agreement between the analyses, the plots can be grouped into two categories: good correlation between laboratory and pLIBS analysis (first row) and moderate correlation (second and third rows). A third category with poor correlation would have been needed for waters with a conductivity greater than 1000 μS/cm or concentrations of several ions greater than $\ll$ 6 mmoleq/L.

For clarity, the uncertainty and the precision of the pLIBS analysis of the bottled waters are reported separately in Table 3.9 in the Appendix A. Standard deviations (SD) for replicates on one sample within the range of 0.003 to 14.01 mg/L for all selected samples and elements are quite acceptable for a portable instrument, taking into account the diverse chemistry, with up to approximately 120 mg/L solution content per element (cf. Table 3.9, highly mineralised waters excluded). Looking at the median relative standard deviation (RSD) for the different elements, the values appear to be quite high. The lowest RSD was 11% (Ca) and the highest 39% (SO_4). However, these values are comparable to the RSDs reported by other authors who analysed aqueous samples by laboratory LIBS.
For example, a precision of 2–6% RSD was achieved for aerosol LIBS and a precision of 13 – 22% for microdrop LIBS (Cahoon and Almirall, 2012). For more similar sample preparation techniques using LSC, 11 – 17% RSD was achieved for geometric constraint LSC and 25 – 36% RSD for unconstrained direct LSC (Ma et al., 2020a). Precision in LIBS analysis is typically low (5 – 20%) due to shot-to-shot variability and matrix effects (Hark and Harmon, 2014). Other effects, such as the slightly different distribution of the EvR, may also occur, resulting in lower precision. It is therefore advisable to perform multiple measurements per sample. At least three, or better five, measurements per sample are recommended for the presented method. Due to the small sample volume required (0.75 μL) and the short measurement time, this can be achieved quickly and easily.
Compared to testing single-element standard solutions (Schlatter and Lottermoser, 2023), it is to be expected that there are more effects affecting the results of an analysis of mixed solutions or natural waters with an even more complex matrix. As LIBS analysis is highly susceptible to the so-called matrix effect (Legnaioli et al., 2022), small changes in the matrix can cause the emitted signal to be no longer proportional to the concentration. There are several indications of matrix effects in the results of mineral water analyses. These are particularly evident in the fact, that more highly mineralised waters such as Aqua Mia, Extaler, and Marius generally showed very poor analytical results and were omitted from the evaluation. If a suitable self-absorption correction is used in the future, these more highly mineralised waters should also be analysable. In addition, especially for Mg and Cl concentrations above 15 mg/L, there is a systematic underestimation, which can even be seen as a recognisable (progressive) exponential function in the correlation plots (cf. Figures 3.16 and 3.17). For the other cations, this effect might also occur if samples with higher concentrations had been analysed. The discarded data for Ca and Sr confirm this assumption. However, the self-absorption effect is difficult to investigate in complex natural waters.
In order to gain a better understanding of this effect, mixed standard solutions were analysed in addition to the bottled mineral waters, and the calibrations developed were used for analysis. A small mixed standard containing Li, Na, and K, and a more comprehensive one containing Li, Na, K, Ca, Mg, and Sr, were analysed. The results of the two test series clearly show that there were both amplifying and attenuating effects that cancelled out the proportionality (cf. Figures 3.19 and 3.20). Nevertheless, a clear correlation is recognisable. This can be described as a degressive proportionality, in which the measured concentration increases less and less as the real concentration increases. Typically, with low concentrations attenuating effects can be recognisable,

especially for the light alkali elements Li, Na, and K. This effect was less pronounced within the test series without the doubly charged cations. As with all elements in both test series, a plateau was reached at higher concentrations, where even higher concentrations did not produce significantly more signal and therefore a predicted concentration, the linearity, was cancelled out. This is a clear hint of self-absorption (Poggialini et al., 2023b).
When using single-element standards, these problems were encountered with concentrations typically above 160 mg/L (Schlatter and Lottermoser, 2023). This limit seems to have dropped significantly for more complex waters and was more pronounced for the alkaline earth metals than for the alkali elements (cf. Figures 3.19 and 3.20). Typically, self-absorption has several effects on the line shape, so these should be visible in the lines used for calibration. Self-reversal can occur in LIBS analysis when there are spatial gradients in plasma temperature and electron number density. This can lead to a dip at the centre of an emission peak, which can be strong enough to erroneously identify two peaks (Samek et al., 2000).
In this work, no line showed typical self-reversal effects such as a dip at any maximum. However, this does not mean that there was no self-absorption (Palleschi, 2022a). Self-absorption was visible in several lines, as the IR did not grow proportionally with increasing concentration (typically above 100 mg/L) and the curve saturated (cf. Figures 3.19 and 3.20). This can also be seen in the broadening of the peaks, which resulted in a higher FWHM (cf. Figure 3.21 a,b).

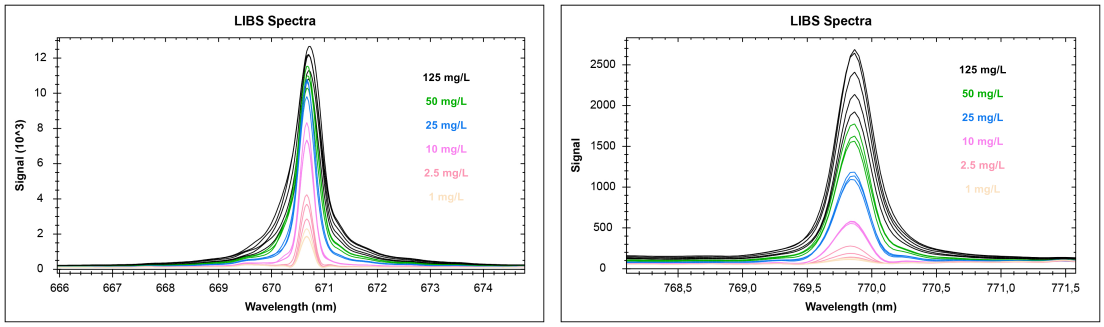

(a) **(b)**

Figure 3.21: Line broadening with increasing concentration (1–125 mg/L). **(a)** Li 670.7 nm; **(b)** K 769.8 nm. Experimental parameters: 5–6 mJ/pulse, 50 Hz, 2 μs gate delay, Ar atmosphere.

It can clearly be seen that for both K (769.8) and Li (670.7) the lines not only increased in height with increasing concentration but also became wider. Between 10 and 25 mg/L there was still a large difference in peak height for K (769.8) (cf. Figure 3.21 b). Between 50 and 125 mg/L the difference was already smaller and the height variation at the same concentration was greater. In addition, the lines at 10 mg/L were only a little more than half a nm wide at the base. At 125 mg/L, it was already more than 2 nm. This made integration more difficult. If the integration range is too large, there may be an overlap with other peaks. If it is too small, the area

under the peaks will be underestimated for higher concentrations. The effect of peak broadening also occurred with all other lines of the other elements and compounds investigated. However, it was particularly pronounced for the higher-intensity peaks. Samek et al. (2000) did not observe any self-reversal or self-absorption when analysing the liquids directly, even at a concentration of 40,000 mg/L. In contrast to Samek et al. (2000), self-absorption played a significant role with increasing concentration when using LSC. However, Samek et al. (2000) also found both self-reversal and self-absorption effects when analysing solids. The main difference in this study is that by analysing the evaporation residue, solids were analysed instead of liquids. This difference was also highlighted by Samek et al. (2000) and attributed to the fact that the atomic densities of analytes in plasma are approximately 1000 times greater for a pure solid than for liquid solutions and are therefore optically thicker. Skrzeczanowski and Długaszek (2022), who used LSC on filter paper in the concentration range of 0 - 1000 mg/L, also experienced self-absorption and therefore had to apply two calibration lines per element to fit the data. At lower concentrations, a steeper straight line could be applied than at higher concentrations (Skrzeczanowski and Długaszek, 2022). This clearly reduced the sensitivity at higher concentrations, as occurred in this work.
The same effect was observed by Bae et al. (2015), who also used an SE LSC method. They explained the increased effect of self-absorption by the fact that analytes and standards are concentrated in a very small area after drying (Bae et al., 2015). It can therefore be assumed that the effect is even stronger with SE methods without filter paper, since the evaporation residue is confined to a smaller area than when a filter paper is used. In this work, a relatively long gate delay of 2 μs was used. The gate delay was initially optimised for Li, Na, and K (Schlatter and Lottermoser, 2023) and not further adjusted in this work to obtain comparable data. Rao et al. (2022) showed that sensitivity is not significantly affected by increasing the gate delay but that precision is increased and self-absorption reduced by a longer gate delay. However, they used significantly shorter gate delays of 250 ns and 500 ns. Tang et al. (2019) also recommended mitigating self-absorption by recording the signal with a longer gate delay, since this effect tends to be more prominent in the early stages of laser-generated plasma.
Looking at the spectra of the gate delay investigations in Schlatter and Lottermoser (2023), which were recorded similarly to the data within this study, it is noticeable that not only the peak height was affected by a change in gate delay at the same concentration (cf. Figure 3.22). There is also a clear broadening of the line at shorter gate delays (more intense grey values). With a longer gate delay, the peaks become significantly narrower and the effect of self-absorption decreases. This effect was observed for the three tested elements of Li, Na, and K.
Due to the strong self-absorption effects, future work will focus on the improvement of the method by the addition of a self-absorption correction to improve accuracy and to compensate for the underestimation of higher predicted concentrations. When applying a self-absorption correction, it may also be possible to have only one calibration curve instead of two or three for different concentration ranges. However, in this work, it was important to show that the method is basically applicable to natural waters and to determine the influencing factors. These seem to be determined

less by the number of different elements than by self-absorption. In addition to filters, used to remove any undissolved components prior to analysis, a mobile hot plate to evaporate the micro droplets is required for future field application of the method.

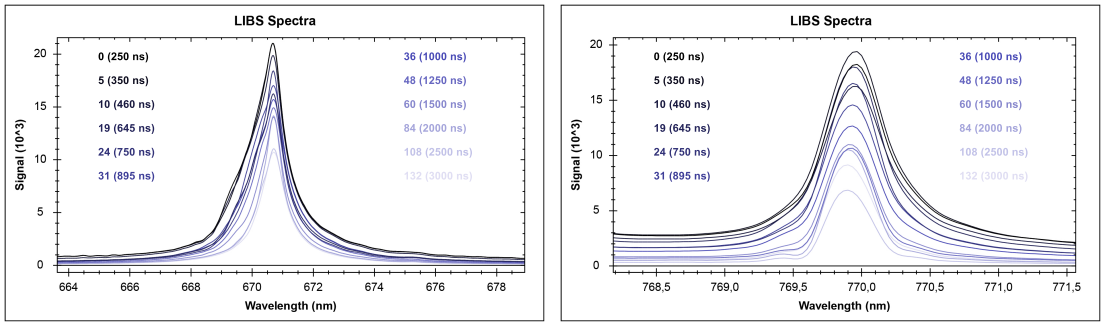

(a) **(b)**

Figure 3.22: Line broadening with increasing gate delay (0–132 IID). **(a)** Li 670.7 nm; **(b)** K 769.8 nm. Experimental parameters: stable concentration of evaporated droplets (1000 mg/L), 5–6 mJ/pulse, 50 Hz, variable gate delay, and Ar atmosphere. Grey value increase with increasing gate delay.

The possibility to set up calibration curves for Zn with high coefficients of determination in standard solutions (cf. Table 3.6) proves that, in principle, it is also possible to analyse environmentally relevant elements in aqueous solutions with portable LIBS. In this work, no correlation could be found for Zn between the results from pLIBS and ICP-MS analyses with the bottled mineral waters used. However, the test series was not very diverse for Zn, with all but one value below 0.1 mg/L in ICP-MS analyses. With an appropriate self-absorption correction and a diverse test series, Zn and possibly other PTEs such as Pb and As should theoretically also be quantifiable.
It is clear that the documented analytical approach is not only applicable to single-element standard solutions but also to low mineralised natural waters with complex matrices. By adding a self-absorption correction, it should also be possible to quantitatively analyse more highly mineralised waters and improve the precision. As demonstrated, there is significant potential for developing field-based pLIBS for quantitative water analysis.

3.2.5 Conclusions

In our previous study, pLIBS was evaluated for the quantitative analysis of dissolved alkali metals in single-element standard solutions. The aim of this work was to show whether pLIBS can also be used for chemical compositional measurements of natural waters. The results of this study demonstrate that it is possible to quantitatively analyse low to medium mineralised bottled mineral waters with pLIBS for some of the main cations and anions. In higher mineralised waters with an EC above approximately 1000 μS/cm, the concentrations of the main cations and anions were mostly

underestimated. This effect was mainly due to self-absorption, which was clearly visible in a strong line broadening with increasing concentration. The effect of self-absorption was quite strong, despite a long gate delay being used, which should have compensated for high self-absorption. However, no self-reversal could be detected in any peak, which should have made self-absorption correction easier. Differences have been observed for singly ionised cations (alkali elements) compared to doubly ionised cations (alkaline earth metals). The self-absorption seems to have been pronounced for alkaline earth metals. Therefore, the analysis of alkali elements is currently more reliable than for alkaline earth metals, and the analysis of higher concentrations is more reliable for alkali elements. Analysis of anions is less reliable, even though LoDs may be calculated to be lower than for the other investigated ions. Of the anions, only Cl showed reasonably reliable results in natural waters. In general, the low detection limits are deceptive and do not reflect how well an EoI can be analysed. An analysable concentration range for natural mineral waters using the method described is approximately between 0.1 and 100 mg/L per element. The next step in the development of the method is the introduction of an adapted self-absorption correction. It is quite promising that more elements will be calibratable (e.g., Zn). It should therefore be possible to analyse environmentally significant elements in the future. In any case, the ability to analyse natural mineral waters with complex matrices for their main ions opens up many new possibilities for pre-screening and on-site water analysis.

3.2.6 Appendix

Table 3.7: Threshold values (THVs) used for selecting the correct formula according to the concentration range and the mean values of the blank IR (mean b), which were subtracted from the calculated IR values. THV I = transition of the first to the second concentration range. THV II = transition of the second to the third concentration range. Unitless IR values are given.

	Li	**Na**	**Mg**	**K**	**Ca**	**Sr**	**SO_4**	**Cl**
THV I	0.100	0.070	0.130	0.020	0.175	0.140	0.0002	0.0028
THV II	3.000	0.600	0.700	0.550	1.000	0.850		
Mean b	0.015	0.0141	0.0222	0.022	0.0093	0.0019	0.0003	0.0001

Table 3.8: Relative standard deviations (RSDs) and detection limits (LoDs) of IC and ICP-MS* analysis.

Abbr.	**Li**	**Na**	**Mg**	**K**	**Ca**	**Sr***	**SO_4**	**Cl**	**Unit**
RSD	0.611	0.476	0.449	0.666	0.355		0.149	0.072	%
LoD	0.028	0.019	0.059	0.053	0.098	0.0000214	0.218	0.075	mg/L

Table 3.9: Standard deviations (SDs) calculated from five pLIBS (Adhz: 15) measurements per water sample and median values of the relative standard deviations (RSDs) for the elements investigated. Readings below the detection limit were not included in the calculation of the RSD. For this reason, no RSD could be calculated for Li.

SD	Li	Na	Mg	K	Ca	Sr	SO_4	Cl	Unit
Adhz	0.06	4.21	4.86	0.73	3.08	0.23	13.51	4.56	mg/L
BeWa	0.06	1.89	0.51	0.54	2.62	0.00	7.00	2.14	
Blk	0.03	0.13	0.05	0.29	0.13	0.01	14.01	3.31	
Gest	0.06	4.23	4.94	0.97	5.28	0.08	7.00	1.65	
Laur	0.04	0.29	0.10	0.34	0.18	0.01	8.58	3.02	
Löng	0.05	3.21	0.21	0.20	3.23	0.01	8.58	3.44	
Nat	0.05	2.44	0.96	0.88	4.33	0.01	13.10	2.70	
Odwq	0.10	1.60	1.78	1.08	3.03	0.09	7.00	1.65	
Rosb	0.07	2.37	3.05	1.08	2.26	0.01	8.58	2.14	
Saw	0.15	9.52	0.74	0.71	4.24	0.03	11.07	2.53	
Vit	0.16	2.34	3.37	1.88	7.22	0.16	7.00	2.14	
Median RSD	-	25	17	29	11	22	39	26	%

3.3 Preliminary Results for Potentially Toxic Elements (PTEs)

Key questions:

- Is it possible to quantitatively determine PTEs in aqueous solutions using pLIBS?
- Is it possible to use mixed standard solutions for calibration?
- Is it possible to create linear calibration curves for all desired concentration ranges of all selected elements?
- What are the detection limits achieved for the selected elements?

In this section some preliminary results for the analysis of PTEs, using the developed method, are presented. The potential use of the developed calibrations for water affected by mining or other anthropogenic sources is outlined. At present, only tests using mixed standard solutions have been conducted. Further research could employ and assess the effectiveness of the calibrations in real samples.

3.3.1 Innovative Field Method for Quantitative Hydrochemical Analysis of Mine Water

The content of this section was originally published as an abstract and poster in German under the original title: *"Innovative Feldmethode zur quantitativen hydrochemischen Analyse von Grubenwasser"* at the conference: *Kassel22 - Let's Talk about Grubenwasser*. Minor typesetting and layout work have been done and the poster can be found in the digital appendix.
DOI: 10.13140/RG.2.2.12667.18726

Authors: Nils Schlatter and Bernd G. Lottermoser

Received: 31 March 2022; **Accepted:** 28 July 2022; **Published:** 6 September 2022

Abstract: Analysing the inorganic solution content of mine water for environmental monitoring requires proper sampling, analysis of the on-site parameters, refrigerated transport and usually time-consuming and cost-intensive analysis in the laboratory. Despite careful monitoring, dissolved substances may precipitate on the way to the laboratory. Sometimes it is also not possible to transport the samples adequately or at all if water at a remote location is being analysed. In this case, and also when time and cost are a factor, it would be helpful to be able to quantify the concentrations of environmentally relevant elements in situ. However, there is currently no portable field method to quantitatively analyse water samples in real time for a variety of elements.

A new innovative field method for the quantitative hydrochemical analysis of mine water is analysis using pLIBS. The spectroscopic method has already been successfully used with large laboratory-based devices for quantitative water analysis in the ng/L range. Miniaturisation and further development now enable hand-held devices that can be used anywhere. In contrast to portable X-ray fluorescence spectrometers, there are hardly any legal restrictions on transport and use. Furthermore, also light elements such as lithium can be detected. On this basis, a field method was developed to analyse natural and anthropogenic waters such as mine water for all dissolved inorganic components. With suitable calibration, all dissolved inorganic constituents can be analysed simultaneously on site in the shortest possible time. Sample preparation, measurement, and analysis only take a few minutes. To date, a number of elements such as Li, Na, Mg, K, Ca, Zn, and Sr have already been successfully calibrated and standard solutions as well as mineral waters have been analysed with relatively low detection limits. Future research is planned on other PTEs such as Cu, Ni, Pb, As, Se, Cd, and Cr. In this context, the method will ultimately be evaluated on various mining-influenced waters.

Keywords: innovative Feldmethode (innovative field method); LIBS; Kalibrierung (calibration); Grubenwasserchemie (mine water chemistry), Umweltüberwachung (environmental monitoring)

3.3.2 On-site Screening of Mine Water Chemistry Using Portable Laser-induced Breakdown Spectroscopy (pLIBS)

Parts of this section were published as poster with abstract under the title: *"On-site screening of mine water chemistry using portable laser-induced breakdown spectroscopy"* at the conference: *TERRA - 1st European Conference on Teaching and Research in Sustainable Resource Extraction*. All texts, figures and tables were newly created for this thesis. The original poster can be found in the digital appendix.
DOI: 10.13140/RG.2.2.29719.55206

Authors: Nils Schlatter and Bernd G. Lottermoser

Received: 11 August 2023; **Accepted:** 11 August 2023; **Published:** 6 September 2023

Sample Preparation

In contrast to the preparation of the standard solutions in Section 3.1, eight aqueous single element AAS standard solutions with a concentration of 1000 mg/L in 2% nitric acid were mixed in equal amounts with each other for calibration (ROTI®Star, Carl Roth, Karlsruhe, Germany). Therefore, a 40 mL initial solution containing 125 mg/L of each element was created by blending 5 mL of every standard solution. This was used to further dilute with a 2% nitric acid to produce a dilution series containing fifteen different concentrations ranging from 0.001 to 50 mg/L. For the dilution of the nitric acid (ROTIPURAN® ≥65 %, Carl Roth, Karlsruhe, Germany) distilled deionised water (18 MΩ) was used. Zinc was already tested in an earlier study to provide an outlook on PTEs. For this purpose, mixed standard solutions with Sr have already been produced in the range of 0.1 to 1000 mg/L. Therefore, the existing calibrations were used for the calibration of Zn at concentrations above 0.1 mg/L and the mixed standard solutions containing the eight elements were only used for lower concentrations.

Acquisition and Calibration Settings

The acquisition settings remained unchanged in comparison to Section 3.1 and 3.2. In addition, the gate delay was not further adjusted to obtain comparable data. All calibration steps of Section 3.1 and 3.2 were applied in the same way. In Table 3.10 the different spectral lines of the eight elements of interest used are listed. Al again was used as an internal standard.

Results

Table 3.10 clearly shows that, in general, for all selected PTEs (Ni, Cu, Zn, As, Se, Cd, Pb), calibrations with the pLIBS are possible. However, no calibration curve could be created for Zn and As below 0.1 mg/L. For Se a calibration curve could be created below 0.1 mg/L, but the R^2 is quite low. For both As (N = 2) and Se (N = 4), only a limited number of weak lines were available for calibration. Consequently, the detection of low concentrations of these elements is compromised. The R^2 is also relatively low for Pb at concentrations lower than 0.1 mg/L. However, Cr, Ni, Cu, and Cd show good R^2 for such low concentrations. All the detection limits calculated were found to be extremely low (ranging between 0.0001 to 0.0107 mg/L), and in several instances, even lower than the minimum concentration of the standard solutions employed.

Table 3.10: Statistical assessment of the calibrations for mixed standard solutions of the PTEs (Cr, Ni, Cu, Zn, As, Se, Cd, and Pb)

z	EoI	State	λ nm	LoD mg/L	Range mg/L	y	R^2	RMSE mg/L
24	Cr	II	205.6	0.0004	0.001-0.5	467.48x+0.9833	0.9848	0.037
		II	206.6		0.5-50	576.15x+0.6763	0.9945	1.855
		II	267.8					
		II	283.5					
		II	284.3					
		II	285					
		I	357.9					
		I	359.4					
		I	360.6					
		I	425.4					
		I	427.5					
		I	437.125					
28	Ni	II	216.5	0.0003	0.001-0.5	1520.8x+0.0822	0.9176	0.07
		II	221.6		0.5-50	1774.5x+0.4438	0.9896	0.303
		II	241.6					
		I	300.3					
		I	301.2					
		I	338					
		I	341.5					
		I	344.6					
		I	351.5					
		I	352.5					
29	Cu	II	224.3	0.0003	0.001-0.5	708.9x+0.0982	0.9649	0.008
		II	224.7		0.5-50	682.62x+0.291	0.9948	0.967
		I	324.8					
		I	327.4					
		I	465.1					
		I	510.6					
		I	515.3					
		I	521.9					
30	Zn	II	202.6		0.001-0.1	-	-	-
		I	213.9	0.0002	0.1-2.5	621.9x-0.1649	0.9883	0.072
		I	334.5		2.5-50	544.01x-0.4883	0.9984	1.378

Table 3.10: Cont.

z	EoI	State	λ nm	LoD mg/L	Range mg/L	y	R^2	RMSE mg/L
		I	468.1		50-1000	$2449.2x^2$+1115.7x-94.322	0.9886	102.144
		I	481.1					
33	As	I	189		0.001-0.1	-	-	-
		I	278.1	0.0001	0.1-50	19531x+0.3696	0.9869	0.29
34	Se	I	204	0.0002	0.001-0.5	1385x+0.5045	0.1691	0.014
		I	473.1		0.5-50	23288x+6.0657	0.9879	0.002
		I	474.2					
		I	891.9					
48	Cd	I	340.3	0.0005	0.001-0.5	1083.8x+0.153	0.9435	0.147
		I	346.7		0.5-50	1585.6x+0.6077	0.9907	1.524
		I	467.8					
		I	480					
		I	508.6					
		I	643.9					
82	Pb	I	261.4	0.0107	0.001-0.1	176.92x+0.0661	0.5881	0.006
		I	266.3		0.1-50	3068.8x+0.9306	0.9892	2.125
		I	283.3					
		I	405.8					
		II	560.8					
13	Al*	I	236.7					
		I	237.3					
		I	308.2					
		I	394.4					
		I	396.1					

z = atomic number, EoI = element of interest, λ = wavelength of the lines used for calibration (* Al used as internal standard), LoD = limit of detection: calculated according to the 3σ-IUPAC criterion (LoD = $3*\sigma B/k$) (IUPAC, 1976), y = formula used for calibration, R^2 = coefficient of determination, RMSE = root mean square error, σ = standard deviation of the background signal at the lowest solution concentration, k = slope of the calibration line.

Discussion and Conclusion

In general, the results show that multi element standard solutions with up to eight elements can be used for calibration, as for all eight elements calibration curves could be established. These are complementary to the existing calibrations of Li, Na, Ca/Mg, K, Zn/Sr, NO_3, SO_4 and Cl. However, calibrations for Zn and As could only be established above 0.1 mg/L. Moreover, if prepared and predicted values are compared below a concentration of 0.1 mg/L, only Cr shows reasonably meaningful results with an R^2 of 0.88 and a systematic overestimation of the concentrations (see Figure 3.23).
For concentrations above 0.1 mg/L, a strong correlation is observed between the prepared and predicted concentrations of all analysed elements (cf. Table 3.11). The lowest correlation, at 0.989, is found for As. Exemplarily, the calibration curves for Cr and Cu between the prepared and the predicted concentration are shown in Figure 3.24.

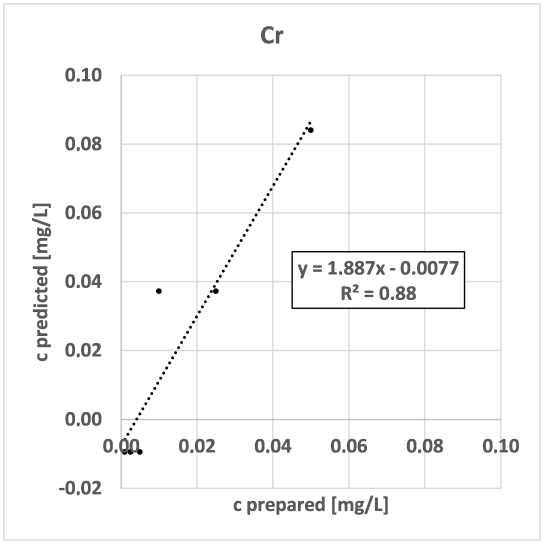

Figure 3.23: Calibration curves for Cr between the prepared and the predicted concentration (in the range of 0.001 to 0.05 mg/L).

Table 3.11: Slope and determination coefficient of the calibrations between the prepared and predicted values.

	Cr	**Ni**	**Cu**	**Zn**	**As**	**Se**	**Cd**	**Pb**
m	0.995	0.993	0.996	0.998	0.989	0.990	0.994	0.996
R^2	0.996	0.992	0.996	0.999	0.989	0.991	0.993	0.990

m = slope

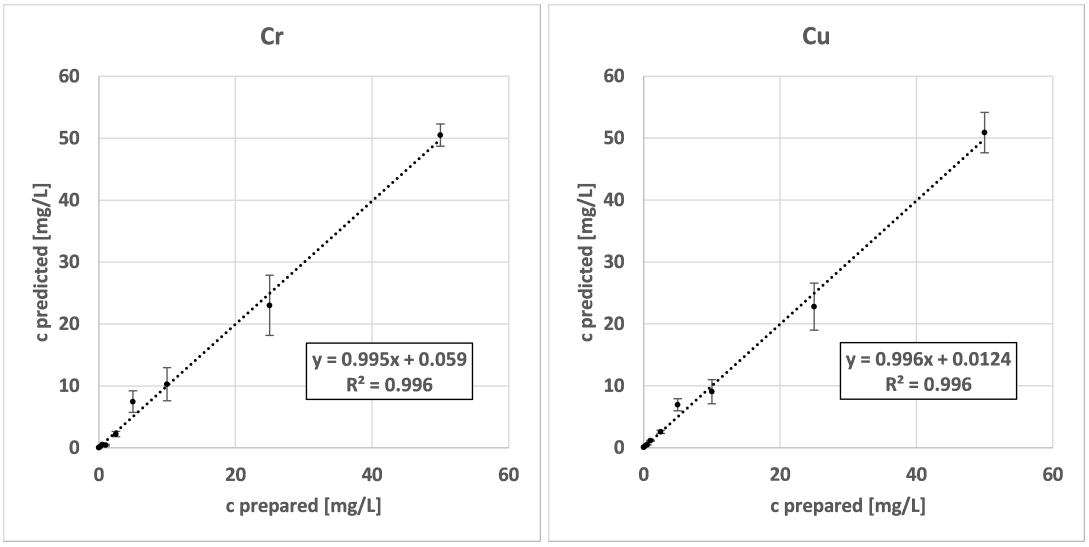

(a) **(b)**

Figure 3.24: Calibration curves for **(a)** Cr and **(b)** Cu between the prepared and the predicted concentration (in the range of 0.1 to 50 mg/L).

This shows that a SE-LSC technique adapted to pLIBS enables quantitative analysis of PTEs in standard solutions. However, this is currently only a proof of concept and has not yet been applied to real-world samples. It is anticipated that more pronounced matrix effects will arise compared to those observed in standard solutions. For instance, it must be determined whether the TDS of an analysed solution affects the outcomes. Furthermore, there could be interference from unanalysed elements, and it is conceivable that both effects could adversely affect the measurement results simultaneously.
In order to investigate this, different types of water should be analysed in future. On the one hand, various mine waters such as highly saline mine waters from coal mining should be considered. On the other hand, mine waters that are only influenced by mining and do not have high EC. For example, samples close to former mine sites in the Meuse river catchment area at the border triangle of Germany, Netherlands, and Belgium as done by Esser et al. (2020) for riverbed sediments. In this study area many pollution sources are given, such as former mine sites, smelters, and other industries. As shown in the literature, these riverbed sediments contain high amounts of the calibrated PTEs, exceeding typical background values in Europe (Esser et al., 2020). These can be mobilised and therefore found in the river water. Waters that are influenced by acid mine drainage (AMD) or acid rock drainage (ARD), such as the Rio Tinto river (Romero-Matos et al., 2023), should also be analysed to evaluate the influence of extreme pH conditions. Although it can be assumed that the pH has no influence on the results with the developed method, this has yet to be proven. The same applies to differently oxidising or reducing waters. It should be tested whether the redox value has an influence too.
Although the LoDs are below all current WHO and German drinking water limits, it is unlikely that the method can quantify precisely enough in the concentration range of the thresholds for non-laboratory prepared solutions, except for Cu (cf. Table 3.12). At present, at least pre-screening for PTEs is possible for a selection of laboratory samples.

Table 3.12: Drinking water limits defined by WHO and TrinkwV.

Element		Cr	Ni	Cu	Zn	As	Se	Cd	Pb	Reference
TrinwV	mg/L	0.025	0.02	2	-	0.01	0.01	0.003	0.01	(BMG, 2023)
WHO	mg/L	0.05	0.07	2	-	0.01	0.04	0.003	0.01	(WHO, 2022)

WHO = World Health Organisation; TrinkwV = Trinkwasserverordnung (Germany)

Chapter 4

Discussion

This chapter briefly discusses the research findings of Chapter 1, 2, and 3 and contextualises them. In Section 4.1, the spread and shape of the EvR is discussed, since improvement of the distribution significantly influences both reproducibility and sensitivity. Introducing a layer of pencil can be a cost-effective and simple way to enhance surfaces. Nevertheless, alternative techniques or improvements could optimise the method. In Section 4.2 matrix effects and self absorption are discussed. Section 4.3 categorises the novel technique within the realm of in-situ analysis and assesses its merits and demerits relative to alternative measuring methods. Finally, the development status will be evaluated in Section 4.4 and assigned a technology readiness level (TRL).

Key questions:

- How can the spread and shape of the evaporation residue be further optimised?
- How can self-absorption be reduced or eliminated?
- How does the developed method compare to other instruments?
- What is the current stage of development of the method?
- What is the market potential of the method?

4.1 Spread and Shape of the Evaporation Residue

As already discussed in Section 3.1.3, the surface enhancement using a pencil layer leads to a more homogenous distribution and shape of the EvR compared to a blank Al-foil. This method is a very cost-effective one, however, there might be improvements possible.

The repeatability of the analysis results also depends on the uniformity of the applied pencil layer. Although no direct differences were found between the analysis results on the Al-foils prepared by three different users, a certain variance can be assumed on each individual foil. This is due to the fact that application by hand is never perfectly homogeneous and that pressure differences result in stronger or weaker application or even bad spots. As a result, an evaporating drop may spread differently. Applying a pencil layer by a machine could prevent this issue. However, a comparison between automated and manual application of the pencil layer was not possible within the scope of this work, as a suitable device would first have to be developed or adapted for the process. Applying the carbon, clay, and wax layer by machine would have a further time-saving effect, as the SE process takes quite a long time by hand. At the same time, instead of the entire surface of the aluminium foil, only the area of the recess in the sample holder could be surface-enhanced in order to save resources and time. Of course, this is only the case if it does not unnecessarily complicate the automated process.
In addition, the contact angle between the droplet and the surface could be increased with advanced surface enhancement substances, as presented in Wu et al. (2021), making the surface even more hydrophobic. This would further homogenise the distribution of the EvR and reduce the surface area covered, leading to an improvement in repeatability and sensitivity. However, care must be taken to ensure that the coating does not become a cost factor. The method developed so far is aimed at a cost-effective solution that excludes the use of an expensive sample carrier as a consumable.
It is also feasible to identify simple molecules using LIBS (Xu et al., 2022). The obtained spectra in this thesis sometimes showed evidence of water in the form of OH molecule peaks, such as at lines 306.4, 306.8, 307.8, 309.0, 308.2, and 309.6 nm. This could imply that the droplets were inadequately dried prior to analysis, or that hydroxides were generated as EvR. However, this does not appear to have a negative impact on the results. Though it would be interesting to study the EvR using microscopic techniques such as scanning electron microscope (SEM), combined with semiquantitative energy-dispersive X-ray spectroscopy (EDX) or wavelength dispersive X-ray analysis (WDX). The homogeneity of the EvR could be investigated and thus better conclusions could provide better insights into the influence of the SE-step. Additionally, a more thorough characterisation of the resulting salts could lead to further interpretations.

4.2 Self-Absorption and Other Factors Limiting the Method

Currently, concentrations higher than approximately 160 mg/L and ECs higher than approximately 1000 μS/cm in the initial solutions result in unreliable results when analysed with the developed method. Self-absorption can be regarded as the main reason for this, as it intensifies with the growth of analyte concentration (Palleschi, 2022a). This can also be observed in Figure 4.1, displaying the median IR values

used for the calibration of Na in this thesis. The plasma becomes optically denser with higher analyte concentration, and stronger absorption occurs (Palleschi, 2022a), cancelling out linearity. This effect must be compensated for mathematically, if higher concentrations need to be analysed. Thereby, also the results of the analysis for lower concentrations could be enhanced.
When self-absorption is absent, the signal intensity is directly proportional to the analyte concentration (Palleschi, 2022a). Consequently, the signal increases proportionally as the concentration rises and a linear calibration line can be established. However, when the plasma is optically denser, the emitted radiation is partly reabsorbed, so the detector no longer receives it (Palleschi, 2022a). This cancels the linearity and results in a saturation effect: as the analyte concentration increases, the measured intensity increases to a lesser degree (Palleschi, 2022a). This is clearly visible in Figure 4.1.

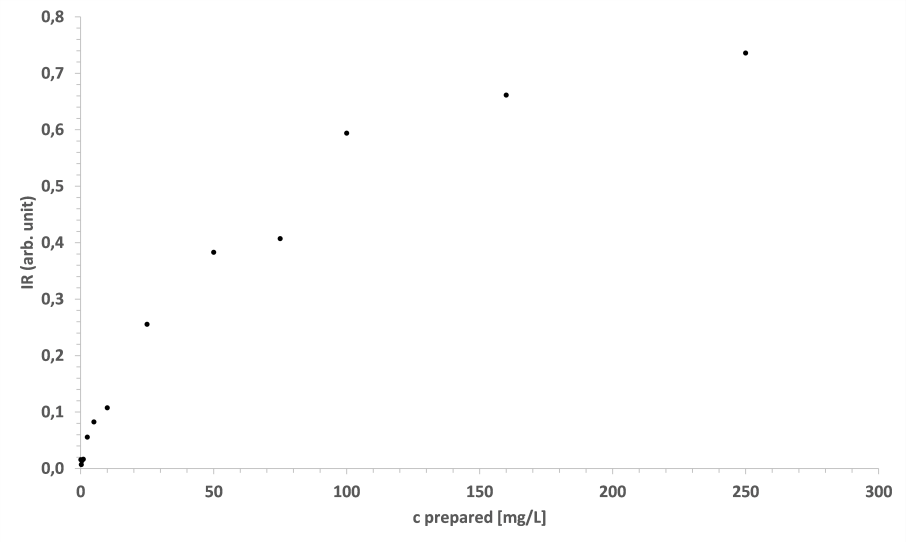

Figure 4.1: Self-absorption visible in the degressive proportionality between the IR and the prepared concentration for Na.

Many diverse formulae have been created for mathematical adaptation. Most need the analysis of physical parameters such as electron density or plasma temperature, which is not easy to analyse with a handheld device. Palleschi (2022a) presents a more straightforward method for compensating self-absorption, considering varying peak widths at different levels of self-absorption.
Firstly, it is assumed that a homogeneous plasma is present, which is in a local thermal equilibrium (Palleschi, 2022a). In this, the number of photons of a certain wavelength λ emitted by the plasma on the path to the detector can be determined as follows (Palleschi, 2022a):

$$\frac{dn_p(\lambda x)}{dx} = \epsilon(\lambda) - k(\lambda)n_p(\lambda, x) \tag{4.1}$$

$\epsilon(\lambda)$ = *"plasma spontaneous emissivity (energy emitted per unit time, unit volume, and unit wavelength)"* (Bredice et al., 2006)
$k(\lambda)$ = absorption coefficient (cm^{-1}) (Bredice et al., 2006)
n_p = photon number (Bredice et al., 2006)

Here, ϵ is *"proportional to the number of emitters and to the spontaneous emission coefficient A_{ki} of the transition"*.

"Following the Einstein treatment of the propagation of radiation in a two-level atomic system [...]", it can be demonstrated that k and ϵ, are linked by the relation (Palleschi, 2022a):

$$B(\lambda)k(\lambda) = \epsilon(\lambda) \tag{4.2}$$

B(λ) = *"Planck black body radiation function at the plasma temperature (T)"* (Palleschi, 2022a)

This equation can be solved for each wavelength along the line of sight of the detector (Palleschi, 2022a). In the case of an optically thin plasma (k(λ)l $\ll$1) the shape of the broadened lines is fitted best with a Lorentzian function. The peak of the lines is found at the wavelength of the transitions.
However, it should be noted that self-absorption has a greater impact at higher emission levels, specifically at the peak of the line (Palleschi, 2022a). This is due to the proportional relationship between the absorption and emission coefficient (Palleschi, 2022a). This alteration modifies the peak's shape, making it harder to compute the integral intensity. However, for low to moderate self-absorption, the line intensity can be calculated by the following equation (Palleschi, 2022a).

$$I \cong I_0 \left(\frac{1 - e^{k(\lambda_0)^l}}{k(\lambda_0)^l} \right)^{\frac{1}{2}} \tag{4.3}$$

k(λ_0) = *"absorption coefficient calculated at the peak of the emission line"* (Palleschi, 2022a)
I_0 = *"integrated intensity (total number of photons emitted) that would have been measured on the detector if the plasma was optically thin"* (Palleschi, 2022a)

Furthermore, the FWHM of a self-absorbed line increases with the same square root behaviour as under conditions of an optically thin plasma (Palleschi, 2022a):

$$\Delta\lambda \cong \Delta\lambda_0 \left(\frac{1 - e^{k(\lambda_0)^l}}{k(\lambda_0)^l} \right)^{\frac{1}{2}} \tag{4.4}$$

$\Delta\lambda$ = *"FWHM of the self-absorbed line"* (Palleschi, 2022a)
$\Delta\lambda_0$ = *"FWHM of the line in the optically thin limit"* (Palleschi, 2022a)

Thus, if $\Delta\lambda$ can be estimated, only $\Delta\lambda_0$ has to be measured to estimate the factor (Palleschi, 2022a):

$$\left(\frac{1 - e^{k(\lambda_0)^l}}{k(\lambda_0)^l} \right)^{\frac{1}{2}} \tag{4.5}$$

The following equation results when the factor above (4.5) is inserted into equation 4.3 (Palleschi, 2022a):

$$I_0 \cong I \frac{\Delta\lambda}{\Delta\lambda_0} \tag{4.6}$$

The following equation leads to better results for the case of strong self-absorption (Palleschi, 2022a):

$$I_0 \cong I \left(\frac{\Delta\lambda}{\Delta\lambda_0} \right)^{0.85} \tag{4.7}$$

Since by definition I_0 is proportional to the number of emitting atoms or ions, this formula allows the linear relationship between the measured intensity I and the concentration in the sample (Palleschi, 2022a). The actual line intensity I_0 (unaffected by self-absorption) can therefore be determined if the FWHM of a line not affected by self-absorption can be determined. However, MLR is utilised in this thesis, hence factors $\Delta\lambda$ and $\Delta\lambda_0$ are reliant on several lines in the spectrum. For Na, the factors are dependent on a total of five Na lines and five Al lines, rather than just one (Na : 330.2, 589.0, 589.6, 818.3, 819.5 nm and Al: 236.7, 237.3, 308.2, 394.4, 396.1 nm). It is also complex to pinpoint a line that remains unaffected by self-absorption to determine $\Delta\lambda_0$.
Furthermore, as the steps involved in calculating the IR, using the software Profile Builder, are not completely transparent and the FWHM would have to be read out individually for each line in an external software, self-absorption compensation as described by Palleschi (2022a) is also difficult to implement. Therefore, it is necessary to find a suitable method of compensating for self-absorption in the future.
Hou et al. (2019) compares advantages and disadvantages of different approaches to

correct or eliminate self-absorption. In order to be able to apply the formulae presented in this work to the calibrations developed, however, either physical parameters that cannot be easily measured with the portable device are missing or a more extensive spectroscopic software would be necessary. In addition to the two applications from the manufacturer (SciAps Utility and Profile Builder, both SciAps, Woburn, MA, USA), the Spectragryph software was tested (Menges, 2023), but FWHM values could only be determined manually. Therefore, compensation for self-absorption was not possible within the scope of this thesis.

Other factors: In addition to self-absorption, there are other limitations that lead to reduced sensitivity, repeatability or difficulties at higher concentrations. Due to the measurement method with a rectangular point grid of 10 * 10 over a circular EvR, some points are analysed without analyte. Some of the spectra will therefore show little or no intensity for lines of the EoI, as only the SE-Al foil was analysed. Four measurements are carried out per measuring point and averaged to form a spectrum. This results in a total of 100 spectra, which show two normal distributions for an EoI contained in a sample: one with increased intensities for the lines of the EoI and one with no or low intensity. The reason for this is the area around the circular EvR containing no or minor concentrations of the EoI. If it were possible to statistically exclude all spectra that did not contain EoI before calculating the IR, it would be possible to increase sensitivity. Furthermore, it would allow for a more accurate analysis of higher concentrations as the effect of two normal distributions is amplified with increasing concentration.
Although a spectrum of a LIBS analysis should be a set of lines, all these lines are broadened to peaks even at any high resolution of the spectrometer (Demtröder, 2011). The frequency of the spectral lines is not entirely monochromatic, instead, there is a range of frequencies surrounding a central value (Demtröder, 2011). This is because of different physical effects when electromagnetic radiation is absorbed or emitted leading to a transition between two energy levels of the atomic system (Demtröder, 2011). The damping of oscillation through spontaneous emission (energy radiation) causes the natural linewidth (Demtröder, 2011). Although usually unobservable, due to masked by other effects, it presents a Lorentz profile (Demtröder, 2011). Doppler broadening is usually the dominant cause of the broadening (Gaussian profile) (Demtröder, 2011). In addition, there is the impact broadening due to elastic and inelastic collisions of the atoms (Voigt profile) (Demtröder, 2011). Self-absorption also affects the width of peaks. As concentration increases, the peaks also become wider (see Figure 3.21). Consequently, at higher concentrations, parts of the peak are no longer detected if the integration range is chosen too small. Nevertheless, the range to be integrated cannot be chosen arbitrarily large, as otherwise, different lines of the same or another element would be detected. This is another reason why higher concentrations ($\geq$ 160 mg/L) are often underestimated in this work. The most straightforward approach would be to dilute higher concentrated solutions.

4.3 Classification of the Analytical Method in Other Aqueous Elemental Analysis Techniques

The significance of analysing aqueous solutions for elemental content is also illustrated by the multitude of measurement techniques that have been developed in recent decades. Zulkifli et al. (2018) gives an overview of the development of techniques used for the detection of pollutants in aqueous solutions. They consider both biological and inorganic contaminants, whereby only the analysis of the latter is considered here. They show that chromatography developed in the 1970s, followed by mass spectrometry and, in the early 1990s, spectroscopic techniques and sensor-based analysis. Biosensors were introduced in the late 1990s.
In this section, first, the developed method is compared and categorised alongside other field methods (cf. Section 4.3.1). Next, transportable instruments are presented and compared (cf. Section 4.3.2). Subsequently, it will also be analysed how the developed method compares to established laboratory methods and how it could potentially complement them in the future (cf. Section 4.3.3). Key criteria for comparison have been established according to Gałuszka et al. (2015):

- Weight and dimensions
- Legal requirements or transport regulations
- Ease of use (trained staff)
- Equipment and chemicals required
- Greenness of the method
- Acquisition cost
- Maintenance and operating costs (cost-effectiveness)
- Analysis time (including preparation)
- Required sample quantity
- Ruggedness of the device
- Handling of data storage and processing
- Sensitivity and LoDs
- Reproducibility

4.3.1 Comparison to Other Field Instruments

There is a rapidly growing market for field instruments for environmental analysis, as technology develops rapidly and there is an urgent need for direct, real-time and cost-effective analysis for many applications (Gałuszka et al., 2015; Mukherjee et al., 2021). Field instruments are commonly used to analyse on-site parameters such as pH, EC, E_h and dissolved oxygen (Gałuszka et al., 2015). To date, multi-elemental analysis of aqueous solutions is mostly conducted in laboratories. However, a diverse range of field instruments are currently under development and utilisation employing a variety of methods. These will be briefly outlined in the following. According to Gałuszka et al. (2015) and Lemière and Harmon (2021) portable devices should:

- be lightweight
- have a compact size
- be able to analyse quickly
- should only need simple hardware additions
- should be ruggedised
- should have an own portable energy source
- data should be similar to laboratory data

Test strips and kits: The stated criteria for field techniques are met for test strips and kits, except for the last two criteria. An energy source is usually not required, since they only indicate concentrations via a colour change on a paper strip, which can be detected by the naked eye (Fan et al., 2023). This makes them very easy to handle and transport. Nevertheless, compared to laboratory analyses, this technique typically provides only semi-quantitative findings as the concentration is usually indicated by multiple increments (Cho et al., 2019). Furthermore, each compound requires individual analysis with its own test strips, or at least with combined test strips, resulting in wastage and significant costs.
For example, Fan et al. (2023) developed photoluminescent chemicals for test strips to detect and quantify Ag^+. Detection limits of 1.56 mg/L and 0.19 mg/L were identified for the fluorometry and colorimetry test strips respectively (Fan et al., 2023).
Das et al. (2014) introduced test strips for As detection in the range between 0.01 - 0.25 mg/L with graduations at 0, 0.01, 0.02, 0.05, 0.1, 0.2, and 0.25 mg/L. The authors reported that the cost per test was $0.6, and compared it to the cost of As kits from Merck ($1.84, range of 0 - 0.5 mg/L), Hach (Hach $1.42, range of 0 - 0.5 mg/L), and Machery-Nagel ($1.01, range of 0 - 0.5 mg/L). Though stated as user friendly by the authors, the detection time is 7 min, different chemicals such as acids and potassium

permanganate have to be used in preparation, and highly poisonous arsine gas is generated in the reaction process (Das et al., 2014). Whilst commercially available test strips such as from Merck and Machery-Nagel may certainly more user-friendly, they result in an excessive amount of waste and prove expensive for large measurement programmes. Additionally, the results obtained are only semi-quantitative and it is not possible to test several compounds simultaneously.

Smartphone based analysis: A relatively new trend is to utilise smartphones in reflectance analysis of test strips (Haque et al., 2018; Golicz et al., 2020). For instance, Haque et al. (2018) conducted an analysis of As levels in groundwater using two commercially available field kits. Images of an unused test strip, a sample strip, and the colour chart were then taken with smartphones and processed (Haque et al., 2018). This approach enabled the assignment of colour gradations to concentrations, resulting in detection limits of 0.0092 mg/L in the laboratory and 0.0219 mg/L in the field (Haque et al., 2018). Although this economical approach turns the semi-quantitative results of the test strips into quantitative results, the method is generally limited to the elements and the concentration range for which the respective test strip is intended.

Photometers: Small and inexpensive photometers such as offered by Hanna® instruments are a superior alternative to chemical test kits (Hanna-instruments, 2024). The Checker® HC series, for example, provide fast and concise measurements with very easy handling. They can be used to analyse a wide variety of elements (e.g. Ca, Cl, Fe, Cr, I, Ni, Cu, Ni, Mn, Mg, and P) and compounds (e.g. silicic acid, NO_3, NO_2, PO_4, and NH_4) for a wide range of applications (e.g. sea water or pool water). The devices operate photometrically, utilising light-emitting diodes (LEDs) of different wavelengths, depending on the substance to be analysed. A reference value can be determined via a comparative measurement of the sample solution in a glass cuvette without any added reagent. Once the reagent has been added, the sample changes the colour and the intensity depends on the concentration. The device then automatically calculates the concentration in the solution by comparing with the stored calibration and subtracting the blank measurement. The results of the measurement can be read directly from an easy-to-read liquid-crystal display (LCD). The resolution varies from analyte to analyte and multiple measuring devices with different concentration ranges are available for each type of analyte. Unfortunately, this presents a significant drawback, as it necessitates not only individual equipment for each analyte, but also for diverse concentration ranges. In addition to this, costly reagents are mandatory, and there is the production of waste (Hanna-instruments, 2024).
Other photometers that are less compact also have the capacity to measure multiple parameters. Nevertheless, they are accompanied by a higher cost and also demand the use of chemicals that are conditional on the analyte. As a result, simultaneous analysis or screening is unattainable as each analyte necessitates its own reagent. Such a method is considerably time-consuming, particularly in cases where more than one compound is required to be analysed.

Electrode probes: Electrode probes are based on electrochemical principles and require the measurement of an electrical current generated by a solution in an electrochemical cell (Dimeski et al., 2010). Electrochemical analysis methods can be divided into three main groups: potentiometry, voltammetry, and coulometry (Dimeski et al., 2010).
To date, potentiometry, which measures the electrical potential as a voltage in a cell, is the most commonly used method (Dimeski et al., 2010). A famous example, the pH electrode, which was the first electrode probe for water analysis, was introduced in approximately 1930 (Yaroshenko et al., 2020). Electrode probes consist of an electrochemical sensor, an electrolyte and an electrochemical measuring instrument. The latter contains two electrodes for ion-selective electrodes (ISEs) to analyse ion concentrations selectively (Dimeski et al., 2010). It can also contain three electrodes - a working electrode, a reference electrode, and a counter electrode (Lu et al., 2018). The working electrode can be modified to detect various kinds of ions (Lu et al., 2018). Benefits include being inexpensive, simple, highly sensitive, easy to use, rapid to analyse, portable, and suitable for field monitoring (Lu et al., 2018).
By using stripping voltammetry, which includes a pre-concentration step, it is even possible to analyse more than one ion (Bernalte et al., 2020). Using single screen-printed electrodes (SPEs), Bernalte et al. (2020) simultaneously detected mining induced Cu^{2+}, Pb^{2+}, and Hg^{2+} pollution in the Amazon River. Within 60 seconds of analysis, Pb^{2+}, Cu^{2+}, and Hg^{2+} could be detected down to 0.015, 1.3, and 0.002 mg/L respectively. Quantification was possible with minor pre-treatment (addition of HCl) between 0.005 and 0.3 mg/L (Bernalte et al., 2020).
These SPEs appear to be the most promising electrode probes due to their low cost and the ability to analyse several ions. However, a true multi-element analysis is not yet possible due to the limited number of analytes per SPEs.

Analysis using pXRF: In in-situ analysis of solid materials, pXRF has been an essential component for many years now (Gałuszka et al., 2015; Lemière and Uvarova, 2020). As this technique is typically not destructive, it is the most environmentally friendly approach to solids analysis (Gałuszka et al., 2015). A direct comparison between pLIBS and pXRF for solid analysis has already been presented in Table 1.1.
Also, in liquid analysis first attempts of multiple elemental analysis have appeared in the last few years. In contrast to solids, where determining the percentage composition is often sufficient, the requirement for liquid analyses is higher. Typically, measurements are expressed in mg/L, which is approximately equivalent to ppm. The detection limits of the hand-held devices must initially be sufficient for this. This makes it clear why the analysis of aqueous samples with pXRF has only developed in recent years. The lower detection limits can only be achieved through technical development and improved statistical methods. The typical penetration depth of X-rays in water is between 2 and 4 mm (Lemière and Harmon, 2021).
In Eksperiandova et al. (2002) the authors describe different sample preparation techniques that allow elemental analysis of aqueous solutions by pXRF. They determined a number of elements in wastewater (Ag, As, Bi, Cd, Co, Cu, Fe, Ga, Ni, Pb, Se, and Zn) using LSC, in particular chelating (che/com) and membrane generation (MeGe)

(Eksperiandova et al., 2002). The detection limits using a pre-concentration step were found to be between 0.01 and 0.04 mg/L (Eksperiandova et al., 2002).
Melquiades et al. (2011) quantified Ca, Ti, Mn, Fe, Ni, Cu, Zn, Pb and other elements by pre-concentration through LSC (chelating/complexation with subsequent filtering). They could analyse 14 samples within a four-hour field work and achieved a SD around 15 % (Melquiades et al., 2011). The LoDs are between 0.0010 and 0.040 mg/L.
Pearson et al. (2017) analysed aqueous solutions for their EC and Cl, K, and Ca concentration utilising pXRF. Therefore, they used simple plastic sample cups covered with Prolene®thin-films typically used in solid analysis (Pearson et al., 2017). In a subsequent study, Pearson et al. (2018) used the same technique to analyse K, Mn, Ca, Fe, Cu, Zn, and Pb in water samples. A wide range of concentrations could be analysed with only 90 s scanning time per sample.
Another approach is the orthogonal triaxial geometry of pXRF measurement used to analyse PTEs in mine water samples (V, Cr, Mn, Fe, Co, Ni, Cu, and Zn) (Pessanha et al., 2020). LSC on FP was used and LoDs between 2 mg/L (Zn) and 18 mg/L (V) were achieved. Analysis time was approximately 600 s (Pessanha et al., 2020).
LSC was also used for pXRF analysis as a combination of adsorption and filtration followed by drying (Tighe et al., 2020). A volume of 2 L per sample was filtered, requiring 5 min for filtering and 30 min for drying (Tighe et al., 2020). With costs of approximately $0,5 per sample Pb concentrations down to 15 ppb could be analysed (Tighe et al., 2020).
Without any sample preparation, Abukashabeh and Abu-Halimeh (2021) analysed U in aqueous solutions. They achieved a RSD of less than 5% for U concentrations above 10 mg/L and a LoD of 2.5 mg/L by using 15 mL propylene tubes (Abukashabeh and Abu-Halimeh, 2021).
Tiihonen et al. (2022) used a self-developed filter to analyse Mn, Ni, Cu, Zn, Pb, and U utilising pXRF. In less than 15 min they could simultaneously analyse these elements in the μg/L range by filtering 10 mL of sample solution.

Analysis using pLIBS: The Z-9 Liquidator by SciAps utilises the newest generation of the Z series (Z-903) to analyse aqueous solutions (SciAps, 2023a). It does not use a LSC step but a LAC (SciAps, 2023b). To generate an aerosol of the sample solution, a Meinhard nebuliser is employed. Only 1 - 2 mL of sample solution are required per test, and no dilution is necessary (SciAps, 2023a). Each analysis typically lasts for approximately five seconds (SciAps, 2023a). Thanks to its small dimensions, moderate weight (6.8 kg + 2.2 kg for the Z-903), and battery-operated capability, this device also permits field analyses (SciAps, 2023a). Currently, the system is tailored for examining Li, B, Na, Mg, K, Ca but has the potential to calibrate all elements. TRL 9 can be assumed for this technology since it has been sold to customers. However, only a preprint and an application note are available to describe the method and to compare the performance.
Preliminary findings on the calibration of Li, B, K, and Ca in synthetic and natural brines are presented in SciAps (2023b). Calibration curves with high R^2 values, varying from 0.9631 (K) to 0.9935 (Ca), were constructed for a broad concentration range

spanning several hundred ppm to low percentages. The calculated RSD are between 6 and 13 % (SciAps, 2023b), and therefore lower than for the method developed within this thesis (cf. 3.9).
The technique is well-suited for the examination of highly concentrated solutions, such as brines, without necessitating any dilution. Nevertheless, self-absorption is noticeable for Ca and to a lesser extent for Li (see SciAps (2023b)). In both cases, quadratic calibrations were utilised, due to the fact that the IR increases at a reducing rate with mounting concentration, impeding proportionality. Linear calibration was feasible for K, with self-absorption playing a relatively minor role (SciAps, 2023b). It is not possible to draw any conclusions for B, as only a three-point calibration was performed (SciAps, 2023b).
On the one hand, the method is presumably less sensitive as the sample preparation does not concentrate the analyte. On the other hand, it can be assumed that the new generation of LIBS instrument is associated with an increase in sensitivity, as the energy of the pulse has also been slightly increased (SciAps, 2023a). Furthermore, less sample preparation is required as the aerosol generation is automated. Ultimately, however, important statistical parameters for the liquidator are missing for a conclusive comparison of both measurement methods.

4.3.2 Comparison to Transportable Instruments:

This category comprises of instruments which can be transported to the field, however, they are either too heavy or large to be truly portable. For example, Gałuszka et al. (2015) defines a threshold of 10 kg for this kind of field instrument category.

Ion chromatography: One example of a transportable instrument is the miniaturisation of a conventional IC described in Elkin (2014). It weighs 27.5 kg including batteries, a solar panel, and measures 62 × 48 × 30 cm. When a power supply is available, the weight is reduced to 13 kg. The instrument is capable of continuous, automated sampling. Using a stored eluent, it can analyse Cl^-, ${NO_3}^-$, ${SO_4}^{2-}$, ${PO_4}^{3-}$ with a RSD of 1%. To reduce waste, it only consumes 23 μL per sample, which is analysed in 15 min. For PO_4 the LoD is 0.55 mg/L.

LIBS: LIBS has already proven successfully in analysing various elements in-situ by utilising miniature versions (Sheng et al., 2019; Sui et al., 2021; Hartzler et al., 2019, 2023), which are transportable, though not entirely portable. For instance, Sui et al. (2021) developed a device which weighs 38.6 kg and has dimensions of 75* 45* 48 cm. It is able to sample and analyse Li, Na, Mg, K, Ca, and Sr automatically by LAC. However, it requires a power supply and consumes 580 W. Higher laser energies in these systems enable lower detection limits compared to truly portable devices. However,

the weight, dimensions, and power requirements of these devices significantly limit their applications.

Telescopic analysis: Samek et al. (2000) already developed a telescopic system in 2000, which was used for remote analysis of technetium in aqueous solutions, aimed at its application in nuclear fuel reprocessing. The system enabled an analysis of the target from a distance of 2 to 5 m and and a LoD of 25 mg/L was estimated (Samek et al., 2000). Unfortunately, the method was not evaluated with other elements, and thus cannot be compared with the method proposed in this thesis. However, it shows the possibility to also develop telescopic LIBS systems.

4.3.3 Comparison to Laboratory Based Instruments

Laboratory instruments such as AAS and ICP-(MS/OES/AES) are considered as *"conventional"* methods for elemental detection in aqueous solutions (Mukherjee et al., 2021). IC analysis is also a widely accepted standard technique for cations and anions.
These conventional methods generally achieve higher sensitivities and reproducibilities than pLIBS, especially ICP analyses, which are highly selective and sensitive to the nanogram level. However, these conventional techniques require trained staff, are expensive to acquire and operate, and need a stationary laboratory space (Mukherjee et al., 2021).

IC: When using IC for analysis, it is important to note that the method is limited to specific cations and anions. For cations, typically Li^+, Na^+, K^+, Ca^{2+}, Mg^{2+}, and Sr^{2+} are analysed. The anions usually include Cl^-, $SO_4{}^{2-}$, $NO_3{}^-$, $NO_2{}^-$, F^-, Br^-, and I^-. In addition, chemicals in the form of the eluent are required for the IC.

AAS: As AAS analysis is less expensive compared to ICP analyses, it is the most commonly utilised method for determining various PTEs, including Zn (Mukherjee et al., 2021). Typical LoDs are within the order of μg/L (Mukherjee et al., 2021), but usually different elements need to be analysed separately.

ICP-MS/ ICP-OES: ICP-MS and inductively coupled plasma optical emission spectroscopy (ICP-OES) are typically the most sensitive techniques for elemental analysis of aqueous solutions for various elements (Mukherjee et al., 2021). Based solely on statistical parameters, the developed field method cannot compete with the trace analysis of ICP-MS or ICP-OES. According to Fichet et al. (2006), even laboratory-based LIBS have detection limits that are approximately three orders of magnitude higher than those of ICP-OES. The pLIBS method cannot achieve comparable values for different

elements in terms of sensitivity or reproducibility. However, it still has advantages over ICP-MS or ICP-OES analyses. These laboratory analyses are quite expensive, require laboratory work, chemicals, and trained staff. This leads to results being available only after several days and at high costs.

4.3.4 Conclusions

Table 4.1 shows a comparison of different analytical techniques capable of simultaneous multi-element quantification. ISEs can be excluded from the comparison as they require one probe per analyte, making multi-element analysis impractical. However, SPEs may remain competitive due to their low price and the possibility to analyse several elements per probe. AAS was also excluded because typically a new analysis is required for each element.

Table 4.1: Comparison of different analytical techniques capable of simultaneous multi-element quantification.

	Port.	**Analyte**	**LoD**	**V**	**t prep.**	**t anal.**	**RSD**	**Range c**	**Ref.**
IC	no	Na	0.019	12	-	-	0.476	-	[1]
ICP-MS	no	U	0.00001	1	180	90	-	-	[2]
ICP-MS	no	Sr	0.0000214	12	-	-	-	-	[1]
ICP-AES	no	U	0.23	1	90	90	-	-	[2]
ICP-OES	no	Na	0.0005	10	-	-	-	-	[3]
WDXRF	no	U	3	20	2	600	-	1-1000	[2]
LIBS	no	Na	0.7	50	-	-	10	100-1500	[3]
tIC	(yes)	PO_4	0.55	23μL	<15	0	<1	-	[4]
tLIBS	(yes)	Ca	0.96	-	-	-	-	1-1124	[5]
tLIBS	(yes)	Na	0.58	-	-	-	-	1-1100	[6]
tLIBS	(yes)	Na	0.01	-	-	13.3	-	0.9-45	[7]
SPEs	yes	Pb	0.015	10	-	60	13.7	0.005-0.3	[8]
pXRF	yes	U	3	<5	0	30-60	<5; 10	1-1000	[2]
pXRF	yes	Pb	0.015	2000	35	-	7	0.001-1	[9]
pXRF	yes	U	0.043	10	13	2	6.3-34.2	0.05-10	[10]
pXRF	yes	Zn	2	200μL	-	600	1-10	50-300	[11]
pLIBS	yes	Na	0.014	0.75μL	<15	120	25	0.1-1000	[1]
unit			mg/L	mL	min	s	%	mg/L	

Abbreviations: port./p- = portable; t- = transportable; (LoD) = Limit of detection; V = sample volume; t prep. = preparation time; t anal. = analysis time; RSD = relative standard deviation; range c = concentration range tested; ref = reference. [1] = Schlatter et al. (2023); Schlatter and Lottermoser (2023); [2] = Abukashabeh and Abu-Halimeh (2021); [3] = Fichet et al. (2006); [4] = Elkin (2014); [5] = Sheng et al. (2019); [6] = Sui et al. (2021); [7] = Hartzler et al. (2023); [8] = Bernalte et al. (2020); [9] = Tighe et al. (2020); [10] = Tiihonen et al. (2022); [11] = Pessanha et al. (2020).

Based on the small selection of different analytical methods and examples by various authors presented in Table 4.1, the lowest detection limits are shown for the laboratory-based methods, as expected. The lowest detection limits within the non-portable methods are documented with ICP-MS, while the highest are with LIBS.
However, there is a tendency for sample preparation and analysis time to be slightly

longer than for the portable methods. It should be noted that this does not include the time required to transport the sample to the laboratory. In most cases, the detection limits for portable instruments are significantly higher than for laboratory analysis. However, some portable methods have comparatively better detection limits than the transportable ones. In addition, it can be seen that portable methods have significantly higher RSDs than laboratory ones.
In general, the portable and transportable techniques may not keep up with the very low detection limits of the laboratory techniques, however, the advantages of flexibility of use over laboratory analysis, no matter how good, are clear. If greater sensitivity is necessary, pLIBS can still be employed for pre-screening.
It can be concluded that both pXRF, and pLIBS are promising field techniques, which can also be applied to the elemental analysis of aqueous solutions. However, the latter has the big advantage that also lighter elements $Z < 12$ can be analysed.
For a portable device, the acquisition costs of well over 40,000 € for the pLIBS are quite high and also higher than for comparable pXRF devices. Tighe et al. (2020) for example stated that their pXRF device costs $25,000, but some may also cost up to 40,000 €. The acquisition costs may be high, but environmental departments could often make use of such devices as they have already been purchased for solid analysis. In addition, the costs for pLIBS and pXRF are still far lower than for laboratory devices such as IC/ICP-MS and the maintenance costs are significantly lower. For example, Tighe et al. (2020) stated that the cost of a pXRF is about 10 - 15% of an ICP-OES or ICP-MS device and typically costs less than $50,000. Moreover, in contrast to large laboratory devices, hardly any maintenance is required, which means that upkeep is significantly cheaper. The main wear and tear on the SciAps Z-300 occurs on the quartz window, which protects the optics inside the device. This window becomes dirty due to frequent analyses and must be cleaned regularly. Sooner or later, however, contamination occurs that cannot be removed even with compressed air, a cotton cloth, or solvents such as isopropanol. In this case, it is necessary to replace the window. However, this can be done cheaply and without any special expertise by unscrewing the nose. The maintenance costs are mainly dependent on the use of argon cartridges, if used. These have proven to be relatively economical, as several hundred measurements are possible with one cartridge costing less than 10 €.
A particular advantage of the pLIBS is that elements for which no calibration is available at the time of analysis can be quantified later. All that is required is that all the measurement settings are kept the same and that the factory wavelength calibration is carried out correctly before the measurements. So, if it is only realised days after sampling that a parameter of interest has not been measured, it is still possible to create a calibration and quantify it.

4.4 Technology Readiness Level (TRL) and Market Potential

Technology Readiness Level: The method that was developed within this thesis, incorporating the 3D-printed sample holder and hot plate, can be classified as having achieved a TRL of four: The initial experimental proof of concept was carried out, and

the technology was subsequently validated in the laboratory. Two initial prototypes, one being a hot plate intended for use in the field and the other being a sample holder, have both been developed and tested in a laboratory environment. There are already ideas in place for the ongoing development of both prototypes for more user-friendly operation. With a proper self-absorption correction, it will also be feasible to analyse highly mineralised waters. So far, an evaluation on natural and anthropogenic waters is still pending for PTEs, but it can be assumed that similar results will be achieved as with the alkali and alkaline earth metals, since calibration lines with a high R^2 could be created. Additionally, thorough in-situ testing of the method is required. However, an initial test performed at the river Inde near the former mine site in Walheim has demonstrated the possibility of executing the analysis steps in the field.

Market Potential: The developed method enables fast, cost-effective, quantitative in situ analysis of aqueous samples for the inorganic solution content. The possible applications are therefore manifold and are determined by the elements to be analysed. Since theoretically any element can be analysed with the LIBS (Senesi et al., 2021), quite a lot of applications are conceivable for which laboratory equipment such as IC, AAS, atomic emission spectroscopy (AES), ICP-AES/ ICP-OES or ICP-MS were previously required.
Although the analytical parameters, such as the detection limits, are typically less favourable compared to conventional laboratory methods, the benefits of low sample preparation, ease of use, and, most importantly, on-site testing offer substantial advantages. Moreover, the developed method contributes to more sustainable analyses as less chemicals are needed in comparison to laboratory methods such as IC (Gałuszka et al., 2015). Because of the data available on site, action can be taken directly on the basis of the data. The number of costly laboratory analyses can be reduced and the method can also be used to pre-select samples. Finally, due to the high measuring speed and the extremely low operating costs, more analyses can be carried out very cost-effectively.
An obvious application is therefore in the field of environmental monitoring of PTEs (e.g. As, Pb, and U). Potential customers may include environmental engineering firms, wastewater management companies, mining corporations (tailings seepage, AMD water), post-mining regulatory bodies, landfill operators dealing with the issue of landfill leachates, water management authorities, environmental agencies, geological services (such as the German *Bundesanstalt für Geowissenschaften und Rohstoffe (BGR)*), and agricultural organisations concerned with nitrate and eutrophication.
In addition, the method may be employed in well construction and maintenance to prevent scaling by continuously analysing the fluid, for instance, in geothermal energy production. Consequently, particular attention should be paid to solved Fe and Mn due to their involvement in well ageing and the formation of oxides and hydroxides that may reduce productivity (Wisotzky et al., 2021). Iron (Fe) and manganese (Mn) were not tested in this thesis, however, previous studies have demonstrated that these elements can be analysed using LIBS, for example by Samek et al. (2000), Aras and Yalçın (2016), and Jijon and Costa Vera (2012).

The use of fluids as a resource, such as in the Upper Rhine Graben with Li from geothermal solutions, could also be an application for the developed method. The lithium content within the Upper Rhine Graben averages at approximately 160 to 190 mg/L (Goldberg et al., 2022a), which falls within the analysable range. It only slightly exceeds the range that can be analysed without the need for self-absorption correction.
Furthermore, the method could be applied in the field of quality control. For example, tap water in households could be tested for PTEs directly at the customer's place. Many homeowners or residents of rented flats are concerned about the quality of tap water and often choose to use bottled water. However, the water quality in German water carriers is high (Grummt, 2007), as the water distributors have to ensure that safe water reaches the water meters in households (Grummt, 2007; Völker et al., 2010). Exceeding limit values for various elements may be present particularly in old houses with obsolete installation such as lead pipes (Grummt, 2007). Despite this, some individuals still choose to opt for water testing from a variety of providers to ensure certainty in water quality. In certain areas in Germany, these tests are even provided for free to households with pregnant women and young children (Grummt, 2007). However, customers frequently have to collect water samples themselves without analytical expertise. Subsequently, the process of receiving results, after submitting samples, may take weeks. This issue can be addressed by carrying out on-site water analysis and using trained professionals to collect and directly analyse the samples.
The German Trinwasserverordnung (*TrinkwV*) obliges water suppliers in Germany to produce and supply drinking water that is safe for human health, and to monitor it themselves (Grummt, 2007; BMG, 2023). Local health authorities conduct independent checks to ensure that drinking water quality parameters are met (Grummt, 2007). Sampling and analysis are necessary for this purpose, and portable analysis would be advantageous. However, the method developed first has to meet specific requirements and receive approval. In Germany, the approved test methods must be applied in accordance with the "generally recognised rules of technology", provide "sufficiently reliable measured values", and comply with the "specified process parameters" (BMG, 2023). It is possible that despite further improvements in method, the sensitivity of the approach may still be inadequate for certain parameters (cf. Section 3.3.2 and Table 3.12). For NO_3, Na, SO_4, Cl, and Cu, it should be possible to comply with the regulations outlined in the *TrinkwV* (refer to Table 4.2).

Table 4.2: Threshold values of measurement uncertainty for approved examination methods in accordance with *TrinkwV* (BMG, 2023)

NO_3	Na	SO_4	Cl	Cr	Ni	Cu	As	Se	Cd	Pb	
15	15	15	15	30	25	25	30	40	25	25	% SD
7.5	30	37.5	37.5	0.0075	0.005	0.5	0.003	0.004	0.00075	0.0025	mg/L SD
50	200	250	250	0.025	0.020	2.0	0.010	0.010	0.0030	0.010	mg/L SD

TrinkwV = Trinkwasserverordnung (Germany)

Moreover, it has already been shown in the laboratory that similar methods can be adapted to other liquids and thus to other fields such as medicine (e.g. analysis of

blood or urine (Metzinger et al., 2014)), analysis of liquid foods (e.g. wine (Bocková et al., 2017, 2018)), and product development and testing (e.g. cosmetics).
Of course, new fields are also opening up for science and the method can be used for low-cost hydrochemical mapping in remote places, for example.
It is theoretically possible to analyse solids following liquid digestion. However, given that this task is typically performed in a laboratory, the only potential benefit is lower costs in comparison to AAS or ICP-MS analyses.
Due to diverse application possibilities and the opening of new market fields, the method also becomes interesting for the manufacturers of portable LIBS and XRF instruments, as the sales market for their products increases (e.g. SciAps, ThermoFisher Sc., Analyticon, Rigaku, Metrohm, StellarNet, Bruker, Olympus).
The market in the field of inorganic water analysis will grow steadily in the coming years, as the rising world population is accompanied by an ever-increasing demand for drinking water. At the same time, climate change is causing a shortage of drinking water in many regions of the world, making it a critical resource. Rapid, cost-effective on-site analyses will contribute to the security of water as a resource.

Chapter 5

Conclusions and Future Work

This thesis concludes by summarising the main findings and outlooks towards future research as well as practical implications. In Section 5.1, the research questions defined in Section 1.2 are answered briefly. In Section 5.2, possible future work is pointed out.

5.1 Answering the Research Questions

The thesis aims to answer the main research question:

(How) can aqueous solutions be quantitatively analysed for their inorganic solution content using a pLIBS, in particular by the SciAps Z-300?

It is possible to utilise the SciAps Z-300 to quantify various elements and simple compounds in aqueous solutions. To date, successful testing has been carried out on Li, Na, Mg, K, Ca, Sr, SO_4, Cl, (NO_3), Cr, Ni, Cu, Zn, As, Se, Cd, and Pb by employing a SE-LSC technique on Al-foil and using a 3D printed sample holder for improved handling.

The remaining subordinate research questions are answered in a structured manner according to their respective chapters.

5.1.1 Chapter 1: Introduction

- When was LIBS developed and how has the technology evolved since its introduction?

  - LIBS was developed shortly after the development of the laser in 1960. In 1981 the acronym *"LIBS"* was introduced and the last centuries have been marked by miniaturisation, with the first prototype of a pLIBS in 1996. Since then, many applications have been found, ranging from simple qualitative scrap sorting to highly specialised applications such as geochemical fingerprinting.

- How long have pLIBS devices been on the market?
  - Real pLIBS devices have been available for purchase since the 2000s. In 2013, the predecessor of the Z-300 was introduced.

- What are the physical principles behind LIBS and how are the devices constructed?
  - A lens focuses a pulsed laser onto the surface of the sample, generating high energy at the focal point. This creates a plasma that atomises and excites the vaporised sample material. Electromagnetic radiation is emitted when the electrons return to their initial state, which can be analysed.

- What are the differences to the comparable pXRF technique?
  - The primary distinction between pXRF and pLIBS is that the latter does not employ ionising radiation, eliminating the need for a radiation safety officer. Additionally, pLIBS can analyse elements with low atomic numbers ($z \leq 12$). However, unlike pXRF, standardless calibration is not feasible, and the analysis is highly dependent on the matrix.

- What needs to be considered when working with pLIBS?
  - Although no ionising radiation is used with LIBS, the high energy density of the laser at the focal point can cause damage to the skin or the eyes. The Z-300 uses a Class 3B laser, which is considered as a Class 1 laser due to the integrated safety feature and can be used without extensive training. However, caution is required, especially with reflective surfaces, as the wavelength of the laser used is outside the range of visible light and does not trigger typical reflexes such as the closing of the eye. The radiation is not recognised, so it is important to be careful.

- Are there safety regulations and legal requirements for transport and use?
  - Currently, there are no legal requirements for transportation. However, regulations for lithium-ion batteries and pressurised gases (Ar-cartridges) do apply.

- What functions are available on current devices?
  - Aside from elemental analysis, the pLIBS offers some special features. These include the ability to create heat maps using a raster mode, cleaning the sample before analysis with cleaning shots, and using Ar as a purge gas to enhance the signal.

- What applications in the raw materials sector are known to date?
  - Several applications have been tested in the raw material sector, such as material identification, geochemistry, chemical imaging, and gold tracing using pLIBS.
- When was elemental analysis of aqueous solutions by LIBS introduced and where is research being carried out on this subject?
  - The first publication on elemental analysis of aqueous solutions using LIBS dates back to 1984.
- What are common challenges encountered during elemental analysis of aqueous solutions using LIBS?
  - The initial publication in 1984 already discussed the challenges of producing the plasma directly on the surface of aqueous solutions. The plasma is cooled by the evaporation of the liquid, and analysis is disrupted by splashing. Analysing inside the liquid results in high pressures that are difficult to manage.
- What methods for sample preparation exist to date and what is their share of use?
  - The literature reviewed distinguishes between four main categories: liquid bulk (LB), liquid-to-solid conversion (LSC), liquid-to-aerosol conversion (LAC), and hydride generation (HG). These categories have a share of 50%, 37%, 12%, and 1%, respectively. LB and LSC can be further subdivided into multiple subcategories, primarily aimed at preventing plasma splashing and cooling.
- Which types of aqueous solutions are analysed?
  - Typically, stock solutions are used for both calibration and verification of the analytical technique. However, artificial (industrial and waste water), biological (blood, urine, wine), natural (rain, river and groundwater), and natural saline waters (seawater, brine) are also analysed.
- Which types of devices are used?
  - LIBS is not only available as a laboratory instrument, but also as a telescopic, online, and portable version.
- What are the most important acquisition settings?
  - The key acquisition settings include the repetition rate, pulse energy, pulse duration, gate delay, laser wavelength, and atmospheric conditions.
- Which elements are usually investigated?
  - The analysis primarily focuses on PTEs such as Cr, Pb, and Cu. However, at least 56 elements have been analysed using LIBS in aqueous solutions, including light elements.

- What LIBS setups exist to enhance analyses?
  - Several different LIBS setups are used to improve the signal, such as double pulse (DP), laser-induced fluorescence (LIF), resonance-enhanced (RE), and microwave enhancement (MW).
- What sensitivities do different methods show for different elements?
  - It is difficult to distinguish the impact of the methods and elements. However, low detection limits were achieved for Ag, Ni, Cu, Li, and Cr, regardless of the method used.
- What could the future development in this field look like?
  - With further miniaturisation and improvement, pLIBS has great potential for liquid analysis due to its capability for simultaneous multi-elemental analyses.

5.1.2 Chapter 2: Method Development

- Is a LSC method appropriate for use with the SciAps Z-300?
  - With some minor adaptations, LSC can be used with pLIBS.
- Which substrate should be selected?
  - The substrate used should be affordable, readily available, and should not bring spectral interferences. Aluminium foil meets all of these criteria.
- What is required to improve the LSC method?
  - As the aluminium substrate is not hydrophobic enough, irregularly shaped and concentrated evaporation residues occur upon drying. Therefore, surface enhancement is required. A pencil layer introduces fat, which makes the surface more hydrophobic.
- What type of standard can be chosen and which elements should be considered?
  - Dilution series of AAS standard solutions, whether as single-element or multi-element standards, can be used to effectively calibrate LIBS. Calibration is necessary for alkali elements, earth alkalines, and typical anions to analyse typical drinking water samples. Additionally, PTEs are selected to assess the method's environmental testing capabilities.
- What are the calibration steps and is the manufacturer's calibration software sufficient?
  - After analysing the dilution series, intensity ratios are calculated by selecting strong lines of the element of interest as the numerator and aluminium lines as the denominator, combined with spectral processing. To

avoid rounding errors caused by the manufacturer's software when creating regressions, a spreadsheet is used instead. Two to three calibrations are defined per element, as the slope changes with increasing concentration.

- How can a pLIBS be held in place during analysis and what can be done to improve the speed and repeatability of the focusing process?
  - Using the screw holes for mounting, a sample holder can be designed to hold the pLIBS in place during analysis.
- How can the process of evaporation also be carried out in the field?
  - A 3D printed hot plate can be used for evaporation. It consists of a circular copper plate as a heating platform, a heating element, and batteries for energy supply.
- How can calibration be managed using a spreadsheet?
  - Several spreadsheets are used to convert the IR values and create calibration curves. Additionally, they can be used for the statistical analysis of the method.
- How can developed calibrations be used to analyse unknown samples?
  - By setting threshold values for the input values of the different elements, the appropriate concentration range is automatically selected, and unknown samples are analysed.

5.1.3 Chapter 3: Application and Evaluation

- Is it possible to quantitatively determine Li, Na, and K in aqueous standard solutions using pLIBS?
  - By employing a SE LSC method, multivariate calibration, and a sample holder, it is possible to quantitatively determine the concentrations of Li, Na, and K in aqueous standard solutions using pLIBS.
- Is the developed SE LSC technique suitable?
  - The surface enhancement results in a relatively homogeneous spread and shape of the evaporation residue (EvR), without any coffee ring effect (CRE).
- Is it possible to create linear calibration curves?
  - Linear calibration curves can be obtained by defining two to three concentration ranges, as the slope changes with increasing concentrations. However, for some higher concentration ranges, a quadratic fit may still be necessary.

- What are the detection limits achieved for the three elements?
  - The detection limits for Li, Na, and K are 0.006, 0.011, and 0.007 mg/L, respectively.
- Which concentration ranges can be analysed?
  - The concentration of Li and Na can be quantified within the range of 0.1 - 100 mg/L, while K can be quantified within the range of 0.1 - 160 mg/L.
- What is the effect of surface enhancement on the spread and shape of the evaporation residue?
  - The evaporation residue is more homogeneous in spread and shape with surface enhancement.
- Does the surface enhancement improve sensitivity or reproducibility?
  - The improved homogeneity of the evaporation residue by the surface enhancement improves reproducibility, but not sensitivity.
- How do the findings compare with other methodologies detailed in literature?
  - The calculated detection limits can be compared with those of stationary laboratory devices. However, they may be slightly optimistic.
- Is it possible to quantitatively determine typical cations and anions in bottled mineral water using pLIBS?
  - Low to medium mineralised water up to 1000 μS/cm can be analysed without self-absorption correction.
- Is it possible to create linear calibration curves for all desired concentration ranges of all selected elements?
  - As previously observed, linearity is lost with higher concentrations. Therefore, two to three concentration ranges are defined for each element. However, for the highest concentration range (typically 160 to 1000 mg/L), quadratic or exponential fits are required. In the case of Mg, no calibration line could be established above 100 mg/L.
- What are the detection limits achieved for the selected elements?
  - The detection limits for Li, Na, Mg, K, Ca, Zn, Sr, N, S, and Cl are 0.006, 0.014, 0.008, 0.006, 0.021, 0.0005, 0.0008, 0.002, 0.0002, and 0.0004 mg/L respectively.
- Which concentration ranges can be analysed?
  - The elements mentioned above can be analysed within the range of 0.1 to 100 mg/L.

- What are the results when the calibrations are applied to mixed standard solutions with a known concentration of the elements?
  - Standard solutions of mixed divalent and monovalent ions were tested to investigate the influence of self-absorption. The results indicate that divalent ions exhibit a higher degree of self-absorption compared to monovalent ions. The series of self-absorption is as follows: K < Li < Na < Mg < Sr < Ca.
- Are there any matrix effects and what is the influence of self-absorption?
  - The matrix effect appears to be low, however, self-absorption strongly influences the results, making it impossible to reliably analyse higher concentrations.
- How do the results compare with other findings detailed in the literature?
  - These results are comparable to the effects observed in other experiments conducted by Skrzeczanowski and Długaszek (2022) and Bae et al. (2015). One possible explanation, as suggested in these publications, is that the analyte becomes more concentrated in a small area as a result of the liquid-to-solid conversion.
- Is it possible to quantitatively determine PTEs in aqueous solutions using pLIBS?
  - Yes, it is also possible to quantitatively determine PTEs in aqueous solutions using pLIBS. However, some elements do not work at concentrations below 0.1 mg/L and, with the exception of Cu, it is not possible to reach typical environmental thresholds.
- Is it possible to use mixed standard solutions for calibration?
  - Mixed standard solutions were used for all PTEs without detectable matrix effects. Zn and Cd share one peak, but this can be compensated by using other strong lines.
- Is it possible to create linear calibration curves for all desired concentration ranges of all selected elements?
  - With the aim of achieving environmentally relevant limit values, concentrations down to 0.001 mg/L were analysed for the PTEs and attempts were made to create calibration curves. For As and Se, calibration curves could only be generated from 0.1 and 0.5 mg/L respectively. For Pb it was possible to create a calibration curve for concentrations between 0.001 and 0.1 mg/L, but this has a low coefficient of determination. However, concentrations above 0.1 mg/L (0.5 mg/L for Se) and up to 50 mg/L can be quantified for all analysed PTEs.
- What are the detection limits achieved for the selected elements?
  - The detection limits were calculated to be between 0.0001 and 0.03 mg/L. However, it has been demonstrated that these values are overly optimistic.

5.1.4 Chapter 4: Discussion

- How can the spread and shape of the evaporation residue be further optimised?
  - There are possibilities to further improve the spread and shape of the evaporation residue by further investigating the surface enhancement.
- How can self-absorption be reduced or eliminated?
  - Self-absorption cannot be eliminated, but it is possible to mathematically compensate for its effect.
- How does the developed method compare to other instruments?
  - Compared to laboratory methods, it is unlikely that pLIBS will be able to keep up, even with further developments. However, for field use and prescreening, there are few alternatives when analysing multiple elements is necessary.
- What is the current stage of development of the method?
  - The current Technology Readiness Level (TRL) is four. Further developments are necessary, especially the introduction of self-absorption compensation, to achieve a final product.
- What is the market potential of the method?
  - There is a significant market potential due to the various possible applications and limited alternatives.

5.2 Future Work

5.2.1 Further Investigations on the Evaporation Residue

As described in Section 4.1, there is evidence of water in the form of OH molecule peaks in several spectra. Therefore, it would be interesting to investigate the EvR further, using microscopic techniques such as SEM combined with semi-quantitative EDX or WDX. It should be studied whether such peaks appeared due to inadequately dried droplets or if hydroxides were formed as EvR. The influence of drying temperature and heating duration on the appearance of OH peaks should also be investigated. If the solution has not completely evaporated, higher temperatures or longer drying times can remedy this. However, if water is present in compounds, its influence on the results should be considered more closely. It may also be possible to use the reaction products to better analyse elements that are more difficult to quantify, such as S or Cl. Further development of surface optimisation using imaging techniques is also possible.

5.2.2 Self-Absorption Correction

Currently, the analysis using the developed method is restricted to lower concentrations ($\leq$ 160 mg/L) due to the cancellation of proportionality between the analyte concentration and the signal intensity at higher concentrations. This is primarily caused by the self-absorption effect, which increases with higher concentrations (see Section 4.2). Although it is possible to correct this effect (Palleschi, 2022a), the chosen calibration technique makes it challenging to find a solution for self-absorption compensation using the available software. Therefore, it is important to find a suitable method to compensate for self-absorption in the future by selecting appropriate software and formulas.

5.2.3 Statistical Improvements

Owing to the rectangular raster of 10 * 10 spots for each evaporated droplet, which is marginally larger than the EvR itself, spots on the surface of the substrate that lack any EvR are also analysed to ensure the complete EvR capture (see Section 4.2). However, this results in two normal distributions when assessing the intensities of the EoI in the one hundred individual spectra, averaged from four measurements each. Despite high element concentrations in the initial solution, certain spectra may exhibit little or no signal of the EoI, due to the analysis of spots outside of the EvR that have a low or no concentration of the EoI. However, the second category of spectra will invariably display a distinguishable signal for the EoIs as these were analysed within the EvR. If the spectra without a signal for the EoI were excluded, the sensitivity and reproducibility would be improved as only the analyte would be analysed. This would facilitate calibrations for higher concentrations since the effect of the two normal distributions is prominent in such cases. Ideally, the combination of self-absorption compensation and this statistical improvement would restore the linearity of the calibration curves while also enhancing sensitivity.

5.2.4 Elemental Additions

A significant benefit of utilising pLIBS for the analysis of aqueous solutions regardless of the applicability in the field is its capability for simultaneous multi-element analysis. It is also possible to calibrate additional elements after the analysis has already been done as long as all measurement settings are kept the same. In contrast to pXRF, even light elements can be analysed. Therefore, depending on the application, it is advisable to test and calibrate additional elements in the future (see Section 3.3.2).
For example, Fe and Mn would be a useful addition for geothermal investigations due to their involvement in well ageing (Wisotzky et al., 2021). Also, more PTEs

such as U could be calibrated for environmental analysis. This is a brief selection of potential extensions. It is theoretically possible to calibrate every element, but the sensitivity of certain elements and compounds using the method selected for this thesis is noticeably lower than that of Li using the same method. Typical anions, as well as Se and As, exhibit significantly lower intensities and fewer lines within the analysable spectrum range. This pattern is evident in all methods when examining literature on the analysis of aqueous solutions with LIBS (cf. Sect. 1.5).
To obtain an initial overview of the possible detection limits for each element, consult the periodic table with median values from the literature (cf. figures 1.7 and 1.21). This will help to determine the ease or difficulty of analysing each element with LIBS. It is expected that this difference will persist in the future. However, it is reasonable to assume that sensitivity will improve with new and superior devices that have detectors with a higher spectral range. Thus, even these elements will be quantified more accurately in the future. Additionally, the use of enhanced data processing and artificial intelligence could also be beneficial (Rezaei et al., 2014).

5.2.5 Improvements of the Hot Plate and the Sample Holder

As stated previously in sections 2.2 and 2.3, the sample holder and the portable hot plate can be further harmonised to create an all-in-one solution. The portable hot plate could serve as the foundation for the sample holder basis if the latter was constructed from metal. The sample holder would heat up along with the substrate, causing the liquid on the surface to evaporate. This would eliminate the need for removing the stencil of the sample holder to take out the sample foil. In order to accommodate the larger rectangular sample holder, the hot plate would have to be slightly larger and fitted with a rectangular heating element. However, Al-foil should continue to be used as a substrate, as it is particularly cost-effective, available and has low spectral interferences. When designing the metal sample holder, however, care should be taken to ensure that not too much additional energy is required to heat the sample holder, as a portable energy source is to be be used. The sample holder should therefore be a good conductor of heat and, if necessary, the stencil and the edges of the sample holder should have an insulating effect.

5.2.6 Accreditation of the Method

Accreditation by an official body would be beneficial for the new method to be widely used outside of research. It should be determined if this is possible after further development to enable the method's broadest possible use (see also Section 4.4).

Appendix A

Appendix: Related Publications

A.1 List of Related Publications

The following section lists all publications that were produced as part of the doctoral thesis. A reference to the full texts is included. The publications are grouped in four categories, namely non-peer-reviewed articles, peer-reviewed articles, conference contributions, and others.

Non-Peer-Reviewed Articles

1. Schlatter, N.; Freutel, G.; Lottermoser, B. G. (2022): Evaluation der Nutzung tragbarer LIBS-Geräte zur chemischen Vor-Ort-Analyse in der Rohstoffindustrie. GeoResources Zeitschrift (2-2022), S. 39–45. Online: https://www.georesources.net/download/GeoResources-Zeitschrift-2-2022.pdf

2. Schlatter, N.; Freutel, G.; Lottermoser, B. G. (2022). Evaluation of the Use of field-portable LIBS Analysers for on-site chemical Analysis in the Mineral Resources Sector. GeoResources Journal (2-2022), pp. 32–38. Online: https://www.georesources.net/download/GeoResources-Journal-2-2022.pdf

Peer-Reviewed Articles

1. Schlatter, N.; Lottermoser, B. G. (2023): Quantitative analysis of Li, Na, and K in single element standard solutions using portable laser-induced breakdown spectroscopy (pLIBS). Geochemistry: Exploration, Environment, Analysis (GEEA).

Volume 23, Issue 2, 2023.
DOI: https://doi.org/10.1144/geochem2023-019

2. Schlatter, N.; Lottermoser, B.G.; Illgner, S.; Schmidt, S. (2023): Utilising Portable Laser-Induced Breakdown Spectroscopy for Quantitative Inorganic Water Testing. Chemosensors 2023, 11, 479.
DOI: https://doi.org/10.3390/chemosensors11090479

3. Schlatter, N.; Lottermoser, B. G. (2024): Laser-Induced Breakdown Spectroscopy Applied to Elemental Analysis of Aqueous Solutions – A Comprehensive Review. Spectroscopy 2024, 2, 1-32.
DOI: https://doi.org/10.3390/spectroscj2010001

Conference Contributions

1. Schlatter, N.; Lottermoser, B. G. (2023): Innovative Feldmethode zur quantitativen hydrochemischen Analyse von Grubenwasser. Kassel 22 - Let's talk about Grubenwasser.
DOI: 10.13140/RG.2.2.12667.18726 (Abstract and Poster)

2. Schlatter, N.; Lottermoser, B. G. (2023): On-site screening of mine water chemistry using portable laser-induced breakdown spectroscopy. 1st European Conference on Teaching and Research in Sustainable Resource Extraction (TERRA), Boppard.
DOI: 10.13140/RG.2.2.29719.55206 (Abstract and Poster)

Others

1. Schlatter, N. (2021): Real-time analysis of the inorganic solution contents of water by means of portable LIBS. 30. Doktorand*innentreffen der Hydrogeologie, Kiel, 14 and 15 July 2021
(Abstract and Presentation)

Appendix B

Appendix: Background data

B.1 Standard Solutions

Table B.1: Standard solutions purchased for this thesis.

z	Element/ compound	Solute	Solvent	Concentration mg/L	SD mg/L
3	Li	Li_2CO_3	2% HNO_3	1003.1	3.8
11	Na	Na_2CO_3	2% HNO_3	999.6	3.2
12	Mg	MgO	2% HNO_3	1003.4	2.2
14	Si	$(NH_4)_2SiF_6$	H_2O	999.6	5
19	K	KNO_3	2% HNO_3	1002.9	4.8
20	Ca	$CaCO_3$	2% HNO_3	1000.9	2.4
24	Cr	$Cr(NO_3)_3$	2% HNO_3	999.8	3.8
28	Ni	$NiNO_3$	2% HNO_3	1001.1	2.5
29	Cu	CuO	2% HNO_3	1001.4	4.8
30	Zn	ZnO	2% HNO_3	1001.2	2.7
33	As	As_2O_3	2% HNO_3	1001.7	7.2
34	Se	Se	2% HNO_3	996.6	6.9
38	Sr	$Sr(NO_3)_2$	2% HNO_3	999.4	2.8
48	Cd	Cd	2% HNO_3	1000.5	3.3
82	Pb	Pb	2% HNO_3	999.2	4.6
7	Cl	NaCl	H_2O	1002	2.2
16	NO_3	KNO_3	H_2O	1002.2	2.2
17	SO_4	Na_2SO_4	H_2O	1000.1	2.2

Data provided by the manufacturer (Carl Roth).

B.2 Working Materials

Table B.2: Working materials utilised within this thesis.

Equipment	Volume range	Volume	SD	Syst. error	Rand. error
Pipettes:					
Eppendorf Research® plus,	0.1 - 2.5 μL	0.1 μL	0.060 μL	$\pm$48.0 %	$\pm$12.0%
single channel, dark grey		0.25 μL	0.045 μL	$\pm$12.0 %	$\pm$6.0 %
		1.25 μL	0.05 μL	$\pm$12.5 %	$\pm$1.5 %
		2.5 μL	0.053 μL	$\pm$1.4 %	$\pm$0.7 %
Eppendorf Research® plus,	0.5 - 5 mL	0.5 mL	0.015 mL	$\pm$2.4 %	$\pm$0.6%
single channel, violet		2.5 mL	0.036 mL	$\pm$1.2 %	$\pm$0.25 %
		5 mL	0.038 mL	$\pm$0.6 %	$\pm$0.15 %
Volumetric flasks:					
Vitlab class B, 1000 mL		1000 mL	0.8 mL		
Vitlab class B, 500 mL		500 mL	0.5 mL		
Vitlab class B, 250 mL		250 mL	0.3 mL		
Vitlab class B, 50 mL		50 mL	0.12 mL		
Centrifuge tubes:					
SPL with border (PP)		50 mL			

Data provided by the manufacturers; syst. error = systematic error; rand. error = random error; PP = polypropylene, SD and errors provided by the manufacturer (Eppendorf, 2013).

B.3 Digital Attachment

The digital attachment to this work contains a digital copy of this thesis, the spreadsheet created for calibration and analysis with the pLIBS, the spreadsheet belonging to the literature review of Section 1.5, the 3D models created, as well as digital copies of all related publications. The data is available in hard copy or can be provided by the author on request (please contact: nils.schlatter@web.de).

Bibliography

Aberkane, S. M., Melikechi, N., and Yahiaoui, K. (2022). LIBS spectral treatment. In Palleschi, V., editor, *Chemometrics and numerical methods in LIBS*, pages 47 – 80. Wiley, Hoboken, NJ, 1st edition.

Abu Kasim, A. F., Wakil, M. A., Grant, K., Hearn, M., and Alwahabi, Z. T. (2022). Aqueous ruthenium detection by microwave-assisted laser-induced breakdown spectroscopy. *Plasma Science and Technology*, 24(084004):1–8.

Abukashabeh, A. and Abu-Halimeh, R. (2021). Quality assurance for *In Situ* uranium concentration measurements of aqueous samples from mineral processing studies using a portable XRF analyser in compliance with ISO/IEC 17025 requirements. *Geostandards and Geoanalytical Research*, 45(3):599–611.

Aguirre, M., Legnaioli, S., Almodóvar, F., Hidalgo, M., Palleschi, V., and Canals, A. (2013). Elemental analysis by surface-enhanced laser-induced breakdown spectroscopy combined with liquid–liquid microextraction. *Spectrochimica Acta Part B: Atomic Spectroscopy*, 79-80:88–93.

Aguirre, M. A., Nikolova, H., Hidalgo, M., and Canals, A. (2015). Hyphenation of single-drop microextraction with laser-induced breakdown spectrometry for trace analysis in liquid samples: A viability study. *Analytical Methods*, 7(3):877–883.

Ahlawat, S., Mukhopadhyay, P. K., Singh, R., Dixit, S. K., and Bindra, K. S. (2023). Laser textured superhydrophilic silicon for uniform solidification and sensitive detection of water based samples using laser induced breakdown spectroscopy. *Journal of Analytical Atomic Spectrometry*, 38(4):883–892.

Ahmad, S. A. and Khan, M. H. (2023). Groundwater arsenic contamination and its health effects in Bangladesh. In Singh Flora, S. J., editor, *Handbook of Arsenic Toxicology*, pages 51–77. Elsevier, 2nd edition.

Alamelu, D., Sarkar, A., and Aggarwal, S. (2008). Laser-induced breakdown spectroscopy for simultaneous determination of Sm, Eu and Gd in aqueous solution. *Talanta*, 77(1):256–261.

Almici, A. (2022). Triple bottom line. In Idowu, S., Schmidpeter, R., Capaldi, N., Zu, L., Del Baldo, M., and Abreu, R., editors, *Encyclopedia of Sustainable Management*, pages 1–4. Springer International Publishing, Cham.

Andrade, J. M., Cal-Prieto, M. J., Gómez-Carracedo, M. P., Carlosena, A., and Prada, D. (2008). A tutorial on multivariate calibration in atomic spectrometry techniques. *J. Anal. At. Spectrom.*, 23(1):15–28.

Aras, N. and Yalçın, S. (2016). Development and validation of a laser-induced breakdown spectroscopic method for ultra-trace determination of Cu, Mn, Cd and Pb metals in aqueous droplets after drying. *Talanta*, 149:53–61.

Aras, N., Yeşiller, S., Ates, D. A., and Yalçın, S. (2012). Ultrasonic nebulization-sample introduction system for quantitative analysis of liquid samples by laser-induced breakdown spectroscopy. *Spectrochimica Acta Part B: Atomic Spectroscopy*, 74-75:87–94.

Arca, G., Ciucci, A., Palleschi, V., Rastelli, S., and Tognoni, E. (1997). Trace element analysis in water by the laser-induced breakdown spectroscopy technique. *Applied Spectroscopy*, 51(8):1102–1105.

Archontaki, H. A. and Crouch, S. R. (1988). Evaluation of an isolated droplet sample introduction system for laser-induced breakdown spectroscopy. *Applied Spectroscopy*, 42(5):741–746.

Asimellis, G., Hamilton, S., Giannoudakos, A., and Kompitsas, M. (2005). Controlled inert gas environment for enhanced chlorine and fluorine detection in the visible and near-infrared by laser-induced breakdown spectroscopy. *Spectrochimica Acta Part B: Atomic Spectroscopy*, 60(7-8):1132–1139.

Babos, D. V., Virgilio, A., Costa, V. C., Donati, G. L., and Pereira-Filho, E. R. (2018). Multi-energy calibration (MEC) applied to laser-induced breakdown spectroscopy (LIBS). *Journal of Analytical Atomic Spectrometry*, 33(10):1753–1762.

Bae, D., Nam, S.-H., Han, S.-H., Yoo, J., and Lee, Y. (2015). Spreading a water droplet on the laser-patterned silicon wafer substrate for surface-enhanced laser-induced breakdown spectroscopy. *Spectrochimica Acta Part B: Atomic Spectroscopy*, 113:70–78.

Banning, A. (2021). Geogenic arsenic and uranium in Germany: Large-scale distribution control in sediments and groundwater. *Journal of Hazardous Materials*, 405(124186):1–10.

Baudelet, M. and Smith, B. W. (2013). The first years of laser-induced breakdown spectroscopy. *Journal of Analytical Atomic Spectrometry*, 28(5):624.

Beckhoff, B., editor (2006). *Handbook of practical X-ray fluorescence analysis*. Springer, Berlin, New York.

Bernalte, E., Arévalo, S., Pérez-Taborda, J., Wenk, J., Estrela, P., Avila, A., and Di Lorenzo, M. (2020). Rapid and on-site simultaneous electrochemical detection of copper, lead and mercury in the Amazon river. *Sensors and Actuators B: Chemical*, 307:127620.

Bertin, E. P. (1978). Qualitative and semiquantitative analysis. In Bertin, E. P., editor, *Introduction to X-Ray Spectrometric Analysis*, pages 255–278. Springer US, Boston, MA.

BGBI (1984). Verordnung über natürliches Mineralwasser, Quellwasser und Tafelwasser (Mineral- und Tafelwasser-Verordnung). "German Mineral and Table Water Ordinance". Last amended by Art. 2 V v. 20.6.2023 I No. 159.

Bhatt, C. R., Goueguel, C. L., Jain, J. C., McIntyre, D. L., and Singh, J. P. (2020a). LIBS application to liquid samples. In Singh, J. P. and N., T. S., editors, *Laser-Induced Breakdown Spectroscopy*, pages 231–246. Elsevier.

Bhatt, C. R., Hartzler, D., Jain, J., and McIntyre, D. L. (2021). Determination of As, Hg, S, and Se in liquid jets by laser-based optical diagnostic technique. *Applied Physics B*, 127(1):8.

Bhatt, C. R., Jain, J. C., Goueguel, C. L., McIntyre, D. L., and Singh, J. P. (2017). Measurement of Eu and Yb in aqueous solutions by underwater laser induced breakdown spectroscopy. *Spectrochimica Acta Part B: Atomic Spectroscopy*, 137:8–12.

Bhatt, C. R., Sanghapi, H. K., Yueh, F. Y., and Singh, J. P. (2020b). LIBS application to powder samples. In Singh, J. P. and Thakur, S. N., editors, *Laser-Induced Breakdown Spectroscopy*, pages 247–262. Elsevier.

Birke, M., Rauch, U., Harazim, B., Lorenz, H., and Glatte, W. (2010a). Major and trace elements in German bottled water, their regional distribution, and accordance with national and international standards. *Journal of Geochemical Exploration*, 107(3):245–271.

Birke, M., Rauch, U., Lorenz, H., and Kringel, R. (2010b). Distribution of uranium in German bottled and tap water. *Journal of Geochemical Exploration*, 107(3):272–282.

Black, C., Poile, C., Langley, J., and Herniman, J. (2006). The use of pencil lead as a matrix and calibrant for matrix-assisted laser desorption/ionisation. *Rapid Communications in Mass Spectrometry*, 20(7):1053–1060.

BMG (2023). Zweite Verordnung zur Novellierung der Trinkwasserverordnung. Bundesgesetzblatt: Ausgegeben zu Bonn am 23. Juni 2023, Nr. 159.

Bocková, J., Marín Roldán, A., Yu, J., and Veis, P. (2018). Potential use of surface-assisted LIBS for determination of strontium in wines. *Applied Optics*, 57(28):8272.

Bocková, J., Tian, Y., Yin, H., Delepine-Gilon, N., Chen, Y., Veis, P., and Yu, J. (2017). Determination of metal elements in wine using laser-induced breakdown spectroscopy (LIBS). *Applied Spectroscopy*, 71(8):1750–1759.

Bol'shakov, A. A., Pandey, S. J., Mao, X., and Liu, C. (2021). Analysis of liquid petroleum using a laser-induced breakdown spectroscopy instrument. *Spectrochimica Acta Part B: Atomic Spectroscopy*, 179:106094.

Boyd, C. E. (2020). Physical properties of water. In *Water Quality*, pages 1–19. Springer International Publishing, Cham.

Bredice, F., Borges, F., Sobral, H., Villagran-Muniz, M., Di Rocco, H., Cristoforetti, G., Legnaioli, S., Palleschi, V., Pardini, L., Salvetti, A., and Tognoni, E. (2006). Evaluation of self-absorption of manganese emission lines in laser induced breakdown spectroscopy measurements. *Spectrochimica Acta Part B: Atomic Spectroscopy*, 61(12):1294–1303.

Bukhari, M., Awan, M. A., Qazi, I. A., and Baig, M. A. (2012). Development of a method for the determination of chromium and cadmium in tannery wastewater using laser-induced breakdown spectroscopy. *Journal of Analytical Methods in Chemistry*, 2012:1–7.

Busser, B., Moncayo, S., Coll, J.-L., Sancey, L., and Motto-Ros, V. (2018). Elemental imaging using laser-induced breakdown spectroscopy: A new and promising approach for biological and medical applications. *Coordination Chemistry Reviews*, 358:70–79.

Bölek, D., Ünal Yeşiller, S., and Yalçın, S. (2018). Determination of arsenic by hydride generation—laser-induced breakdown spectroscopy: Characterization of interelement interferences. *Analytical Letters*, 51(10):1605–1621.

Cahoon, E. M. and Almirall, J. R. (2012). Quantitative analysis of liquids from aerosols and microdrops using laser induced breakdown spectroscopy. *Analytical Chemistry*, 84(5):2239–2244.

Carvalho, A. A., Silvestre, D. M., Leme, F. O., Naozuka, J., Intima, D. P., and Nomura, C. S. (2019). Feasibility of measuring Cr(III) and Cr(VI) in water by laser-induced breakdown spectroscopy using ceramics as the solid support. *Microchemical Journal*, 144:33–38.

Casanova, L., Beldjilali, S. A., Gonca, B., Sezer, B., Motto-Ros, V., Pelascini, F., Bănaru, D., and Hermann, J. (2023). Evaluation of limits of detection in laser-induced breakdown spectroscopy: Demonstration for food. *Spectrochimica Acta Part B: Atomic Spectroscopy*, 207:106760.

Charfi, B. and Harith, M. (2002). Panoramic laser-induced breakdown spectrometry of water. *Spectrochimica Acta Part B: Atomic Spectroscopy*, 57(7):1141–1153.

Chen, C., Niu, G., Shi, Q., Lin, Q., and Duan, Y. (2015). Laser-induced breakdown spectroscopy technique for quantitative analysis of aqueous solution using matrix conversion based on plant fiber spunlaced nonwovens. *Applied Optics*, 54(28):8318.

Chen, Z., Godwal, Y., Tsui, Y. Y., and Fedosejevs, R. (2010). Sensitive detection of metals in water using laser-induced breakdown spectroscopy on wood sample substrates. *Applied Optics*, 49(13):C87–C94.

Chen, Z., Li, H., Zhao, F., and Li, R. (2008). Ultra-sensitive trace metal analysis of water by laser-induced breakdown spectroscopy after electrical-deposition of the analytes on an aluminium surface. *Journal of Analytical Atomic Spectrometry*, 23(6):871.

Cheri, M. S. and Tavassoli, S. H. (2011). Quantitative analysis of toxic metals lead and cadmium in water jet by laser-induced breakdown spectroscopy. *Applied Optics*, 50(9):1227.

Chiulan, I., Frone, A., Brandabur, C., and Panaitescu, D. (2017). Recent advances in 3D printing of aliphatic polyesters. *Bioengineering*, 5(1):2.

Cho, J. H., Gao, Y., and Choi, S. (2019). A portable, single-use, paper-based microbial fuel cell sensor for rapid, on-site water quality monitoring. *Sensors*, 19(24):5452.

Choi, D., Gong, Y., Nam, S.-H., Han, S.-H., Yoo, J., and Lee, Y. (2014). Laser-induced breakdown spectroscopy (LIBS) analysis of calcium ions dissolved in water using filter paper substrates: An ideal internal standard for precision improvement. *Applied Spectroscopy*, 68(2):198–212.

Coldewey, W. G. and Göbel, P. (2015). *Hydrogeologische Gelände- und Kartiermethoden*. Springer, Berlin, Heidelberg.

Cong, Z.-b., Sun, L.-x., Xin, Y., Li, Y., and Qi, L.-f. (2013). Comparison of calibration curve method and partial least square method in the laser-induced breakdown spectroscopy quantitative analysis. *Journal of Computer and Communications*, 01(07):14–18.

Connors, B., Somers, A., and Day, D. (2016). Application of handheld laser-induced breakdown spectroscopy (LIBS) to geochemical analysis. *Applied Spectroscopy*, 70(5):810–815.

Contreras, V., Valencia, R., Peralta, J., Sobral, H., Meneses-Nava, M. A., and Martinez, H. (2018). Chemical elemental analysis of single acoustic-levitated water droplets by laser-induced breakdown spectroscopy. *Optics Letters*, 43(10):2260.

Cooper, C. (2019). You can handle it: 3D printing for museums. *Advances in Archaeological Practice*, 7(4):443–447.

Costa, V., Babos, D., Castro, J., Andrade, D., Gamela, R., Machado, R., Sperança, M., Araújo, A., Garcia, J., and Pereira-Filho, E. (2021). Calibration strategies applied to laser-induced breakdown spectroscopy: A critical review of advances and challenges. *Journal of the Brazilian Chemical Society*, 31(12):2439–2451.

Cremers, D. A. and Chinni, R. C. (2009). Laser-induced breakdown spectroscopy—capabilities and limitations. *Applied Spectroscopy Reviews*, 44(6):457–506.

Cremers, D. A. and Radziemski, L. J. (2013). *Handbook of laser-induced breakdown spectroscopy*. Wiley, Chichester, West Sussex, 2nd edition.

Cremers, D. A., Radziemski, L. J., and Loree, T. R. (1984). Spectrochemical analysis of liquids using the laser spark. *Applied Spectroscopy*, 38(5):721–729.

Crocombe, R. A., Leary, P. E., and Kammrath, B. W., editors (2021). *Portable spectroscopy and spectrometry*. Wiley, Hoboken, NJ, 1st edition.

Cáceres, J., Tornero López, J., Telle, H., and González Ureña, A. (2001). Quantitative analysis of trace metal ions in ice using laser-induced breakdown spectroscopy. *Spectrochimica Acta Part B: Atomic Spectroscopy*, 56(6):831–838.

Das, J., Sarkar, P., Panda, J., and Pal, P. (2014). Low-cost field test kits for arsenic detection in water. *Journal of Environmental Science and Health, Part A*, 49(1):108–115.

De Giacomo, A., Koral, C., Valenza, G., Gaudiuso, R., and Dell'Aglio, M. (2016). Nanoparticle enhanced laser-induced breakdown spectroscopy for microdrop analysis at subppm level. *Analytical Chemistry*, 88(10):5251–5257.

de Jesus, A. M. D., Aguirre, M. A., Hidalgo, M., Canals, A., and Pereira-Filho, E. R. (2014). The determination of V and Mo by dispersive liquid–liquid microextraction (DLLME) combined with laser-induced breakdown spectroscopy (LIBS). *Journal of Analytical Atomic Spectrometry*, 29(10):1813–1818.

de Oliveira Borges, F., Ospina, J. U., de Holanda Cavalcanti, G., Farias, E. E., Rocha, A. A., Ferreira, P. I. L. B., Gomes, G. C., and Mello, A. (2018). CF-LIBS analysis of frozen aqueous solution samples by using a standard internal reference and correcting the self-absorption effect. *Journal of Analytical Atomic Spectrometry*, 33(4):629–641.

Deegan, R. D., Bakajin, O., Dupont, T. F., Huber, G., Nagel, S. R., and Witten, T. A. (1997). Capillary flow as the cause of ring stains from dried liquid drops. *Nature*, 389(6653):827–829.

Demetriades, A., Reimann, C., Birke, M., and The Eurogeosurveys Geochemistry EGG Team (2012). European ground water geochemistry using bottled water as a sampling medium. In Quercia, F. F. and Vidojevic, D., editors, *Clean Soil and Safe Water*, pages 115–139. Springer Netherlands, Dordrecht. Series Title: NATO Science for Peace and Security Series C: Environmental Security.

Demtröder, W. (2011). *Laserspektroskopie 1*. Springer, Berlin, Heidelberg.

Dimeski, G., Badrick, T., and John, A. S. (2010). Ion selective electrodes (ISEs) and interferences—A review. *Clinica Chimica Acta*, 411(5-6):309–317.

DIN-38402-62:2014-12 (2014). *German Standard Methods for the Examination ofWater, Waste Water and Sludge—Part 62: Plausibility Check of Analytical Data by Performing an Ion Balance.* Beuth Verlag GmbH, Berlin.

Donati, G. L. and Amais, R. S. (2019). Fundamentals and new approaches to calibration in atomic spectrometry. *Journal of Analytical Atomic Spectrometry*, 34(12):2353–2369.

Duffus, J. H. (2002). "Heavy metals" a meaningless term? (IUPAC technical report). *Pure and Applied Chemistry*, 74(5):793–807.

Eksperiandova, L. P., Blank, A. B., and Makarovskaya, Y. N. (2002). Analysis of waste water by x-ray fluorescence spectrometry. *X-Ray Spectrometry*, 31(3):259–263.

Elkin, K. R. (2014). Portable, fully autonomous, ion chromatography system for on-site analyses. *Journal of Chromatography A*, 1352:38–45.

Eppendorf (2013). Eppendorf research plus - adjustment factory. https://www.google.com/url?sa=t&source=web&rct=j&opi=89978449&url=https://www.eppendorf.com/product-media/doc/de/327080/Eppendorf_Liquid-Handling_Adjustment_Research-plus_Factory-Adjustment.pdf&ved=2ahUKEwiW34SozY2FAxX3gv0HHQxSCvUQFnoECB0QAQ&usg=AOvVaw08iMKLKsl1GDw-W3FRHWfJ, last accessed: 24.03.2024.

Esser, V., Buchty-Lemke, M., Schulte, P., Podzun, L. S., and Lehmkuhl, F. (2020). Signatures of recent pollution profiles in comparable central European rivers – Examples from the international river basin district Meuse. *CATENA*, 193:104646.

Ezer, M., Gondi, R., Kennehan, E., and Simeonsson, J. B. (2019). Trace determination of germanium by continuous flow hydride generation laser-induced fluorescence spectrometry. *Analytical Letters*, 52(7):1125–1137.

Fabre, C. (2020). Advances in laser-induced breakdown spectroscopy analysis for geology: A critical review. *Spectrochimica Acta Part B: Atomic Spectroscopy*, 166:105799.

Fabre, C., Ourti, N. E., Ballouard, C., Mercadier, J., and Cauzid, J. (2022). Handheld LIBS analysis for in situ quantification of Li and detection of the trace elements (Be, Rb and Cs). *Journal of Geochemical Exploration*, 236:106979.

Fabre, C., Ourti, N. E., Mercadier, J., Cardoso-Fernandes, J., Dias, F., Perrotta, M., Koerting, F., Lima, A., Kaestner, F., Koellner, N., Linnen, R., Benn, D., Martins, T., and Cauzid, J. (2021). Analyses of Li-rich minerals using handheld LIBS tool. *Data*, 6(6):68.

Fan, X., Lv, J., Li, R., Chen, Y., Zhang, S., Liu, T., Zhou, S., Shao, X., Wang, S., Hu, G., and Yue, Q. (2023). Paper test strip for silver ions detection in drinking water samples based on combined fluorometric and colorimetric methods. *Arabian Journal of Chemistry*, 16(2):104492.

Fang, X. and Ahmad, S. R. (2012). Detection of mercury in water by laser-induced breakdown spectroscopy with sample pre-concentration. *Applied Physics B*, 106(2):453–456.

Fichet, P., Mauchien, P., Wagner, J.-F., and Moulin, C. (2001). Quantitative elemental determination in water and oil by laser induced breakdown spectroscopy. *Analytica Chimica Acta*, 429(2):269–278.

Fichet, P., Tabarant, M., Salle, B., and Gautier, C. (2006). Comparisons between LIBS and ICP/OES. *Analytical and Bioanalytical Chemistry*, 385(2):338–344.

Fichet, P., Toussaint, A., and Wagner, J.-F. (1999). Laser-induced breakdown spectroscopy: A tool for analysis of different types of liquids. *Applied Physics A: Materials Science & Processing*, 69(7):591–592.

Foucaud, Y., Fabre, C., Demeusy, B., Filippova, I., and Filippov, L. (2019). Optimisation of fast quantification of fluorine content using handheld laser induced breakdown spectroscopy. *Spectrochimica Acta Part B: Atomic Spectroscopy*, 158:105628.

Free, G., Van de Bund, W., Gawlik, B., Van Wijk, L., Wood, M., Guagnini, E., Koutelos, K., Annunziato, A., Grizzetti, B., Vigiak, O., Gnecchi, M., Poikane, S., Christiansen, T., Whalley, C., Antognazza, F., Zerger, B., Hoeve, R. J., and Stielstra, H. (2023). An EU analysis of the ecological disaster in the Oder River of 2022: lessons learned and research based recommendations to avoid future ecological damage in EU rivers, a joint analysis from DG ENV, JRC and the EEA. JRC Technical Report, European Commission. Joint Research Centre, Luxembourg.

Fu, H., Jia, J., Wang, H., Ni, Z., and Dong, F. (2018a). Calibration methods of laser-induced breakdown spectroscopy. In Stauffer, M. T., editor, *Calibration and Validation of Analytical Methods - A Sampling of Current Approaches*, pages 85–108. InTech.

Fu, X., Li, G., Tian, H., and Dong, D. (2018b). Detection of cadmium in soils using laser-induced breakdown spectroscopy combined with spatial confinement and resin enrichment. *RSC Advances*, 8(69):39635–39640.

Gaubeur, I., Aguirre, M. A., Kovachev, N., Hidalgo, M., and Canals, A. (2015a). Dispersive liquid–liquid microextraction combined with laser-induced breakdown spectrometry and inductively coupled plasma optical emission spectrometry to elemental analysis. *Microchemical Journal*, 121:219–226.

Gaubeur, I., Aguirre, M. A., Kovachev, N., Hidalgo, M., and Canals, A. (2015b). Speciation of chromium by dispersive liquid–liquid microextraction followed by laser-induced breakdown spectrometry detection (DLLME–LIBS). *Journal of Analytical Atomic Spectrometry*, 30(12):2541–2547.

Gałuszka, A., Migaszewski, Z. M., and Namieśnik, J. (2015). Moving your laboratories to the field – Advantages and limitations of the use of field portable instruments in environmental sample analysis. *Environmental Research*, 140:593–603.

Gey, M. H. (2021). *Instrumentelle Analytik und Bioanalytik: Biosubstanzen, Trennmethoden, Strukturanalytik, Applikationen*. Springer, Berlin, Heidelberg.

Godwal, Y., Kaigala, G., Hoang, V., Lui, S.-L., Backhouse, C., Tsui, Y., and Fedosejevs, R. (2008). Elemental analysis using micro laser-induced breakdown spectroscopy in a microfluidic platform. *Optics Express*, 16(17):12435.

Goldberg, V., Kluge, T., and Nitschke, F. (2022a). Herausforderungen und Chancen für die Lithiumgewinnung aus geothermalen Systemen in Deutschland – Teil 1: Literaturvergleich bestehender Extraktionstechnologien. *Grundwasser - Zeitschrift der Fachsektion Hydrogeologie*, 27:239–259.

Goldberg, V., Nitschke, F., and Kluge, T. (2022b). Herausforderungen und Chancen für die Lithiumgewinnung aus geothermalen Systemen in Deutschland – Teil 2: Potenziale und Produktionsszenarien in Deutschland. *Grundwasser - Zeitschrift der Fachsektion Hydrogeologie*, 27:261–275.

Golicz, K., Hallett, S., Sakrabani, R., and Ghosh, J. (2020). Adapting smartphone app used in water testing, for soil nutrient analysis. *Computers and Electronics in Agriculture*, 175:105532.

Golik, S. S., Bukin, O. A., Il'in, A. A., Sokolova, E. B., Kolesnikov, A. V., Babiy, M. Y., Kul'chin, Y. N., and Gal'chenko, A. A. (2012). Determination of detection limits for elements in water by femtosecond laser-induced breakdown spectroscopy. *Journal of Applied Spectroscopy*, 79(3):471–476.

Golik, S. S., Ilyin, A. A., Babiy, M. Y., Biryukova, Y. S., Lisitsa, V. V., and Bukin, O. A. (2015). Determination of iron in water solution by time-resolved femtosecond laser-induced breakdown spectroscopy. *Plasma Science and Technology*, 17(11):975–978.

Goueguel, C., McIntyre, D. L., Jain, J., Karamalidis, A. K., and Carson, C. (2015). Matrix effect of sodium compounds on the determination of metal ions in aqueous solutions by underwater laser-induced breakdown spectroscopy. *Applied Optics*, 54(19):6071.

Goueguel, C., Singh, J. P., McIntyre, D. L., Jain, J., and Karamalidis, A. K. (2014). Effect of sodium chloride concentration on elemental analysis of brines by laser-induced breakdown spectroscopy (LIBS). *Applied Spectroscopy*, 68(2):213–221.

Groh, S., Diwakar, P. K., Garcia, C. C., Murtazin, A., Hahn, D. W., and Niemax, K. (2010). 100% efficient sub-nanoliter sample introduction in laser-induced breakdown spectroscopy and inductively coupled plasma spectrometry: Implications for ultralow sample volumes. *Analytical Chemistry*, 82(6):2568–2573.

Grummt, H.-J. (2007). Die Trinkwasserbeschaffenheit in Deutschland: Eine Übersicht für die Jahre 2002–2004. *Bundesgesundheitsblatt - Gesundheitsforschung - Gesundheitsschutz*, 50(3):276–283.

Guezenoc, J., Gallet-Budynek, A., and Bousquet, B. (2019). Critical review and advices on spectral-based normalization methods for LIBS quantitative analysis. *Spectrochimica Acta Part B: Atomic Spectroscopy*, 160:105688.

Haider, A., Hedayet Ullah, M., Khan, Z., Kabir, F., and Abedin, K. (2014). Detection of trace amount of arsenic in groundwater by laser-induced breakdown spectroscopy and adsorption. *Optics & Laser Technology*, 56:299–303.

Hanna-instruments (2024). Mini-Photometer CHECKER HC. https://hannainst.de/shop/photometer/hanna-checker-hc/?order=name-asc&p=1, last accessed: 24.03.2024.

Haque, E., Mailloux, B. J., De Wolff, D., Gilioli, S., Kelly, C., Ahmed, E., Small, C., Ahmed, K. M., Van Geen, A., and Bostick, B. C. (2018). Quantitative drinking water arsenic concentrations in field environments using mobile phone photometry of field kits. *Science of The Total Environment*, 618:579–585.

Hark, R. R. and Harmon, R. S. (2014). Geochemical fingerprinting using LIBS. In Musazzi, S. and Perini, U., editors, *Laser-Induced Breakdown Spectroscopy*, volume 182, pages 309–348. Springer, Berlin, Heidelberg. Series Title: Springer Series in Optical Sciences.

Harmon, R. S., Khashchevskaya, D., Morency, M., Owen, L. A., Jennings, M., Knott, J. R., and Dortch, J. M. (2021). Analysis of rock varnish from the Mojave desert by handheld laser-induced breakdown spectroscopy. *Molecules*, 26(17):5200.

Harmon, R. S., Remus, J., McMillan, N. J., McManus, C., Collins, L., Gottfried, J. L., DeLucia, F. C., and Miziolek, A. W. (2009). LIBS analysis of geomaterials: Geochemical fingerprinting for the rapid analysis and discrimination of minerals. *Applied Geochemistry*, 24(6):1125–1141.

Harmon, R. S. and Senesi, G. S. (2021). Laser-induced breakdown spectroscopy – A geochemical tool for the 21st century. *Applied Geochemistry*, 128:104929.

Harris, D. C. (2010). *Quantitative chemical analysis*. W.H. Freeman and Co, New York, 8th edition.

Harris, D. C. and Harris, D. C. (2014). *Lehrbuch der quantitativen Analyse*. Lehrbuch. Springer Spektrum, Berlin, Heidelberg, 2nd edition.

Hartzler, D. A., Bhatt, C. R., and McIntyre, D. L. (2023). Design, construction, and validation of an in-situ groundwater trace element analyzer with applications in carbon storage. *Scientific Reports*, 13(1):7516.

Hartzler, D. A., Jain, J. C., and McIntyre, D. L. (2019). Development of a subsurface LIBS sensor for in situ groundwater quality monitoring with applications in CO_2 leak sensing in carbon sequestration. *Scientific Reports*, 9(1):4430.

Harun, H. A. and Zainal, R. (2018a). Improvement of laser induced breakdown spectroscopy signal for sodium chloride solution. *Malaysian Journal of Fundamental and Applied Sciences*, 14:429–433.

Harun, H. A. and Zainal, R. (2018b). Laser-induced breakdown spectroscopy measurement for liquids: Experimental configurations and sample preparations. *Journal of Nonlinear Optical Physics & Materials*, 27(02):1850023.

Hasiuk, F. (2014). Making things geological: 3-D printing in the geosciences. *GSA Today*, pages 28–29.

He, Y., Wang, X., Guo, S., Li, A., Xu, X., Wazir, N., Ding, C., Lu, T., Xie, L., Zhang, M., Hao, Y., Guo, W., and Liu, R. (2019). Lithium ion detection in liquid with low detection limit by laser-induced breakdown spectroscopy. *Applied Optics*, 58(2):422.

Hou, J., Zhang, L., Zhao, Y., Wang, Z., Zhang, Y., Ma, W., Dong, L., Yin, W., Xiao, L., and Jia, S. (2019). Mechanisms and efficient elimination approaches of self-absorption in LIBS. *Plasma Science and Technology*, 21(3):034016.

Huang, J.-S., Ke, C.-B., Huang, L.-S., and Lin, K.-C. (2002). The correlation between ion production and emission intensity in the laser-induced breakdown spectroscopy of liquid droplets. *Spectrochimica Acta Part B: Atomic Spectroscopy*, 57(1):35–48.

Huang, J.-S., Ke, C.-B., and Lin, K.-C. (2004). Matrix effect on emission/current correlated analysis in laser-induced breakdown spectroscopy of liquid droplets. *Spectrochimica Acta Part B: Atomic Spectroscopy*, 59(3):321–326.

Huang, J.-S. and Lin, K.-C. (2005). Laser-induced breakdown spectroscopy of liquid droplets: correlation analysis with plasma-induced current versus continuum background. *Journal of Analytical Atomic Spectrometry*, 20(1):53.

Huang, J.-S., Liu, H.-T., and Lin, K.-C. (2007). Laser-induced breakdown spectroscopy in analysis of Al^{3+} liquid droplets: On-line preconcentration by use of flow-injection manifold. *Analytica Chimica Acta*, 581(2):303–308.

Huang, L., Yao, M., Xu, Y., and Liu, M. (2013). Determination of Cr in water solution by laser-induced breakdown spectroscopy with different univariate calibration models. *Applied Physics B*, 111(1):45–51.

Hölting, B. and Coldewey, W. G. (2019). *Hydrogeology*. Springer Textbooks in Earth Sciences, Geography and Environment. Springer, Berlin, Heidelberg.

IPCC (2023). Climate change 2023: Synthesis report. Technical report, Intergovernmental Panel on Climate Change (IPCC). 1st edition.

IUPAC (1976). Nomenclature, symbols, units and their usage in spectrochemical analysis—II. Data interpretation. *Pure and Applied Chemistry Division*, 45(2):99–103.

Jan, F., Min-Allah, N., and Düştegör, D. (2021). IoT based smart water quality monitoring: Recent techniques, trends and challenges for domestic applications. *Water*, 13(13):1729.

Janzen, C., Fleige, R., Noll, R., Schwenke, H., Lahmann, W., Knoth, J., Beaven, P., Jantzen, E., Oest, A., and Koke, P. (2005). Analysis of small droplets with a new detector for liquid chromatography based on laser-induced breakdown spectroscopy. *Spectrochimica Acta Part B: Atomic Spectroscopy*, 60(7-8):993–1001.

Jarvikivi, M. (2018). What is laser induced breakdown spectroscopy (LIBS)? https://hha.hitachi-hightech.com/en/blogs-events/blogs/2018/01/03/what-is-libs/, accessed: 2024-03-18.

Jiang, L., Sui, M., Fan, Y., Su, H., Xue, Y., and Zhong, S. (2021). Micro-gas column assisted laser induced breakdown spectroscopy (MGC-LIBS): A metal elements detection method for bulk water in-situ analysis. *Spectrochimica Acta Part B: Atomic Spectroscopy*, 177:106065.

Jijon, D. and Costa Vera, C. (2012). Laser-induced breakdown spectroscopy analysis of dried liquids on solid surfaces. *Optica Pura y Aplicada*, 45(4):475–484.

Jijón, D. and Costa, C. (2011). Pencil lead scratches on steel surfaces as a substrate for LIBS analysis of dissolved salts in liquids. *Journal of Physics: Conference Series*, 274:012077.

Judge, E. J., Campbell, K., and Kelly, D. (2021). Uranium corrosion characterization by handheld laser-induced breakdown spectroscopy. *Spectrochimica Acta Part B: Atomic Spectroscopy*, 186:106325.

Järvinen, S. T., Saarela, J., and Toivonen, J. (2013). Detection of zinc and lead in water using evaporative preconcentration and single-particle laser-induced breakdown spectroscopy. *Spectrochimica Acta Part B: Atomic Spectroscopy*, 86:55–59.

Järvinen, S. T., Saari, S., Keskinen, J., and Toivonen, J. (2014). Detection of Ni, Pb and Zn in water using electrodynamic single-particle levitation and laser-induced breakdown spectroscopy. *Spectrochimica Acta Part B: Atomic Spectroscopy*, 99:9–14.

Kang, J., Li, R., Wang, Y., Chen, Y., and Yang, Y. (2017). Ultrasensitive detection of trace amounts of lead in water by LIBS-LIF using a wood-slice substrate as a water absorber. *Journal of Analytical Atomic Spectrometry*, 32(11):2292–2299.

Keerthi, K., George, S. D., Sebastian, J. G., Warrier, A. K., Chidangil, S., and Unnikrishnan, V. K. (2022). Optimization of different sampling approaches in liquid LIBS analysis for environmental applications. *Journal of Analytical Atomic Spectrometry*, 37(12):2625–2636.

Kim, T., Ricchia, M. L., and Lin, C.-T. (2010). Analysis of copper in an aqueous solution by ion-exchange concentrator and laser-induced breakdown spectroscopy. *Journal of the Chinese Chemical Society*, 57(4B):829–835.

Knopp, R., Scherbaum, F. J., and Kim, J. I. (1996). Laser induced breakdown spectroscopy (LIBS) as an analytical tool for the detection of metal ions in aqueous solutions. *Fresenius Journal of Analytical Chemistry*, 355(1):16–20.

Kocot, K., Pytlakowska, K., Zawisza, B., and Sitko, R. (2016). How to detect metal species preconcentrated by microextraction techniques? *TrAC Trends in Analytical Chemistry*, 82:412–424.

Kraus, D. (2014). Consolidated data analysis and presentation using an open-source add-in for the microsoft excel® spreadsheet software. *Medical Writing*, 23:25–28.

Krogh, M., Dorani, F., Foulsham, E., MxSorley, A., and Hoey, D. (2013). Hunter catchment salinity assessment. EPA 2013/0787.

Kumar, A., Yueh, F. Y., Miller, T., and Singh, J. P. (2003). Detection of trace elements in liquids by laser-induced breakdown spectroscopy with a Meinhard nebulizer. *Applied Optics*, 42(30):6040.

Kurniawan, K. H., Pardede, M., Hedwig, R., Abdulmadjid, S. N., Lahna, K., Idris, N., Jobiliong, E., Suyanto, H., Suliyanti, M. M., Tjia, M. O., Lie, T. J., Lie, Z. S., Kurniawan, D. P., and Kagawa, K. (2015). Practical and highly sensitive elemental analysis for aqueous samples containing metal impurities employing electrodeposition on indium-tin oxide film samples and laser-induced shock wave plasma in low-pressure helium gas. *Applied Optics*, 54(25):7592.

Kuwako, A., Uchida, Y., and Maeda, K. (2003). Supersensitive detection of sodium in water with use of dual-pulse laser-induced breakdown spectroscopy. *Applied Optics*, 42(30):6052.

Lawley, C. J., Somers, A. M., and Kjarsgaard, B. A. (2021). Rapid geochemical imaging of rocks and minerals with handheld laser induced breakdown spectroscopy (LIBS). *Journal of Geochemical Exploration*, 222:106694.

Lazic, V. and Jovićević, S. (2014). Laser induced breakdown spectroscopy inside liquids: Processes and analytical aspects. *Spectrochimica Acta Part B: Atomic Spectroscopy*, 101:288–311.

Lee, D.-H., Han, S.-C., Kim, T.-H., and Yun, J.-I. (2011). Highly sensitive analysis of boron and lithium in aqueous solution using dual-pulse laser-induced breakdown spectroscopy. *Analytical Chemistry*, 83(24):9456–9461.

Lee, Y., Oh, S.-W., and Han, S.-H. (2012). Laser-induced breakdown spectroscopy (LIBS) of heavy metal ions at the sub-parts per million level in water. *Applied Spectroscopy*, 66(12):1385–1396.

Legnaioli, S., Botto, A., Campanella, B., Poggialini, F., Raneri, S., and Palleschi, V. (2022). Univariate linear methods. In Palleschi, V., editor, *Chemometrics and numerical methods in LIBS*, pages 259 – 276. Wiley, Hoboken, NJ, 1st edition.

Lemière, B. (2018). A review of pXRF (field portable X-ray fluorescence) applications for applied geochemistry. *Journal of Geochemical Exploration*, 188:350–363.

Lemière, B. and Harmon, R. S. (2021). XRF and LIBS for field geology. In Crocombe, R., Leary, P., and Kammrath, B., editors, *Portable Spectroscopy and Spectrometry*, pages 455–497. Wiley, 1st edition.

Lemière, B. and Uvarova, Y. A. (2020). New developments in field-portable geochemical techniques and on-site technologies and their place in mineral exploration. *Geochemistry: Exploration, Environment, Analysis*, 20(2):205–216.

Li, X., Chen, R., You, Z., Pan, T., Yang, R., Huang, J., Fang, H., Kong, W., Peng, J., and Liu, F. (2022). Chitosan homogenizing coffee ring effect for soil available potassium determination using laser-induced breakdown spectroscopy. *Chemosensors*, 10(9):374.

Lin, J., Yang, J., Gao, X., Huang, Y., and Lin, X. (2022). The effect of solution temperature on the quantitative analysis of laser-induced breakdown spectroscopy. *Applied Physics B*, 128(7):127.

Lin, Q., Han, X., Wang, J., Wei, Z., Liu, K., and Duan, Y. (2016). Ultra-trace metallic element detection in liquid samples using laser induced breakdown spectroscopy based on matrix conversion and crosslinked PVA polymer membrane. *Journal of Analytical Atomic Spectrometry*, 31(8):1622–1630.

Liu, K., Tang, Z., Zhou, R., Zhang, W., Li, Q., Zhu, C., He, C., Liu, K., and Li, X. (2021). Determination of lead in aqueous solutions using resonant surface-enhanced LIBS. *Journal of Analytical Atomic Spectrometry*, 36(11):2480–2484.

Liu, Y., Pan, J., Hu, Z., Chu, Y., Khan, M. S., Tang, K., Guo, L., and Lau, C. (2020). Stability improvement for dried droplet pretreatment by suppression of coffee ring effect using electrochemical anodized nanoporous tin dioxide substrate. *Microchimica Acta*, 187(12):664.

Loree, T. R. and Radziemski, L. J. (1981). Laser-induced breakdown spectroscopy: Time-integrated applications. *Plasma Chemistry and Plasma Processing*, 1(3):271–279.

Lottermoser, B. G. (2010). *Mine wastes: characterization, treatment and environmental impacts*. Springer, Berlin, Heidelberg, 3rd edition.

Lottermoser, B. G. (2017). *Environmental indicators in metal mining*. Springer Cham, New York.

Loudyi, H., Rifaï, K., Laville, S., Vidal, F., Chaker, M., and Sabsabi, M. (2009). Improving laser-induced breakdown spectroscopy (LIBS) performance for iron and lead determination in aqueous solutions with laser-induced fluorescence (LIF). *Journal of Analytical Atomic Spectrometry*, 24(10):1421.

Lu, Y., Li, Y., Wu, J., Zhong, S., and Zheng, R. (2010). Guided conversion to enhance cation detection in water using laser-induced breakdown spectroscopy. *Applied Optics*, 49(13):C75.

Lu, Y., Liang, X., Niyungeko, C., Zhou, J., Xu, J., and Tian, G. (2018). A review of the identification and detection of heavy metal ions in the environment by voltammetry. *Talanta*, 178:324–338.

Ma, S., Cao, F., Wen, X., Xu, F., Tian, H., Fu, X., and Dong, D. (2022a). Detection of heavy metal ions using laser-induced breakdown spectroscopy combined with filter paper modified with Ptag bimetallic nanoparticles. *SSRN Electronic Journal*.

Ma, S., Guo, L., and Dong, D. (2022b). A molecular laser-induced breakdown spectroscopy technique for the detection of nitrogen in water. *Journal of Analytical Atomic Spectrometry*, 37(3):663–667.

Ma, S., Tang, Y., Ma, Y., Chen, F., Zhang, D., Dong, D., Wang, Z., and Guo, L. (2020a). Stability and accuracy improvement of elements in water using LIBS with geometric constraint liquid-to-solid conversion. *Journal of Analytical Atomic Spectrometry*, 35(5):967–971.

Ma, S., Tang, Y., Ma, Y., Chu, Y., Chen, F., Hu, Z., Zhu, Z., Guo, L., Zeng, X., and Lu, Y. (2019). Determination of trace heavy metal elements in aqueous solution using surface-enhanced laser-induced breakdown spectroscopy. *Optics Express*, 27(10):15091.

Ma, S., Tang, Y., Zhang, S., Ma, Y., Sheng, Z., Wang, Z., Guo, L., Yao, J., and Lu, Y. (2020b). Chlorine and sulfur determination in water using indirect laser-induced breakdown spectroscopy. *Talanta*, 214:120849.

Maity, U., Manoravi, P., Joseph, M., and Sivaraman, N. (2022). Laser-induced breakdown spectroscopy for simultaneous determination of lighter lanthanides in actinide matrix in aqueous medium. *Spectrochimica Acta Part B: Atomic Spectroscopy*, 190:106393.

Manard, B. T., Wylie, E. M., and Willson, S. P. (2018). Analysis of rare earth elements in uranium using handheld laser-induced breakdown spectroscopy (HH LIBS). *Applied Spectroscopy*, 72(11):1653–1660.

Matsumoto, A., Shimazu, Y., Nakano, H., Murakami, K., and Yae, S. (2021). Signal stability of surface-enhanced laser-induced breakdown spectroscopy for microdroplet analysis using a porous silicon substrate. *Spectrochimica Acta Part B: Atomic Spectroscopy*, 178:106143.

Melquiades, F., Parreira, P., Appoloni, C., Silva, W., and Lopes, F. (2011). Quantification of metals in river water using a portable EDXRF-system. *Applied Radiation and Isotopes*, 69(2):327–333.

Meneses-Nava, M., Pichardo, J., Rodriguez, M., Rosas-Roman, I., and Maldonado, J. (2021). Detection enhancement at parts per billion level of aluminum in water droplets by a combination of acoustic levitation and nanoparticle enhanced laser induced breakdown spectroscopy. *Spectrochimica Acta Part B: Atomic Spectroscopy*, 184:106280.

Menges, F. (2023). Spectragryph - optical spectroscopy software. Version 1.2.16.1, http://www.effemm2.de/spectragryph/.

Mermet, J.-M. (2010). Calibration in atomic spectrometry: A tutorial review dealing with quality criteria, weighting procedures and possible curvatures. *Spectrochimica Acta Part B: Atomic Spectroscopy*, 65(7):509–523.

Metzinger, A., Kovács-Széles, E., Almási, I., and Galbács, G. (2014). An assessment of the potential of laser-induced breakdown spectroscopy (LIBS) for the analysis of cesium in liquid samples of biological origin. *Applied Spectroscopy*, 68(7):789–793.

Mukherjee, S., Bhattacharyya, S., Ghosh, K., Pal, S., Halder, A., Naseri, M., Mohammadniaei, M., Sarkar, S., Ghosh, A., Sun, Y., and Bhattacharyya, N. (2021). Sensory development for heavy metal detection: A review on translation from conventional analysis to field-portable sensor. *Trends in Food Science & Technology*, 109:674–689.

Musazzi, S. and Perini, U., editors (2014). *Laser-induced breakdown spectroscopy: Theory and applications*, volume 182 of *Springer Series in Optical Sciences*. Springer, Berlin, Heidelberg, 1st edition.

Méndez-López, C., Fernández-Menéndez, L. J., González-Gago, C., Pisonero, J., and Bordel, N. (2023). Nebulization assisted molecular LIBS for sensitive and fast fluorine determination in aqueous solutions. *Journal of Analytical Atomic Spectrometry*, 38(1):80–89.

Nakanishi, R., Ohba, H., Saeki, M., Wakaida, I., Tanabe-Yamagishi, R., and Ito, Y. (2021). Highly sensitive detection of sodium in aqueous solutions using laser-induced breakdown spectroscopy with liquid sheet jets. *Optics Express*, 29(4):5205.

NCBI (2024). Periodic table of elements. National Center for Biotechnology Information, accessed Jan. 14, 2024.

Niu, S., Zheng, L., Qayyum Khan, A., and Zeng, H. (2019). Laser-induced breakdown spectroscopic (LIBS) analysis of trace heavy metals enriched by Al_2O_3 nanoparticles. *Applied Spectroscopy*, 73(4):380–386.

Olechowski, A. L., Eppinger, S. D., Joglekar, N., and Tomaschek, K. (2020). Technology readiness levels: Shortcomings and improvement opportunities. *Systems Engineering*, 23(4):395–408.

Oleksy, M., Dynarowicz, K., and Aebisher, D. (2023). Rapid prototyping technologies: 3D printing applied in medicine. *Pharmaceutics*, 15(8):2169.

Palleschi, V. (2022a). Avoiding misunderstanding self-absorption in laser-induced breakdown spectroscopy (LIBS) analysis. *Spectroscopy*, pages 60–62.

Palleschi, V., editor (2022b). *Chemometrics and numerical methods in LIBS*. Wiley, Hoboken, NJ, 1st edition.

Papai, R., da Silva Mariano, C., Pereira, C. V., Ferreira da Costa, P. V., de Oliveira Leme, F., Nomura, C. S., and Gaubeur, I. (2019). Matte photographic paper as a low-cost material for metal ion retention and elemental measurements with laser-induced breakdown spectroscopy. *Talanta*, 205:120167.

Pearman, W., Scaffidi, J., and Angel, S. M. (2003). Dual-pulse laser-induced breakdown spectroscopy in bulk aqueous solution with an orthogonal beam geometry. *Applied Optics*, 42(30):6085.

Pearson, D., Chakraborty, S., Duda, B., Li, B., Weindorf, D. C., Deb, S., Brevik, E., and Ray, D. (2017). Water analysis via portable X-ray fluorescence spectrometry. *Journal of Hydrology*, 544:172–179.

Pearson, D., Weindorf, D. C., Chakraborty, S., Li, B., Koch, J., Van Deventer, P., de Wet, J., and Kusi, N. Y. (2018). Analysis of metal-laden water via portable X-ray fluorescence spectrometry. *Journal of Hydrology*, 561:267–276.

Pessanha, S., Marguí, E., Carvalho, M. L., and Queralt, I. (2020). A simple and sustainable portable triaxial energy dispersive X-ray fluorescence method for in situ multielemental analysis of mining water samples. *Spectrochimica Acta Part B: Atomic Spectroscopy*, 164:105762.

Pierce, W. and Christian, S. M. (2006). Portable LIBS instrumentation can identify trace levels of environmental pollutants. *Photonik international*, pages 92 –94.

Piorek, S. (2019). Rapid sorting of aluminum alloys with handheld μLIBS analyzer. *Materials Today: Proceedings*, 10:348–354.

Piper, A. M. (1944). A graphic procedure in the geochemical interpretation of water-analyses. *Transactions, American Geophysical Union*, 25(6):914.

Pochon, A., Desaulty, A.-M., and Bailly, L. (2020). Handheld laser-induced breakdown spectroscopy (LIBS) as a fast and easy method to trace gold. *Journal of Analytical Atomic Spectrometry*, 35(2):254–264.

Poggialini, F., Campanella, B., Cocciaro, B., Lorenzetti, G., Palleschi, V., and Legnaioli, S. (2023a). Catching up on calibration-free LIBS. *Journal of Analytical Atomic Spectrometry*, 38(9):1751–1771.

Poggialini, F., Campanella, B., Legnaioli, S., Pagnotta, S., Raneri, S., and Palleschi, V. (2020). Improvement of the performances of a commercial hand-held laser-induced breakdown spectroscopy instrument for steel analysis using multiple artificial neural networks. *Review of Scientific Instruments*, 91(7):073111.

Poggialini, F., Campanella, B., Palleschi, V., Hidalgo, M., and Legnaioli, S. (2022). Graphene thin film microextraction and nanoparticle enhancement for fast LIBS metal trace analysis in liquids. *Spectrochimica Acta Part B: Atomic Spectroscopy*, 194:106471.

Poggialini, F., Legnaioli, S., Campanella, B., Cocciaro, B., Lorenzetti, G., Raneri, S., and Palleschi, V. (2023b). Calculating the limits of detection in laser-induced breakdown spectroscopy: Not as easy as it might seem. *Applied Sciences*, 13(6):1–14.

Popov, A. M., Drozdova, A. N., Zaytsev, S. M., Biryukova, D. I., Zorov, N. B., and Labutin, T. A. (2016). Rapid, direct determination of strontium in natural waters by laser-induced breakdown spectroscopy. *Journal of Analytical Atomic Spectrometry*, 31(5):1123–1130.

Pourret, O. and Hursthouse, A. (2019). It's time to replace the term "heavy metals" with "potentially toxic elements" when reporting environmental research. *International Journal of Environmental Research and Public Health*, 16(22):4446.

Rai, N. K., Rai, A. K., Kumar, A., and Thakur, S. N. (2008). Detection sensitivity of laser-induced breakdown spectroscopy for Cr II in liquid samples. *Applied Optics*, 47(31):G105.

Rai, V. and Thakur, S. N. (2020). Instrumentation for LIBS and recent advances. In *Laser-Induced Breakdown Spectroscopy*, pages 107–136. Elsevier, Amsterdam, Oxford, Cambridge, 2nd edition.

Raimundo, I. M., Michael Angel, S., and Colón, A. M. (2021). Detection of low lithium concentrations using laser-induced breakdown spectroscopy (LIBS) in high-pressure and high-flow conditions. *Applied Spectroscopy*, 75(11):1374–1381.

Ramli, M., Khumaeni, A., Kurniawan, K. H., Tjia, M. O., and Kagawa, K. (2017). Spectrochemical analysis of Cs in water and soil using low pressure laser induced breakdown spectroscopy. *Spectrochimica Acta Part B: Atomic Spectroscopy*, 132:8–12.

Rao, A. P., Jenkins, P. R., Auxier, J. D., Shattan, M. B., and Patnaik, A. K. (2022). Analytical comparisons of handheld LIBS and XRF devices for rapid quantification of gallium in a plutonium surrogate matrix. *Journal of Analytical Atomic Spectrometry*, 37(5):1090–1098.

Reimann, C. and Birke, M., editors (2010). *Geochemistry of European bottled water*. Borntraeger Science Publishers, Stuttgart.

Rezaei, F., Cristoforetti, G., Tognoni, E., Legnaioli, S., Palleschi, V., and Safi, A. (2020). A review of the current analytical approaches for evaluating, compensating and exploiting self-absorption in laser induced breakdown spectroscopy. *Spectrochimica Acta Part B: Atomic Spectroscopy*, 169:105878.

Rezaei, F., Karimi, P., and Tavassoli, S. H. (2014). Effect of self-absorption correction on LIBS measurements by calibration curve and artificial neural network. *Applied Physics B*, 114(4):591–600.

Rezk, R., Galmed, A., Abdelkreem, M., Ghany, N. A., and Harith, M. (2016). Quantitative analysis of Cu and Co adsorbed on fish bones via laser-induced breakdown spectroscopy. *Optics & Laser Technology*, 83:131–139.

Rifai, K., Laville, S., Vidal, F., Sabsabi, M., and Chaker, M. (2012). Quantitative analysis of metallic traces in water-based liquids by UV-IR double-pulse laser-induced breakdown spectroscopy. *J. Anal. At. Spectrom.*, 27(2):276–283.

Rifai, K., Vidal, F., Chaker, M., and Sabsabi, M. (2013). Resonant laser-induced breakdown spectroscopy (RLIBS) analysis of traces through selective excitation of aluminum in aluminum alloys. *Journal of Analytical Atomic Spectrometry*, 28(3):388.

Ripoll, L. and Hidalgo, M. (2019). Electrospray deposition followed by laser-induced breakdown spectroscopy (ESD-LIBS): a new method for trace elemental analysis of aqueous samples. *Journal of Analytical Atomic Spectrometry*, 34(10):2016–2026.

Ripoll, L., Navarro-González, J., Legnaioli, S., Palleschi, V., and Hidalgo, M. (2021). Evaluation of thin film microextraction for trace elemental analysis of liquid samples using LIBS detection. *Talanta*, 223:121736.

Romero-Matos, J., Cánovas, C. R., Macías, F., Pérez-López, R., León, R., Millán-Becerro, R., and Nieto, J. M. (2023). Wildfire effects on the hydrogeochemistry of a river severely polluted by acid mine drainage. *Water Research*, 233:119791.

Rossum, J. R. (1949). Conductance method for checking accuracy of water analyses. *Analytical Chemistry*, 21(5):631–631.

Ruas, A., Matsumoto, A., Ohba, H., Akaoka, K., and Wakaida, I. (2017). Application of laser-induced breakdown spectroscopy to zirconium in aqueous solution. *Spectrochimica Acta Part B: Atomic Spectroscopy*, 131:99–106.

Ruiz, F., Ripoll, L., Hidalgo, M., and Canals, A. (2019). Dispersive micro solid-phase extraction (DμSPE) with graphene oxide as adsorbent for sensitive elemental analysis of aqueous samples by laser induced breakdown spectroscopy (LIBS). *Talanta*, 191:162–170.

Samek, O., Beddows, D., Kaiser, J., Kukhlevsky, S. V., Liska, M., Telle, H., and Whitehouse, A. J. (2000). Application of laser-induced breakdown spectroscopy to in situ analysis of liquid samples. *Optical Engineering*, 39(8):2248.

Sarkar, A., Aggarwal, S. K., Sasibhusan, K., and Alamelu, D. (2010). Determination of sub-ppm levels of boron in ground water samples by laser induced breakdown spectroscopy. *Microchimica Acta*, 168(1-2):65–69.

Sarkar, A., Alamelu, D., and Aggarwal, S. K. (2008). Determination of thorium and uranium in solution by laser-induced breakdown spectrometry. *Applied Optics*, 47(31):G58.

Sarkar, A., Alamelu, D., and Aggarwal, S. K. (2012). Gallium quantification in solution by LIBS in the presence of bulk uranium. *Optics & Laser Technology*, 44(1):30–34.

Sawaf, S. and Tawfik, W. (2014). Analysis of heavy elements in water with high sensitivity using laser induced breakdown spectroscopy. *Optoelectronics and Advanced Materials - Rapid Communications*, 8(5-6):414 – 417.

Schilder, C., Schlemminger, A., and Ahsan, A. (2021). In-situ slag analysis with LIBS - the future technology to analyze slag sample fast and preparation free. *Proceedings of the 7th International Slag Valorisation Symposium*, (7):51 – 52.

Schlatter, N., Freutel, G., and Lottermoser, B. (2022). Evaluation of the use of field-portable LIBS analysers for on-site chemical analysis in the mineral resources sector. *GeoResources*, 2:32–38.

Schlatter, N. and Lottermoser, B. G. (2023). Quantitative analysis of Li, Na, and K in single element standard solutions using portable laser-induced breakdown spectroscopy (pLIBS). *Geochemistry: Exploration, Environment, Analysis*, 23(geochem2023-019):1–13.

Schlatter, N. and Lottermoser, B. G. (2024). Laser-induced breakdown spectroscopy applied to elemental analysis of aqueous solutions—a comprehensive review. *Spectroscopy Journal*, 2(1):1–32.

Schlatter, N., Lottermoser, B. G., Illgner, S., and Schmidt, S. (2023). Utilising portable laser-induced breakdown spectroscopy for quantitative inorganic water testing. *Chemosensors*, 11(479):1–22.

Schmidt, N. E. and Goode, S. R. (2002). Analysis of aqueous solutions by laser-induced breakdown spectroscopy of ion exchange membranes. *Applied Spectroscopy*, 56(3):370–374.

Schoeller, H. (1965). Hydrodynamique dans le karst: écoulement et emmagasinement. *Symposium on Hydrology of Fractured Rocks*.

Schäffer, R. (2018). *Hydrochemische Methoden zur geothermalen Erkundung und Charakterisierung von Thermalwässern*. PhD thesis, Technische Universität Darmstadt, Darmstadt.

Schäffer, R. and Dietz, A. (2023). Standardized Schoeller diagrams - A Matlab plotting tool. *Grundwasser - Zeitschrift der Fachsektion Hydrogeologie*, 28:345–355.

Schäffer, R., Götz, E., Schlatter, N., Schubert, G., Weinert, S., Schmidt, S., Kolb, U., and Sass, I. (2022). Fluid–rock interactions in geothermal reservoirs, germany: Thermal autoclave experiments using sandstones and natural hydrothermal brines. *Aquatic Geochemistry*, 28(2):63–110.

Schäffer, R., Sass, I., Blümmel, C., and Schmidt, S. (2021). Hydrochemistry of the Tuxertal, NW Tauern Window, Austria: water use and drinking water supply in an alpine environment. *Journal of Maps*, 17(2):197–213.

SciAps (2020). Best practices guide for developing LIBS calibrations. Internal document.

SciAps (2021). LIBS CCD integration delay and period. Internal document.

SciAps (2023a). SciAps Z-9 Liquidator specifications. Internal document, https://www.sciaps.com/resources/product-brochures, Last accessed: 24.03.2024.

SciAps (2023b). Z-9 Liquidator for rapid multi-element analysis of lithium brines. Internal document, https://www.sciaps.com/resources/product-brochures, last accessed: 24.03.2024.

Scott, J. R., Effenberger, A. J., and Hatch, J. J. (2014). Influence of atmospheric pressure and composition on LIBS. In Musazzi, S. and Perini, U., editors, *Laser-Induced Breakdown Spectroscopy*, number 182 in Springer Series in Optical Sciences, pages 91–116. Springer, Berlin, Heidelberg, 1st edition.

Senesi, G. S. (2014). Laser-induced breakdown spectroscopy (LIBS) applied to terrestrial and extraterrestrial analogue geomaterials with emphasis to minerals and rocks. *Earth-Science Reviews*, 139:231–267.

Senesi, G. S., Harmon, R. S., and Hark, R. R. (2020). Field-portable and handheld LIBS. In Singh, J. P. and Thakur, S. N., editors, *Laser-Induced Breakdown Spectroscopy*, pages 537–560. Elsevier, Amsterdam, Oxford, Cambridge, 2nd edition.

Senesi, G. S., Harmon, R. S., and Hark, R. R. (2021). Field-portable and handheld laser-induced breakdown spectroscopy: Historical review, current status and future prospects. *Spectrochimica Acta Part B: Atomic Spectroscopy*, 175(106013):1–27.

Shao, Y., Ma, S., Zhao, X., Tian, H., Chen, S., Dong, D., and Zhou, J. (2023). Determination of phosphorus in water using iron hydroxide assisted laser-induced breakdown spectroscopy. *Journal of Analytical Atomic Spectrometry*, (3).

Sheng, P., Jiang, L., Sui, M., and Zhong, S. (2019). Micro-hole array sprayer-assisted laser-induced breakdown spectroscopy technology and its application in the field of sea water analysis. *Spectrochimica Acta Part B: Atomic Spectroscopy*, 154:1–9.

Shi, Q., Niu, G., Lin, Q., Wang, X., Wang, J., Bian, F., and Duan, Y. (2014). Exploration of a 3D nano-channel porous membrane material combined with laser-induced breakdown spectrometry for fast and sensitive heavy metal detection of solution samples. *Journal of Analytical Atomic Spectrometry*, 29(12):2302–2308.

Shimazu, Y., Matsumoto, A., Nakano, H., and Yae, S. (2021). Sensitive quantitative analysis of strontium in microdroplet by surface-enhanced laser-induced breakdown spectroscopy using porous silicon. *Analytical Sciences*, 37:1839–1841.

Simeonsson, J. and Williamson, L. (2011). Characterization of laser induced breakdown plasmas used for measurements of arsenic, antimony and selenium hydrides. *Spectrochimica Acta Part B: Atomic Spectroscopy*, 66(9-10):754–760.

Singh, J. P. and Thakur, S. N. (2020). *Laser-induced breakdown spectroscopy*. Elsevier, Amsterdam, Oxford, Cambridge, 2nd edition.

Singh, M. and Sarkar, A. (2019). Analytical evaluation of cesium emission lines using laser-induced breakdown spectroscopy. *Pramana*, 93(1):2.

Skrzeczanowski, W. and Długaszek, M. (2021). Al and Si quantitative analysis in aqueous solutions by LIBS method. *Talanta*, 225(121916).

Skrzeczanowski, W. and Długaszek, M. (2022). Application of laser-induced breakdown spectroscopy in the quantitative analysis of elements-K, Na, Ca, and Mg in liquid solutions. *Materials*, 15(3736):1–10.

Sobral, H., Sanginés, R., and Trujillo-Vázquez, A. (2012). Detection of trace elements in ice and water by laser-induced breakdown spectroscopy. *Spectrochimica Acta Part B: Atomic Spectroscopy*, 78:62–66.

Song, R., Schlecht, P. C., and Ashley, K. (2001). Field screening test methods: performance criteria and performance characteristics. *Journal of Hazardous Materials*, 83(1-2):29–39.

St-Onge, L., Kwong, E., Sabsabi, M., and Vadas, E. B. (2004). Rapid analysis of liquid formulations containing sodium chloride using laser-induced breakdown spectroscopy. *Journal of Pharmaceutical and Biomedical Analysis*, 36(2):277–284.

Stiff, H. A. (1951). The interpretation of chemical water analysis by means of patterns. *Journal of Petroleum Technology*, 3(10):15–3.

Sui, M., Fan, Y., Jiang, L., Xue, Y., Zhou, J., and Zhong, S. (2021). Online ultrasonic nebulizer assisted laser induced breakdown spectroscopy (OUN-LIBS): An online metal elements sensor for marine water analysis. *Spectrochimica Acta Part B: Atomic Spectroscopy*, 180(106201):1–11.

Tang, Y., Ma, S., Chu, Y., Wu, T., Ma, Y., Hu, Z., Guo, L., Zeng, X., Duan, J., and Lu, Y. (2019). Investigation of the self-absorption effect using time-resolved laser-induced breakdown spectroscopy. *Optics Express*, 27(4).

Tang, Z., Hao, Z., Zhou, R., Li, Q., Liu, K., Zhang, W., Yan, J., Wei, K., and Li, X. (2021). Sensitive analysis of fluorine and chlorine elements in water solution using laser-induced breakdown spectroscopy assisted with molecular synthesis. *Talanta*, 224(121784).

Tian, H., Jiao, L., and Dong, D. (2019). Rapid determination of trace cadmium in drinking water using laser-induced breakdown spectroscopy coupled with chelating resin enrichment. *Scientific Reports*, 9(1):10443.

Tian, H., Li, C., Jiao, L., Zhao, X., and Dong, D. (2022). Study on rapid detection method of water heavy metals by laser-induced breakdown spectroscopy coupled with liquid-solid conversion and morphological constraints. In Lu, Y., Gu, Y., and Chen, S., editors, *International Conference on Optoelectronic Materials and Devices (ICOMD 2021)*, page 44, Guangzhou, China. SPIE.

Tighe, M., Bielski, M., Wilson, M., Ruscio-Atkinson, G., Peaslee, G. F., and Lieberman, M. (2020). A sensitive XRF screening method for lead in drinking water. *Analytical Chemistry*, 92(7):4949–4953.

Tiihonen, T. E., Nissinen, T. J., Turhanen, P. A., Vepsäläinen, J. J., Riikonen, J., and Lehto, V.-P. (2022). Real-time on-site multielement analysis of environmental waters with a portable X-ray fluorescence (pXRF) system. *Analytical Chemistry*, 94(34):11739–11744.

Timms, W. and Holley, C. (2016). Mine site water-reporting practices, groundwater take and governance frameworks in the Hunter Valley coalfield, Australia. *Water International*, 41(3):351–370.

Tolstonogova, Y. S., Golik, S. S., Mayor, A. Y., Ilyin, A. A., Proschenko, D. Y., and Bukin, O. A. (2021). Effect of laser pulse repetition rate on the detection limits of the elemental composition of pollutants in aqueous solutions by femtosecond laser induced breakdown spectroscopy. *Atmospheric and Oceanic Optics*, 34(6):553–559.

United Nations (2015). *Transforming our world: the 2030 Agenda for Sustainable Development*. United Nations Publications, New York.

United Nations (2023). *The sustainable development goals report 2023: Special edition*. United Nations Publications, New York.

van Vliet, M. T. H., Jones, E. R., Flörke, M., Franssen, W. H. P., Hanasaki, N., Wada, Y., and Yearsley, J. R. (2021). Global water scarcity including surface water quality and expansions of clean water technologies. *Environmental Research Letters*, 16(2):024020.

Vander Wal, R. L., Ticich, T. M., West, J. R., and Householder, P. A. (1999). Trace metal detection by laser-induced breakdown spectroscopy. *Applied Spectroscopy*, 53(10):1226–1236.

Völker, S., Schreiber, C., and Kistemann, T. (2010). Drinking water quality in household supply infrastructure—A survey of the current situation in Germany. *International Journal of Hygiene and Environmental Health*, 213(3):204–209.

Wachter, J. R. and Cremers, D. A. (1987). Determination of uranium in solution using laser-induced breakdown spectroscopy. *Applied Spectroscopy*, 41(6):1042–1048.

Wakil, M. A. and Alwahabi, Z. T. (2019). Microwave-assisted laser induced breakdown molecular spectroscopy: quantitative chlorine detection. *Journal of Analytical Atomic Spectrometry*, 34(9):1892–1899.

Wakil, M. A. and Alwahabi, Z. T. (2020). Quantitative fluorine and bromine detection under ambient conditions *via* molecular emission. *Journal of Analytical Atomic Spectrometry*, 35(11):2620–2626.

Walker, M. and Humphries, S. (2019). 3D printing: Applications in evolution and ecology. *Ecology and Evolution*, 9(7):4289–4301.

Wall, M., Sun, Z., and Alwahabi, Z. T. (2016). Quantitative detection of metallic traces in water-based liquids by microwave-assisted laser-induced breakdown spectroscopy. *Optics Express*, 24(2):1507.

Walser, H. (2011). *Statistik für Naturwissenschaftler*. Number 3541 in UTB Biologie, Geographie, Geologie, Chemie. Haupt Verlag, Bern Stuttgart Wien, 1st edition.

Wang, Q., Ge, T., Liu, Y., Jiang, L., Chen, A., Han, J., and Jin, M. (2022). Highly sensitive analysis of trace elements in aqueous solutions using surface-enhanced and discharge-assisted laser-induced breakdown spectroscopy. *Journal of Analytical Atomic Spectrometry*, 37(2):233–239.

Wang, Q., Liu, Y., Jiang, L., Chen, A., Han, J., and Jin, M. (2023). Metal micro/nanostructure enhanced laser-induced breakdown spectroscopy. *Analytica Chimica Acta*, 1241:340802.

Wang, X., Shi, L., Lin, Q., Zhu, X., and Duan, Y. (2014). Simultaneous and sensitive analysis of Ag(I), Mn(II), and Cr(III) in aqueous solution by LIBS combined with dispersive solid phase micro-extraction using nano-graphite as an adsorbent. *Journal of Analytical Atomic Spectrometry*, 29(6):1098.

Wang, Y. R., Kang, J., Chen, Y. Q., and Li, R. H. (2019). Sensitive analysis of copper in water by LIBS–LIF assisted by simple sample pretreatment. *Journal of Applied Spectroscopy*, 86(2):353–359.

Wang, Z., Afgan, M. S., Gu, W., Song, Y., Wang, Y., Hou, Z., Song, W., and Li, Z. (2021). Recent advances in laser-induced breakdown spectroscopy quantification: From fundamental understanding to data processing. *TrAC Trends in Analytical Chemistry*, 143:116385.

Wang, Z. Z., Yan, J. J., Liu, J. P., Deguchi, Y., Katsumori, S., and Ikutomo, A. (2015). Sensitive cesium measurement in liquid sample using low-pressure laser-induced breakdown spectroscopy. *Spectrochimica Acta Part B: Atomic Spectroscopy*, 114:74–80.

Wen, X., Hu, Z., Nie, J., Gao, Z., Zhang, D., Guo, L., Ma, S., and Dong, D. (2023). Detection of lead in water at ppt levels using resin-enrichment combined with LIBS-LIF. *Journal of Analytical Atomic Spectrometry*, (5).

Wen, X., Lin, Q., Niu, G., Shi, Q., and Duan, Y. (2016). Emission enhancement of laser-induced breakdown spectroscopy for aqueous sample analysis based on Au nanoparticles and solid-phase substrate. *Applied Optics*, 55(24):6706.

WHO (2022). *Guidelines for drinking-water quality*. World-Health-Organization, Geneva, 4th edition.

Williams, A. N. and Phongikaroon, S. (2016). Elemental detection of cerium and gadolinium in aqueous aerosol using laser-induced breakdown spectroscopy. *Applied Spectroscopy*, 70(10):1700–1708.

Wise, M. A., Harmon, R. S., Curry, A., Jennings, M., Grimac, Z., and Khashchevskaya, D. (2022). Handheld LIBS for Li exploration: An example from the Carolina Tin-Spodumene Belt, USA. *Minerals*, 12(1):77.

Wisotzky, F., Cremer, N., and Lenk, S. (2018). *Angewandte Grundwasserchemie, Hydrogeologie und hydrogeochemische Modellierung: Grundlagen, Anwendungen und Problemlösungen*. Springer, Berlin, Heidelberg, 2nd edition.

Wisotzky, F., Cremer, N., and Lenk, S., editors (2021). *Angewandte Grundwasserchemie, Hydrogeologie und hydrogeochemische Modellierung: Grundlagen, Anwendungen und Problemlösungen*. Springer, Berlin, Heidelberg, 3rd edition.

Wu, K., Shen, J., Cao, D., Cheng, H., Sun, S., and Hu, B. (2018). Coulombic effect of amphiphiles with metal nanoparticles on laser-induced breakdown spectroscopy enhancement. *The Journal of Physical Chemistry C*, 122(33):19133–19138.

Wu, M., Wang, X., Niu, G., Zhao, Z., Zheng, R., Liu, Z., Zhao, Z., and Duan, Y. (2021). Ultrasensitive and simultaneous detection of multielements in aqueous samples based on biomimetic array combined with laser-induced breakdown spectroscopy. *Analytical Chemistry*, 93(29):10196–10203.

Wójcik, M., Brinkmann, P., Zdunek, R., Riebe, D., Beitz, T., Merk, S., Cieślik, K., Mory, D., and Antończak, A. (2020). Classification of copper minerals by handheld laser-induced breakdown spectroscopy and nonnegative tensor factorisation. *Sensors*, 20(105946):1–17.

Xing, P., Dong, J., Yu, P., Zheng, H., Liu, X., Hu, S., and Zhu, Z. (2021). Quantitative analysis of lithium in brine by laser-induced breakdown spectroscopy based on convolutional neural network. *Analytica Chimica Acta*, 1178:338799.

Xiu, J., Zhong, S., Hou, H., Lu, Y., and Zheng, R. (2014). Quantitative determination of manganese in aqueous solutions and seawater by laser-induced breakdown spectroscopy (LIBS) using paper substrates. *Applied Spectroscopy*, 68(9):1039–1045.

Xu, F., Ma, S., Zhao, C., and Dong, D. (2022). Application of molecular emissions in laser-induced breakdown spectroscopy: A review. *Frontiers in Physics*, 10:821528.

Yamamoto, K. Y., Cremers, D. A., Ferris, M. J., and Foster, L. E. (1996). Detection of metals in the environment using a portable laser-induced breakdown spectroscopy instrument. *Applied Spectroscopy*, 50(2):222–233.

Yang, X., Hao, Z., shen, M., Yi, R., Li, J., Yu, H., Guo, L., Li, X., Zeng, X., and Lu, Y. (2017). Simultaneous determination of La, Ce, Pr, and Nd elements in aqueous solution using surface-enhanced laser-induced breakdown spectroscopy. *Talanta*, 163:127–131.

Yang, X., Yi, R., Li, X., Cui, Z., Lu, Y., Hao, Z., Huang, J., Zhou, Z., Yao, G., and Huang, W. (2018). Spreading a water droplet through filter paper on the metal substrate for surface-enhanced laser-induced breakdown spectroscopy. *Optics Express*, 26(23):30456.

Yang, X. Y., Hao, Z. Q., Li, C. M., Li, J. M., Yi, R. X., Shen, M., Li, K. H., Guo, L. B., Li, X. Y., Lu, Y. F., and Zeng, X. Y. (2016). Sensitive determinations of Cu, Pb, Cd, and Cr elements in aqueous solutions using chemical replacement combined with surface-enhanced laser-induced breakdown spectroscopy. *Optics Express*, 24(12):13410.

Yant, M. H., Lewis, K. W., H., P. A., Hörst, A. M., and Team, E. (2020). Project ESPRESSO: Exploration roles of handheld LIBS for field geology on Earth and planetary surfaces at the palisades sill. *LPSC*, 51(2326):2.

Yao, M., Lin, J., Liu, M., and Xu, Y. (2012). Detection of chromium in wastewater from refuse incineration power plant near Poyang Lake by laser induced breakdown spectroscopy. *Applied Optics*, 51(10):1552.

Yaroshenko, I., Kirsanov, D., Marjanovic, M., Lieberzeit, P. A., Korostynska, O., Mason, A., Frau, I., and Legin, A. (2020). Real-time water quality monitoring with chemical sensors. *Sensors*, 20(12):3432.

Yi, R., Guo, L., Li, C., Yang, X., Li, J., Li, X., Zeng, X., and Lu, Y. (2016). Investigation of the self-absorption effect using spatially resolved laser-induced breakdown spectroscopy. *Journal of Analytical Atomic Spectrometry*, 31(4):961–967.

Ytsma, C. R., Knudson, C. A., Dyar, M. D., McAdam, A. C., Michaud, D. D., and Rollosson, L. M. (2020). Accuracies and detection limits of major, minor, and trace element quantification in rocks by portable laser-induced breakdown spectroscopy. *Spectrochimica Acta Part B: Atomic Spectroscopy*, 171:17.

Yueh, F.-Y., Sharma, R. C., Singh, J. P., Zhang, H., and Spencer, W. A. (2002). Evaluation of the potential of laser-induced breakdown spectroscopy for detection of trace element in liquid. *Journal of the Air & Waste Management Association*, 52(11):1307–1315.

Zhang, D., Chen, A., Chen, Y., Wang, Q., Li, S., Jiang, Y., and Jin, M. (2021a). Influence of substrate temperature on the detection sensitivity of surface-enhanced LIBS for analysis of heavy metal elements in water. *Journal of Analytical Atomic Spectrometry*, 36(6):1280–1286.

Zhang, D. C., Hu, Z. Q., Su, Y. B., Hai, B., Zhu, X. L., Zhu, J. F., and Ma, X. (2018). Simple method for liquid analysis by laser-induced breakdown spectroscopy (LIBS). *Optics Express*, 26(14):18794.

Zhang, Y., Zhang, T., and Li, H. (2021b). Application of laser-induced breakdown spectroscopy (LIBS) in environmental monitoring. *Spectrochimica Acta Part B: Atomic Spectroscopy*, 181:106218.

Zhang, Z., Jia, W., Shan, Q., Hei, D., Wang, Z., Wang, Y., and Ling, Y. (2022). Determining metal elements in liquid samples using laser-induced breakdown spectroscopy and phase conversion technology. *Analytical Methods*, 14(2):147–155.

Zhao, F., Chen, Z., Zhang, F., Li, R., and Zhou, J. (2010). Ultra-sensitive detection of heavy metal ions in tap water by laser-induced breakdown spectroscopy with the assistance of electrical-deposition. *Analytical Methods*, 2(4):408.

Zhao, N. J., Meng, D. S., Jia, Y., Ma, M. J., Fang, L., Liu, J. G., and Liu, W. Q. (2019). Online quantitative analysis of heavy metals in water based on laser-induced breakdown spectroscopy. *Optics Express*, 27(8):A495.

Zheng, P., Ding, N., Wang, J., Zhao, H., Liu, R., and Yang, Y. (2021). Separation and determination of Cr(III) and Cr(VI) in aqueous solution using laser-induced breakdown spectroscopy coupled with resin substrate preconcentration. *Journal of Analytical Atomic Spectrometry*, 36(12):2631–2638.

Zhong, S., Zheng, R., Lu, Y., Cheng, K., and Xiu, J. (2015). Ultrasonic nebulizer assisted LIBS: A promising metal elements detection method for aqueous sample analysis. *Plasma Science and Technology*, 17(11):979–984.

Zhong, S.-L., Lu, Y., Kong, W.-J., Cheng, K., and Zheng, R. (2016). Quantitative analysis of lead in aqueous solutions by ultrasonic nebulizer assisted laser induced breakdown spectroscopy. *Frontiers of Physics*, 11(4):114202.

Zhu, D., Wu, L., Wang, B., Chen, J., Lu, J., and Ni, X. (2011). Determination of Ca and Mg in aqueous solution by laser-induced breakdown spectroscopy using absorbent paper substrates. *Applied Optics*, 50(29):5695.

Zhu, Y., Ma, S., Yang, G., Tian, H., and Dong, D. (2023). Rapid automatic detection of water Ca, Mg elements using laser-induced breakdown spectroscopy. *Frontiers in Physics*, 11:1179574.

Zuber, A., Bachhuka, A., Tassios, S., Tiddy, C., Vasilev, K., and Ebendorff-Heidepriem, H. (2020). Field deployable method for gold detection using gold pre-concentration on functionalized surfaces. *Sensors*, 20(2):492.

Zulkifli, S. N., Rahim, H. A., and Lau, W.-J. (2018). Detection of contaminants in water supply: A review on state-of-the-art monitoring technologies and their applications. *Sensors and Actuators B: Chemical*, 255:2657–2689.

Ünal, S. and Yalçın, S. (2010). Development of a continuous flow hydride generation laser-induced breakdown spectroscopic system: Determination of tin in aqueous environments. *Spectrochimica Acta Part B: Atomic Spectroscopy*, 65(8):750–757.

Ünal Yeşiller, S. and Yalçın, S. (2013). Optimization of chemical and instrumental parameters in hydride generation laser-induced breakdown spectrometry for the determination of arsenic, antimony, lead and germanium in aqueous samples. *Analytica Chimica Acta*, 770:7–17.

Typeset August 26, 2024